

In presenting this dissertation/thesis as a partial fulfillment of the requirements for an advanced degree from Emory University, I agree that the Library of the University shall make it available for inspection and circulation in accordance with its regulations governing materials of this type. I agree that permission to copy from, or to publish, this thesis/dissertation may be granted by the professor under whose direction it was written when such copying or publication is solely for scholarly purposes and does not involve potential financial gain. In the absence of the professor, the dean of the Graduate School may grant permission. It is understood that any copying from, or publication of, this thesis/dissertation which involves potential financial gain will not be allowed without written permission.

Kimberlynn Becnel Davis

Part I: Synthesis of Cyclobutyl Nucleoside and Nucleotide Analogues as HIV-1 Reverse Transcriptase Inhibitors

Part II: Improvement of Glycosylation Regioselectivity in Purine Nucleoside Analogue Synthesis

Part III: Enantioselective Synthesis of β -D-Dioxolane-T and β -D-FDOC

By

Kimberlynn Becnel Davis
Doctor of Philosophy

Department of Chemistry

Dennis C. Liotta, PhD.
Adviser

Simon Blakey, Ph.D.
Committee Member

Lanny S. Liebeskind, Ph.D.
Committee Member

Accepted:

Lisa A. Tedesco, Ph.D.
Dean of the Graduate School

Date

Part I: Synthesis of Cyclobutyl Nucleoside and Nucleotide Analogues as HIV-1 Reverse Transcriptase Inhibitors

Part II: Improvement of Glycosylation Regioselectivity in Purine Nucleoside Analogue Synthesis

Part III: Enantioselective Synthesis of β -D-Dioxolane-T and β -D-FDOC

By

Kimberlynn Becnel Davis
B.S., Xavier University of Louisiana, 2004

Adviser: Dennis C. Liotta, Ph.D.

An abstract of a dissertation submitted to the Faculty of the Graduate School of Emory University in partial fulfillment of the requirements of the degree of Doctor of Philosophy

Department of Chemistry

2008

Abstract

Part I of this dissertation describes the synthesis and biological activity of novel cyclobutyl nucleoside analogues. The cyclobutane portion of the analogues was synthesized via a [2+2] ketene cycloaddition and an S_N2 coupling strategy for glycosylation. The EC_{50} values in human PBM cell lines ranged from 6.5 to $>100 \mu\text{M}$ with no toxicity in PBM, CEM, and Vero cells up to $100 \mu\text{M}$ (with the exception of the 6-chloropurine derivative, which showed some toxicity). The guanine derivative was proven as the most active compound in the entire cyclobutyl series, including the previously synthesized pyrimidine analogues. Ring-expanded nucleobases, including tricyclic and bicyclic with an extended chain (fatty), were also explored. None showed significant anti-HIV activity without an accompanying cytotoxicity. Certain compounds that showed significant cytotoxicity were evaluated for anti-cancer activity. Triphosphates of each class of compounds were synthesized as well, in order to determine if these derivatives serve as substrates for reverse transcriptase. It was found that the purine and tricyclic compounds are suitable as nucleoside reverse transcriptase inhibitors; however, the fatty base analogue was not incorporated into the elongating DNA chain.

Part II of this dissertation describes efforts toward the improvement of regioselective base coupling of purines. A problem often encountered in glycosylation reactions with purines is the N9 vs N7 competition. This issue was addressed by synthesizing the purine with a bulky silane group in the C-6 position. This should allow a method of blocking the N7 position to accomplish

selective N9 glycosylation, but also a strategy to create a variety of derivatives through the easily substituted silyl group. The synthesis of the silyl purine was explored through a variety of methods, including cross-coupling reactions and organometallic/halogen exchanges. The product was synthesized, but was not able to be isolated as the pure silyl purine due to decomposition.

Part III of this dissertation depicts the studies performed towards enantioselectively synthesizing β -D-FDOC and β -D-dioxolane-T. This was explored in both the glycosylation and lactonization steps of the synthesis. Chiral auxiliaries on the dioxolane component as well as chiral Lewis acids to induce enantioselectivity were employed.

Part I: Synthesis of Cyclobutyl Nucleoside and Nucleotide Analogues as HIV-1 Reverse Transcriptase Inhibitors

Part II: Improvement of Glycosylation Regioselectivity in Purine Nucleoside Analogue Synthesis

Part III: Enantioselective Synthesis of β -D-Dioxolane-T and β -D-FDOC

By

Kimberlynn Becnel Davis
B.S., Xavier University of Louisiana, 2004

Adviser: Dennis C. Liotta, PhD

A dissertation submitted to the Faculty of the Graduate School of Emory University in partial fulfillment of the requirements of the degree of Doctor of Philosophy

Department of Chemistry

2008

Acknowledgements

I vividly remember the first time that I met Dr. Dennis Liotta. He asked, "What do you want to do in the future?" Young and confused, I honestly answered "I don't know" and proceeded with an extensive list of interests. He listened patiently before replying, "That's the perfect response to that question." Encouraged by this initial conversation, the decision that has been deemed as the most important for the graduate student had become simple - Dr. Liotta would be my graduate advisor. I would like to thank Dr. Liotta for all of the insight and guidance that he has provided, not only with chemistry, but also with life. He has truly been a source of comfort throughout these trying years of self-discovery. Thank you for assisting in my personal growth and your constant encouragement and support.

I would also like to thank my committee members, Dr. Blakey and Dr. Liebeskind, for their helpfulness throughout my yearly reports. I would like to thank Dr. McDonald as well, for graciously serving on my proposal committee. Thanks also go to Dr. Mohler and Dr. Padwa, for their instruction in departmental courses.

I am fortunate to have been surrounded by a group of very talented scientists, including Dr. Larry Wilson, Dr. Marike Herold-Dublin, Dr. Ustun Sunay, Dr. Jose Soria, and Dr. Mike Hager. Your help over these years has been instrumental and is greatly appreciated.

Being a member of the Liotta group is a special honor. My graduate school experience has been enhanced due to the encouragement and support of

my group members. Special thanks are given to the “4th floor crew” (past and present), whom I’ve shared lab space with for the last few years. Thanks for all of the interesting discussions and food scouting missions. It has also been great working with the members of the nucleoside project, including Dr. Shuli Mao, Dr. Yongfeng Li, Dr. Xingang Fang, Sanna Malick, Annette Neuman, and Greg Bluemling. Thanks for assisting in my growth as a chemist. I also want to thank the entire synthetic group, especially Dr. Weiqiang Zhan and Cara Mosley, as well as the computational division and Dr. Snyder.

Without the support of the chemistry department staff, life as a graduate student would have been much harder. I want to thank Cindy Gaillard and Ethel Ellington for their helpfulness throughout this process and for being sources of comfort. Special thanks go to the stockroom staff as well – sorry for all of the “I need it yesterday” visits. I also want to thank Dr. Wu, Dr. Wang, Donna Hudson, Dr. Stroebel, and Dr. Hardcastle for their assistance.

I also send my gratitude to my OTT family. My time spent with you was great. I was fortunate to acquire a second boss during this process, Dr. Cory Acuff, who has been instrumental throughout this process. Thank you not only taking the time to train me and expose me to the biotech industry, but also for your genuine concern about me as a person.

To the BCA, including Ronald Hunter, Dr. Rhonda Moore, Kornelius Bankston, Muhsinah Morris, and Dr. Tamara Henderson, it has definitely been a fun ride. Thanks for keeping it interesting and supporting me with all of my “causes”.

Finally, I want to thank the backbone of my life – my family. I want to thank my parents for always believing in me and providing consistent encouragement throughout my life, even with all of the surprises. Thanks also go to my extended family, especially Aunt Perlae who has assumed the grandmother role in my life. I want to thank my in-laws as well, who have been unbelievably supportive throughout this process – including late night lab visits. Most importantly, I want to thank Stephen Davis - my helpmate, my better half, my biggest fan. It is so encouraging to know that I have someone in my corner that believes I can conquer it all. Thank you for being that constant source of support.

“Now unto Him that is able to do exceeding abundantly above all that we ask or think, according to the power that worketh in us...” - Ephesians 3:20.

It is overwhelming to imagine how incomplete my life would be without the power of God working through me. Thank You for blessing me with abundant life and allowing me to accomplish all that I've asked. I realize that none of this would have been possible without You.

Dedicated to my parents

“Making your mark on the world is hard. If it were easy, everybody would do it. But it's not. It takes patience, it takes commitment, and it comes with plenty of failure along the way. The real test is not whether you avoid this failure, because you won't. It's whether you let it harden or shame you into inaction, or whether you learn from it; whether you choose to persevere.”

- *Barack Obama*

Table of Contents

Part I: Synthesis of Cyclobutyl Nucleoside and Nucleotide Analogues as HIV-1 Reverse Transcriptase Inhibitors

1.1	Statement of purpose	1
1.2	Introduction	3
1.2.1	Current status of the HIV/AIDS pandemic.....	3
1.2.2	HIV replication cycle	5
1.2.3	FDA approved anti-HIV treatments	7
1.2.4	NRTI mechanism of action	11
1.2.5	Mechanism of NRTI resistance	12
1.3	Background	16
1.3.1	Carbocyclic oxetanocins as nucleoside analogues	16
1.3.2	Synthesis of 2,3-disubstituted cyclobutanes as nucleoside analogue intermediates	16
1.3.3	Synthesis of modified cyclobutanes as intermediates for nucleoside reverse transcriptase inhibitors	24
1.3.4	Methods of synthesizing carbocyclic cyclobutyl nucleoside analogues	28
1.3.5	Methods of synthesizing nucleoside triphosphates	31
1.3.6	Synthesis and anti-HIV activity of 3'-hydroxymethyl cyclobutyl nucleosides	35
1.4	Results and Discussion	40
1.4.1	Design and synthesis of purine cyclobutyl nucleosides	40
1.4.2	Design and synthesis of tricyclic nucleobase cyclobutyl analogues	48
1.4.3	Design and synthesis of ring expanded ("fat") nucleoside analogues	65
1.4.4	Synthesis of 4'-O-triphosphate of cyclobutyl nucleosides	67
1.4.5	Biological activity of synthesized compounds	69
1.5	Conclusion	74
1.6	Experimental	75
1.7	References	138

Part II: Improvement of Glycosylation Regioselectivity in Purine Nucleoside Analogue Synthesis

2.1	Statement of purpose	148
2.2	Introduction and Background	150
2.2.1	Organolithium reagents	151
2.2.2	Organomagnesium reagents	152
2.2.3	Organozinc reagents	153

2.2.4	Organostannane reagents	154
2.3	Results and Discussion	155
2.3.1	Organolithium generation	155
2.3.2	Palladium catalyzed cross-couplings	161
2.3.3	Halogen/magnesium exchange	163
2.4	Conclusion	167
2.5	Experimental	168
2.6	References	173

Part III: Enantioselective Synthesis of β -D-Dioxolane-T and β -D-FDOC

3.1	Statement of Purpose	178
3.2	Introduction and Background	180
3.3	Results and Discussion	184
3.3.1	Asymmetric glycosylation	184
3.3.2	Asymmetric lactonization	188
3.4	Conclusion	190
3.5	Experimental	191
3.6	References	203

List of Figures

Part I: Synthesis of Cyclobutyl Nucleoside and Nucleotide Analogues as HIV-1 Reverse Transcriptase Inhibitors

Figure 1	Structures of 3TC, FTC, and Oxetanocin A	2
Figure 2	Adults and children estimated to be living with HIV/AIDS in 2007	4
Figure 3	Global estimates of deaths due to AIDS from 1990 to 2007	4
Figure 4	HIV replication cycle	5
Figure 5	FDA approved nucleoside reverse transcriptase inhibitors	8
Figure 6	FDA approved non-nucleoside reverse transcriptase inhibitors	8
Figure 7	FDA approved protease inhibitors	9
Figure 8	FDA approved entry and integrase inhibitors	10
Figure 9	NRTI mechanism of action	12
Figure 10	Mechanism of nucleoside excision	14
Figure 11	Mechanism of nucleoside discrimination (3TC and M184V)	15
Figure 12	Structures of oxetanocin A, cyclobut-A, and cyclobut-G	16
Figure 13	Purine cyclobutyl analogues synthesized by Reese	35
Figure 14	Pyrimidine cyclobutyl analogues synthesized by Reese	36
Figure 15	Purine cyclobutyl nucleoside targets	40
Figure 16	X-ray structure of 9-[<i>cis</i> -3-(hydroxymethyl)cyclobutyl]-guanine 101	45
Figure 17	X-ray structure of 9-[<i>cis</i> -3-(hydroxymethyl)cyclobutyl]purine 117	46
Figure 18	Expanded tricyclic nucleoside adenine 132 and guanine 133 analogues	49
Figure 19	Structure of triciribine	49
Figure 20	Structures of tricyclic nucleoside analogues	51
Figure 21	Benzyl protecting groups used for tricyclic base synthesis	53
Figure 22	Electron withdrawing protecting groups used for tricyclic base synthesis	56
Figure 23	Other protecting groups used for tricyclic base synthesis	57
Figure 24	Ring-expanded “fatty” nucleoside analogues as West Nile virus inhibitors	65
Figure 25	Ring-expanded “fatty” cyclobutyl nucleoside analogues	65
Figure 26	Synthesized cyclobutyl nucleoside 4'-O-triphosphates	67
Figure 27	Structures of tested cyclobutyl nucleosides	69
Figure 28	K _d curve for cyclobutyl adenine triphosphate 184	71
Figure 29	K _d curve for cyclobutyl expanded adenine triphosphate 185	71
Figure 30	Structure of gemcitabine HCl	73

Part II: Improvement of Glycosylation Regioselectivity in Purine Nucleoside Analogue Synthesis

Figure 1	Representative FDA approved purine nucleoside analogues	148
Figure 2	Hypothesized N9 vs. N7 glycosylation regioselectivity with 6-silyl substituted purines	149

Part III: Enantioselective Synthesis of β -D-Dioxolane-T and β -D-FDOC

Figure 1	Structures of 3TC and FTC	180
Figure 2	Structures of dioxolane nucleoside analogues	181
Figure 3	Chiral Lewis acid ligands used in asymmetric glycosylation reactions	186

List of Schemes

Part I: Synthesis of Cyclobutyl Nucleoside and Nucleotide Analogues as HIV-1 Reverse Transcriptase Inhibitors

Scheme 1	Synthesis of 3,3-diethoxy-1,2-cyclobutanedicarboxylate using [2+2] cycloaddition	17
Scheme 2	Diastereoselective [2+2] cycloaddition using chiral substrate	18
Scheme 3	Asymmetric [2+2] cycloaddition mediated by chiral Lewis acid	18
Scheme 4	Rearrangement of oxaspiropentane to cyclobutanone	19
Scheme 5	Second generation synthesis of oxaspiropentane	19
Scheme 6	Synthesis of cyclobutamine through pyridone photolysis	20
Scheme 7	Enantioselective cyclobutamine synthesis through asymmetric [2+3] cycloaddition	21
Scheme 8	Synthesis of cyclobutamine through photolysis of chromium carbene complex	21
Scheme 9	Chemoenzymatic synthesis of cyclobutanol	22
Scheme 10	Synthesis of cyclobutyl epoxide through enantioselective enzymatic hydrolysis	23
Scheme 11	Synthesis of cyclobutanol derivative through photoirradiation	23
Scheme 12	Cyclobutanol synthesis through zirconium-mediated ring contraction	24
Scheme 13	Cyclobutamine synthesis through Hoffman rearrangement	25
Scheme 14	Synthesis of olefin cyclobutane intermediate	25
Scheme 15	Synthesis of 3'-fluoro-3'-(acetoxymethyl)cyclobutane derivative	26
Scheme 16	Synthesis of <i>trans</i> -3-(benzyloxymethyl)cyclobutanol	26
Scheme 17	Synthesis of unsaturated nucleoside analogues	27
Scheme 18	Pinene and verbenone as chiral building blocks for nucleoside analogues	27

Scheme 19	Coupling of tetrabutylammonium salt of purine to triflate	28
Scheme 20	Mitsunobu coupling between <i>trans</i> -3-(benzyloxymethyl)-cyclobutanol and substituted adenine	29
Scheme 21	Regioselective coupling between purine and epoxide	30
Scheme 22	Michael addition between 6-chloropurine 82 and methyl 4,4-diethoxycyclobut-1-ene-1-carboxylate 81	30
Scheme 23	Construction of pyrimidine bases	31
Scheme 24	Construction of purine bases	31
Scheme 25	Yoshikawa/Ludwig "one-pot, three-step" triphosphate synthesis	33
Scheme 26	Moffatt triphosphate synthesis using phosphoramidate intermediate	34
Scheme 27	Ludwig/Eckstein triphosphate synthesis using activated phosphite	35
Scheme 28	Synthesis of 5-fluoro-1-[<i>cis</i> -3-(hydroxymethyl)cyclobutyl] cytosine 112	37
Scheme 29	Synthesis of 5-fluoro-1-[<i>cis</i> -3-(hydroxymethyl)cyclobutyl] cytosine triphosphate 116	38
Scheme 30	Synthesis of <i>trans</i> -3-(benzyloxymethyl)cyclobutanol 63	41
Scheme 31	Synthesis of 9-[<i>cis</i> -3-(benzyloxymethyl)cyclobutyl]adenine 77a	42
Scheme 32	Deprotection of 9-[<i>cis</i> -3-(benzyloxymethyl)cyclobutyl]adenine 77a	42
Scheme 33	Attempted guanine coupling via tetrabutylammonium salt	43
Scheme 34	Synthesis of O ⁶ -benzylguanine 79	43
Scheme 35	Coupling of <i>trans</i> -3-(benzyloxymethyl)cyclobutyl mesylate 122 and O ⁶ -benzylguanine 79	44
Scheme 36	Deprotection of 9-[<i>cis</i> -3-(benzyloxymethyl)cyclobutyl]O ⁶ -benzylguanine 127	44
Scheme 37	Synthesis of purine analogue 117	46
Scheme 38	Synthesis of 6-chloropurine analogue 118	46
Scheme 39	Synthesis of 2-amino-6-chloropurine analogue 119	47
Scheme 40	Synthesis of 2,6-diamino analogue 120 using 2-amino-6-chloropurine precursor 130	47
Scheme 41	Synthesis of diamino analogue 120 by direct coupling of 2,6-diaminopurine	48
Scheme 42	Late coupling disconnection approach for synthesis of tricyclic nucleoside analogues	50
Scheme 43	Early coupling disconnection approach for synthesis of tricyclic nucleoside analogues	50
Scheme 44	Synthesis of 7-deazapurine backbone of expanded bases	51
Scheme 45	General method of preparing intact expanded adenine 152 and guanine 135 nucleobases	52
Scheme 46	Eissenstat and Weaver transfer of activation mechanism	54
Scheme 47	Synthesis of expanded adenine base 152 using SEM protecting group	58

Scheme 48	Synthesis of expanded guanine base 135 using SEM protecting group	59
Scheme 49	Conversion of protected expanded adenine 156 into deprotected expanded guanine 135	60
Scheme 50	Attempted coupling between expanded adenine 152 and <i>trans</i> -cyclobutanol 63	60
Scheme 51	Attempted coupling between expanded guanine 135 and oxathiolane 160	61
Scheme 52	Attempted coupling between expanded guanine 135 and dioxolane 163	61
Scheme 53	Synthesis of expanded adenine cyclobutyl nucleoside analogue 132 using early coupling strategy	62
Scheme 54	Synthesis of expanded guanine cyclobutyl nucleoside analogue 133 using early coupling strategy	63
Scheme 55	Synthesis of expanded guanine oxathiolane nucleoside analogue 162 using early coupling strategy	64
Scheme 56	Synthesis of β -anomer of dodecylguanidine cyclobutyl analogue	66
Scheme 57	Synthesis of α -anomer of dodecylguanidine cyclobutyl analogue	66
Scheme 58	Synthesis of 4'-O-triphosphate of 9-[<i>cis</i> -3-hydroxymethyl) cyclobutyl]adenine 184	68

Part II: Improvement of Glycosylation Regioselectivity in Purine Nucleoside Analogue Synthesis

Scheme 1	Glycosylation regioselectivity on cyclobutyl coupling with adenine and O ⁶ -benzylguanine	149
Scheme 2	Regioselectivity in C6 vs. C8 lithiated purine generation	151
Scheme 3	Silyl group migration in purine derivatization	152
Scheme 4	Purine cross-coupling with organomagnesium reagents	153
Scheme 5	Silylation of iodozinc uracil	153
Scheme 6	Use of 6-zincated iodopurine for C6 derivatization	154
Scheme 7	Purine cross-coupling with organostannane reagents	154
Scheme 8	Synthesis of 6-iodopurine	155
Scheme 9	Attempts towards the synthesis of 6-trimethylsilyl purine	156
Scheme 10	Attempts towards the synthesis of 6-trimethylsilyl purine Using Li naphthalenide	158
Scheme 11	Use of trimethylammonium purine for silylation	159
Scheme 12	Use of DABCO purine to generate silyl purine	160
Scheme 13	Use of lithium/tin exchange to prepare silyl purine	160
Scheme 14	Stille coupling used for nucleobase silylation	161
Scheme 15	Negishi coupling used for nucleobase silylation	162
Scheme 16	Attempted Negishi coupling using iodozinc purine	163
Scheme 17	Reaction of aldehydes with 6-magnesiated purines	164

Scheme 18	Functionalization of unprotected nucleobases using magnesium/halogen exchange	164
Scheme 19	Attempted silylation of magnesiated purine	165

Part III: Enantioselective Synthesis of β -D-Dioxolane-T and β -D-FDOC

Scheme 1	Synthesis of FDOC 8 using Vorbruggen ribosylation	181
Scheme 2	β -Selective glycosylation using $\text{TiCl}_3(\text{O}i\text{Pr})$	182
Scheme 3	Mechanism of titanium mediated glycosylation reaction	182
Scheme 4	Generation of oxonium ion with TMSOTf	183
Scheme 5	Glycosylation with racemic dioxolane acetate and silylated 5-fluorocytosine	184
Scheme 6	Asymmetric glycosylation general reaction	186
Scheme 7	Asymmetric glycosylation general reaction with chiral dioxolane	187
Scheme 8	Asymmetric lactonization general reaction with chiral Lewis acid	189

List of Tables

Part I: Synthesis of Cyclobutyl Nucleoside and Nucleotide Analogues as HIV-1 Reverse Transcriptase Inhibitors

Table 1	Comparison of inhibition of HIV-RT in cell-free assays	38
Table 2	Anti-HIV activity and toxicity of cyclobutyl nucleosides	69
Table 3	Summary of <i>in vitro</i> results with triphosphates	72
Table 4	Anti-HCV activity and toxicity of cyclobutyl nucleosides	72
Table 5	Crystal data and structure refinement for Kba68fs	86
Table 6	Atomic coordinates ($\times 10^4$) and equivalent isotropic displacement parameters ($\text{\AA}^2 \times 10^3$) for Kba68fs	87
Table 7	Bond lengths [\AA] and angles [$^\circ$] for Kba68fs	88
Table 8	Anisotropic displacement parameters ($\text{\AA}^2 \times 10^3$) for Kba68fs	89
Table 9	Hydrogen coordinates ($\times 10^4$) and isotropic displacement parameters ($\text{\AA}^2 \times 10^3$) for Kba68fs	90
Table 10	Torsion angles [$^\circ$] for Kba68fs	91
Table 11	Hydrogen bonds for Kba68fs [\AA and $^\circ$]	92
Table 12	Crystal data and structure refinement for KB78	94
Table 13	Atomic coordinates ($\times 10^4$) and equivalent isotropic displacement parameters ($\text{\AA}^2 \times 10^3$) for KB78	95
Table 14	Bond lengths [\AA] and angles [$^\circ$] for KB78	96
Table 15	Anisotropic displacement parameters ($\text{\AA}^2 \times 10^3$) for Kba68fs	98
Table 16	Hydrogen coordinates ($\times 10^4$) and isotropic displacement	98

Table 17	parameters ($\text{\AA}^2 \times 10^3$) for KB78	99
Table 18	Torsion angles [$^\circ$] for KB78	99
Table 18	Hydrogen bonds for KB78 [\AA and $^\circ$]	100

Part II: Improvement of Glycosylation Regioselectivity in Purine Nucleoside Analogue Synthesis

Table 1	Conditions used for 6-iodopurine silylation using <i>t</i> -BuLi	157
Table 2	Conditions used for 6-iodopurine silylation using LiTMS	157
Table 3	Conditions for Negishi coupling	162
Table 4	Conditions for halogen/magnesium exchange	165

Part III: Enantioselective Synthesis of β -D-Dioxolane-T and β -D-FDOC

Table 1	Attempts at asymmetric glycosylation using chiral Lewis acids	186
Table 2	Attempts at asymmetric glycosylation using menthol dioxolane	188
Table 3	Attempts at asymmetric lactonization using chiral Lewis acids	189

List of Abbreviations

abs	Absolute
AcOH	Acetic acid
Ac ₂ O	Acetic anhydride
Ac	Acetyl
Bn	Benzyl
Bz	Benzoyl
9-BBN	9-Borabicyclo[3.3.1]nonane
bp	Boiling point
<i>n</i> -BuLi	<i>n</i> -Butyl lithium
<i>t</i> -BuLi	<i>t</i> -Butyl lithium
cat	Catalytic
CAN	Ceric ammonium nitrate
CBN	Cyclobutyl nucleoside
DBU	1,8-Diazabicyclo[5.4.0]undec-7-ene
1,2-DCE	1,2-Dichloroethane
DCC	1,3-Dicyclohexylcarbodiimide
DDQ	2,3-dichloro-5,6-dicyano-1,4-benzoquinone
DAST	(Diethylamino)sulfur trifluoride
DEAD	Diethyl azodicarboxylate
DIAD	Diisopropyl azodicarboxylate
DIBAL-H	Diisobutylaluminum hydride

DMAP	N,N-Dimethylaminopyridine
DME	1,2-Dimethoxyethane
DMF	N,N-Dimethylformamide
DMS	Dimethyl sulfide
DMSO	Dimethyl sulfoxide
EC50	Effective concentration of a drug that is required for 50% inhibition of viral replication <i>in vitro</i>
EC90	Effective concentration of a drug that is required for 90% inhibition of viral replication <i>in vitro</i>
EI-MS	Electron Ionization Mass Spectroscopy
EtOAc	Ethyl acetate
Et ₂ O	Diethyl ether
HIV-RT	HIV-reverse transcriptase
HMPT	Hexamethylphosphorous triamide
HMDS	1,1,1,3,3,3-Hexamethyldisilazane
HPLC	High Pressure Liquid Chromatography
HR	High Resolution
IC50	Concentration of an inhibitor that is required for 50% inhibition of an enzyme <i>in vitro</i>
IR	Infrared Spectroscopy
LDA	Lithium diisopropylamide
L-Selectride	Lithium tri-sec-butylborohydride
<i>m</i> CPBA	<i>meta</i> -Chloroperoxy benzoic acid
min	Minutes
mp	Melting point

MS	Mass Spectroscopy
MsCl	Methanesulfonyl chloride
NaHMDS	Sodium hexamethyldisilazide
NIS	N-Iodosuccinimide
NMO	N-methylmorpholine N-oxide
NMR	Nuclear Magnetic Resonance
Ph	Phenyl
PMB	<i>p</i> -Methoxybenzyl
Py	Pyridine
RT	Room temperature
Sat.	Saturated
TBAF	Tetrabutylammonium fluoride
Tf ₂ O	Trifluoromethanesulfonic anhydride
THF	Tetrahydrofuran
TIPSCI	Triisopropylsilyl chloride
TLC	Thin layer chromatography
TMSCl	Trimethylsilyl chloride
TMSOTf	Trimethylsilyl trifluoromethanesulfonate
TBDPSCI	<i>t</i> -Butyldiphenylsilyl chloride
TsCl	<i>p</i> -Toluenesulfonyl chloride

Part I: Synthesis of Cyclobutyl Nucleoside and Nucleotide Analogues as HIV-1 Reverse Transcriptase Inhibitors

1.1 Statement of Purpose

The case of the “mysterious disease” that resulted in the death of an African tribesman in 1959 has been identified as the earliest known account of AIDS (Acquired Immune Deficiency Syndrome).¹ Now, only fifty years later, this disease has claimed the lives of a staggering 22 million people. It is estimated that over 42 million people are currently living with AIDS or its causative agent, HIV (Human Immunodeficiency Virus). Of the 14,000 new infections occurring daily, 95% are within developing countries with approximately 74% of infected individuals living in sub-Saharan Africa. An alarming fact is that HIV/AIDS is now described as a “disease of young people”, as half of the 5 million new infections each year occur among people ages 15 to 24.²

There have been major efforts by public and private organizations to prevent the spread of this virus, which is transmitted through bodily fluids. Though a cure for AIDS has not yet been found, there are therapeutic agents that effectively increase the life span of infected individuals. The currently accepted regimen involves the co-administration of HIV therapies, and always includes nucleoside reverse transcriptase inhibitors (NRTIs) as a component.

The effectiveness of NRTIs as anti-HIV agents has been demonstrated throughout the course of the disease, with the first HIV treatment (AZT) belonging to this class of compounds. However, there are some limitations associated with these therapies, including toxicities resulting from long term

usage, poor compliance due to high and frequent dosages, and the development of viral resistance.³ The M184V/I mutation is one form of viral resistance that has been intensely studied. Codon 184 is located near the reverse transcriptase active site and has direct interaction with incoming nucleotides.⁴ Mutations of the methionine codon at position 184 to β -branched amino acids (namely valine and isoleucine) result in increased nucleotide discrimination due to steric hindrances. Both 3TC and FTC (Figure 1) have large oxathiolane rings, and tend to select for the M184V/I mutation. In fact, the mutation is seen as early as one week after initiation of 3TC therapy and in almost all patients after three months of monotherapy.⁴

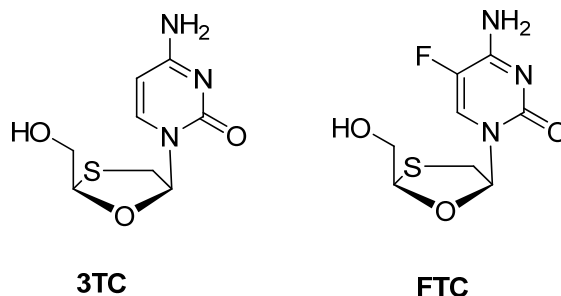


Figure 1: Structures of 3TC and FTC

The Liotta group has chosen to address this problem of resistance with the development of cyclobutyl nucleoside analogues. We postulate that these analogues should be less susceptible to this form of resistance due to a decrease in size, which should eliminate or reduce steric interactions in the M184V/I mutants. Pyrimidine cyclobutyl nucleoside analogues previously developed in our laboratory were inactive against HIV.⁵ Thus, cyclobutyl rings coupled to larger nucleoside bases will be studied.

1.2 Introduction

1.2.1 Current Status of the HIV/AIDS Pandemic

In 1959, an African tribesman sought treatment at a local clinic for symptoms similar to those of sickle-cell anemia. A sample of the patient's blood, retained by clinic physicians, was genetically tested after forty years. Though a certain amount of decomposition occurred, researchers were able to identify this case as the earliest known account of the human immunodeficiency virus type 1 (HIV-1).¹

An estimated 33.2 million people are currently living with HIV or AIDS (Acquired Immune Deficiency Syndrome), which is the most advanced stage of the virus (Figure 2). Recent epidemiologic studies revealed that on any given day, over 6,800 people become infected with the virus and over 5,700 people die from AIDS. In 2007, there were approximately 2.1 million deaths globally, with 76% occurring in sub-Saharan Africa.⁶

Though these figures are alarming, they do display a reduction in annual deaths due to AIDS (Figure 3), which is attributed to increased treatment access and intervention methods. In addition, there was a net decrease in the number of new infections as well as a decline in prevalence within certain regions. Nevertheless, AIDS remains a leading cause of death worldwide and is the primary cause of death in sub-Saharan Africa.

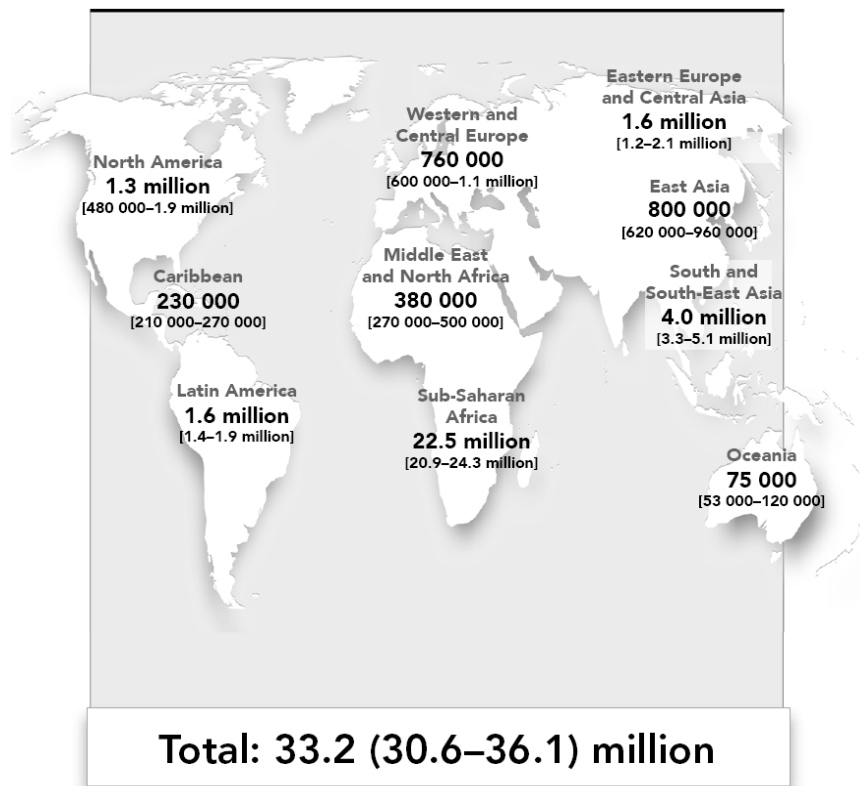


Figure 2. Adults and children estimated to be living with HIV/AIDS in 2007⁶

Estimated number of adult and child deaths due to AIDS globally, 1990–2007

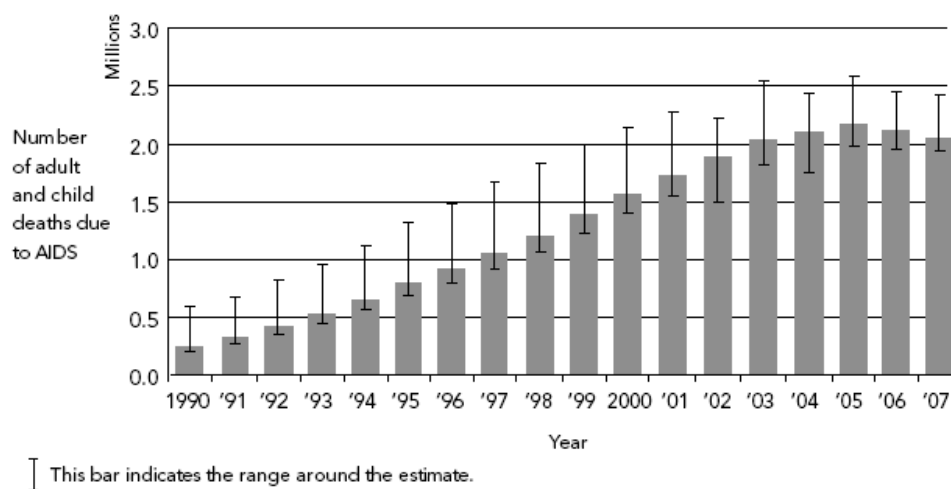


Figure 3. Global estimates of deaths due to AIDS from 1990 to 2007⁶

1.2.2 HIV Replication Cycle

HIV mainly infects cells of the immune system, including T-helper lymphocytes, macrophages, and dendritic cells. Several steps (Figure 4) are required in order to invade the host cell (early phase) and to produce mature viral particles that are able to subsequently invade other host cells (late phase).⁷⁻⁹

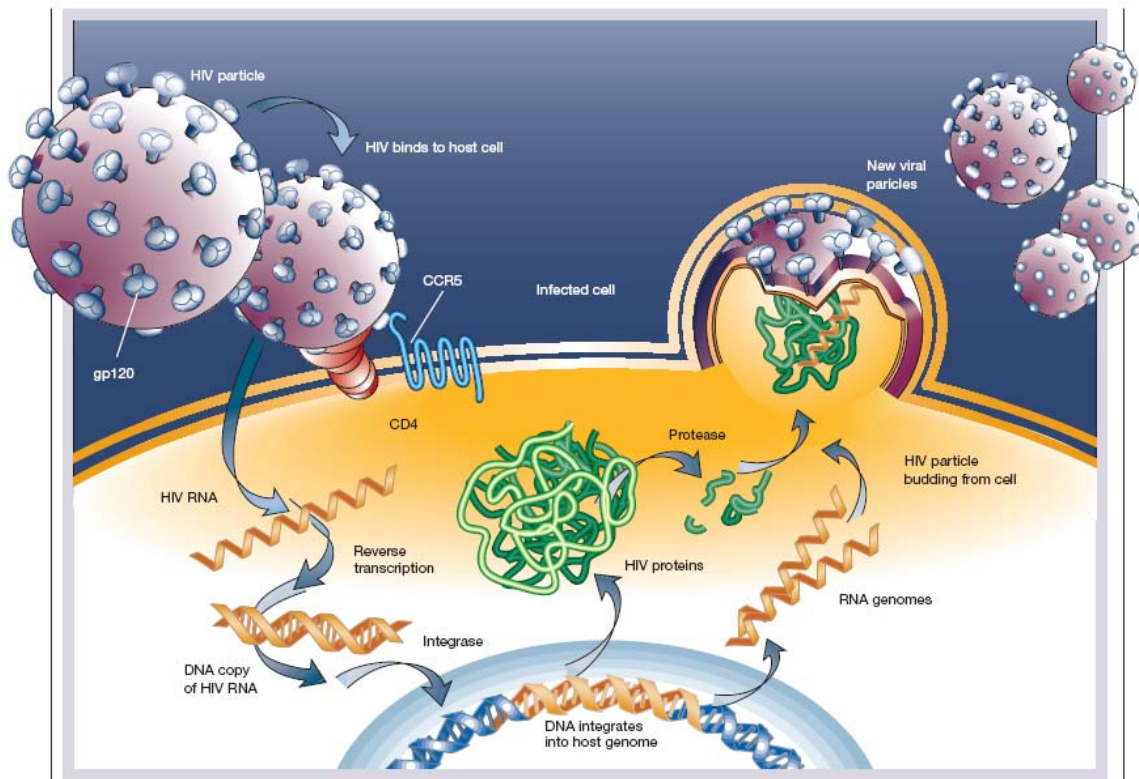


Figure 4: HIV replication cycle¹⁰

Early Phase

1. Attachment/Penetration

The first step of the viral invasion process involves the binding of HIV-1 surface glycoprotein 120 (gp120) to a CD4 molecule on the plasma membrane of the host cell. Following this, the complex interacts with a co-receptor, which includes different G-protein-coupled receptors. Studies have identified that

CXCR4 is the co-receptor for HIV-1 strains that target T cells, while CCR5 is the co-receptor for those strains that infect macrophages. The binding to the co-receptor results in a conformational change that exposes the transmembrane protein gp41, enabling fusion of the viral and cellular membranes. This allows the protein core, which contains the viral genome, to enter the cell.

2. Reverse Transcription

The two RNA copies of the viral genome are released from the capsid into the cell. Reverse transcriptase (RT) performs three enzymatic roles in converting single-stranded RNA into double-stranded DNA. Reverse transcriptase acts as an RNA-dependent DNA polymerase, transcribing single-stranded RNA genome into single-stranded DNA. As DNA is being made, the RNA genome is degraded by the ribonuclease H activity of RT. A complementary DNA strand is then synthesized through reverse transcriptase's role as a DNA-dependent DNA polymerase to produce double-stranded DNA, which is able to enter the nucleus and begin the integration process.

3. Integration

The process of integration begins with the removal of two nucleotides from each 3'-end of the viral DNA. Following this, integrase cleaves the host DNA. The modified viral DNA is now able to be joined to the host DNA through a strand transfer reaction. This process results in formation of the HIV-1 provirus.

Late Phase

4. Transcription

The integrated provirus may then lie dormant, which is referred to as the latent stage of HIV infection. The presence of cellular transcription factors, including NF- κ B, promotes the production of the active virus. The provirus is copied into mRNA, which is then spliced into the regulatory proteins Tat, Rev, and Nef. The accumulation of Rev causes the inhibition of mRNA splicing, which results in the translation of unspliced viral mRNA into the Gag and Gag-Pro-Pol polyproteins.

5. Assembly/Budding/Maturation

The viral envelope protein (gp160) is cleaved by cellular proteases and processed into the surface proteins gp120 and gp41. These envelope proteins are assembled with the viral genomic RNA and polyproteins at the surface of the infected cell. New virions are released from the surface of the host cell through budding. Maturation occurs when HIV protease cleaves the polyproteins into functional HIV proteins and enzymes. The mature virion is then able to infect other cells and continue the replication cycle.

1.2.3 FDA Approved Anti-HIV Treatments

The U.S. Food and Drug Administration (FDA) has approved several drugs as anti-HIV therapeutics. These drugs can be divided into five general classes. Nucleoside reverse transcriptase inhibitors (NRTIs) act as chain terminators of reverse transcriptase, thus stalling viral reproduction. There are currently eight approved compounds in this class (Figure 5): zidovudine (AZT),

didanosine (ddI), dideoxycytidine (ddC), stavudine (d4T), lamivudine (3TC), emtricitabine (FTC), abacavir (ABC), and tenofovir disoproxil fumarate (TDF).

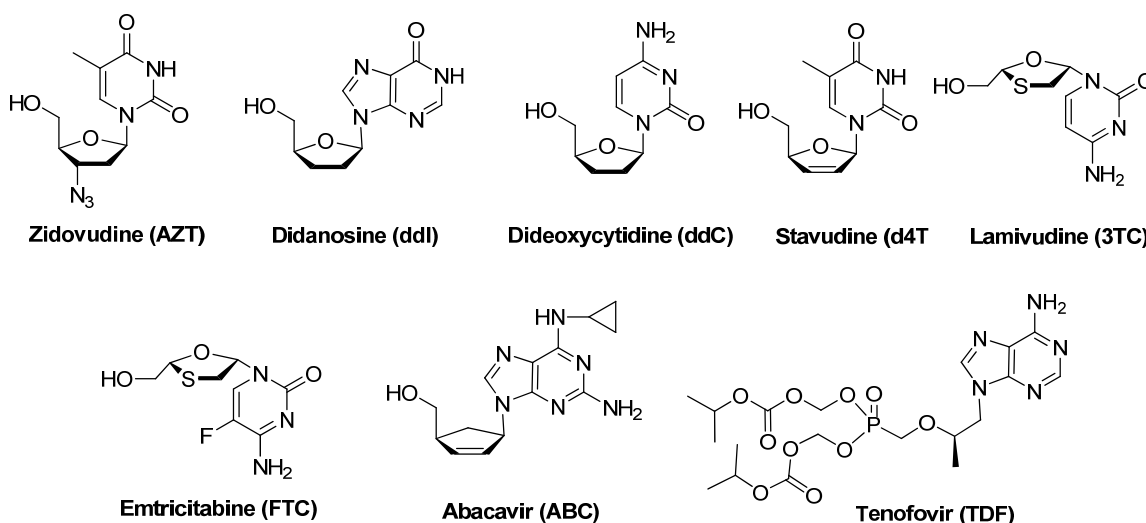


Figure 5: FDA Approved Nucleoside Reverse Transcriptase Inhibitors

Non-nucleoside reverse transcriptase inhibitors (NNRTIs), are able to directly bind to reverse transcriptase and disable it. These include nevirapine (NVP), delavirdine (DLV), efavirenz (EFV), and the newly approved etravirine (Figure 6).

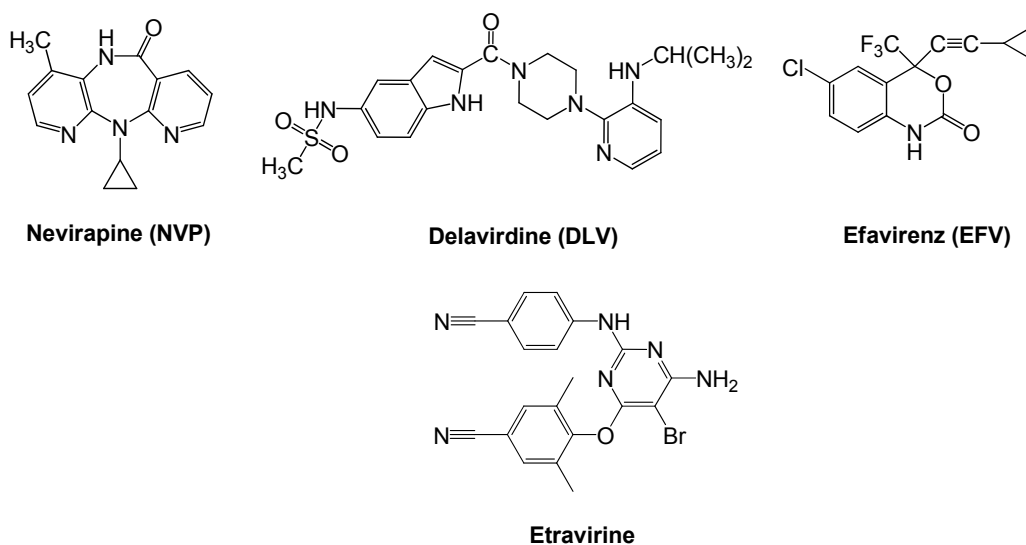


Figure 6: FDA Approved Non-Nucleoside Reverse Transcriptase Inhibitors

Protease inhibitors (PIs) are able to disable the protease enzyme that cuts the viral protein into smaller fragments. There are currently nine approved protease inhibitors on the market: saquinavir (SQV), indinavir (IDV), ritonavir (RTV), nelfinavir (NFV), amprenavir (APV), lopinavir (LPV), atazanavir (ATV), tipranavir (TPV), and darunavir (Figure 7).

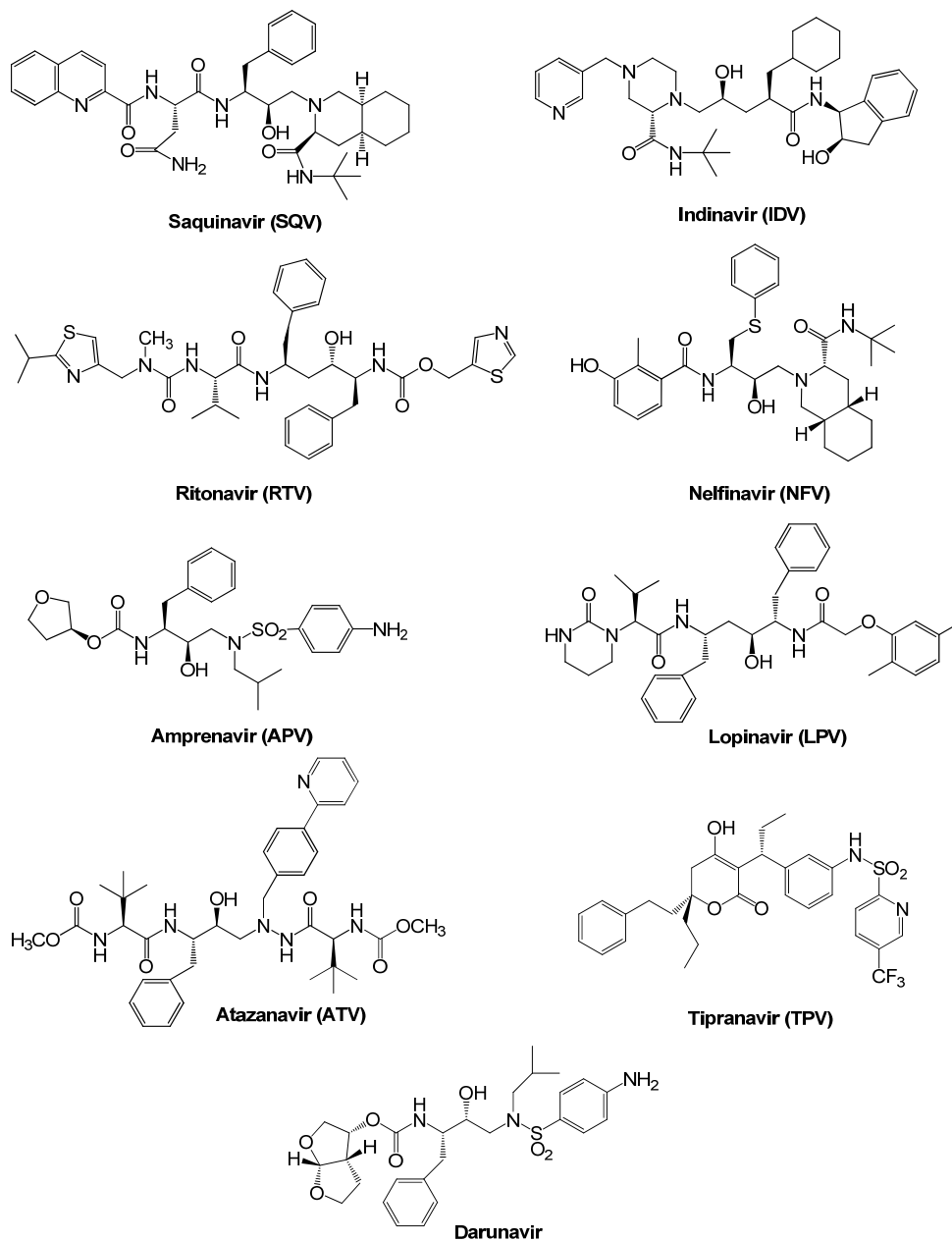


Figure 7: FDA Approved Protease Inhibitors

Fusion/entry inhibitors block the entry of HIV into the host cell. There are currently two approved drugs of this class. Enfuvirtide (Figure 8) was the first viral entry inhibitor to be approved, and is a peptide that corresponds to amino acid residues 643-678 of gp160. Maraviroc (Figure 8) acts as a CCR5 co-receptor antagonist and prevents entry of the virus into the cell. The first integrase inhibitor, raltegravir (Figure 8), was approved in late 2007. It functions to block the integration of genetic material from the virus into the host cell.

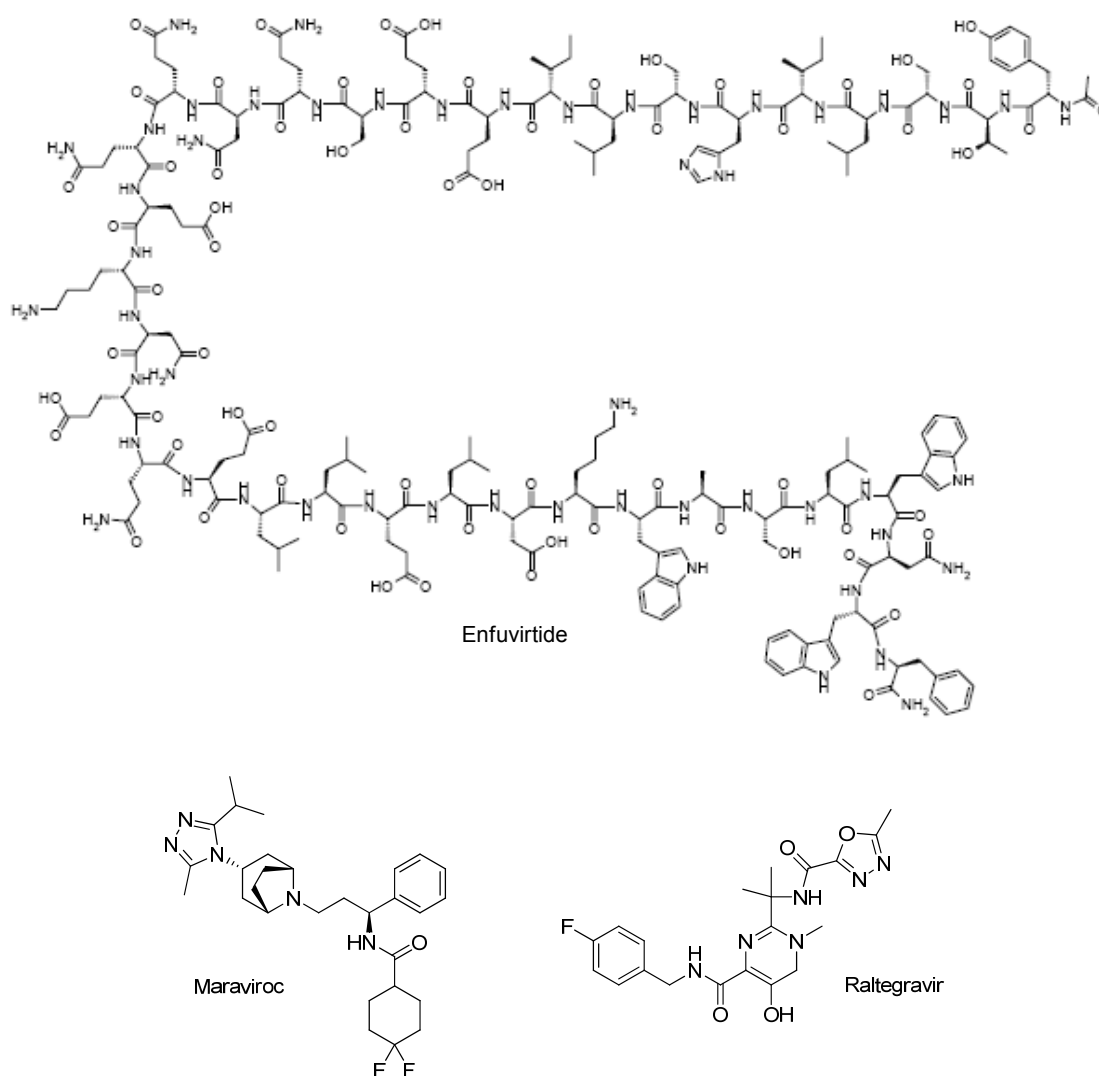


Figure 8: FDA Approved Entry and Integrase Inhibitors

Researchers have found that the best way to treat the infection is by employing the highly active anti-retroviral therapy (HAART), which combines three or more antiviral drugs. This treatment has been shown to significantly reduce short-term mortality and opportunistic disease.¹¹

1.2.4 NRTI Mechanism of Action

Drug design for HIV has been based upon an understanding of the viral replication cycle.¹² The conversion of viral RNA into double-stranded DNA, catalyzed by reverse transcriptase, is a major target in therapeutic design. This viral enzyme serves as an attractive target, as no cellular counterpart exists. In fact, the first FDA approved anti-HIV agent, AZT, is a reverse transcriptase inhibitor. There are two targets for inhibition on HIV reverse transcriptase: the allosteric binding site and the deoxynucleotide triphosphate (dNTP) binding site. NNRTIs are able to directly bind to this allosteric binding site and disable enzyme activity. NRTIs target the catalytic substrate binding site and act as chain terminators of the enzyme, thus stalling viral reproduction.^{3,8,12,13}

In order to accomplish inhibition of the RT enzyme, the NRTI must first be converted into its active metabolite (Figure 9). The 5'-hydroxyl group of the inhibitor, which is a 2',3'-dideoxynucleoside analogue, is converted by cellular kinases into the triphosphate through three distinct phosphorylation steps (note that only two steps are required for the activation of tenofovir, which is administered in its monophosphate form). The nucleoside triphosphate, or nucleotide, is then able to compete with natural nucleotide substrates (dATP,

dGTP, dCTP, and dTTP) for the catalytic substrate binding site. The lack of the 3'-hydroxyl group, which is necessary to elongate the DNA strand, results in chain termination.^{9,12,14,15}

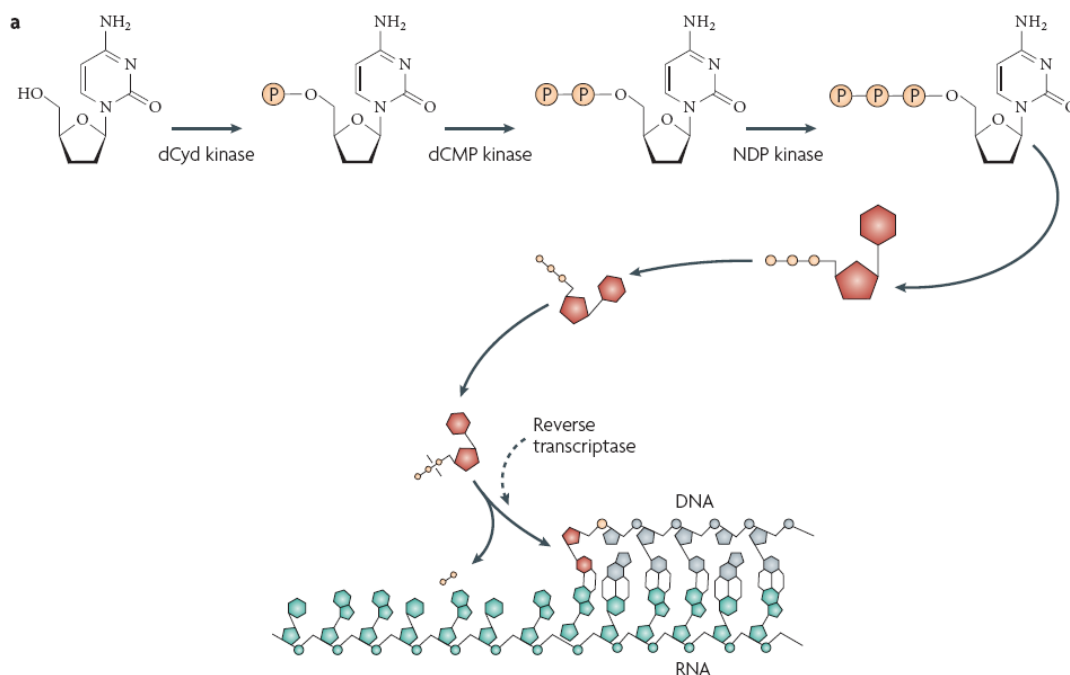


Figure 9: NRTI Mechanism of Action¹²

The success of NRTI therapy relies upon two characteristics of reverse transcriptase. It has a natural affinity for dNTPs, and will readily utilize chemically altered analogues of these substrates. In addition, the enzyme lacks formal proofreading ability. This allows the inhibitor to be incorporated into the DNA chain.¹⁶

1.2.5 Mechanism of NRTI Resistance

Current HAART treatment involves the use of two nucleoside reverse transcriptase inhibitors with either a protease inhibitor or a non-nucleoside reverse transcriptase inhibitor.¹⁵ Studies have shown that combination therapies

of this type improve the efficacy of the drugs being used and also delay drug resistance.^{14,17} The success of the treatment, however, may be compromised due to insufficient potency, complicated regimens, poor tolerability, and adverse interactions with other medications.¹⁸⁻²²

The common use of NRTIs in HIV treatment causes issues of resistance to eventually arise and hinders the long-term efficacy of the therapeutics. In fact, even under the most favorable treatment conditions, there are several features of HIV that cause the inevitable development of drug resistance. HIV has a very high replication rate; it is estimated that in untreated patients at least 10^{10} new virions are produced daily, with 10^7 replication cycles occurring per day. The virus also has a very high mutation rate, as 1 mutation in 10^4 replications occurs per cycle. In addition, these drug-resistant mutants can remain latent in resting CD4+ T cells, monocytes, and macrophages.¹⁸ Thus, incomplete viral suppression, which may result from non-adherence, pharmacokinetics, or lack of drug potency, allows for the selection of these drug resistant variants.²³

Two mechanisms of resistance to NRTIs have been proposed: excision and discrimination.²⁴ Nucleoside excision is the reverse of a normal polymerization reaction (Figure 10). It involves the nucleophilic attack of a polyphosphate unit, either ATP or pyrophosphate (PPi), on the phosphodiester bond between the last two nucleotides of the primer. This results in the removal of the chain terminating NRTI.^{4,23,25-27} Thymidine analogs, such as zidovudine and stavudine, were found to select for this type of resistance through the following RT mutants: M41L, D67N, K70R, T215Y/F, and K219Q/E/N.

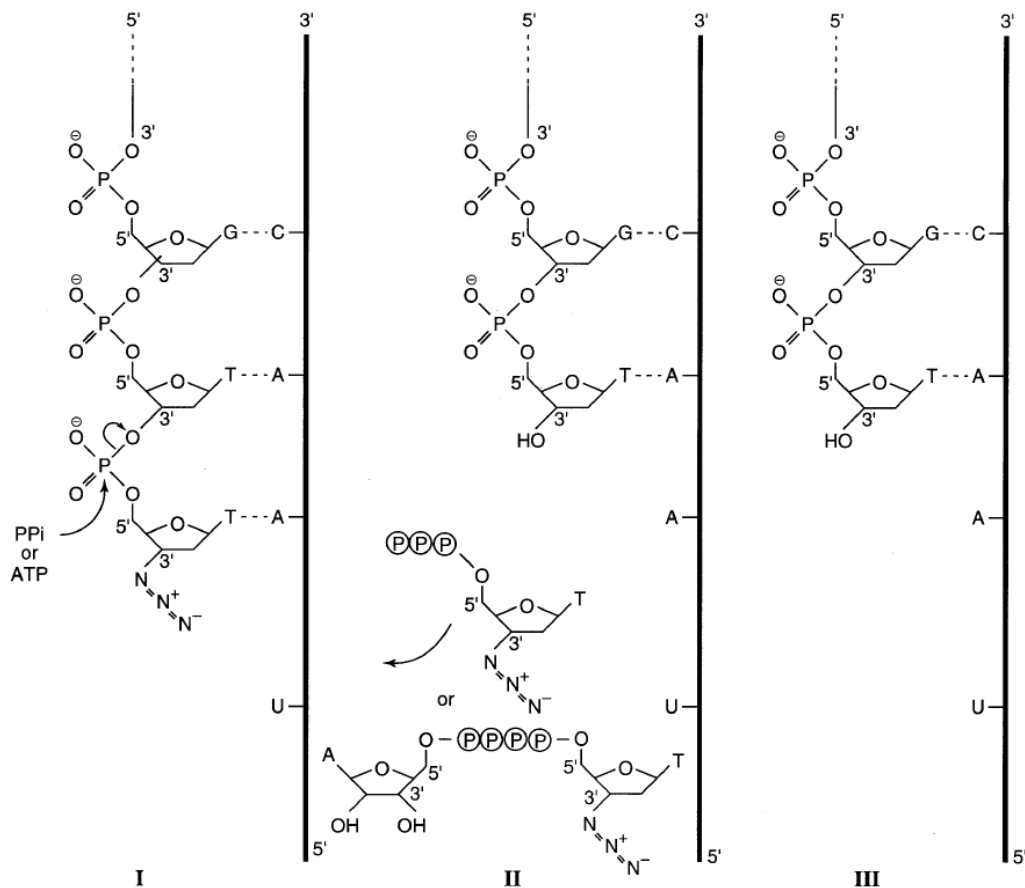


Figure 10: Mechanism of Nucleoside Excision¹⁶

Nucleoside discrimination is caused by mutations within reverse transcriptase that allow it to recognize structural differences between the inhibitors and the natural substrates. This results from changes in those amino acids of the enzyme that are responsible for positioning the incoming nucleotide. Mutations that cause this form of resistance include Q151M, L74V, K65R, and M184V/I.^{4,23,28} A well-known example of this type of resistance is the M184V/I mutation that confers high-level resistance to 3TC (Figure 11). This resistance is caused by steric interaction between β -branched amino acids and the oxathiolane ring of 3TC.^{29,30} Natural dNTPs substrates are not affected by this

mutation and are able to be incorporated at the 3' end of the extending primer, thus continuing viral replication and inducing selective pressure of the mutant.³¹

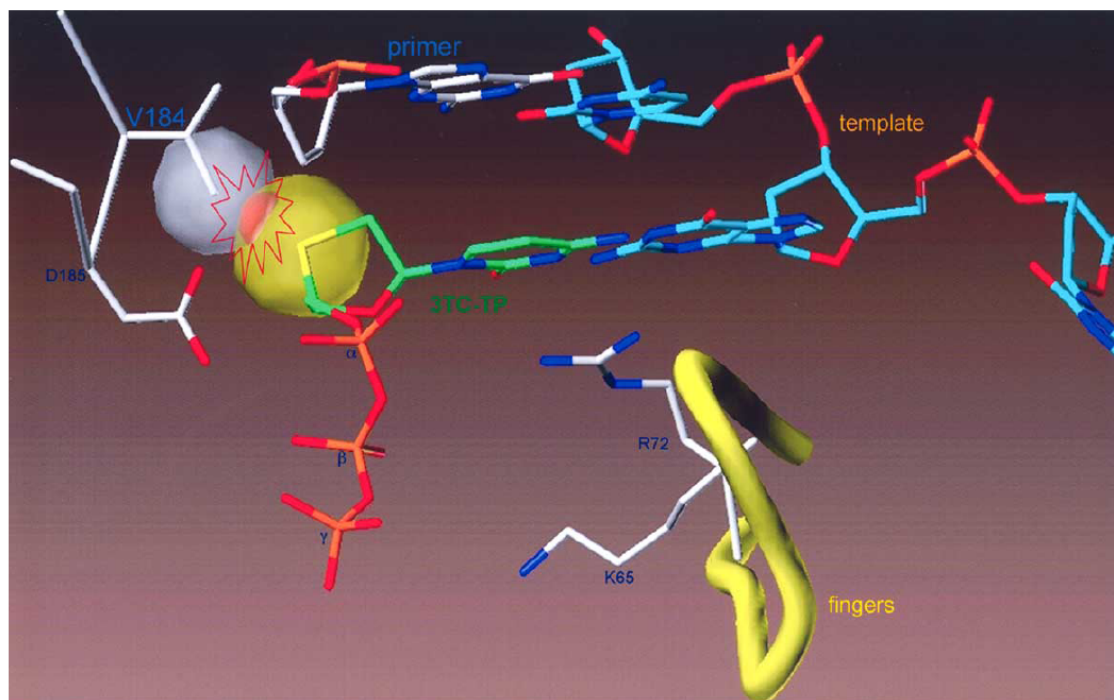


Figure 11: Mechanism of Nucleoside Discrimination (3TC and M184V)¹⁹

1.3 Background

1.3.1 Carbocyclic Oxetanocins as Nucleoside Analogues

The interest in cyclobutyl nucleoside analogues as therapeutic agents was initiated with the discovery that natural product oxetanocin A displays potent anti-HIV activity (Figure 12).^{32,33} Several analogues of this compound have been developed with modifications in the carbohydrate and/or base portions of the molecule. Molecular model studies showed that the cyclobutane ring may serve as a suitable substitute for the oxetane ring. This led to the development of cyclobut-A and cyclobut-G, which were both considered as promising anti-viral agents (Figure 12).³⁴ This resulted in a surge of interest in cyclobutyl nucleosides and the development of numerous methods of synthesizing these analogues.

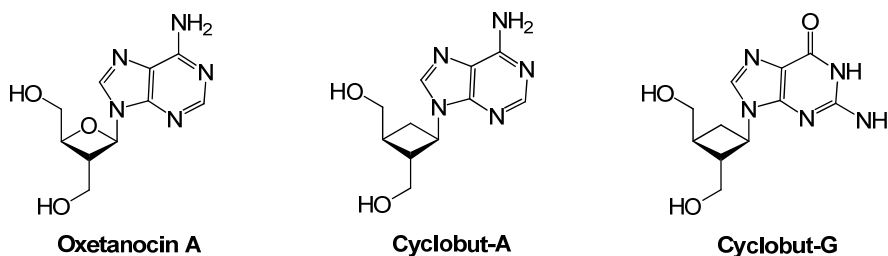


Figure 12: Structures of oxetanocin A, cyclobut-A, and cyclobut-G

1.3.2 Synthesis of 2,3-Disubstituted Cyclobutanes as Nucleoside Analogue Intermediates

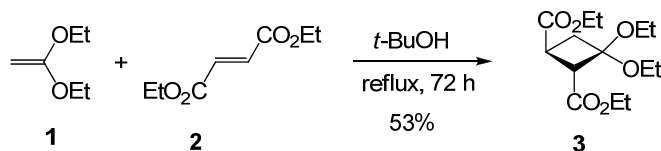
Cyclobutanes are highly strained molecules that adopt a puckered conformation due to 1,3 (non-bonded) carbon-carbon interactions.³⁵ This level of strain, which has been calculated as 26.4 kcal, allows cyclobutanes to undergo facile ring openings to acyclic products, enlargements to five or six membered

rings, and even contractions to cyclopropanes.³⁶ There are many methods that reliably generate the four-membered carbocyclic ring. The main strategies used include [2+2] cycloadditions, cyclization of acyclic compounds, ring expansion of cyclopropanes, and ring contraction of cyclopentanes. In the following sections, common methods of synthesizing 2,3-disubstituted cyclobutyl rings for use in the construction of nucleoside analogues are described, with the categorization based upon the key intermediate used to generate the nucleoside (cyclobutanone, cyclobutamine, or cyclobutanol). Methods of synthesizing the 2,3-disubstituted cyclobutanes are highlighted, as these have been most explored due to their similarities to oxetanocin A.³⁷⁻³⁹

Cyclobutanone Derivatives

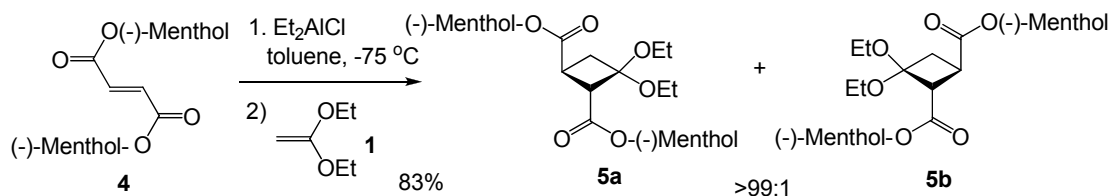
One of the key intermediates used in the synthesis of cyclobutyl nucleosides is the cyclobutanone. The cyclobutanone intermediate has been synthesized by several methods. Notable routes are described below.

In the synthesis of the 2,3-disubstituted ketal **3**, diethyl fumarate **2** and ketene diethylacetal **1** underwent a thermal [2+2] cycloaddition reaction (Scheme 1).^{40,41} Hydrolysis of the ketal (not shown) afforded the cyclobutanone derivative.



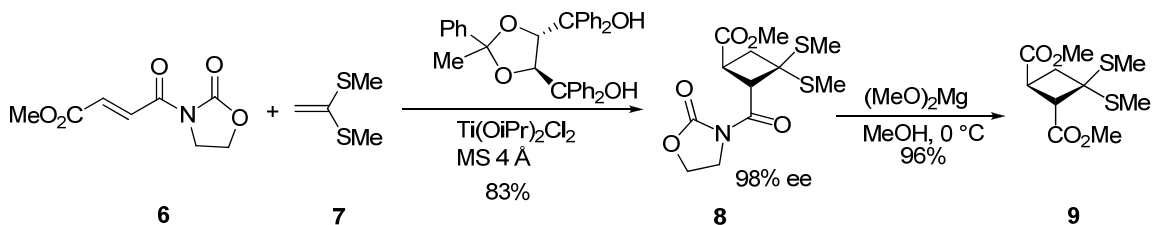
Scheme 1: Synthesis of 3,3-diethoxy-1,2-cyclobutanedicarboxylate using [2+2] cycloaddition

A Lewis acid catalyzed asymmetric [2+2] cycloaddition between ketene diethylacetal **1** and chiral dimethyl fumarate **4** provided the cyclobutyl product **5a** in high yield (Scheme 2). A diastereomeric excess of >99:1 was obtained following recrystallization.⁴²



Scheme 2: Diastereoselective [2+2] cycloaddition using chiral substrate

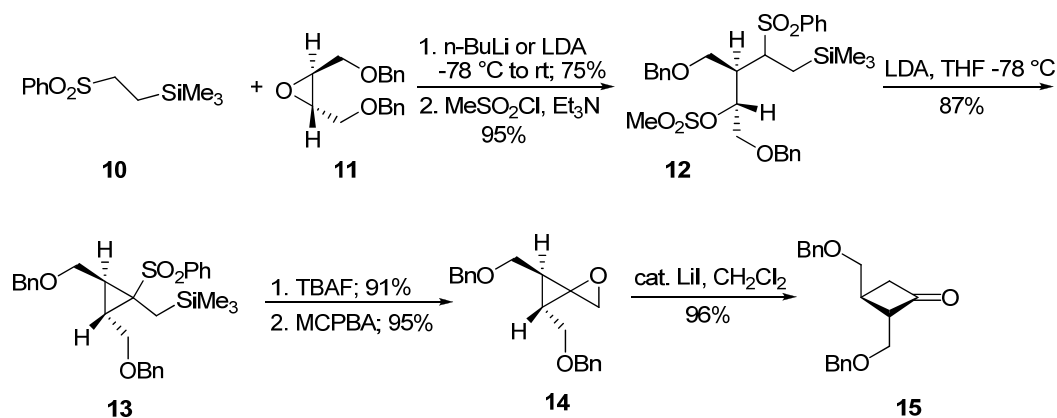
A [2+2] cycloaddition performed with oxazolidinone **6** and methylthioethylene **7** produced cyclobutane **8** in 83% yield and greater than 98% ee (Scheme 3).⁴³ The reaction was conducted with a catalytic amount of chiral titanium Lewis acid.



Scheme 3: Asymmetric [2+2] cycloaddition mediated by chiral Lewis acid

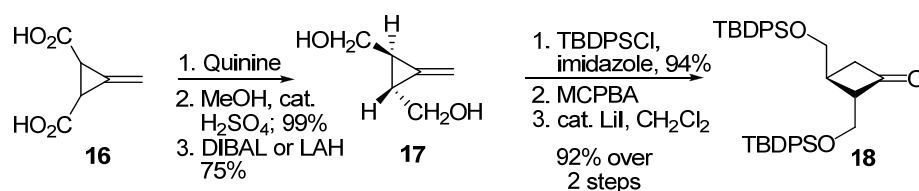
Abbott labs released the synthesis of the chiral cyclobutanone **15** through an oxaspiropentane rearrangement (Scheme 4).⁴⁴ Treatment of symmetric epoxide **11** with sulfonyl **10** afforded **12**. Deprotonation with LDA followed by cyclization gives **13**. An elimination induced by TBAF provides the cyclopropyl

alkene, which is epoxidized to form **14**. Rearrangement of the oxaspiropentane results in cyclobutanone **15**.



Scheme 4: Rearrangement of oxaspiropentane to cyclobutanone

This strategy was modified by the Abbott group using Feist's acid **16** as the starting material (Scheme 5).⁴⁴ Resolution of the racemic acid as its quinine salt followed by treatment with methanol in acid and diester reduction provided **17**. Protection of the alcohols and epoxidation affords a compound (not shown) similar to **14** from the first approach. Rearrangement of the oxaspiropentane provides cyclobutanone **18**.

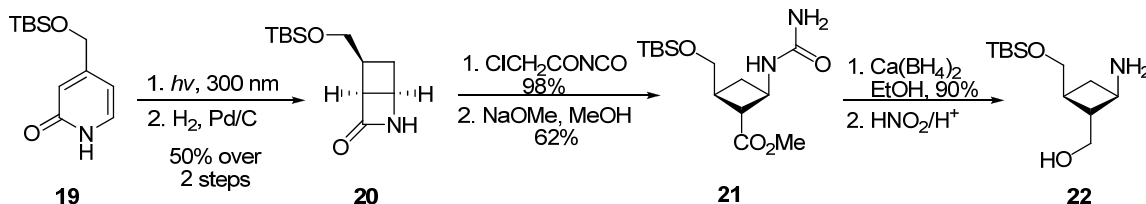


Scheme 5: Second generation synthesis of oxaspiropentane

Cyclobutamine Derivatives

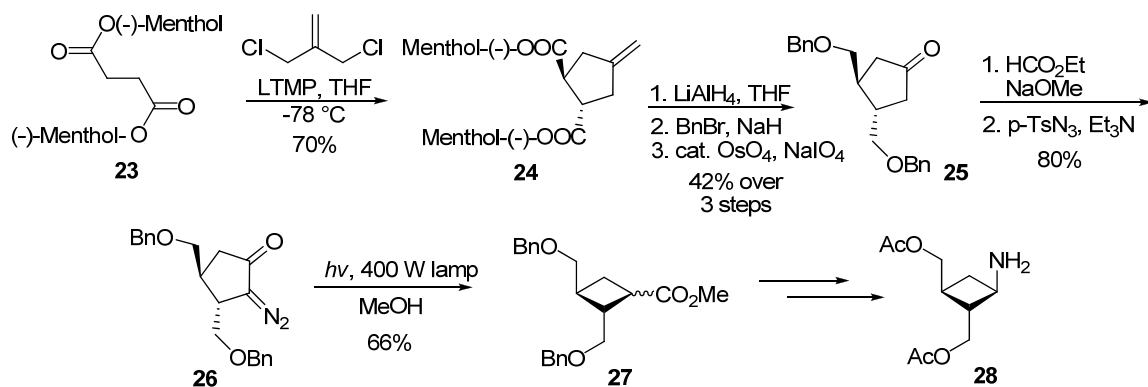
Another commonly employed cyclobutyl nucleoside building block is the cyclobutamine. Direct routes of synthesizing this intermediate are listed below.

In a method described by Katagiri, the substituted pyridone **19** was converted into bicyclic compound **20** through photolysis and catalytic hydrogenation at the less hindered exo side (Scheme 6).⁴⁵ Ring opening of the N-chloroacetylcarbamoyl derivative produced compound **21**. Reduction using calcium borohydride and treatment with acid afforded the free amine **22**. It should be noted that both **21** and **22** are useful intermediates in the synthesis of cyclobutyl nucleosides.



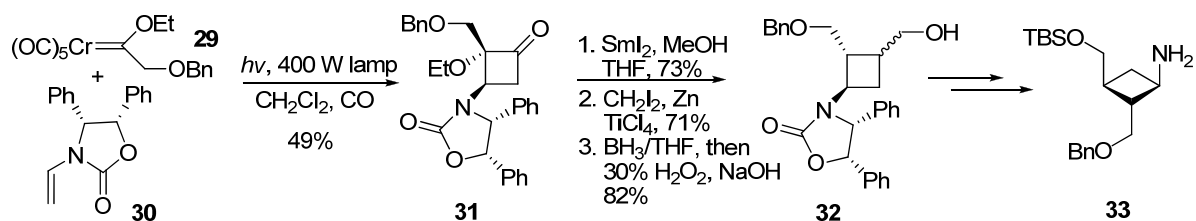
Scheme 6: Synthesis of cyclobutamine through pyridone photolysis

An enantioselective synthesis of cyclobutamine **28** has been developed that employs an asymmetric [2+3] formation of cyclopentane ring **24** from (-)-dimethyl succinate **23** and 3-chloro-2-(chloromethyl)-1-propene (Scheme 7).⁴⁶ A series of transformations provided diazocyclopentanone **26**, which then underwent a Wolff rearrangement to provide **27**. Further transformations, including a Curtius rearrangement of an acylazide to the isocyanate, provided the desired cyclobutamine **28**.



Scheme 7: Enantioselective cyclobutamine synthesis through asymmetric [2+3] cycloaddition

The Hegedus group reported the synthesis of the cyclobutamine **33** through the photolysis of chromium carbene complex **29** and reaction with ene-carbamate **30** (Scheme 8).⁴⁷ This reaction proceeded in six days and 49% yield. The cyclobutanone **31** was deoxygenated with inversion of stereochemistry, methylenated, and converted into the primary alcohol through hydroboration. Subsequent transformations provided amine **33**.

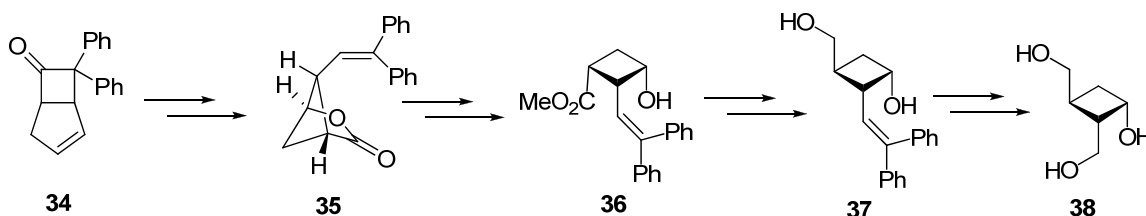


Scheme 8: Synthesis of cyclobutamine through photolysis of chromium carbene complex

Cyclobutanol Derivatives

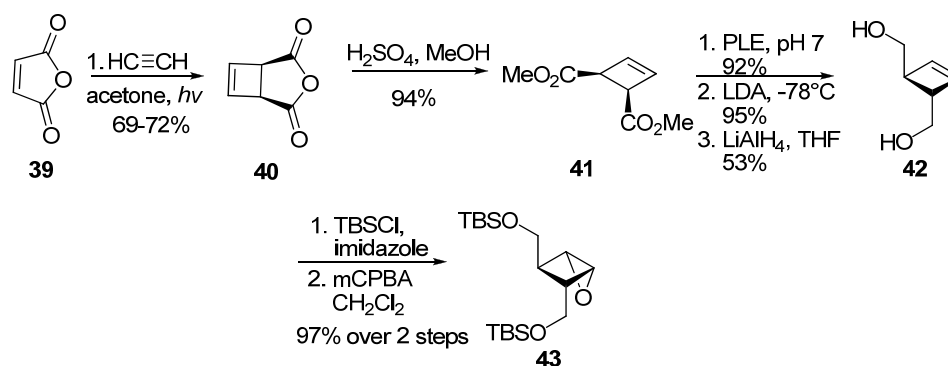
Cyclobutanol intermediates have been used extensively in the synthesis of cyclobutyl derivatives. Selected methods of synthesizing the cyclobutanol are described.

Roberts reported the synthesis of cyclobutanol derivative **38** using a chemoenzymatic method (Scheme 9).⁴⁸ Compound **34**, synthesized through the cycloaddition of cyclopentadiene and diphenylketene, was treated with NBS to provide isomeric bromohydrins (which were easily separated). Enzymatic resolution and photolysis provided compound **35**. Methanolysis of **35** and subsequent transformations provided the cyclobutanol **38**.



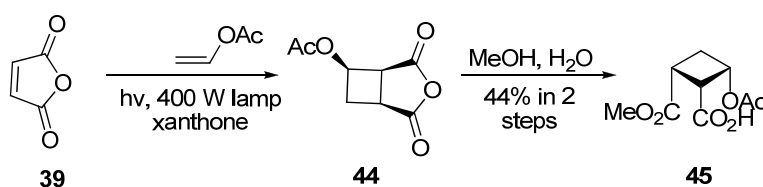
Scheme 9: Chemoenzymatic synthesis of cyclobutanol

Jung reported the synthesis of epoxide **43** as an intermediate in the synthesis of cyclobutyl analogues (Scheme 10).⁴⁹ The photocycloaddition of maleic anhydride **39** and acetylene resulted in compound **40**. Anhydride opening with acid and methanol afforded compound **41**, which was enzymatically hydrolyzed. Isomerization to create the trans-monoester and reduction produced the diol **42**. Epoxidation provided compound **43**, which provides an intermediate that can be directly glycosylated with nucleoside bases.



Scheme 10: Synthesis of cyclobutyl epoxide through enantioselective enzymatic hydrolysis

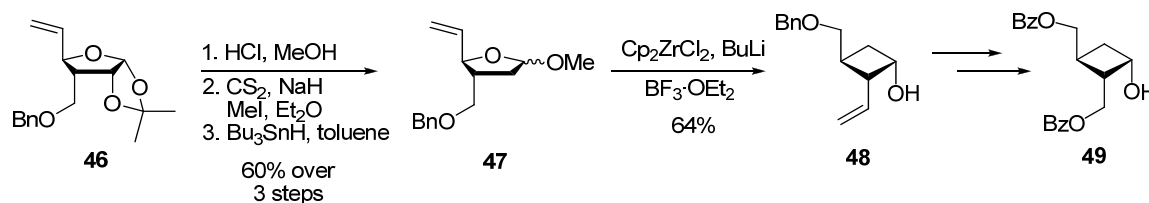
A facile method of synthesizing cyclobutyl nucleosides through photoirradiation was reported by Somekawa (Scheme 11).⁵⁰ The photoaddition of maleic anhydride **39** with vinyl acetate followed by treatment with methanol produced the all *cis*-methyl ester **45**.



Scheme 11: Synthesis of cyclobutanol derivative through photoirradiation

Taguchi synthesized the cyclobutanol intermediate **49** through a ring-contraction method.⁵¹ It was found that treatment of vinylpyrano- or furano-side derivatives could be converted into *cis*-vinylcyclopentanol or *cis*-vinylcyclobutanol derivatives using zirconocene equivalents. The reaction proceeds stereoselectively through a chair-like transition state with the *Z*-allylic zirconium species. In this particular synthesis, furanose derivative **46** was converted into vinyl furanoside **47**. The zirconium-mediated ring contraction was then

performed to give **48**, which was transformed into compound **49** through ozonolysis and aldehyde reduction.



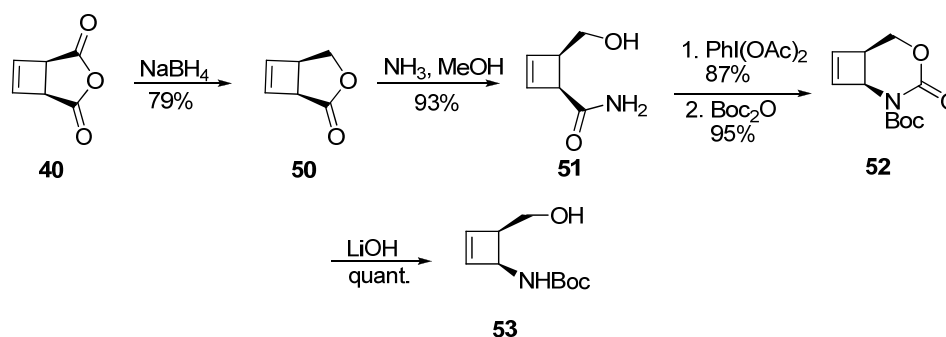
Scheme 12: Cyclobutanol synthesis through zirconium-mediated ring contraction

1.3.3 Synthesis of Modified Cyclobutanes as Intermediates for Nucleoside Reverse Transcriptase Inhibitors

The presence of the 3'-hydroxyl group in the above described nucleosides allows them to be phosphorylated by cellular kinases. The 2'-hydroxyl motif enables their incorporation into growing strands of DNA. In order to develop potential nucleoside reverse transcriptase inhibitors, it is necessary to exclude the 2'-hydroxyl group. This will allow the analogues to be incorporated into the DNA chain as the final nucleotide, as elongation will be terminated due to the missing linker group. This section describes the synthesis of cyclobutyl rings for analogues that are able to function as NRTIs through the exclusion of the 2'-hydroxyl group.

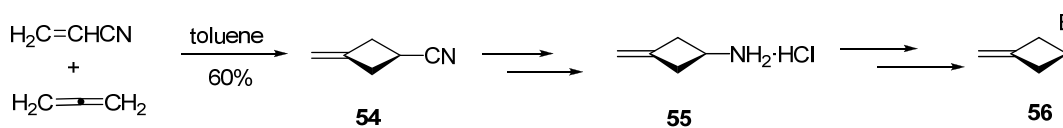
Norcarbovir analogues, the cyclobutyl derivatives of carbovir, were synthesized according to the following procedure.⁵² The photoaddition product **40** of maleic anhydride and acetylene was reduced to the lactone and reacted with ammonia to create **51** (Scheme 13). A Hoffman rearrangement led to the cyclic carbamate, which was Boc protected to form **52**. Ring opening produced

compound **53**, which served as a cyclobutamine intermediate for nucleoside analogue synthesis.



Scheme 13: Cyclobutamine synthesis through Hoffman rearrangement

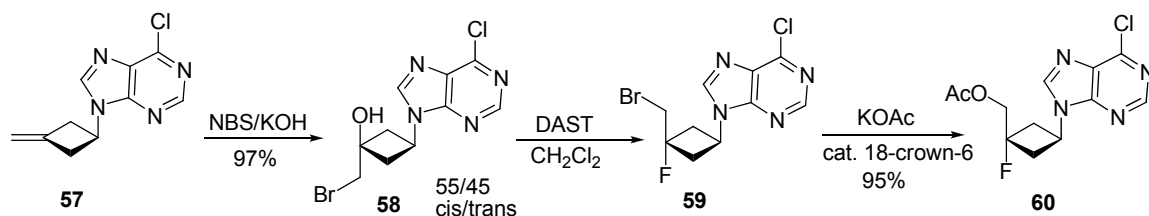
Legraverend and coworkers synthesized a number of cyclobutyl analogues that lack the 2'-hydroxyl group.⁵³ Each series of analogues employed the olefin cyclobutane **56**, which was then efficiently derivatized. The synthesis was initiated by a [2+2] cycloaddition between acrylonitrile and allene (Scheme 14).⁵⁴ Further transformations, including the introduction of the nucleoside base, gave intermediate **56**.



Scheme 14: Synthesis of olefin cyclobutane intermediate

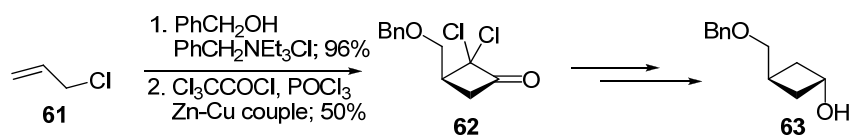
Intermediate **56** was then converted into different 3'-substituted derivatives, including 3'-fluoro-3'-(hydroxymethyl)cyclobutyl, 3'-hydroxy-3'-(phosphonomethyl)cyclobutyl, and 3'-fluoro-3'-(phosphonomethyl)cyclobutyl compounds. Scheme **15** displays the synthesis of the 3'-fluoro-3'-

(acetoxymethyl)cyclobutane moiety. Treatment of the 6-chloropurine olefin cyclobutane with NBS and KOH resulted in a mixture of the cis/trans bromohydrins. Treatment of the **58** with DAST resulted in fluorination with an inversion of configuration to give **59**. This intermediate was acetylated to afford compound **60**, which was converted into both the adenylyl and hypoxanthyl derivatives.



Scheme 15: Synthesis of 3'-fluoro-3'-(acetoxymethyl)cyclobutane derivative

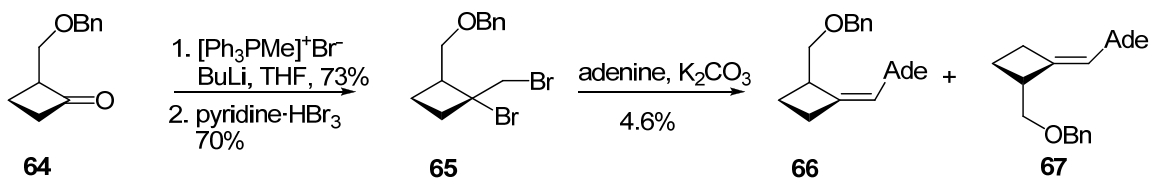
In 1995, the Reese group described the synthesis of cyclobutyl nucleoside derivatives through the *trans*-cyclobutanol **63**.⁵⁵ Allyl chloride was converted into allyl benzyl ether in high yield, and then underwent a [2+2] cycloaddition with trichloroacetyl chloride to form the dichloro species **62**. Further transformations rendered **63**, which was glycosylated with nucleoside bases.



Scheme 16: Synthesis of *trans*-3-(benzyloxymethyl)cyclobutanol

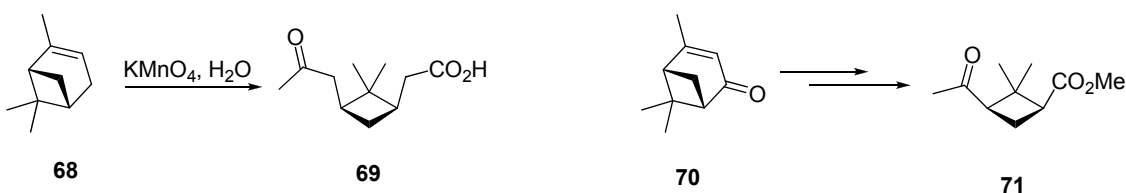
The synthesis of unsaturated nucleoside analogues was initiated with the [2+2] cycloaddition of ethyl acrylate and ketene dimethyl thioacetal.⁵⁶ Subsequent transformations produced compound **64**, which was methylenated

under Wittig conditions and brominated to form **65** (Scheme 17). Treatment with adenine and base yielded the *E*- and *Z*-methylenecyclobutane analogues **66** and **67** in low yield. The major products of this transformation were the *E/Z*-bromomethylenecyclobutanes, which resulted from HBr elimination.



Scheme 17: Synthesis of unsaturated nucleoside analogues

Enantioselective syntheses of these cyclobutyl compounds have also been developed through the use of chiral precursors, such as α -pinene **68**.⁵⁷ Conversion of α -pinene (both enantiomers have been used) into the *cis*-pinonic acid allows the synthesis of cyclobutamines of varying chain lengths.⁵⁸ Verbenone **70** has also been used as a chiral building block in the stereoselective synthesis of analogues.⁵⁹



Scheme 18: Pinene and verbenone as chiral building blocks for nucleoside analogues

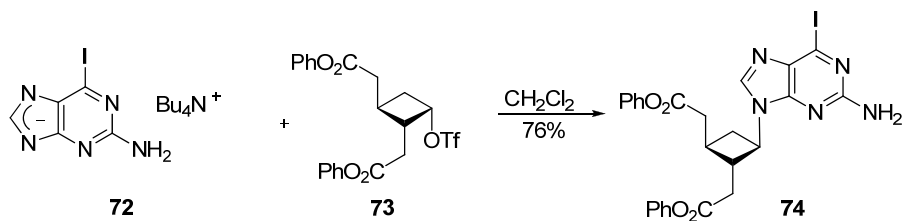
1.3.4 Methods of Synthesizing Carbocyclic Cyclobutyl Nucleoside Analogues

In the synthesis of nucleosides, glycosylation is typically accomplished using the Vorbruggen ribosylation method.⁶⁰ This method, however, is not applicable in the synthesis of carbocyclic nucleosides due to the replacement of the oxygen with a methylene group. Thus, alternative coupling methods have been employed and are described below.

Coupling of Intact Nucleoside Bases

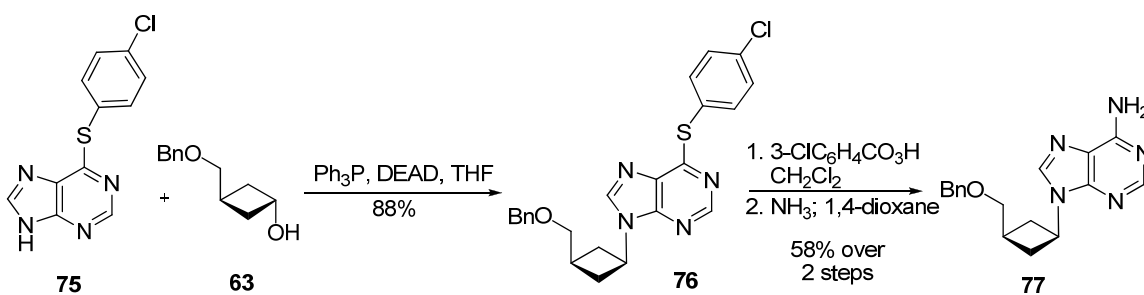
An intact nucleoside base can be directly coupled to the carbocyclic cyclobutane through a variety of methods. These methods include substitution of activated cyclobutanols, opening of epoxides, and the Michael addition.

Cyclobutanols can be activated for displacement through conversion into the mesylate, tosylate, or other suitable leaving groups. Through an S_N2 mechanism, the nucleoside base can be introduced while inverting the affected stereocenter. In the example shown in Scheme 19, the 2-amino-6-iodopurine tetraalkylammonium salt **72** is coupled to the cyclobutyl ring **73** through displacement of the triflate.⁶¹ This method is reported to regioselectively produce the desired N9 coupled product **74** over the N7 product. In addition, no elimination was observed.



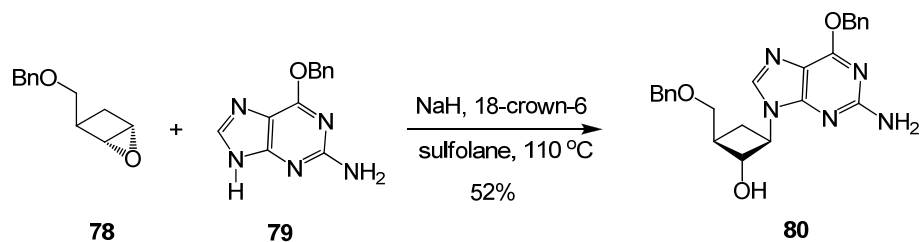
Scheme 19: Coupling of tetrabutylammonium salt of purine to triflate

Because elimination is a typical problem experienced in these reactions that are often performed under harsh conditions, an alternative method using a Mitsunobu coupling has been used.⁶² The reaction was employed in the synthesis of a cyclobutyl adenine analogue reported by Reese.⁵⁵ The coupling between *trans*-3-(benzyloxymethyl)cyclobutanol **63** and the substituted adenine **75** was accomplished in high yield.



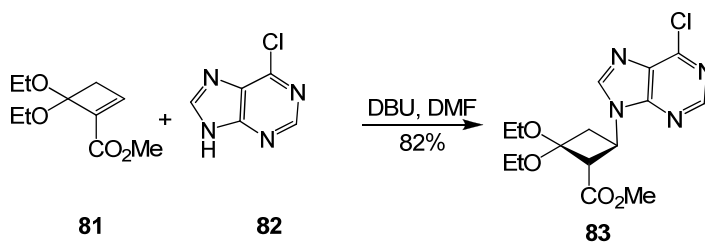
Scheme 20: Mitsunobu coupling between *trans*-3-(benzyloxymethyl)cyclobutanol and substituted adenine

Ring openings of epoxides are another method of introducing nucleoside bases. This strategy provides the coupled product with an inversion of stereochemistry at the affected center. However, nucleophilic attack on the epoxide can occur at both carbon centers of the epoxide. Thus, efforts to control the regioselectivity have been explored. One such method was described in the synthesis of a guanine cyclobutyl product **80** (Scheme 21).⁶³ It was anticipated that nucleophilic attack at the position alpha to the benzyloxymethyl group would be hindered due to steric interaction. Thus, attack should occur preferentially at the beta position. This was indeed the outcome, as the beta coupled product **80** was obtained in 52% yield, while only 5% of the alpha product was isolated.



Scheme 21: Regioselective coupling between purine and epoxide

The Michael addition has also been employed in the coupling of nucleoside bases. The addition of 6-chloropurine **82** to methyl 4,4-diethoxycyclobut-1-ene-1-carboxylate **81** produced mainly the *trans* N-9 adduct **83**.⁶⁴ Only a trace amount of the *cis* isomer was isolated.



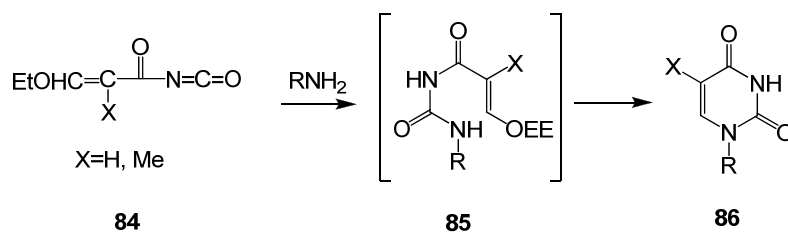
Scheme 22: Michael addition between 6-chloropurine **82** and methyl 4,4-diethoxycyclobut-1-ene-1-carboxylate **81**

Construction of nucleoside carbocycles through precursors

The use of cyclobutamines as intermediates in the synthesis of nucleoside analogues allows the stepwise construction of the nucleoside base. Methods for constructing both purine and pyrimidine bases have been established, with the most common method for each detailed below.

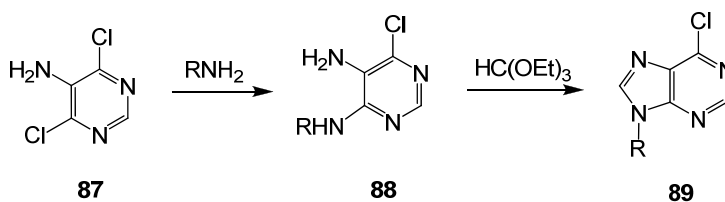
Pyrimidines are most often synthesized according to the Shaw and Warrenner method.⁶⁵⁻⁶⁸ The reaction of isocyanate **84** with an amine results in the

acryloylurea intermediate **85** (Scheme 23). Cyclization under acidic or basic conditions provides uracil or thymine **86**.⁶⁹



Scheme 23: Construction of pyrimidine bases

Purines have been synthesized through the reaction of 5-amino-4,6-dichloropyrimidine **87** and an amine (Scheme 24).⁷⁰ Ring closure is then induced using triethyl orthoformate to form the 6-chloropurine derivative **89**. The 6-chloropurine nucleobase can be easily derivatized into the adenine or hypoxanthine analogues through treatment with ammonia or hydroxide.



Scheme 24: Construction of purine bases

1.3.5 Methods of Synthesizing Nucleoside Triphosphates

Nucleoside triphosphates are often used in research as tools for understanding biological pathways. However, synthesizing these compounds is often challenging. This is in part due to the differing nature of the substrate and reagents. It is necessary to use conditions that will cater to both the lipophilic substrate as well as the charged ionic reagents. They are also inherently

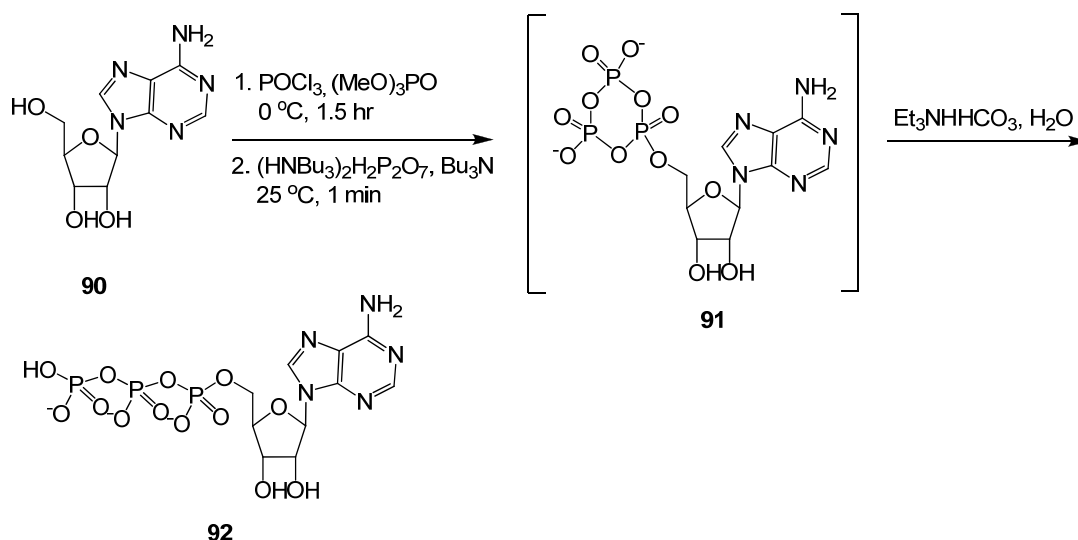
unstable, and are reported to decompose over a few days even at low temperature. The hydrolysis of the triphosphate is accelerated under both acidic and basic conditions.⁷¹ It has been revealed, however, that under certain conditions (neutral pH, low temperatures) the trialkylammonium triphosphate salts can be stable for extended periods.

Several methods have been developed to synthesize these compounds. None, however, provide a universal procedure for the conversion of all substrates into their triphosphate forms in high yield.⁷² The most common and useful methods that have been developed are described herein.

Triphosphate synthesis using dichlorophosphates

The most widely used method of synthesizing nucleoside triphosphates involves the nucleophilic attack of pyrophosphate on an activated monophosphate. In this method, only the activated nucleoside monophosphate needs to be prepared, as the pyrophosphate salts are commercially available. One of the most utilized methods for monophosphate synthesis was initially discovered by Yoshikawa, who discovered that the rate of phosphorylation was accelerated through trialkylphosphate solvents.⁷³ These solvents have the capability of dissolving both the nucleoside and the reagents to give homogeneous solutions. An attractive component of this method is that isolation of the monophosphate is not necessary in the synthesis of triphosphates. Instead, the chlorophosphate intermediate can be reacted directly with the

pyrophosphate salts, as demonstrated by Ludwig, to provide a one-pot, three-step method of triphosphorylation (Scheme 25).⁷⁴



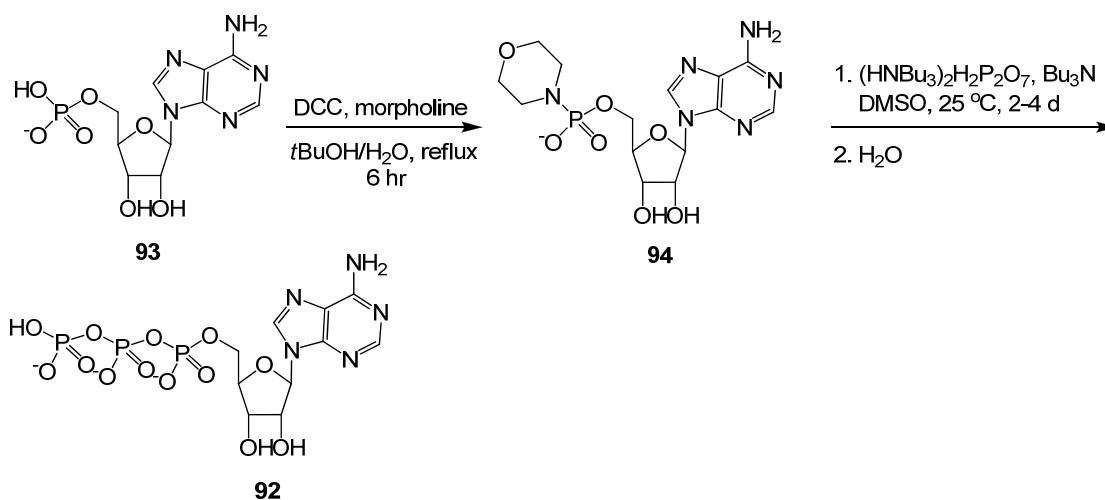
Scheme 25: Yoshikawa/Ludwig “one-pot, three-step” triphosphate synthesis

Triphosphate synthesis using phosphoramidates

The synthesis of triphosphates using nucleoside phosphoramidates is similar to the above method as it also involves the nucleophilic attack of pyrophosphate on an activated monophosphate. In this method, the nucleoside monophosphates are isolated prior to further phosphorylation. Thus, it addresses the problem of determining the efficiency of monophosphorylation in one-pot methods.

Initial studies performed to activate nucleoside monophosphates involved the use of DCC in pyridine. However, it was noted that substantial amounts of the undesired mono-, di-, and inorganic polyphosphates were also generated.⁷⁵ This problem was solved with modifications developed by Moffatt (Scheme 26).⁷⁶ Moffatt employed amines with DCC to form an intermediate phosphoramidate **94**,

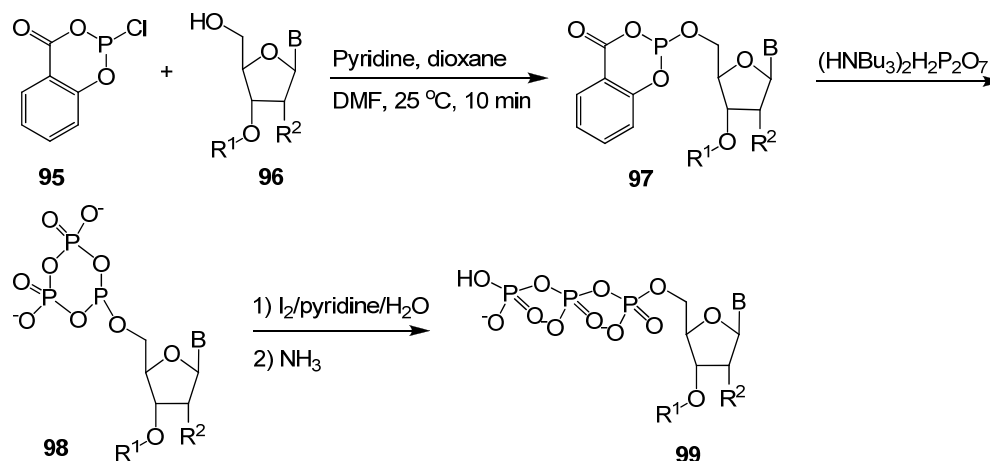
and also discontinued the use of pyridine as this promotes disproportionation of the triphosphates.



Scheme 26: Moffatt triphosphate synthesis using phosphoramidate intermediate

Triphosphate synthesis using activated phosphites

The Ludwig and Eckstein method for developing triphosphates through activated phosphite intermediates can be applied to a wide variety of nucleoside derivatives.⁷⁷ The general nucleoside analogue **96** was reacted with 2-chloro-4*H*-1, 3, 2-benzodioxaphosphorin-4-one **95** to form activated phosphite **97**. The phosphite was then reacted with pyrophosphate to form cyclic intermediate **98**. Hydrolysis and oxidation provided triphosphate **99**.



Scheme 27: Ludwig/Eckstein triphosphate synthesis using activated phosphite

1.3.6 Synthesis and anti-HIV activity of 3'-hydroxymethyl cyclobutyl nucleosides

The synthesis of 9-[*cis*-3-(hydroxymethyl)cyclobutyl]-adenine **100** and guanine **101** was reported by Reese and co-workers (Figure 13).⁵⁵ They later reported the synthesis of the pyrimidine analogues: 1-[*cis*-3-(hydroxymethyl)cyclobutyl]-uracil **102**, -cytosine **103** and -thymine **104** (Figure 14).⁷⁸

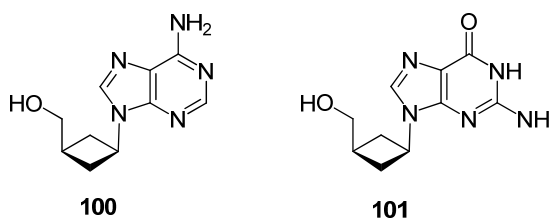


Figure 13: Purine cyclobutyl analogues synthesized by Reese

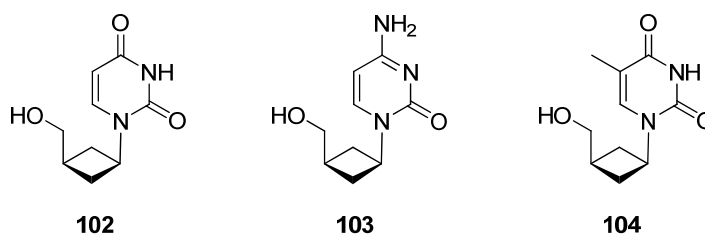
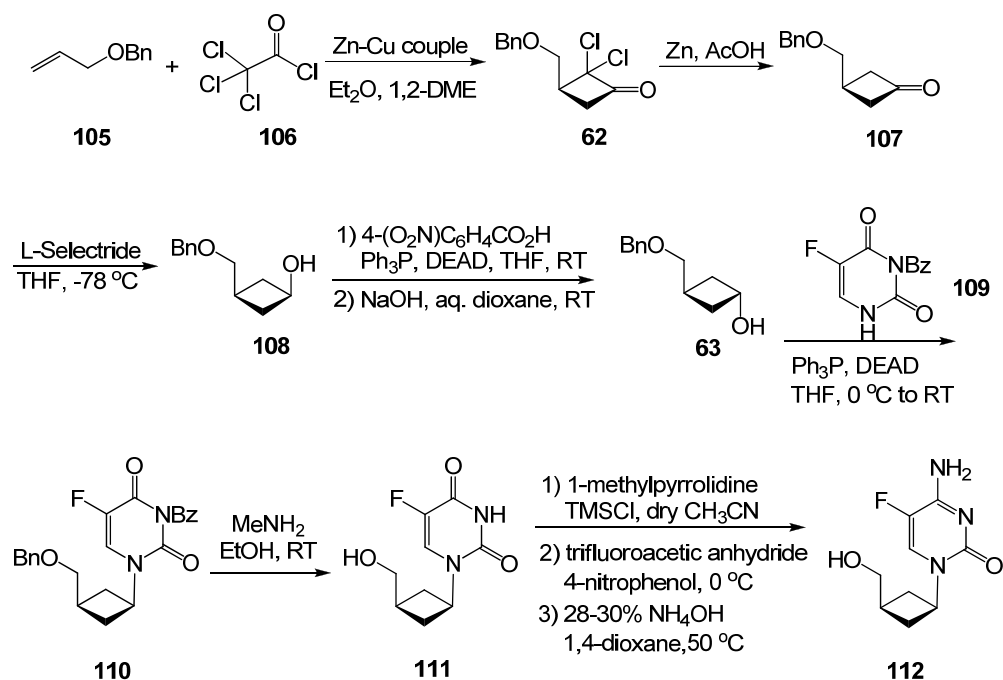


Figure 14: Pyrimidine cyclobutyl analogues synthesized by Reese

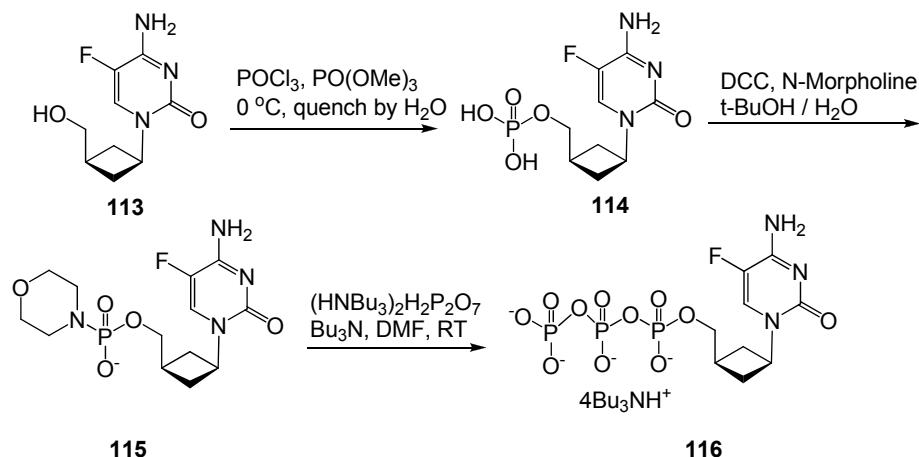
It was reported that the adenine analogue **100** showed anti-HIV activity of 0.8 μM and no toxicity up to 1000 μM .⁵⁵ The guanine analogue **101** displayed anti-HIV activity of 8 μM and no toxicity up to 1000 μM . None of the pyrimidine analogues displayed any HIV activity or toxicity.⁷⁸

In the Liotta group, 5-fluoro-1-[*cis*-3-(hydroxymethyl)-cyclobutyl]-cytosine **112** was synthesized according to the Reese procedure.⁷⁹ The synthesis featured a cycloaddition reaction between dichloroketene and allyl benzyl ether **105** to construct the cyclobutyl ring (Scheme 28). A Mitsunobu coupling was performed between the *trans*-cyclobutanol **63** and the nucleoside base **109** to form the coupled product **110**. Subsequent transformations converted the 5-fluorouracil analogue into the 5-fluorocytosine analogue **112**.



Scheme 28: Synthesis of 5-fluoro-1-[*cis*-3-(hydroxymethyl)cyclobutyl] cytosine **112**

The 5-fluorocytosine analogue **112** was evaluated for anti-HIV activity. Although the analogue was found to be non-toxic, it proved to be inactive up to 100 μM in primary human lymphocytes infected with HIV-1.⁵ Thus, the triphosphate of **112** was synthesized and tested in efforts of elucidating the mechanism of nucleotide incorporation into the viral DNA chain. The triphosphate **116** was prepared according to the procedure by Moffatt using the activated morpholine intermediate **115**.⁷⁶



Scheme 29: Synthesis of 5-fluoro-1-[*cis*-3-(hydroxymethyl)cyclobutyl] cytosine triphosphate **116**

The triphosphate **116** displayed anti-HIV activity comparable to 3TC-TP against recombinant HIV-RT ($\text{IC}_{50} = 4.7\ \mu\text{M}$) and wild-type HIV-RT ($\text{IC}_{50} = 6.9\ \mu\text{M}$). In addition, the triphosphate exhibited high activity against M184I ($\text{IC}_{50} = 6.1\ \mu\text{M}$) and M184V ($\text{IC}_{50} = 6.9\ \mu\text{M}$) mutant RT enzymes (Table 1).

HIV-RT	Inhibition of RT Activity (IC_{50} , μM)			
	3TC-TP		DLS183-TP	
Recombinant HIV RT (WT)	2.99	0.7	4.74	0.34
HIV RT (WT)	6.53	1.46	6.85	1.79
HIV RT (M/I)	>10		6.06	0.75
HIV RT (M/V)	>10		6.91	1.50

All the HIV RT used, except the recombinant RT, was obtained from viral lysates from PBM cells infected with respective HIV.

Table 1: Comparison of inhibition of HIV-RT in cell-free assays

These results suggest that the cyclobutyl nucleotide can be incorporated into the DNA chains of HIV-RT wild type and M184V/I mutants to terminate DNA elongation. Thus, the inactivity of nucleoside **113** is likely to be the result of not

being phosphorylated by cellular kinases. The cellular kinases may not recognize the cyclobutyl nucleoside analogues due to structural and conformational differences from the natural nucleoside substrates.⁵

1.4 Results and Discussion

1.4.1 Design and Synthesis of Purine Cyclobutyl Nucleosides

Preliminary data performed by the Liotta group (as described in section 1.3.6) revealed that the 5'-fluorocytosine cyclobutyl triphosphate analogue **116** is able to be incorporated into viral DNA. This, along with the fact that none of the cyclobutyl nucleosides exhibited toxicity, deems this series worthy of further exploration. Though Reese synthesized and tested the cyclobutyl adenine **100**, guanine **101**, uracil **102**, cytosine **103**, and thymine **104** analogues for anti-HIV activity, the identities of the cell lines used were not revealed.^{55,78}

Though the pyrimidine derivatives were all inactive in these unknown cell lines, the purine analogues were reported as moderately active in their free nucleoside forms. In order to determine if these purine analogues are able to act as NRTIs and to also gauge the degree of their activity in comparison to current anti-HIV therapeutics, it is necessary to synthesize these and other compounds. Thus, the goal of this project became to synthesize several purine analogues (Figure 15) and assess their anti-HIV activity in known assays.

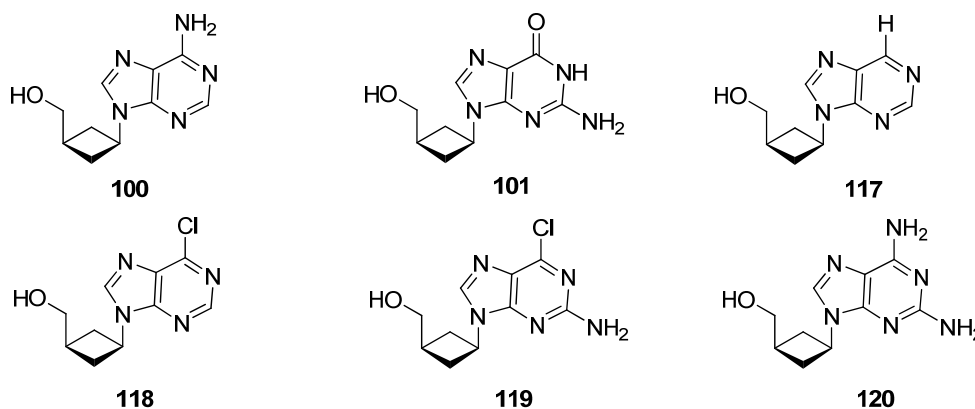
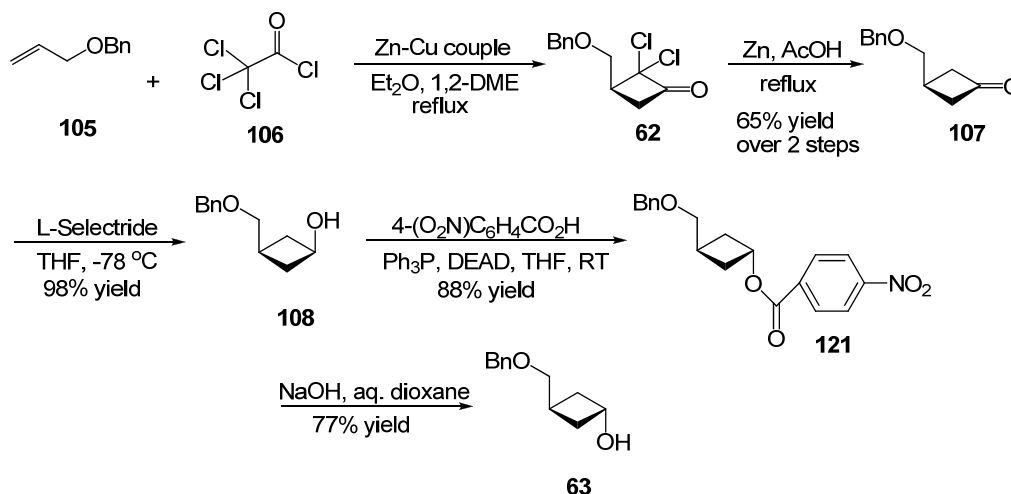


Figure 15: Purine cyclobutyl nucleoside targets

Synthesis of *trans*-3-(benzyloxymethyl)cyclobutanol (**63**)

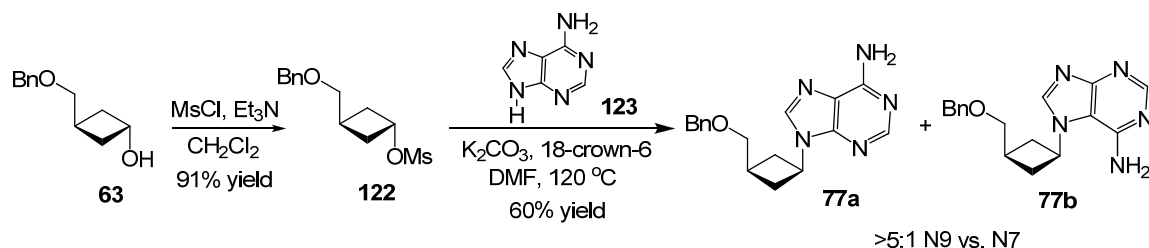
Each of the analogues shown in Figure 15 were derived from a common source - *trans*-3-(benzyloxymethyl)cyclobutanol **63**. This compound was synthesized using the method described by Reese (Scheme 30).^{55,78} The reaction of allyl benzyl ether **105** and the dichloroketene (generated *in situ* from trichloroacetyl chloride **106** and activated zinc) afforded the [2 + 2] cycloaddition product **62**. Compound **62** was then dechlorinated to give 3-(benzyloxymethyl)cyclobutanone **107** in 65% yield over two steps. The cyclobutanone was then reduced with L-Selectride to provide a mixture of alcohols in a 20:1 ratio favoring the *cis*-cyclobutanol **108**. A Mitsunobu inversion afforded the *trans* alcohol **63**, which will serve as an intermediate in the synthesis of each of the cyclobutyl purine nucleosides in Figure 15.



Scheme 30: Synthesis of *trans*-3-(benzyloxymethyl)cyclobutanol **63**

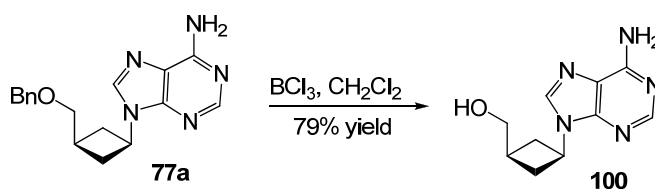
Synthesis of 9-[*cis*-3-(hydroxymethyl)cyclobutyl]adenine (**100**)

A displacement of an activated cyclobutanol was performed in the synthesis of the cyclobutyl adenine compound. Mesylate **122** was prepared from cyclobutanol **63**, and was then coupled with adenine **123** in the presence of base. The N9 coupled product **77a** was produced selectively over the N7 product **77b** in a 5:1 ratio (Scheme 31).



Scheme 31: Synthesis of 9-[*cis*-3-(benzyloxymethyl)cyclobutyl]adenine **77a**

Attempts to deprotect **77a** using hydrogenolysis failed. However, the use of Lewis acids (both BCl_3 and AlCl_3) provided the desired compound **100** (Scheme 31).

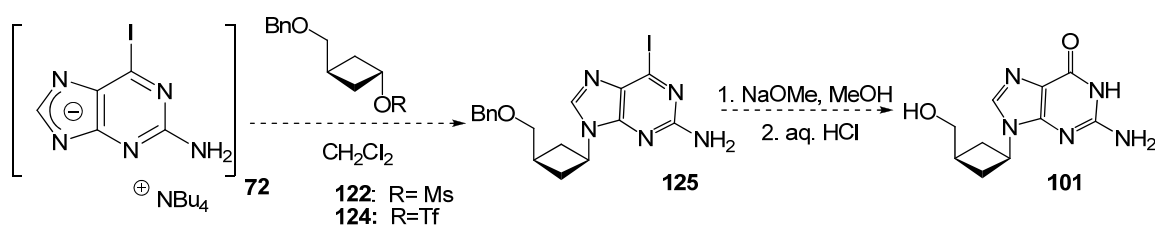


Scheme 32: Deprotection of 9-[*cis*-3-(benzyloxymethyl)cyclobutyl]adenine **77a**

Synthesis of 9-[*cis*-3-(hydroxymethyl)cyclobutyl]guanine (**101**)

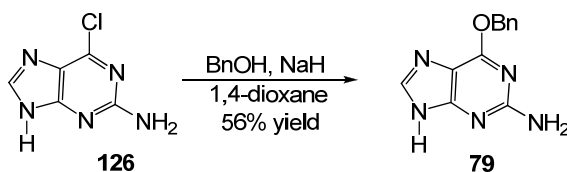
Synthesis of the guanine analogue **101** proved to be more challenging. Initially, a procedure described by Bissachi and coworkers was used in which the 2-amino-6-iodopurine tetrabutylammonium salt **72** would be coupled to mesylate

122 (Scheme 33).⁶¹ The group reported that the N9 product was formed selectively over the N7 product. This is in accordance with previous studies that proved that halogens attached to C6, especially the iodo group, promote regioselective N9 coupling.⁸⁰ Following this, treatment of coupled product **125** with sodium methoxide in methanol should afford the 6-methoxy product. Deprotection using acid would then form the desired product **101**. However, there was no product obtained from the mesylate coupling. The use of the triflate leaving group on the cyclobutyl ring also failed.



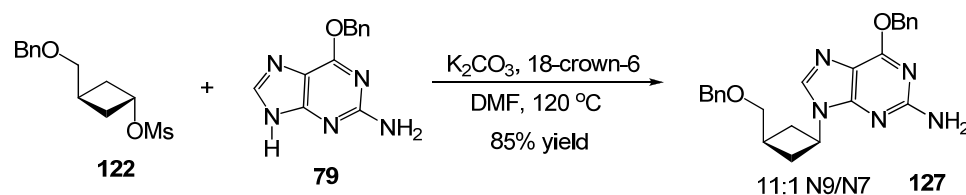
Scheme 33: Attempted guanine coupling via tetrabutylammonium salt

A method described by Slusarchyk and coworkers that used 6-benzyloxy-2-aminopurine **79**, successfully gave the guanine analogue **101**.⁴¹ The protected guanine nucleobase **79** was synthesized by treating commercially available 2-amino-6-chloropurine **126** with benzyl alcohol in the presence of sodium hydride (Scheme 34).



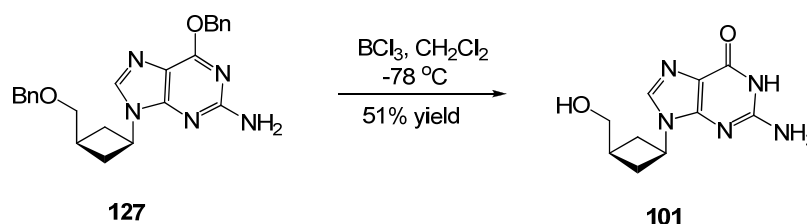
Scheme 34: Synthesis of O⁶-benzylguanine **79**

Treatment of O⁶-benzylguanine **79** with the cyclobutyl mesylate **122** produced a mixture of the N9 and N7 coupled product **127** in an 85% yield, with the N9 product formed selectively over the N7 product (Scheme 35). It should be noted that the 11:1 ratio of N9 to N7 product is significantly higher in this coupling than that of adenine (5:1 N9 to N7). This is due to the blocking effect that the bulky O-benzyl group presents. The regioisomers were separable.



Scheme 35: Coupling of *trans*-3-(benzyloxymethyl)cyclobutyl mesylate **122** and O⁶-benzylguanine **79**

Both benzyl groups were then removed using boron trichloride (Scheme 36). This afforded the final product **101** in 51% yield. Alternatively, the deprotection can be performed by single electron reduction with sodium in liquid ammonia at -78 °C, which affords the desired product in 34% yield. The product structure was verified by X-ray crystallography (Figure 16).



Scheme 36: Deprotection of 9-[*cis*-3-(benzyloxymethyl)cyclobutyl]O⁶-benzylguanine **127**

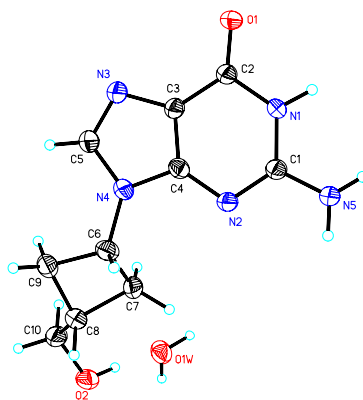
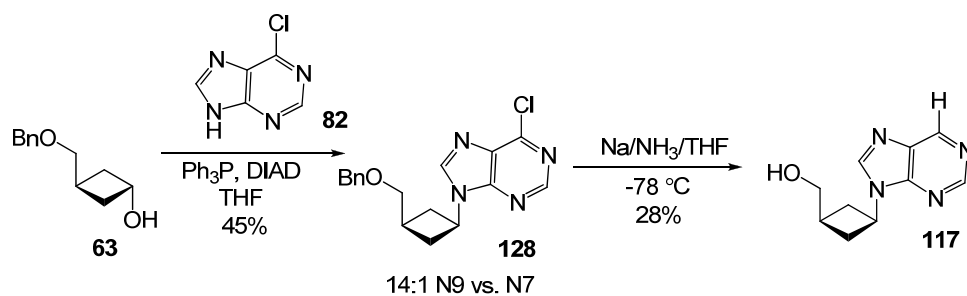


Figure 16: X-ray structure of 9-[*cis*-3-(hydroxymethyl)cyclobutyl]guanine **101**

Synthesis of 9-[*cis*-3-(hydroxymethyl)cyclobutyl]purine (**117**)

Additional purines, including the chloropurine nucleoside analogues were also synthesized in this series. Initially, the coupling of 6-chloropurine **82** with cyclobutyl mesylate **122** was attempted in the presence of K_2CO_3 . However, there was significant decomposition after heating at high temperatures (120 °C) and no product formation when heating at lower temperature (50 °C). Thus, the Mitsunobu reaction was employed (Scheme 37). This produced compound **128** in 45% yield and a 14:1 N9 vs. N7 ratio. Deprotection was accomplished using the single electron reduction method described previously. However, after analysis by 1H -NMR, it was suspected that the deprotection reaction may have caused dechlorination and subsequent protonation of C6 (indicated by an additional signal in the 1H -NMR spectrum at 8.9 ppm). This was confirmed by mass spectrometry and X-ray crystallography (Figure 17).



Scheme 37: Synthesis of purine analogue **117**

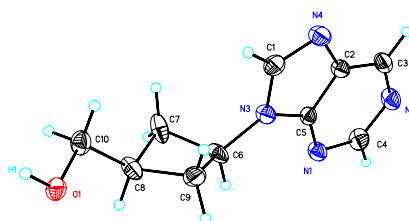
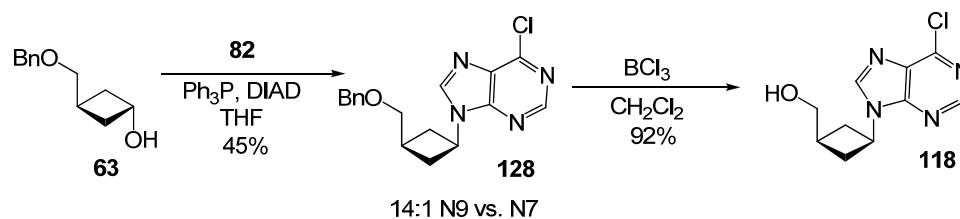


Figure 17: X-ray structure of 9-[*cis*-3-(hydroxymethyl)cyclobutyl]purine **117**

Synthesis of 9-[*cis*-3-(hydroxymethyl)cyclobutyl]-6-chloropurine (**118**)

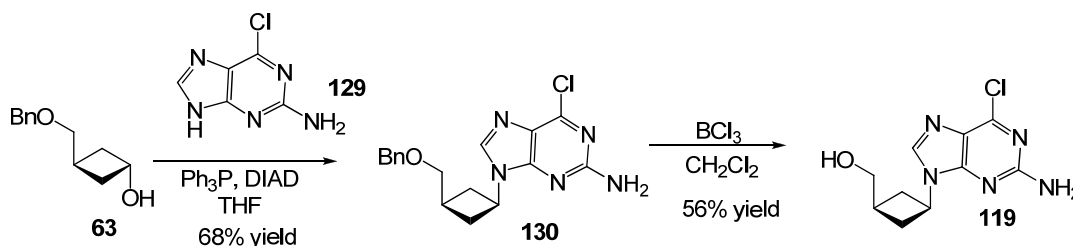
The deprotection of the 6-chloropurine analogue **128** was attempted again using the Lewis acid BCl_3 (Scheme 38). This successfully gave the deprotected product **118**.



Scheme 38: Synthesis of 6-chloropurine analogue **118**

Synthesis of 9-[*cis*-3-(hydroxymethyl)cyclobutyl]-2-amino-6-chloropurine (119)

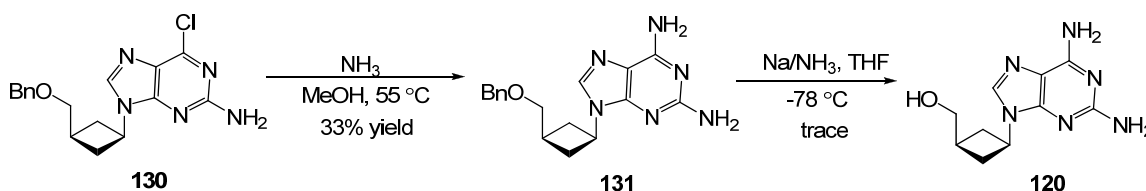
The 2-amino-6-chloropurine nucleobase **129** was coupled in a similar manner using Mitsunobu conditions (Scheme 39). Only N9 coupled product **130** was isolated. The deprotection was performed in a non-compromising method to the chlorine group with boron trichloride to provide the product in 56% yield.



Scheme 39: Synthesis of 2-amino-6-chloropurine analogue **119**

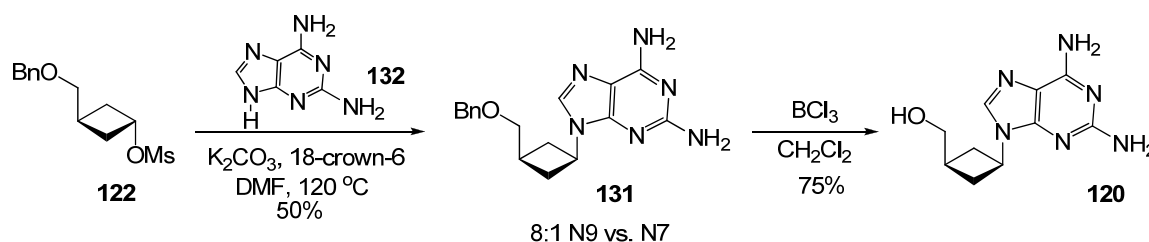
Synthesis of 9-[*cis*-3-(hydroxymethyl)cyclobutyl]-2,6-diaminopurine (120)

The diamino analogue **120** was synthesized by treating coupled product **130** with methanolic ammonia at 55 °C (Scheme 40). The 6-halo derivative was employed due to literature precedents describing regioselective N9 coupling with these compounds.^{61,80} After deprotection of **131** using sodium in ammonia, very little compound was obtained. In addition, it was difficult to separate the isolated product from impurities.



Scheme 40: Synthesis of 2,6-diamino analogue **120** using 2-amino-6-chloropurine precursor **130**

Thus, an alternative method that would efficiently provide the coupled product was sought. Mesylate **122** was directly coupled with commercially available 2,6-diaminopurine **132** by treatment with K_2CO_3 in DMF under refluxing conditions (Scheme 41). This coupling gave an 8:1 ratio of the N9 to N7 coupled product. The desired N9 coupled product **131** was isolated in 50% yield. Following this, compound **131** was deprotected using BCl_3 to give desired compound **120** in 75% yield.



Scheme 41: Synthesis of diamino analogue **120** by direct coupling of 2,6-diaminopurine

1.4.2 Design and Synthesis of Tricyclic Nucleobase Cyclobutyl Analogues

Studies performed by the Reese and Liotta groups have confirmed that the cyclobutyl purine nucleoside analogues are innately more active than the cyclobutyl pyrimidine analogues. Examination of these results in terms of steric reasoning suggests that the active site of HIV-RT may be better suited for larger bases. The extent of this theory was evaluated through the synthesis and anti-HIV activity testing of ring-expanded tricyclic bases (Figure 18). These analogues were chosen in particular due to their resemblances to adenine and guanine. This may aid in the recognition of these analogues by cellular kinases and promote cellular phosphorylation of the compounds.

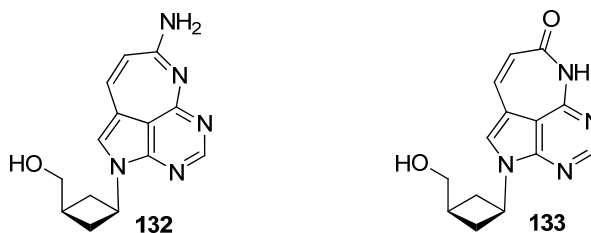


Figure 18: Expanded tricyclic nucleoside adenine **132** and guanine **133** analogues

Upon initial examination of these tricyclic nucleoside analogues, it may seem unreasonable to expect cellular kinases to recognize structures so dissimilar. However, the use of these tricyclic compounds in nucleoside analogues has literature precedence. Triciribine is a well studied tricyclic nucleoside that has exhibited potent activity against cancer and viral cells (Figure 19). Studies have shown that this compound is recognized by adenosine kinase and converted into its monophosphate.⁸¹ In fact, triciribine and its monophosphate have been involved in advanced clinical trials. Since then, several tricyclic bases have been coupled to modified sugars as potential treatments for viral infections and infectious diseases.⁸²⁻⁸⁴

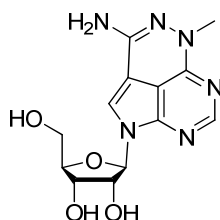
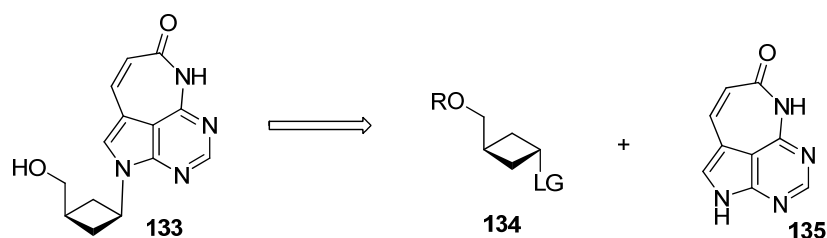


Figure 19: Structure of triciribine

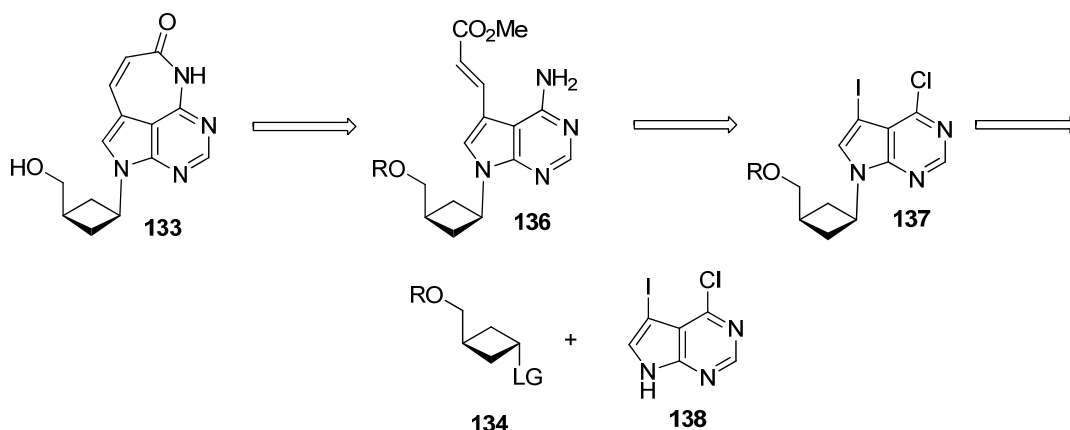
The synthesis of these compounds can be envisioned by two disconnection approaches: the late coupling and early coupling methods. The

late coupling method involves the synthesis of the intact expanded nucleobase and the subsequent coupling to the activated cyclobutanol (Scheme 42).



Scheme 42: Late coupling disconnection approach for synthesis of tricyclic nucleoside analogues

The early coupling method involves the coupling of a simple precursor of the expanded base to the cyclobutyl ring. The tricyclic base will then be built stepwise (Scheme 43). This was the method employed by the Biota corporation in the synthesis of their tricyclic analogues.⁸²



Scheme 43: Early coupling disconnection approach for synthesis of tricyclic nucleoside analogues

The late coupling method was chosen as the ideal strategy, as this method would allow the facile synthesis of a number of derivatives with different pseudosugars. Thus, the goal is to synthesize the intact expanded guanine and

adenine bases. Following this, the bases will be coupled to the cyclobutyl, oxathiolane, and dioxolane pseudosugars (Figure 20).

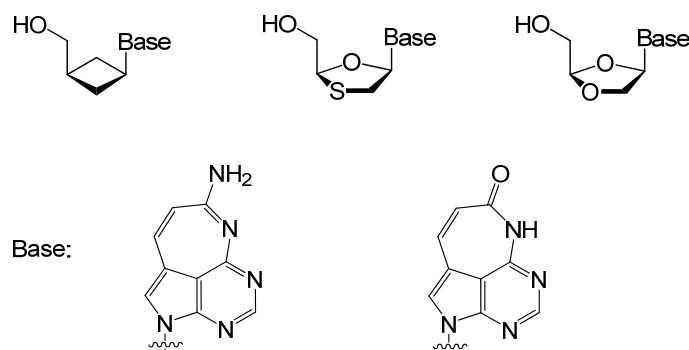
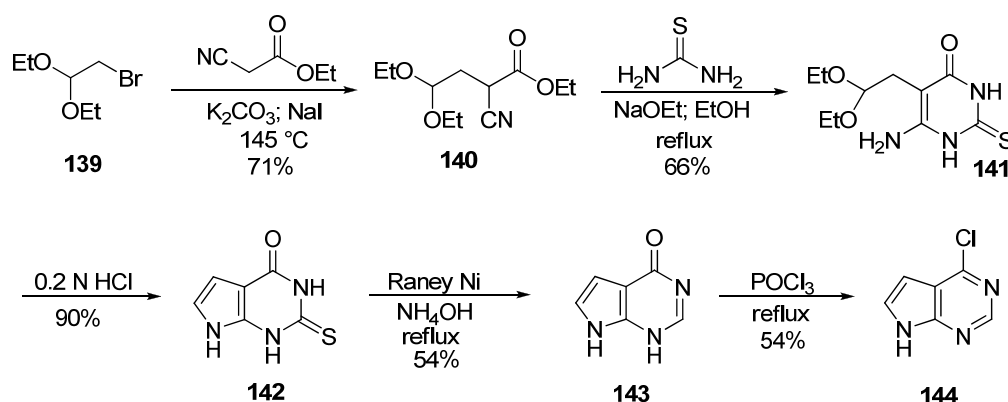


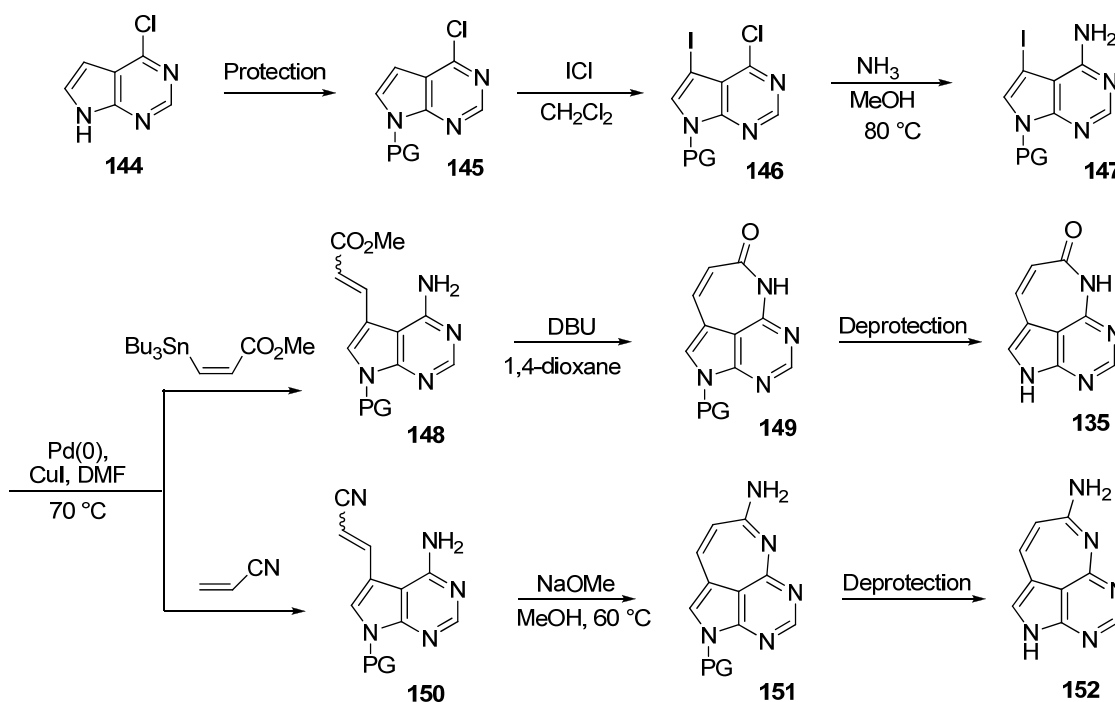
Figure 20: Structures of tricyclic nucleoside analogues

Both tricyclic nucleobases share a common 7-deazapurine precursor **144**, which was synthesized according to a literature procedure (Scheme 44).⁸⁵ Bromoacetal **139** and ethyl cyanoacetate were condensed to form the diethoxycyanoacetate **140**. This compound was then cyclized into the pyrimidine **141** using thiourea. Treatment of the cyclized base with acid formed the deazapurine **142**. Desulfurization was performed with Raney nickel to give intermediate **143**, which was then treated with POCl_3 to produce the 6-chloro-7-deazapurine **144**.



Scheme 44: Synthesis of 7-deazapurine backbone of expanded bases

The late coupling strategy involves the production of intact bases **135** and **152**. In order to synthesize these bases, it is necessary to protect the N9 position. Following this, iodination of the C7 position provides the 6-chloro-7-iodo-7-deazapurine **146**. Subsequent amination of the C6 position results in **147**, which is the final common intermediate for both expanded base derivatives. Cross-coupling with tributylstannyl methyl acrylate or acrylonitrile provides compounds **148** and **150**, respectively. Cyclization will then be induced using base, which forms the intact expanded adenine **149** and guanine **151** derivatives. Deprotection will afford the free expanded nucleobases, which can be coupled with the pseudosugars.



Scheme 45: General method of preparing intact expanded adenine **152** and guanine **135** nucleobases

Several protecting groups were employed in order to achieve the desired free expanded nucleobases. However, there were significant problems with most of these groups undergoing each proposed transformation. Among these was the inability to remove the protecting group in the final step, which was experienced when using the benzyl derivatives.

Benzyl derived protecting groups

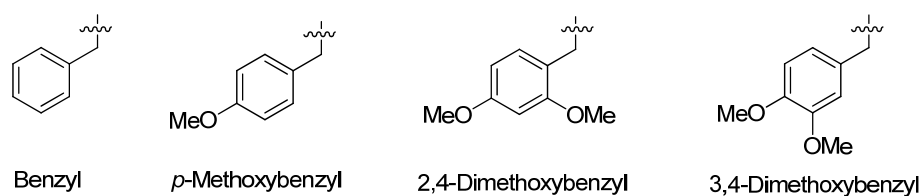
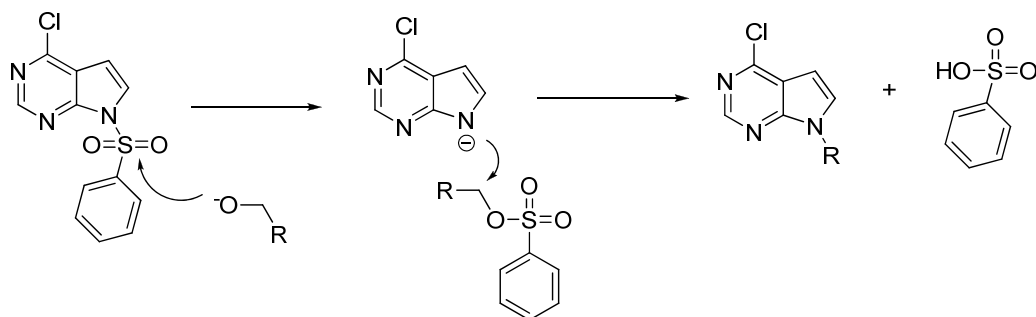


Figure 21: Benzyl protecting groups used for tricyclic base synthesis

The benzyl protecting group was employed initially, which was not able to be deprotected using Lewis acids. It did, however, allow an understanding of the nature of the 7-deazapurine system, which is dissimilar from the purine system. Instead, it behaves similarly to pyrroles, indoles, and related heterocycles. This was displayed with the intention of protecting the N9 position of the deazapurine using base and benzyl chloride. Instead of obtaining the expected product, a mixture of N9 and C7 alkylation was found. Poor N-alkylation vs. C-3 alkylation is a common problem experienced in pyrroles.⁸⁶ However, this problem has been solved through a transfer of activation method, in which the benzene sulfonyl group is used to regioselectively alkylate the N7 position.⁸⁷ This has been proposed to occur through a bimolecular reaction, in which a pre-formed

alkoxide attacks the sulfonamide to provide an alkyl sulfonate and the nitrogen anion. The nitrogen anion is then able to displace the sulfonate and become alkylated. This method has also been applied to the 7-deazapurine system, and produces the N9 benzylated derivative in 62% yield (Scheme 46).⁸⁸



Scheme 46: Eissenstat and Weaver transfer of activation mechanism⁸⁷

Though the problem of protecting the deazapurine was solved, the deprotection of benzylated **149** and **152** failed with all attempts. Thus, the *para*-methoxybenzyl group was substituted due to its extensive use as a nitrogen protecting group in many heterocyclic systems, including pyrazoles and imidazoles.⁸⁹ In addition, it can be removed under acidic, hydrogenolytic, and oxidative methods. However, none of these conditions proved effective in removing this group. The use of this group did, however, allow the development of alternative reaction conditions. Instead of using the low-yielding iodine monochloride reagent for the iodination step, NIS was used in its place. This increased the yield of the iodination reaction from 30 - 45% to 80 - 90%. Also, the amination step using ammonia in methanol was changed to ammonium hydroxide in 1,4-dioxane. This was done because the use of ammonia in

methanol often resulted in the C6-methoxy derivative instead of the expected aminated derivative. Thus, the ammonium hydroxide conditions were used instead, which reliably afforded the desired product in high yields.

Because the electron donating effect of the methoxy groups aid in the formation of the benzyl cation and hence deprotonation, an additional methoxy group was added in the *ortho* position of the phenyl ring by using the 2,4-dimethoxybenzyl protecting group. This group seemed promising, as it was successfully deprotected in the synthesis of the natural product rigidin, which is also a deazapurine derivative.⁹⁰ However, this group was not suitable for this method, as deprotection of the system failed using known conditions, including trifluoroacetic acid in dichloromethane, hydrochloric acid in methanol, and oxidative removal using DDQ.

A literature procedure describing the synthesis of the antitumor agent ALIMTA used the 3,4-dimethoxybenzyl group as a protecting group for the 7-deazapurine.⁹¹ The use of this group seemed counterintuitive, as a *meta*-methoxy group would not add to the electron delocalization needed to form the benzyl cation. However, it was reported that although the benzyl and PMB groups failed, this method was able to effectively undergo the deprotection. In addition, the group has been shown to undergo facile deprotection from pyrroles.⁹² Thus, this protecting group was selected and deprotection was attempted using the reported conditions of TFA and sulfuric acid at room temperature. Needless to say, these harsh conditions resulted in a small amount

of deprotected base, which was detected in the reaction mixture by mass spectrometry. No product, however, was isolated.

Electron withdrawing protecting groups

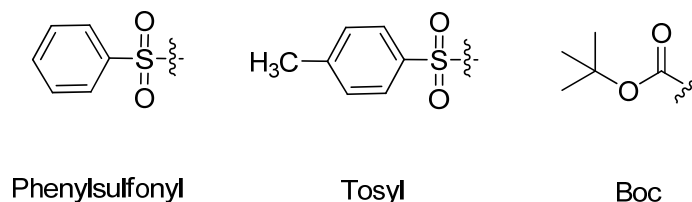


Figure 22: Electron withdrawing protecting groups used for tricyclic base synthesis

A few electron withdrawing protecting groups were used as well. The phenylsulfonyl group was used because this analogue was used in order to achieve the benzyl derivative. Thus, it was brought through the transformation. However, the electron withdrawing nature of the protecting group hindered the iodination. Thus, the iodine was installed prior to protecting the deazapurine, which became a practice that was maintained because of the high yields that were attained in this step.⁹³ Protection with the group after this step worked well; however, the group did not survive the amination step. Efforts to circumvent this problem by reprotecting after amination failed, as very low yields of the protected base were obtained. Similar outcomes were witnessed with the use of the Boc and also the tosyl protecting group, which was chosen because of its reported use in indoles and the 7-deazapurine system and ease of deprotection using cesium carbonate.⁹⁴

Other protecting groups

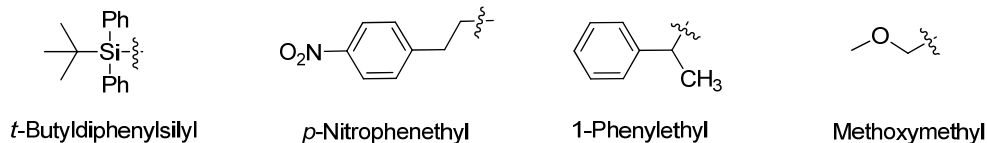
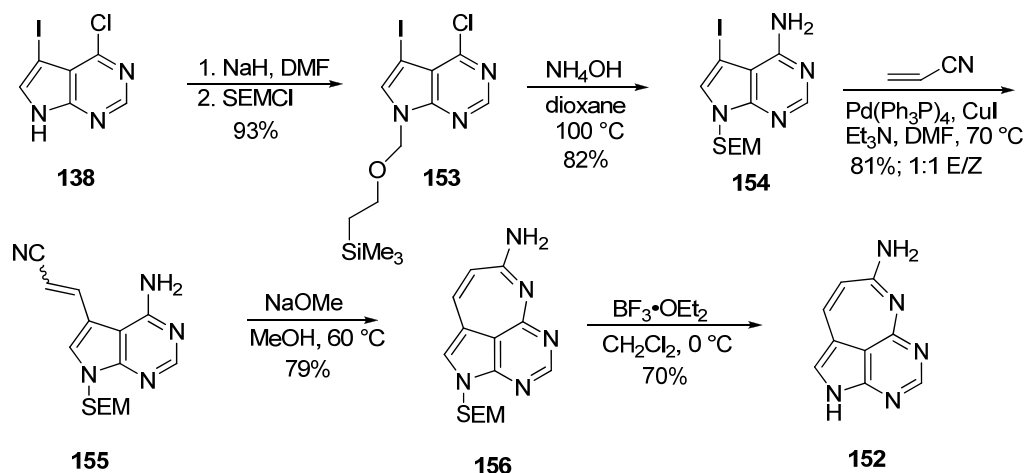


Figure 23: Other protecting groups used for tricyclic base synthesis

Other protecting groups were tried as well, including the TBDPS group which is reported to be robust enough to protect a nitrogen group in heterocyclic compounds.⁹⁵ However, this group was lost at the amination step. The *p*-nitrophenethyl group was also tried, which was successfully used in the synthesis of the 7-deazapurine system of 2'-deoxycadeguomycin and other pyrroles.^{96,97} However, this group produced many side products which resulted in very low yields. The 1-phenylethyl group was also employed, which was reported to be ideal for such systems.⁹⁸⁻¹⁰⁰ However, deprotection failed under acidic conditions. The MOM group was also tried, which has been used as a protecting group in the synthesis of 7-deazapurines.^{101,102} This group underwent the transformations in moderate yields, and was actually deprotected in the final step. However, a two step deprotection method was needed in order to accomplish this. In addition, the product yield was low and it co-eluted with salts. Thus, it was necessary to choose a similar protecting group, but one with more options for deprotection.

SEM protecting group

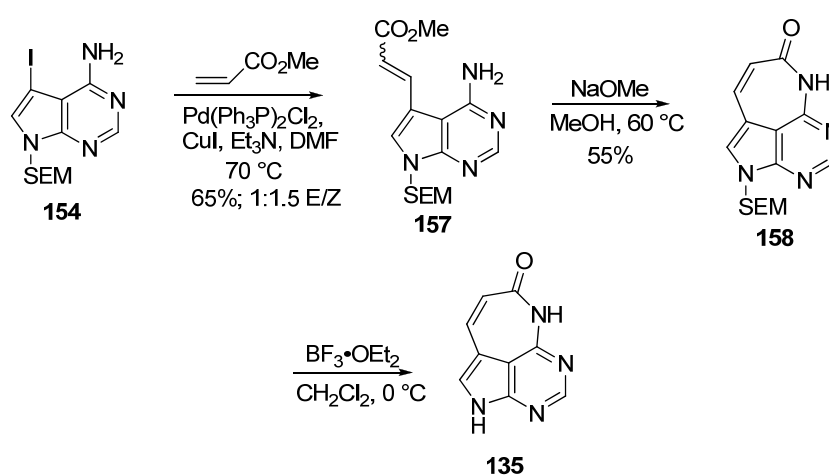
The SEM group was chosen due to its similarity to the MOM protecting group. In addition, it has been used in the total synthesis of dapiramycin B, which contains the 7-deazapurine backbone.¹⁰³ The 7-iodo-6-chloro-7-deazapurine **138** was protected using sodium hydride and SEMCl. It should be noted that the transfer of activation needed in the benzyl protection is not needed in this instance, since the C7 position is substituted. The amination was then performed to provide **153**. A Heck coupling was then used to install the acrylonitrile component, which produced **155** in a 1:1 E/Z mixture. Cyclization induced by sodium methoxide formed the tricyclic expanded adenine base **156**, which was then deprotected using Lewis acid to form **152**.



Scheme 47: Synthesis of expanded adenine base **152** using SEM protecting group

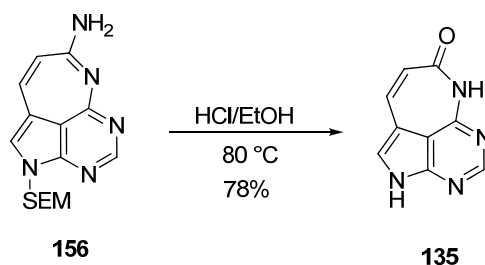
Similarly, the expanded guanine base was synthesized by performing the Heck coupling with methyl acrylate. It should be noted that this cross-coupling differs from that originally proposed for the synthesis of the expanded guanine derivative. The original cross coupling was performed under Stille conditions using the cis stannane. This is because the researchers noted that in this case,

only the cis isomer would cyclize. Thus, efforts to make only the cis isomer were employed. However, isomerization was noted even when using the cis stannane. Therefore, the cross coupling technique was changed to the Heck, which would give mixtures of the E and Z isomers as well, but without the difficult removal of the stannyl reagents. Cyclization was performed using sodium methoxide, and deprotection accomplished with a Lewis acid to give the expanded guanine base **135**.



Scheme 48: Synthesis of expanded guanine base **135** using SEM protecting group

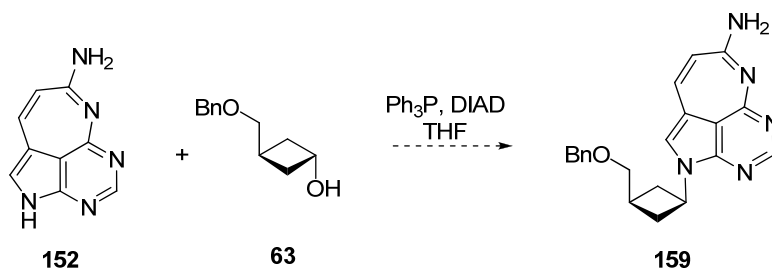
The use of the Lewis acids for deprotection resulted in the generation of a large amount of salts, which made purification difficult. Thus, an alternative method for deprotection, HCl in refluxing ethanol was explored. After two hours under these conditions, deprotection of the SEM group and complete conversion of the protected expanded adenine **156** to the expanded guanine **135** occurred. This results in a completely convergent method, with the final two bases diverging only in the final deprotection step. Retention of the expanded base can be performed using Lewis acids.



Scheme 49: Conversion of protected expanded adenine **156** into deprotected expanded guanine **135**

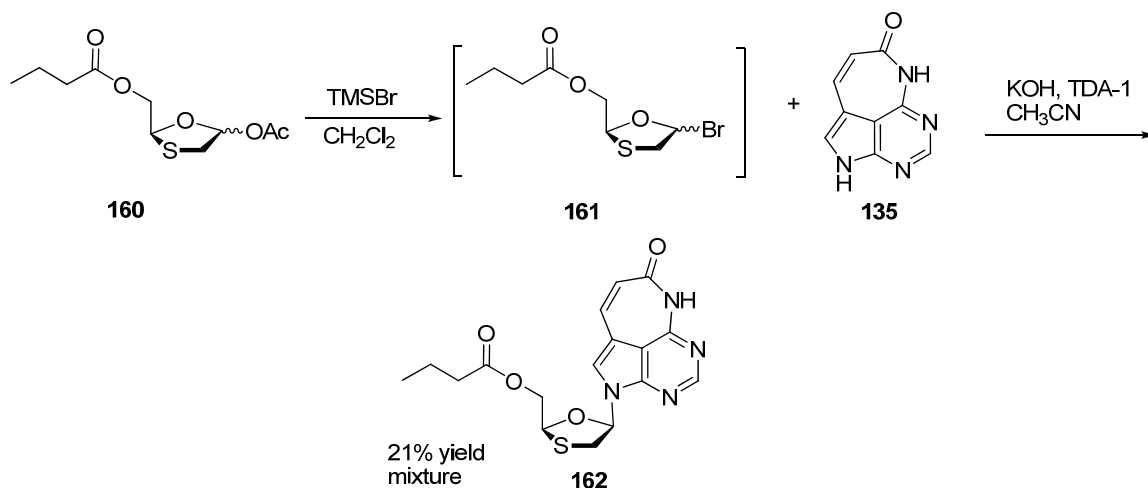
Glycosylation of expanded nucleobases

The coupling of expanded adenine base **152** and the *trans*-cyclobutanol ring **63** was attempted using Mitsunobu conditions. This reaction, however, failed. There are other methods, including the use of the activated cyclobutanol derivative, to be explored.



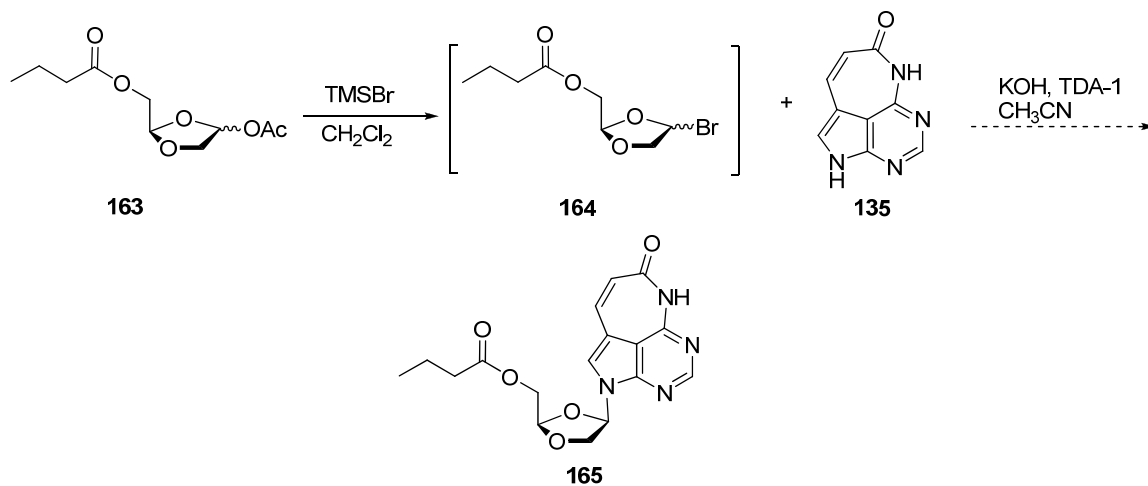
Scheme 50: Attempted coupling between expanded adenine **152** and *trans*-cyclobutanol **63**

The coupling of the expanded guanine base **135** and the oxathiolane acetate was attempted under Vorbruggen conditions.¹⁰⁴ However, the base was unreactive under these conditions. Thus, the bromide **161** was formed *in situ* and reacted with base **135** under solid-liquid phase transfer conditions.¹⁰⁵ A small amount of product was detected by ¹H-NMR and mass spectrometry in an inseparable mixture.



Scheme 51: Attempted coupling between expanded guanine **135** and oxathiolane **160**

The same coupling was attempted with the expanded guanine base **135** and the dioxolane bromide (Scheme 52). There was no product obtained.

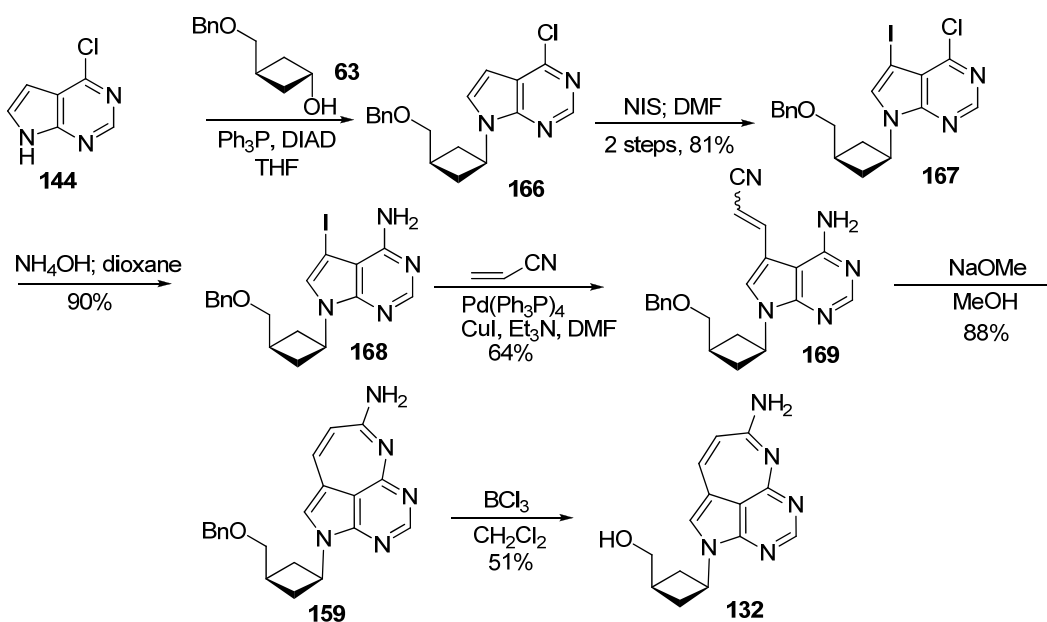


Scheme 52: Attempted coupling between expanded guanine **135** and dioxolane **163**

Early coupling strategy

Although the late coupling strategy was able to effectively produce the free expanded adenine and guanine bases, the coupling techniques used are in need of further refinement. Thus, the early coupling strategy was employed in order to synthesize the desired coupled nucleoside analogues.

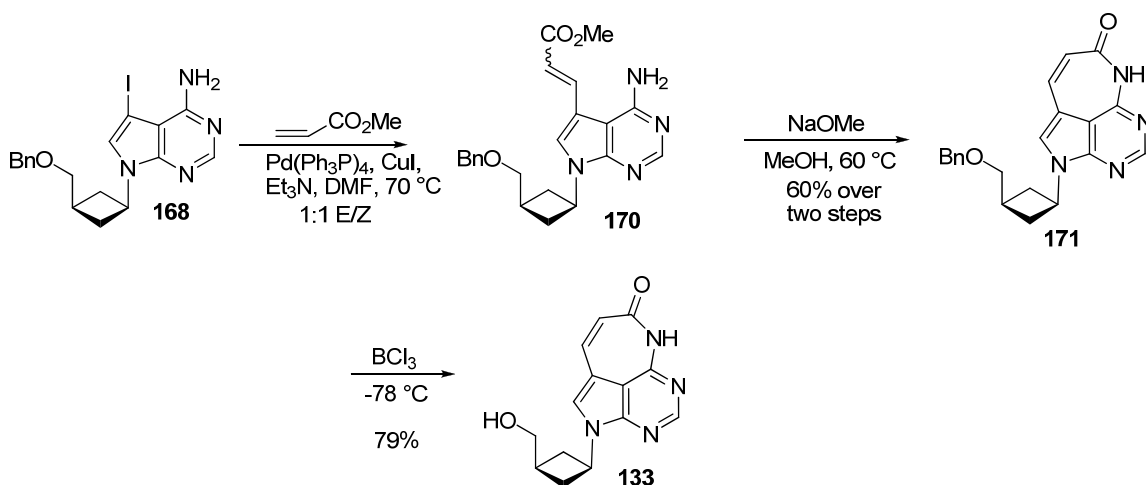
The 7-deazapurine **144** was coupled to the *trans*-cyclobutanol **63** using a Mitsunobu reaction to form **166**. Iodination using NIS resulted in **167** in 81% yield over two steps. Amination was accomplished using ammonium hydroxide and 1,4-dioxane heated to 100 °C to give **168**. A Heck coupling was then employed with acrylonitrile to form **169**. Cyclization was then induced using sodium methoxide, which formed the protected tricyclic analogue **159**. Deprotection of the benzyl group provided **132** in 51% yield (Scheme 53).



Scheme 53: Synthesis of expanded adenine cyclobutyl nucleoside analogue **132** using early coupling strategy

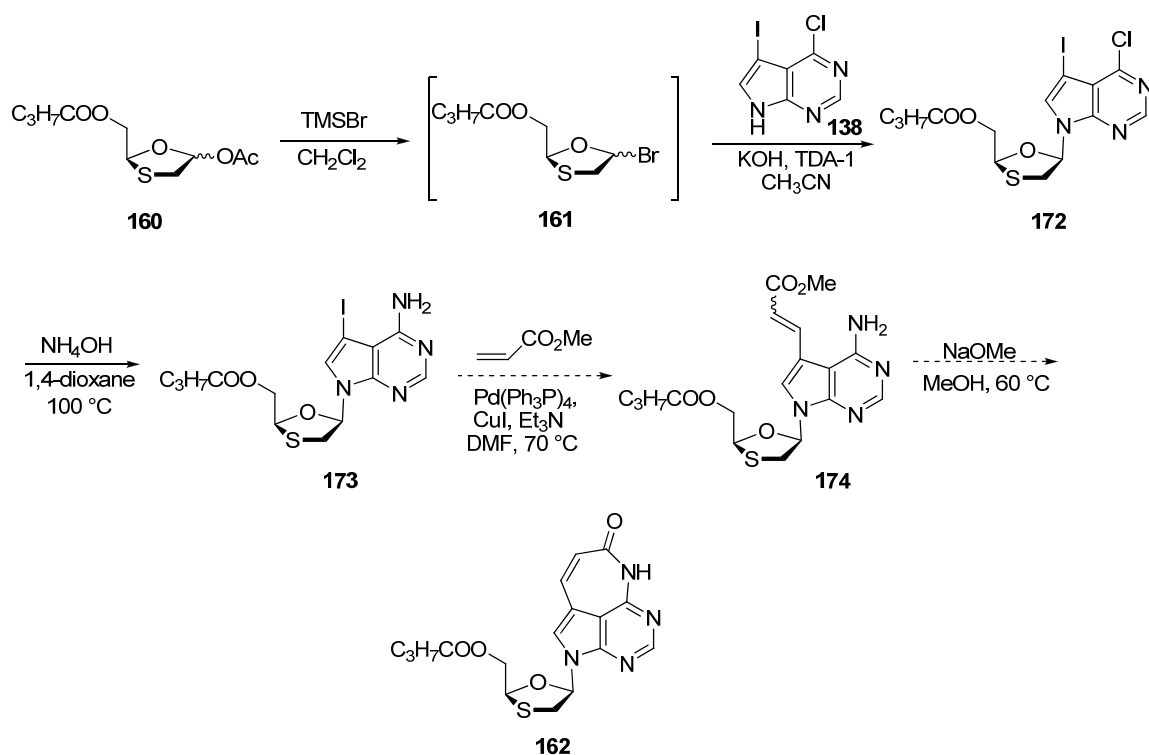
An advantage of the early coupling strategy is that each intermediate can serve as a potential analogue. Thus, each intermediate was subjected to deprotection to form the free nucleoside. Intermediate **167** was successfully deprotected to form its free cyclobutyl nucleoside analogue which was tested for anti-HIV activity. This was attempted with the aminated intermediate **168**. However, no product was isolated when deprotection was attempted using Lewis acids. Hydrogenolysis of **168** resulted in loss of the iodide with no effect on the benzyl group.

This strategy was also used in the synthesis of the expanded guanine derivative **133** (Scheme 54). Intermediate **168** was coupled with methyl acrylate under Heck conditions to form **170** as a 1:1 E/Z mixture. Cyclization using sodium methoxide was done to give the protected expanded guanine derivative **171** in 60% yield over two steps. Deprotection using BCl_3 was done to give **133** in 79% yield.



Scheme 54: Synthesis of expanded guanine cyclobutyl nucleoside analogue **133** using early coupling strategy

The synthesis of the oxathiolane analogue was also attempted using this strategy. The 7-iodo-6-chloro-7-deazapurine **138** was coupled to the bromo oxathiolane **161** formed *in situ* from the oxathiolane acetate **160**. The desired β coupled product was then aminated using ammonium hydroxide in 1,4-dioxane. Heck coupling was then performed on **173** using methyl acrylate. There was product detected in a complex mixture, but was not able to be isolated. Treatment of the mixture with sodium methoxide did not result in product formation. Similar outcomes were produced when performing the Heck coupling with acrylonitrile. Thus, the early coupling method is not suitable for the synthesis of this analogue.



Scheme 55: Synthesis of expanded guanine oxathiolane nucleoside analogue **162** using early coupling strategy

1.4.3 Design and Synthesis of Ring Expanded (“Fat”) Nucleoside Analogues

An additional mode of attack for nucleoside analogues is to disrupt the ability of helicases to unwind RNA structures. It is expected that an expanded “fatty” base will inhibit the unwinding by presenting steric interference in translocation of the enzyme along the polynucleotide chain.¹⁰⁶ In the synthesis of certain fatty base analogues as inhibitors of the West Nile virus, it was discovered that the α -anomer **176** displayed more potent and selective activity than the β -anomer **175** (Figure 24).^{107,108} Thus, both the β - (**177**) and α -anomers (**178**) of the dodecylguanidine cyclobutyl analogues were prepared and submitted for anti-HIV activity testing (Figure 25).

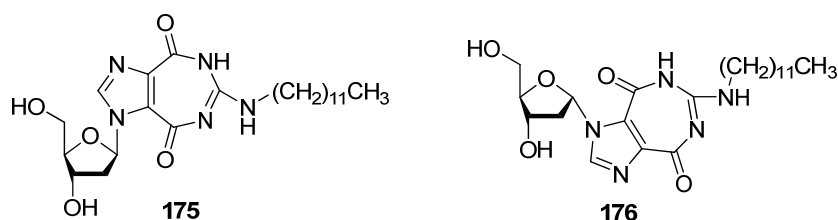


Figure 24: Ring-expanded “fatty” nucleoside analogues as West Nile virus inhibitors

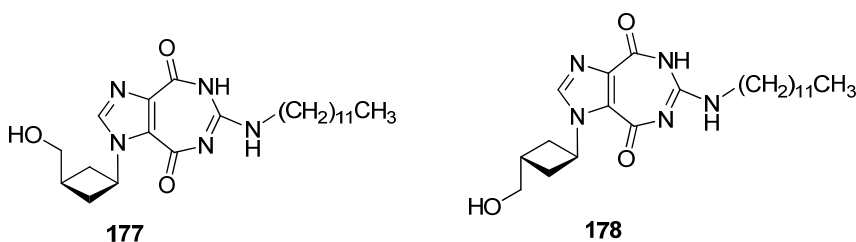
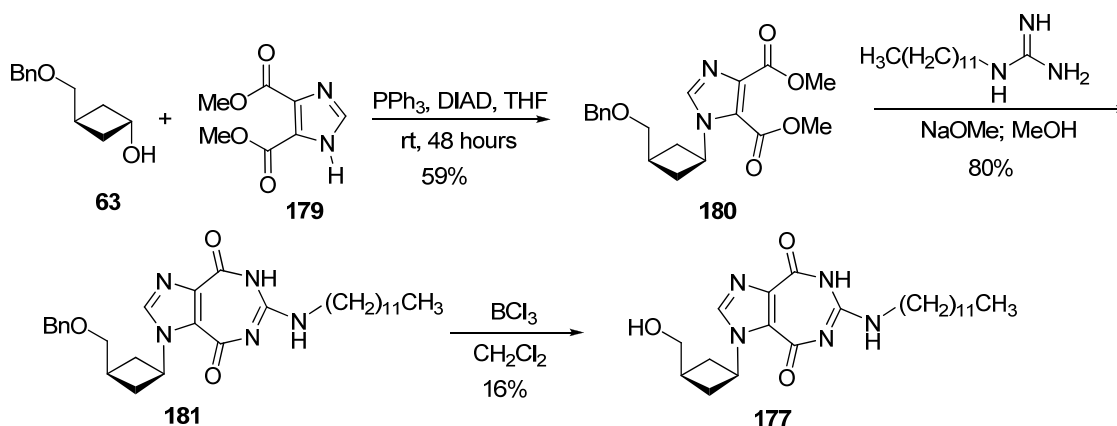


Figure 25: Ring-expanded “fatty” cyclobutyl nucleoside analogues

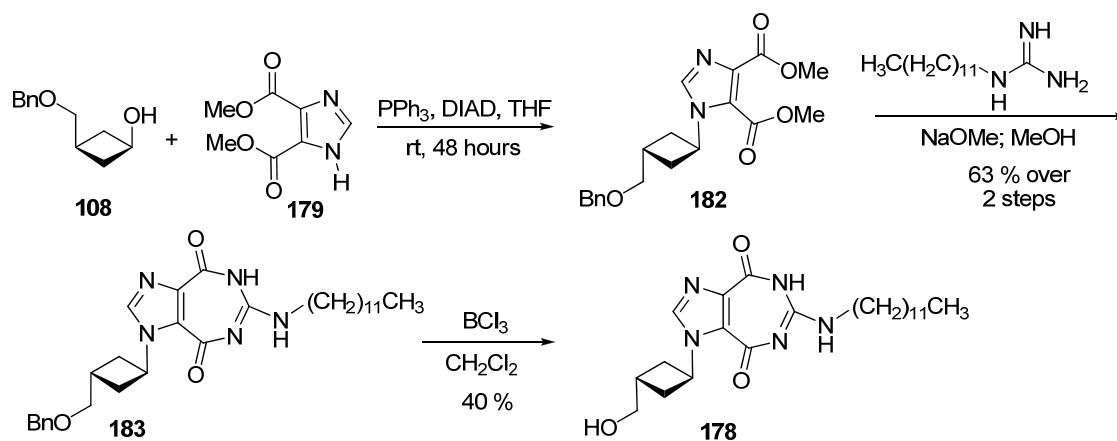
The *trans*-cyclobutanol ring **63** was coupled to the imidazole **179** under Mitsunobu conditions (Scheme 56). Treatment with dodecylguanidine resulted in

the fatty base analogue **181**. Deprotection using Lewis acid gives the product **177**.



Scheme 56: Synthesis of β -anomer of dodecylguanidine cyclobutyl analogue

Similar transformations were employed in the synthesis of the α -anomer (Scheme 57). Instead of using the *trans*-cyclobutanol, the *cis* isomer was employed for the Mitsunobu coupling.



Scheme 57: Synthesis of α -anomer of dodecylguanidine cyclobutyl analogue

1.4.4 Synthesis of 4'-O-triphosphate of cyclobutyl nucleosides

A triphosphate of each representative class of compounds, purine, tricyclic, and ring-expanded “fatty” cyclobutyl analogues, was synthesized (Figure 26).

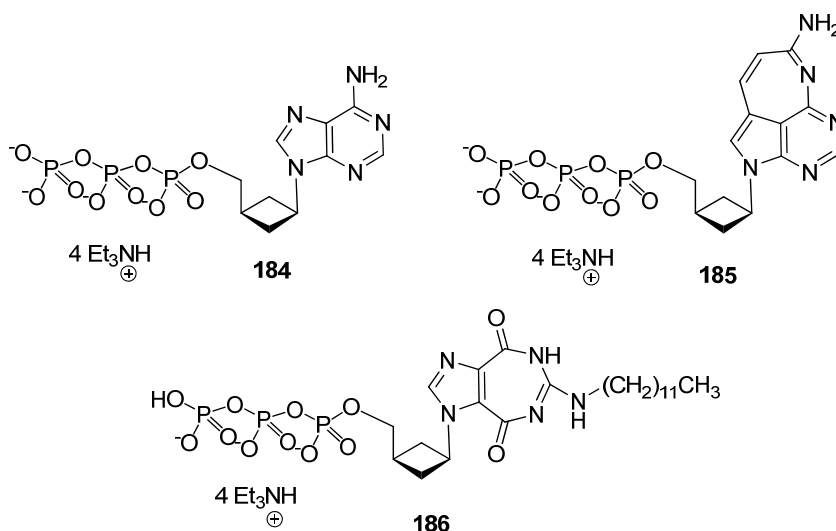
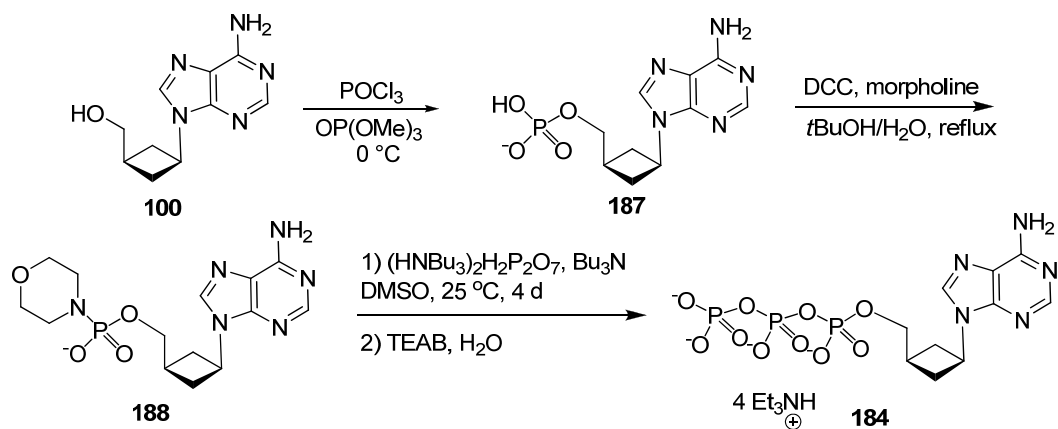


Figure 26: Synthesized cyclobutyl nucleoside 4'-O-triphosphates

The triphosphates were all synthesized according to the method developed by Moffatt involving the phosphoramidate intermediate. The synthesis of the cyclobutyl adenine triphosphate is shown as a representative example (Scheme 58). The nucleoside **100** was allowed to react with phosphorus oxytrichloride in trimethyl phosphate and quenched with water, which allowed the isolation of the monophosphate intermediate **187**. The morpholine phosphoramidate **188** was then prepared, which was allowed to react with bis-(*tri-n*-butylammonium)pyrophosphate and quenched with triethylammonium bicarbonate (TEAB) to obtain the triphosphate **184**.



Scheme 58: Synthesis of 4'-O-triphosphate of 9-[*cis*-3-hydroxymethyl)cyclobutyl]adenine **184**

1.4.5 Biological Activity of Synthesized Compounds

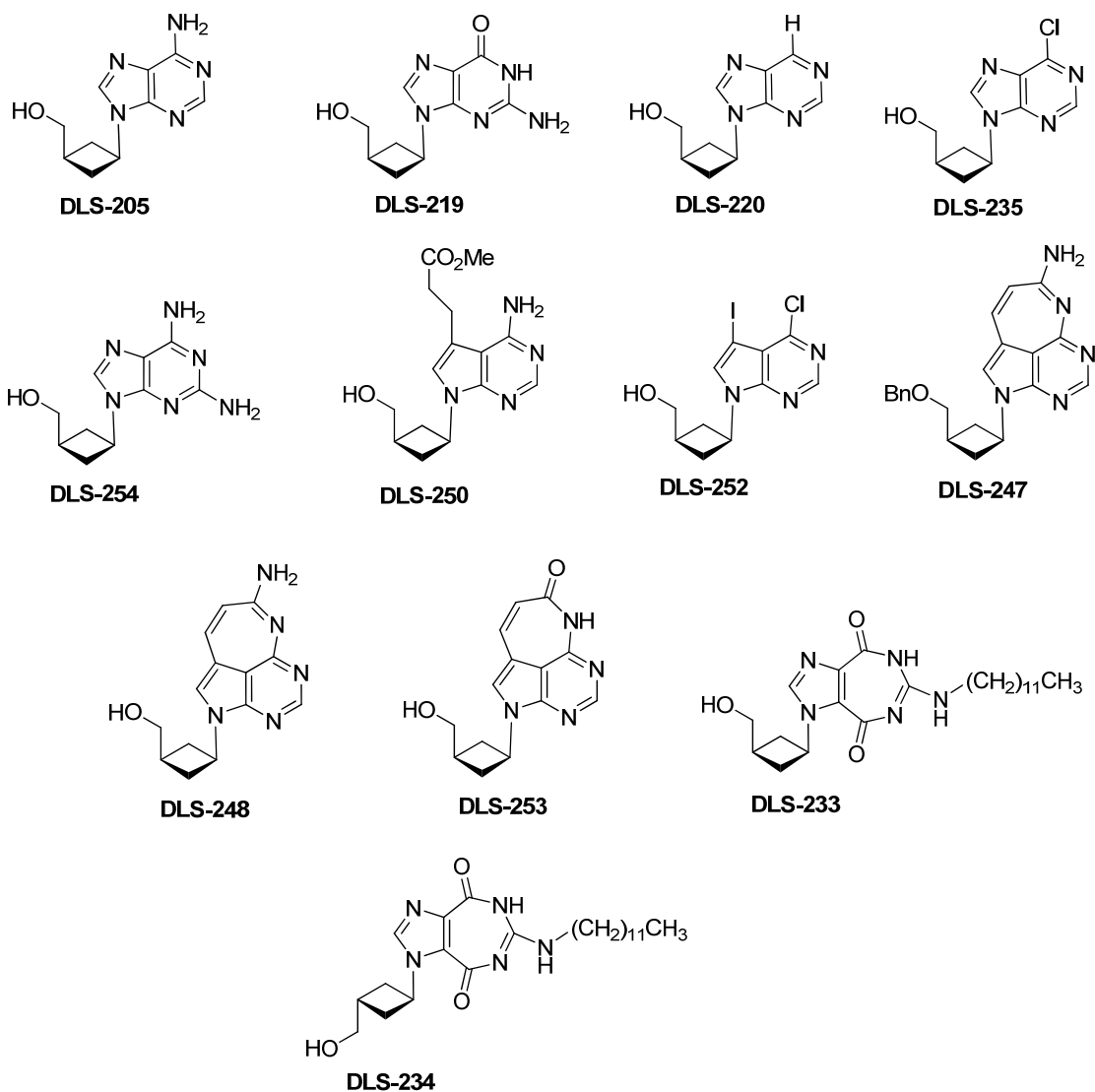


Figure 27: Structures of tested cyclobutyl nucleosides

Anti-HIV Activity

Compound	Activity (PBM)		Toxicity (IC ₅₀)		
	EC ₅₀ (μM)	EC ₉₀ (μM)	PBM (μM)	CEM (μM)	Vero (μM)
DLS-205	67.9	> 100	> 100	> 100	> 100
DLS-219	6.5	21.8	> 100	> 100	> 100
DLS-220	> 100	> 100	> 100	> 100	> 100
DLS-235	8.7	55.8	> 100	55.3	> 100
DLS-254	70.1	> 100	> 100	> 100	> 100

DLS-250	9.1	26.6	11.8	2.1	3.2
DLS-252	24.8	> 100	68.3	> 100	27.0
DLS-247	3.2	5.4	1.5	< 1.0	1.3
DLS-248	> 100	> 100	> 100	> 100	> 100
DLS-253	46.1	> 100	20.7	88.9	70.1
DLS-233	12.0	40.9	8.9	8.2	6.1
DLS-234	15.1	43.0	13.3	17.0	3.3

Table 2: Anti-HIV activity and toxicity of cyclobutyl nucleosides

The synthesized compounds were tested for anti-HIV activity and cytotoxicity in PBM, CEM, and Vero cells.^{109,110} The anti-HIV data obtained showed that the cyclobutyl adenine, guanine, and 2,6 - diamino derivatives were moderately active against HIV. In fact, the guanine derivative **DLS-219** has proven to be the most active of the cyclobutyl series developed by the Liotta group thus far. These compounds also displayed no cytotoxicity. The 6-chloropurine analogue **DLS-235** displayed mild activity, but also cytotoxicity in CEM cells. The expanded bases analogues, including both the tricyclic and fatty bases exhibited activity, but also cytotoxicity. In fact, the strong toxicity in vero cells displayed with DLS-234 and DLS-247 suggests that these compounds are highly toxic in rapidly proliferating cells. Thus, they may be useful as non-specific anti-cancer agents.

In addition to the evaluation of nucleoside analogs, the effectiveness of the triphosphates as competitive inhibitors against HIV RT. Thus, triphosphates **184**, **185**, and **186** were submitted for *in vitro* testing. It was found that both **184** and **185** are able to adequately be incorporated as adenine analogs by RT-wt during DNA polymerization (Figures 28 and 29). These compounds are less

efficient than the natural dATP substrate, however (Table 3). Compounds **184** and **185** are both being explored for activity as guanine mimics as well. Compound **186** does not serve as a substrate for the enzyme. It is currently being examined for activity as a competitive inhibitor of enzyme.

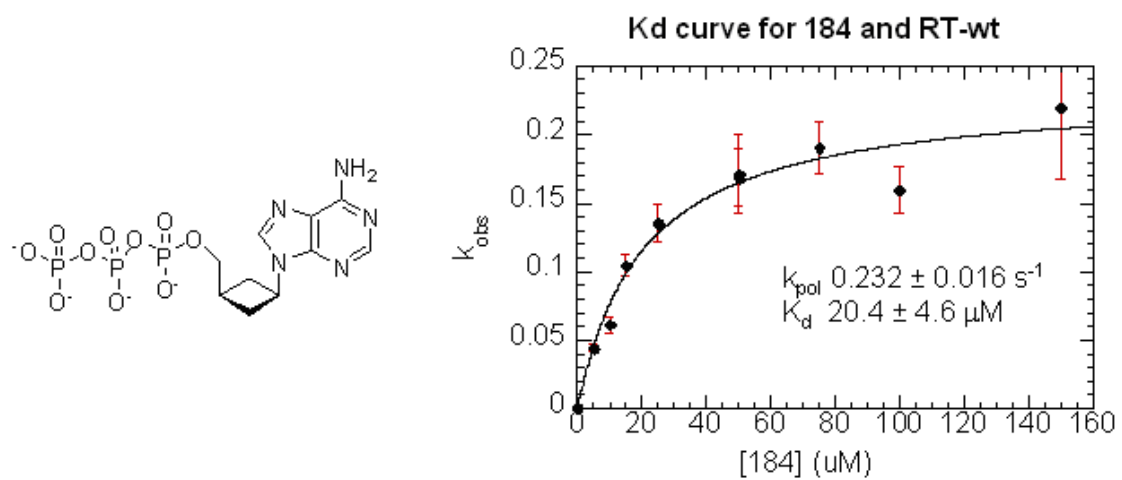


Figure 28: K_{d} curve for cyclobutyl adenine triphosphate **184**

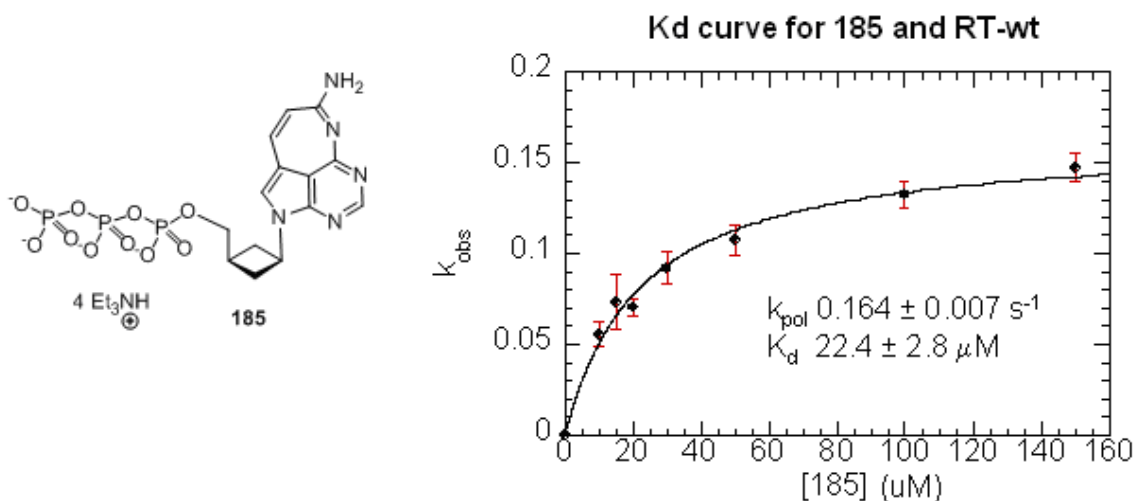


Figure 29: K_{d} curve for cyclobutyl expanded adenine triphosphate **185**

	Nucleotide	k _{pol} (s ⁻¹)	K _d (μM)	Efficiency (s ⁻¹ μM ⁻¹)
RT ^{WT}	dATP	12.3 ± 1.0	4.6 ± 1.6	2.7
	184	0.232 ± 0.016	20.4 ± 4.6	0.011
	185	0.163 ± 0.007	22.4 ± 2.8	0.007
	186	N/A	N/A	N/A

Table 3: Summary of *in vitro* results with triphosphates

Anti-HCV Activity

Certain analogues were also evaluated for anti-HCV activity. The assays were performed using Huh 7 clone B cells containing HCV replicon RNA.¹¹¹ Interesting compounds include the toxic analogues DLS -234 and DLS-247. The level of toxicity displayed with these analogues in both HCV and HIV assays prompted the anti-cancer testing of these compounds.

Compound	Activity (Huh-7)		Toxicity		% Inhibition
	EC ₉₀ (μM)	Conclusion	IC ₅₀ (μM)	Conclusion	
DLS-233	> 10	Not active	> 10	Slightly Toxic	N/A
DLS-234	> 10	Slightly active	> 10	Toxic	65%
DLS-235	> 10	Slightly active	> 10	Not toxic	50%
DLS-247	< 10	Active	> 10	Toxic	98.9%
DLS-248	> 10	Not active	> 10	Not toxic	N/A

Table 4: Anti-HCV activity and toxicity of cyclobutyl nucleosides

Anti-cancer Activity

The anti-cancer testing was performed on a malignant pancreatic cancer cell line. The compounds were tested to determine their ability to inhibit cell growth. Gemcitabine was used as the control for this experiment. It is an FDA approved nucleoside analogue that exhibits significant antitumor activity (Figure

30). This compound was shown to decrease cell proliferation by 70% after 48 hours. Upon testing the analogues from this series, DLS-234 and DLS-247 decreased proliferation by only 20 and 40%, respectively.

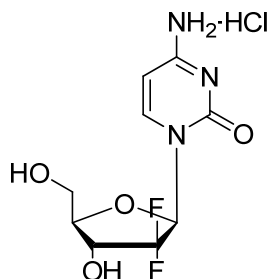


Figure 30: Structure of gemcitabine HCl

1.5 Conclusion

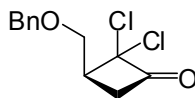
Several cyclobutyl nucleoside analogues have been synthesized and evaluated in HIV, HCV, and cancer cell lines. Among the cyclobutyl compounds synthesized, the cyclobutyl guanine (DLS-219) was the most promising. It exhibited moderate anti-HIV activity and also was not cytotoxic up to 100 μ M in PBM, CEM, and Vero cell lines. The expanded tricyclic base and fatty base cyclobutyl analogues all displayed significant cytotoxicity, with the exception of the expanded adenine analogue DLS-248. The high toxicity of DLS-234 and DLS-247 in both HIV and HCV assays warranted the further testing in a pancreatic cancer cell line. However, these compounds were not as effective as the current nucleoside analogue treatment on the market.

The origin of the cytotoxicity for these compounds, however, is unknown. Thus, representative triphosphates of these compounds have been synthesized and will be tested for anti-HIV activity. Upon receipt of positive data for these compounds, it may be necessary to synthesize phosphonate prodrugs of the analogues. In addition, different expanded bases should also be explored. The fact that the expanded adenine base DLS-248 is non-toxic demonstrates the potential use of this class as HIV-RT inhibitors.

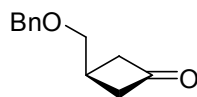
1.6 Experimental

General: ^1H -NMR spectra were recorded at either 400 MHz on an INOVA-400 spectrometer, or at 600 MHz on an INOVA-600 spectrometer. ^{13}C -NMR spectra were recorded at either 100 MHz or 150 MHz on the above mentioned instruments, respectively. NMR samples were prepared in either deuterated chloroform (CDCl_3), methanol (CD_3OD), dimethyl sulfoxide (d^6 -DMSO), or deuterium oxide (D_2O) with residual solvent peaks serving as the internal standards. ^{31}P NMR spectra were recorded on a Varian 400 spectrometer. Chemical shifts (δ) are reported in parts per million, and the coupling constants (J) are reported in Hertz. Mass spectra were obtained on either a VG 70-S Nier Johnson or JEOL Mass Spectrometer. HPLC analyses were conducted on a Varian ProStar system. Infrared spectra were recorded on a Thermo Nicolet Avatar 370 FT-IR spectrometer as neat films. Elemental analyses were performed by Atlantic Microlab (Norcross, GA). Analytical TLC was performed on Whatman precoated glass plates (0.25 mm) with silica gel (60 F254). Flash column chromatography was performed with silica gel 60 (230 – 400 mesh, EM Science). Anhydrous reactions were performed with anhydrous solvents in flame-dried, argon-filled glassware. Reagents were obtained from commercial suppliers and used without further purification. Solvents were purchased as anhydrous or dried over 4Å molecular sieves. Organic extracts were dried over commercially available anhydrous MgSO_4 or Na_2SO_4 . Evaporations were performed under reduced pressure using a Buchi rotary evaporator at 35 °C, unless otherwise noted.

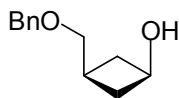
3-(Benzyloxymethyl)-2,2-dichlorocyclobutanone (62)



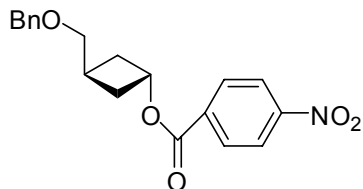
To a dry 3-necked 500 mL round bottomed flask under argon was added 250 mL of dry diethyl ether followed by 33 mL of 1,2-dimethoxyethane. To this solution was then added 13.3 g of freshly prepared Zn-Cu couple (*J. Org. Chem.* **1978**, 43, 14, 2879-2882) followed by allyl benzyl ether **105** (10.4 mL, 67.3 mmol). The mixture was allowed to stir and trichloroacetyl chloride **106** (20.0 mL, 0.178 mol) was added dropwise. The mixture was gently heated at 30 °C for 68 hours. The mixture was then vacuum filtered and the zinc residue was washed with diethyl ether. The washings were concentrated to approximately 50 mL and 100 mL of petroleum ether was added. The mixture was stirred vigorously for five minutes and the supernatant was decanted. An additional 40 mL of petroleum ether was added, the mixture was stirred, and the supernatant was decanted. The combined layers were washed with saturated aqueous NaHCO₃ (2 x 200 mL) and brine (100 mL). The organic layers were dried over anhydrous MgSO₄ and concentrated to give the crude product (20.5 g) as an orange oil (Rf: 0.35; 9:1 Hex/EtOAc). ¹H-NMR (CDCl₃, 400 MHz): σ 3.12 – 3.24 (m, 2H), 3.39 – 3.48 (m, 1H), 3.69 – 3.73 (m, 1H), 3.84 – 3.88 (m, 1H), 4.59 (s, 2H), 7.30 – 7.40 (m, 5H). ¹³C-NMR (CDCl₃, 100 Mz): σ 45.3, 45.6, 69.1, 73.6, 87.7, 127.9, 128.1, 128.7, 137.7, 192.4. HRMS (APCI): expected for C₁₂H₁₃Cl₂O₂ (M+H)⁺ 259.02871. Found 259.01029. IR(neat): ν_{\max} 2862, 1807, 1097 cm⁻¹.

3-(Benzyloxymethyl)-cyclobutanone (107)

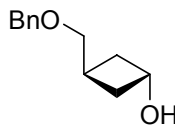
Glacial acetic acid (130 mL) was added to the 250 round bottomed flask containing crude 3-(benzyloxymethyl)-2,2-dichlorocyclobutanone **62** (18.7 g, 72.3 mmol). Zinc dust (28.3 g, 0.434 mol) was added slowly to the solution with vigorous stirring. Addition of zinc caused the flask to heat and a reflux condenser was attached. The mixture was allowed to stir for two hours, as the flask slowly cooled to room temperature. Diethyl ether (100 mL) was added to the cooled mixture which was then vacuum filtered. The zinc residue was washed with 50 mL of diethyl ether. The filtrate and washings were then concentrated. The remaining oil was then dissolved in 200 mL of dichloromethane and 50 mL of saturated aqueous NaHCO₃ was added to react with the remaining acetic acid. The solution was then washed carefully with saturated aqueous NaHCO₃ (2 x 200 mL) and water (100 mL). The organic layer was dried over anhydrous MgSO₄, filtered, and concentrated. Purification by column chromatography (5:1 Hex/EtOAc) gave 8.36 g (65% yield over two steps) of product as a colorless oil (Rf: 0.23; 9:1 Hex/EtOAc). ¹H-NMR (CDCl₃, 400 MHz): σ 2.67 – 2.74 (m, 1H), 2.86 – 2.93 (m, 2H), 3.09 – 3.18 (m, 2 H), 3.60 (d, 2H, J = 6.4 Hz), 4.57 (s, 2H), 7.29 – 7.39 (m, 5H). ¹³C-NMR (CDCl₃, 100 Mz): σ 23.8, 50.2, 73.0, 73.3, 127.8, 127.9, 128.6, 138.2, 207.7. HRMS (APCI): expected for C₁₂H₁₅O₂ (M+H)⁺ 191.10666. Found 191.10665. IR(neat): ν_{\max} 2855, 1778, 1089 cm⁻¹.

cis-3-(Benzyloxymethyl)cyclobutanol (108)

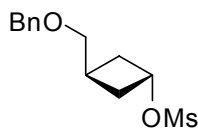
To a 250 mL round bottomed flask under argon containing 8.3 g (43 mmol) of 3-(benzyloxymethyl)-cyclobutanone **107** was added 100 mL of dry THF. The flask was cooled to -78°C and 54 mL of an L-selectride solution (1.0 M in THF, 54 mmol) was added dropwise over 30 minutes. After the addition was complete, the flask was warmed to room temperature and saturated aqueous NaHCO_3 (80 mL) was added over 5 minutes. The mixture was then cooled in an ice bath and 30 mL of 30% aqueous hydrogen peroxide was added dropwise (to maintain the temperature below 28°C). Water (140 mL) was added followed by 345 mL of ethyl acetate. The organic layer was separated and then washed with water (3 x 175 mL) and brine (100 mL). The organic layer was then dried over anhydrous MgSO_4 , filtered, and concentrated to give 8.1 g (98% yield) of product as a colorless oil (R_f : 0.29; 1:1 Hex/EtOAc). $^1\text{H-NMR}$ (CDCl_3 , 600 MHz): σ 1.66 – 1.70 (m, 2H), 2.05 – 2.10 (m, 1H), 2.41 – 2.46 (m, 2H), 2.78 (s, 1H), 3.44 (d, 2H, $J = 6$ Hz), 4.09 – 4.14 (m, 1H), 4.53 (s, 2H), 7.28 – 7.37 (m, 5H). $^{13}\text{C-NMR}$ (CDCl_3 , 150 Mz): σ 25.9, 36.6, 64.1, 73.1, 74.5, 127.7, 127.8, 128.5, 138.5. HRMS (FAB): expected for $\text{C}_{12}\text{H}_{17}\text{O}_2$ ($\text{M}+\text{H}$) $^+$ 193.12231. Found 193.12220. IR(neat): ν_{max} 3345, 2929, 1071 cm^{-1} .

***trans*-3-(Benzyloxymethyl)cyclobutyl 4-nitrobenzoate (121)**

To a dry 500 mL round bottomed flask under argon was added 21.5 g (82.2 mmol) of Ph_3P , 13.0 g (78.3 mmol) of 4-nitrobenzoic acid, and 7.5 g (38.9 mmol) of *cis*-3-(benzyloxymethyl)cyclobutanol **108**. The solids and oil were placed under vacuum overnight and then the flask was refilled with argon. Dry THF (70 mL) was added and the flask was cooled to 0°C. A solution of DIAD (16.2 mL, 82.2 mmol) in 35 mL of dry THF was added dropwise over 20 minutes. The mixture was allowed to warm to room temperature and was stirred for 7.5 hours. The reaction mixture was then concentrated to give a viscous yellow oil. Purification of the crude material by column chromatography (96:4 Hex/EtOAc) gave 11.6 g (88 % yield) of product as a white flaky solid (R_f : 0.41, 3:1 Hex/EtOAc). mp: 69-70 °C. $^1\text{H-NMR}$ (CDCl_3 , 600 MHz): σ 2.38 – 2.45 (m, 4H), 2.65 – 2.69 (m, 1H), 3.55 (d, 2H, $J = 7.2$ Hz), 4.58 (s, 2H), 5.35 – 5.39 (m, 1H), 7.30 – 7.33 (m, 1H), 7.35 – 7.39 (m, 4H), 8.21 – 8.23 (m, 2H), 8.28 – 8.30 (m, 2H). $^{13}\text{C-NMR}$ (CDCl_3 , 150 Mz): σ 28.7, 32.4, 70.3, 73.3, 73.4, 123.6, 127.8, 128.6, 130.9, 135.9, 138.5, 150.6, 164.3. HRMS (EI^+): expected for $\text{C}_{19}\text{H}_{19}\text{NO}_5$ (M^+) 341.1263. Found. 341.1261. IR(neat): ν_{max} 2938, 2854, 1708, 1525, 1277 cm^{-1} .

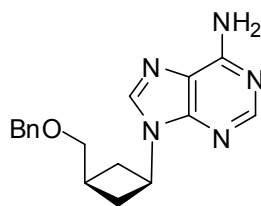
***trans*-3-(Benzyloxymethyl)cyclobutanol (63)**

To a 500 mL round bottomed flask containing 10.6 g (31.1 mmol) of *trans*-3-(benzyloxymethyl)cyclobutyl 4-nitrobenzoate **121** was added 225 mL of 1,4-dioxane. The solution was stirred and 150 mL of 0.4 M NaOH (60.0 mmol) was added to the solution. The mixture was stirred for 30 minutes and then quenched with the dropwise addition of 2.68 mL (46.6 mmol) of acetic acid. The solution was then concentrated to give a white residue. The residue was dissolved in ethyl acetate (125 mL) and the solution was washed with saturated aqueous NaHCO₃ (3 x 125 mL). The organic layers were dried over MgSO₄, filtered, and concentrated to give 4.6 g (77% yield) of a light yellow oil (R_f: 0.32; 1:1 Hex/EtOAc). ¹H-NMR (CDCl₃, 600 MHz): σ 2.04 – 2.09 (m, 2H), 2.17 – 2.21 (m, 2H), 2.24 (s, br, 1H), 2.46 – 2.51 (m, 1H), 3.46 (d, 2H, *J* = 6.6 Hz), 4.35 – 4.40 (m, 1H), 4.54 (s, 1H), 7.27 – 7.38 (m, 5H). ¹³C-NMR (CDCl₃, 150 Mz): σ 26.9, 35.4, 66.3, 73.1, 74.1, 127.7, 127.8, 128.5, 138.6. HRMS (EI⁺): expected for C₁₂H₁₆O₂ (M)⁺ 192.1150. Found: 192.1154. IR(neat): ν_{\max} 3355, 2930, 2852, 1453, 1090 cm⁻¹.

***trans*-3-(Benzyloxymethyl)cyclobutyl methanesulfonate (122)**

To a dry round bottomed flask under argon was added 5.75 g (29.9 mmol) of *trans*-3-(benzyloxymethyl)cyclobutanol **63** and 37.5 mg (0.299 mmol) of DMAP. The oil and solid were dissolved in CH₂Cl₂ (225 mL) and the solution was stirred. Triethylamine (20.8 mL, 150 mmol) was then added and the solution was cooled to 0°C. After five minutes of stirring in the ice bath, 2.79 mL (35.9 mmol) of MsCl was added dropwise. The solution was then allowed to warm to room temperature and was stirred for 20 hours. The reaction mixture was quenched with water and was then washed with water (2 x 200 mL) and brine (200 mL). The organic layers were dried over anhydrous MgSO₄, filtered, and concentrated. The product was purified by column chromatography with 4:1 Hex/EtOAc to give 7.35 g of product as a yellow oil. (R_f: 0.51; 1:1 Hex/EtOAc). ¹H-NMR (CDCl₃, 600 MHz): σ 2.35 – 2.39 (m, 2H), 2.45 – 2.50 (m, 2H), 2.58 – 2.63 (m, 1H), 2.97 (s, 3H), 3.47 (d, 2H, *J* = 5.4 Hz), 4.55 (s, 2H), 5.11 – 5.16 (m, 1H), 7.27 – 7.38 (m, 5H). ¹³C-NMR (CDCl₃, 150 Mz): σ 28.2, 33.1, 38.3, 72.9, 73.3, 74.3, 127.8, 127.9, 128.6, 138.4. HRMS (FAB): expected for C₁₃H₁₉O₄S (M+H)⁺ 271.09986. Found: 271.09922. IR(neat): ν_{\max} 2942, 2856, 1350, 1170 cm⁻¹.

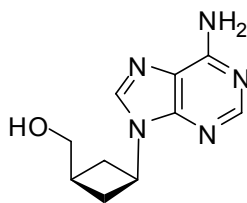
9-[*cis*-3-(Benzyloxymethyl)cyclobutyl]adenine (**77**)



To a dry 3-necked 100 mL round bottomed flask fitted with a condenser under argon was added 1.03 g (3.82 mmol) of *trans*-3-(benzyloxymethyl)cyclobutyl methanesulfonate **42**, 1.01 g (7.47 mmol) of adenine, 1.04 g (7.54 mmol) of

K_2CO_3 , and 1.04 g (3.96 mmol) of 18-crown-6. The contents of the flask were dried under high vacuum for five hours to ensure dryness and then the flask was refilled with argon. Dry DMF (39 mL) was added and the mixture was refluxed at 120°C. After 22 hours of reflux, the flask was cooled to room temperature and water (100 mL) was added. The solution was extracted with EtOAc (5 x 50 mL) and the organic layers were washed with brine (2 x 50 mL). The organic layers were then dried over anhydrous $MgSO_4$, filtered, and concentrated. Purification by column chromatography (10:1 $CH_2Cl_2/MeOH$) afforded the product in 60% yield (0.725 g) as yellowish-white crystals. R_f : 0.51 (9:1 $CH_2Cl_2/MeOH$). mp: 105°C. 1H -NMR ($CDCl_3$, 600 MHz): σ 2.44 – 2.55 (m, 3H), 2.68 – 2.73 (m, 2H), 3.55 (d, 2H, $J = 4.8$), 4.57 (s, 2H), 4.92 – 4.98 (m, 1 H), 6.19 (s, 2H), 7.28 – 7.38 (m, 5H), 7.95 (s, 1H), 8.34 (s, 1H). ^{13}C -NMR ($CDCl_3$, 150 Mz): σ 28.8, 33.3, 45.1, 72.9, 73.4, 119.9, 127.8, 127.9, 128.6, 138.4, 139.0, 150.1, 152.9, 155.8. HRMS (FAB): expected for $C_{17}H_{20}N_5O$ ($M+H$)⁺ 310.16624. Found: 310.16495. IR(neat): ν_{max} 3323, 3152, 1662, 1595 cm^{-1} .

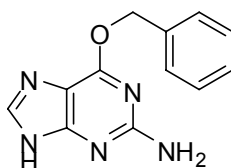
9-[*cis*-3-Hydroxymethyl)cyclobutyl]adenine (100)



To the 250 mL round bottomed flask containing 0.65 g (2.11 mmol) of 9-[*cis*-3-(benzyloxymethyl)cyclobutyl]adenine **77** was added 15 mL of dry CH_2Cl_2 . The solution was cooled to -78°C and 10 mL of boron trichloride (1.0 M in CH_2Cl_2) was added dropwise. The solution was allowed to stir at -78°C for five hours and

was then warmed to room temperature. The reaction was quenched with 5 mL of 7N methanolic ammonia and was then concentrated. The crude material was purified by column chromatography using 9:1 CH₂Cl₂/MeOH. The product was then crystallized from EtOAc to give fine white crystals (0.36 g; 79% yield). R_f: 0.16, 9:1 CH₂Cl₂/MeOH. mp: 130°C. ¹H-NMR ([CD₃)₂SO], 400 MHz): σ 2.24 – 2.39 (m, 3H), 2.46 – 2.52 (m, 2H), 3.48 – 3.50 (m, 2H), 4.64 (t, 1H, *J* = 5.6), 4.77 – 4.89 (m, 1H), 7.21 (br s, 1H), 8.13 (s, 1H), 8.28 (s, 1H). ¹³C-NMR ([CD₃)₂SO], 100 Mz): σ 30.3, 32.4, 44.5, 64.4, 119.0, 139.3, 149.4, 152.3, 156.0. HRMS (FAB): expected for C₁₀H₁₄N₅O (M+H)⁺ 220.11929. Found: 220.11882. IR(neat): ν_{max} 3099, 1594, 1326 cm⁻¹. Elemental Analysis for C₁₀H₁₃N₅O·H₂O: Found: C, 51.08; H, 6.50; N, 29.09. Calculated: C, 50.62; H, 6.37; N, 29.52.

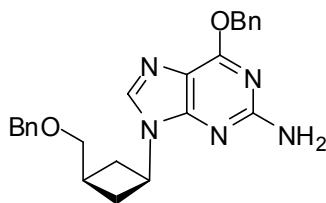
O⁶-Benzylguanine (79)



To a dry 3-necked round bottomed flask under argon was added 530 mg (13.5 mmol) of NaH (60% in mineral oil) followed by 30 mL of dry 1,4-dioxane. To this mixture was then added benzyl alcohol (1.40 mL, 13.5 mmol) dropwise. The mixture was allowed to stir at room temperature. After three hours, 2-amino-6-chloropurine **126** (1.14 g, 6.74 mmol) was added all at once. The mixture was heated to 105°C and allowed to stir overnight. The solution was then warmed to room temperature and 100 mL of H₂O was added. The solution was filtered and the pH was adjusted to 6. Overnight refrigeration allowed fine crystals to form

which were filtered by vacuum. The crude material was then purified by column chromatography (15:1 CH₂Cl₂/ MeOH) which gave the product as white crystals (56% yield). R_f: 0.29 (9:1 CH₂Cl₂/MeOH). mp: 198 – 199 °C. ¹H-NMR ([[(CD₃)₂SO], 400 MHz): σ 4.11 (s, br, 1H), 5.48 (s, 1H), 6.30 (s, br, 2H), 7.32 – 7.42 (m, 3H), 7.50 (d, 2H, *J* = 6.8 Hz), 7.83 (s, 1H). ¹³C-NMR ([[(CD₃)₂SO], 150 Mz): σ 48.5, 66.7, 66.8, 108.9, 128.1, 128.3, 128.4, 128.5, 136.8, 137.8, 159.7. HRMS (FAB): expected for C₁₂H₁₁N₅O (M+H)⁺ 242.10364. Found: 242.10337. IR(neat): ν_{max} 3188, 2797, 1589 cm⁻¹.

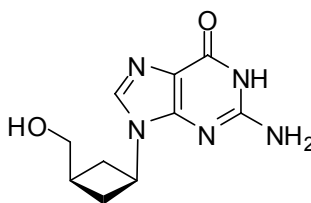
9-[*cis*-3-(Benzyloxymethyl)cyclobutyl]O⁶-benzylguanine (**127**)



To a dry 100 mL round bottomed flask fitted with a condenser was added 0.56 g (2.31 mmol) of O⁶-benzylguanine **79**, 0.31 g (1.15 mmol) of *trans*-3-(benzyloxymethyl)cyclobutyl methanesulfonate **122**, 0.33 g (2.39 mmol) of anhydrous K₂CO₃, and 0.33 g (1.23 mmol) of 18-crown-6. The contents of the flask were placed under high vacuum for six hours to ensure the dryness of the reagents. The flask was refilled with argon and 13 mL of dry DMF was added. The mixture was heated to 115 °C for 25 hours. The reaction was then cooled to room temperature and quenched with 50 mL of water. The product was extracted using EtOAc (5 x 50 mL) and the organic layers were washed with brine and concentrated. The crude material was purified by column chromatography (15:1 CH₂Cl₂/MeOH) to give 0.393 mg (85% yield) of product as

a yellow oil (R_f ; 0.75; 15:1 $\text{CH}_2\text{Cl}_2/\text{MeOH}$). $^1\text{H-NMR}$ (CDCl_3 , 400 MHz): σ 2.40 – 2.50 (m, 3H), 2.62 – 2.68 (m, 2H), 3.54 (d, 2H, $J = 4.8$ Hz), 4.57 (s, 2H), 4.78 – 4.89 (m, 1H), 5.56 (s, 2H), 7.24 – 7.52 (m, 10 H), 7.76 (s, 1H). $^{13}\text{C-NMR}$ (CDCl_3 , 100 Mz): σ 28.7, 33.4, 44.9, 46.9, 68.1, 73.4, 116.1, 127.8, 127.9, 128.1, 128.4, 128.5, 128.7, 136.7, 138.0, 138.5, 154.2, 159.1, 161.2. HRMS (FAB): expected for $\text{C}_{24}\text{H}_{26}\text{N}_5\text{O}_2$ ($\text{M}+\text{H}$) $^+$ 416.20810. Found: 416.20803. IR(neat): ν_{max} 3329, 3199, 2360, 1579 cm^{-1} . Elemental Analysis for $\text{C}_{24}\text{H}_{25}\text{N}_5\text{O}_2$: Found: C, 70.33; H, 6.71; N, 15.01. Calculated: C, 69.38; H, 6.06; N, 16.86.

9-[*cis*-3-(Hydroxymethyl)cyclobutyl]guanine (101)



To a round bottomed flask containing 0.11 g (0.273 mmol) of 9-[*cis*-3-(benzyloxymethyl)cyclobutyl]O⁶-benzylguanine **127** was added 2.5 mL of dry CH_2Cl_2 . The solution was cooled to -78°C and 2.8 mL of boron trichloride (1.0 M in CH_2Cl_2) was added dropwise. The solution was allowed to stir at -78°C for five hours and was then warmed to room temperature. The reaction was quenched with 3 mL of 7N methanolic ammonia and was then concentrated. The crude material was purified by column chromatography using 4:1 $\text{CH}_2\text{Cl}_2/\text{MeOH}$ to give 32.7 mg (51 % yield) of pure product. (R_f : 0.10, 9:1 $\text{CH}_2\text{Cl}_2/\text{MeOH}$). mp: 271°C . $^1\text{H-NMR}$ ($[(\text{CD}_3)_2\text{SO}]$, 600 MHz): σ 2.17 – 2.26 (m, 3H), 2.39 – 2.43 (m, 2H), 3.46 (s, 2H), 4.58 – 4.64 (m, 2H), 6.43 (br s, 2H), 7.85 (s, 1H), 10.63 (s, 1H). $^{13}\text{C-NMR}$ ($[(\text{CD}_3)_2\text{SO}]$, 150 Mz): σ 30.2, 32.6, 43.8, 64.3, 116.7, 135.5, 150.9, 153.5,

157.0. HRMS (FAB): expected for $C_{10}H_{14}N_5O_2$ (M+H)⁺ 236.11420. Found: 236.11408. IR(neat): ν_{max} 3392, 3310, 3191, 1627 cm^{-1} . Elemental Analysis for $C_{10}H_{15}N_5O_3 \cdot H_2O$: Found: C, 46.61; H, 5.76; N, 27.00. Calculated: C, 47.42; H, 5.97; N, 27.65. The relative stereochemistry was established by X-ray crystallographic analysis.

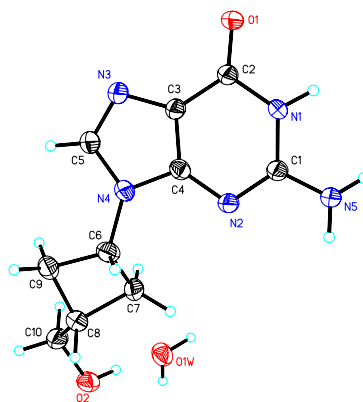


Table 5. Crystal data and structure refinement for Kba68fs.

Identification code	kba68fs	
Empirical formula	C ₁₀ H ₁₅ N ₅ O ₃	
Formula weight	253.27	
Temperature	173(2) K	
Wavelength	0.71073 Å	
Crystal system	Monoclinic	
Space group	P2(1)/c	
Unit cell dimensions	a = 12.486(4) Å	a = 90°.
	b = 11.582(3) Å	b = 101.770(6)°.
	c = 8.391(3) Å	g = 90°.
Volume	1188.0(6) Å ³	
Z	4	
Density (calculated)	1.416 Mg/m ³	
Absorption coefficient	0.108 mm ⁻¹	
F(000)	536	
Crystal size	0.42 x 0.22 x 0.12 mm ³	

Theta range for data collection	1.67 to 28.31°.
Index ranges	-16<=h<=16, -15<=k<=15, -11<=l<=11
Reflections collected	16020
Independent reflections	2954 [R(int) = 0.0391]
Completeness to theta = 28.31°	99.9 %
Absorption correction	Semi-empirical from equivalents
Max. and min. transmission	0.9872 and 0.9562
Refinement method	Full-matrix least-squares on F ²
Data / restraints / parameters	2954 / 0 / 223
Goodness-of-fit on F ²	1.096
Final R indices [I>2sigma(I)]	R1 = 0.0555, wR2 = 0.1389
R indices (all data)	R1 = 0.0643, wR2 = 0.1450
Largest diff. peak and hole	0.395 and -0.200 e.Å ⁻³

Table 6. Atomic coordinates ($\times 10^4$) and equivalent isotropic displacement parameters ($\text{Å}^2 \times 10^3$) for Kba68fs. U(eq) is defined as one third of the trace of the orthogonalized U_{ij} tensor.

	x	y	z	U(eq)
C(1)	1220(1)	8900(1)	4469(2)	24(1)
C(2)	111(1)	7446(1)	2760(2)	24(1)
C(3)	807(1)	6640(1)	3729(2)	23(1)
C(4)	1635(1)	7057(1)	4938(2)	23(1)
C(5)	1663(1)	5166(2)	4838(2)	29(1)
C(6)	3119(1)	6129(2)	7009(2)	29(1)
C(7)	4199(1)	6693(2)	6790(2)	32(1)
C(8)	4793(1)	5762(2)	7966(2)	29(1)
C(9)	3745(2)	5010(2)	7505(3)	36(1)
C(10)	5859(2)	5275(2)	7688(2)	33(1)
N(1)	383(1)	8577(1)	3214(2)	24(1)
N(2)	1888(1)	8160(1)	5374(2)	24(1)
N(3)	836(1)	5442(1)	3680(2)	28(1)
N(4)	2193(1)	6105(1)	5641(2)	26(1)
N(5)	1362(1)	10032(1)	4740(2)	32(1)

O(1)	-661(1)	7238(1)	1607(2)	31(1)
O(2)	6715(1)	6103(1)	8080(2)	34(1)
O(1W)	7152(1)	7310(1)	5610(2)	41(1)

Table 7. Bond lengths [Å] and angles [°] for Kba68fs.

C(1)-N(2)	1.322(2)
C(1)-N(5)	1.337(2)
C(1)-N(1)	1.376(2)
C(2)-O(1)	1.2415(19)
C(2)-N(1)	1.387(2)
C(2)-C(3)	1.415(2)
C(3)-C(4)	1.380(2)
C(3)-N(3)	1.389(2)
C(4)-N(2)	1.349(2)
C(4)-N(4)	1.371(2)
C(5)-N(3)	1.304(2)
C(5)-N(4)	1.375(2)
C(6)-N(4)	1.454(2)
C(6)-C(9)	1.527(2)
C(6)-C(7)	1.542(2)
C(7)-C(8)	1.546(2)
C(8)-C(10)	1.506(3)
C(8)-C(9)	1.554(2)
C(10)-O(2)	1.424(2)
N(2)-C(1)-N(5)	119.45(15)
N(2)-C(1)-N(1)	123.76(14)
N(5)-C(1)-N(1)	116.78(14)
O(1)-C(2)-N(1)	120.36(14)
O(1)-C(2)-C(3)	127.41(15)
N(1)-C(2)-C(3)	112.22(13)
C(4)-C(3)-N(3)	110.56(14)
C(4)-C(3)-C(2)	118.16(14)
N(3)-C(3)-C(2)	131.26(14)

N(2)-C(4)-N(4)	125.06(14)
N(2)-C(4)-C(3)	129.07(14)
N(4)-C(4)-C(3)	105.86(14)
N(3)-C(5)-N(4)	113.58(15)
N(4)-C(6)-C(9)	118.64(15)
N(4)-C(6)-C(7)	119.21(15)
C(9)-C(6)-C(7)	88.91(13)
C(6)-C(7)-C(8)	86.90(13)
C(10)-C(8)-C(7)	119.11(16)
C(10)-C(8)-C(9)	118.51(16)
C(7)-C(8)-C(9)	87.81(13)
C(6)-C(9)-C(8)	87.15(13)
O(2)-C(10)-C(8)	110.94(15)
C(1)-N(1)-C(2)	124.91(13)
C(1)-N(2)-C(4)	111.86(13)
C(5)-N(3)-C(3)	104.12(14)
C(4)-N(4)-C(5)	105.86(14)
C(4)-N(4)-C(6)	125.18(14)
C(5)-N(4)-C(6)	128.89(14)

Symmetry transformations used to generate equivalent atoms:

Table 8. Anisotropic displacement parameters ($\text{\AA}^2 \times 10^3$) for Kba68fs. The anisotropic displacement factor exponent takes the form: $-2p^2 [h^2 a^* 2U^{11} + \dots + 2hka^* b^* U^{12}]$

	U ¹¹	U ²²	U ³³	U ²³	U ¹³	U ¹²
C(1)	20(1)	24(1)	26(1)	-1(1)	3(1)	0(1)
C(2)	21(1)	23(1)	26(1)	-1(1)	2(1)	1(1)
C(3)	23(1)	20(1)	26(1)	-2(1)	3(1)	1(1)
C(4)	20(1)	24(1)	24(1)	1(1)	4(1)	4(1)
C(5)	31(1)	22(1)	33(1)	0(1)	0(1)	3(1)
C(6)	26(1)	31(1)	26(1)	-2(1)	-1(1)	3(1)
C(7)	28(1)	23(1)	41(1)	4(1)	-1(1)	1(1)

C(8)	29(1)	29(1)	28(1)	1(1)	0(1)	1(1)
C(9)	29(1)	32(1)	41(1)	13(1)	-2(1)	-3(1)
C(10)	29(1)	28(1)	40(1)	-2(1)	-2(1)	1(1)
N(1)	22(1)	21(1)	26(1)	2(1)	-2(1)	2(1)
N(2)	21(1)	23(1)	25(1)	-2(1)	1(1)	1(1)
N(3)	28(1)	21(1)	33(1)	-1(1)	0(1)	2(1)
N(4)	24(1)	23(1)	28(1)	1(1)	0(1)	5(1)
N(5)	29(1)	22(1)	37(1)	-2(1)	-9(1)	1(1)
O(1)	27(1)	26(1)	35(1)	-4(1)	-8(1)	1(1)
O(2)	26(1)	37(1)	35(1)	4(1)	-2(1)	-4(1)
O(1W)	30(1)	38(1)	51(1)	13(1)	1(1)	-2(1)

Table 9. Hydrogen coordinates ($\times 10^4$) and isotropic displacement parameters ($\text{\AA}^2 \times 10^3$) for Kba68fs.

	x	y	z	U(eq)
H(1)	-1(18)	9130(20)	2610(30)	36(5)
H(2)	955(18)	10530(19)	4180(30)	35(6)
H(3)	1886(18)	10212(18)	5590(30)	34(5)
H(4)	1879(16)	4418(18)	5130(20)	29(5)
H(5)	2865(17)	6468(18)	7920(30)	37(6)
H(6)	4342(13)	6551(14)	5730(20)	12(4)
H(7)	4319(19)	7540(20)	7080(30)	45(6)
H(8)	4920(20)	6031(19)	9190(30)	47(6)
H(9)	3496(19)	4500(20)	8280(30)	49(7)
H(10)	3807(15)	4554(17)	6550(20)	25(5)
H(11)	5742(19)	5030(20)	6520(30)	47(6)
H(12)	6061(18)	4600(20)	8380(30)	39(6)
H(13)	6750(20)	6540(20)	7250(30)	54(7)
H(1W)	6910(20)	7810(20)	4790(40)	61(8)
H(2W)	7850(20)	7450(20)	5960(30)	53(7)

Table 10. Torsion angles [°] for Kba68fs.

O(1)-C(2)-C(3)-C(4)	178.71(16)
N(1)-C(2)-C(3)-C(4)	-0.5(2)
O(1)-C(2)-C(3)-N(3)	0.2(3)
N(1)-C(2)-C(3)-N(3)	-178.97(16)
N(3)-C(3)-C(4)-N(2)	179.76(15)
C(2)-C(3)-C(4)-N(2)	1.0(3)
N(3)-C(3)-C(4)-N(4)	0.51(18)
C(2)-C(3)-C(4)-N(4)	-178.28(14)
N(4)-C(6)-C(7)-C(8)	-145.45(15)
C(9)-C(6)-C(7)-C(8)	-22.86(14)
C(6)-C(7)-C(8)-C(10)	144.15(16)
C(6)-C(7)-C(8)-C(9)	22.46(14)
N(4)-C(6)-C(9)-C(8)	145.82(16)
C(7)-C(6)-C(9)-C(8)	22.73(14)
C(10)-C(8)-C(9)-C(6)	-144.91(17)
C(7)-C(8)-C(9)-C(6)	-22.68(14)
C(7)-C(8)-C(10)-O(2)	71.7(2)
C(9)-C(8)-C(10)-O(2)	176.36(15)
N(2)-C(1)-N(1)-C(2)	1.7(2)
N(5)-C(1)-N(1)-C(2)	-179.69(15)
O(1)-C(2)-N(1)-C(1)	-179.99(15)
C(3)-C(2)-N(1)-C(1)	-0.7(2)
N(5)-C(1)-N(2)-C(4)	-179.74(15)
N(1)-C(1)-N(2)-C(4)	-1.2(2)
N(4)-C(4)-N(2)-C(1)	179.00(15)
C(3)-C(4)-N(2)-C(1)	-0.1(2)
N(4)-C(5)-N(3)-C(3)	-0.7(2)
C(4)-C(3)-N(3)-C(5)	0.11(19)
C(2)-C(3)-N(3)-C(5)	178.70(17)
N(2)-C(4)-N(4)-C(5)	179.82(15)
C(3)-C(4)-N(4)-C(5)	-0.89(18)
N(2)-C(4)-N(4)-C(6)	2.5(3)
C(3)-C(4)-N(4)-C(6)	-178.22(15)

N(3)-C(5)-N(4)-C(4)	1.1(2)
N(3)-C(5)-N(4)-C(6)	178.25(16)
C(9)-C(6)-N(4)-C(4)	-171.99(16)
C(7)-C(6)-N(4)-C(4)	-65.7(2)
C(9)-C(6)-N(4)-C(5)	11.3(3)
C(7)-C(6)-N(4)-C(5)	117.6(2)

Symmetry transformations used to generate equivalent atoms:

Table 11. Hydrogen bonds for Kba68fs [\AA and $^\circ$].

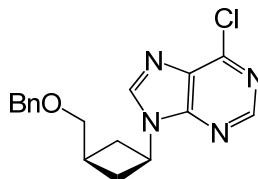
D-H...A	d(D-H)	d(H...A)	d(D...A)	\angle (DHA)
N(1)-H(1)...N(3)#1	0.90(2)	2.02(2)	2.919(2)	177(2)
N(5)-H(2)...O(1)#1	0.84(2)	2.09(2)	2.858(2)	150(2)
N(5)-H(3)...O(2)#2	0.89(2)	2.14(2)	2.976(2)	157.4(19)
O(2)-H(13)...O(1W)	0.87(3)	1.79(3)	2.648(2)	166(3)
O(1W)-H(1W)...O(2)#3	0.90(3)	1.89(3)	2.777(2)	168(3)
O(1W)-H(2W)...O(1)#4	0.87(3)	1.86(3)	2.738(2)	178(3)

Symmetry transformations used to generate equivalent atoms:

#1 $-x, y+1/2, -z+1/2$ #2 $-x+1, y+1/2, -z+3/2$ #3 $x, -y+3/2, z-1/2$

#4 $x+1, -y+3/2, z+1/2$

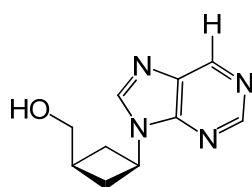
9-[*cis*-3-(Benzyloxymethyl)cyclobutyl]-6-chloropurine (**128**)



To a dry 100 mL flask filled with argon was added *trans*-3-(benzyloxymethyl)cyclobutanol **63** (0.32 g, 1.67 mmol), triphenylphosphine (0.93 g, 3.5 mmol), and 6-chloropurine **82** (0.52 g, 3.4 mmol). To the reagents was

added 3 mL of dry THF and the mixture was cooled to 0°C. A solution of diisopropyl azodicarboxylate (DIAD) (0.69 mL, 3.5 mmol) in 1.4 mL of dry THF was added dropwise. The mixture was allowed to warm to room temperature and was stirred for 24 hours before quenching with 10 mL of methanol. The solution was then concentrated and purified by short column using 3:1 to 1:1 Hex/EtOAc. This yielded 203 mg (45%) of pure product (R_f : 0.22, 1:1 Hex/EtOAc). mp: 78-79°C. ^1H NMR (CDCl_3 , 600 MHz): δ 2.57 (3H, m), 2.74 (2H, m), 3.57 (2H, d, $J = 3.6\text{Hz}$), 4.58 (2H, s), 5.03 (1H, m), 7.27-7.40 (5H, m), 8.29 (1H, s), 8.73 (1H, s); ^{13}C NMR (CDCl_3 , 150 MHz): δ 28.8, 32.1, 32.9, 45.9, 72.5, 73.5, 127.8, 128.0, 128.7, 131.9, 138.4, 144.0, 151.1, 151.9, 156.6. HRMS (ESI): expected for $\text{C}_{17}\text{H}_{18}\text{N}_4\text{O}$ ($\text{M}+\text{H}$) $^+$ 329.11637. Found: 329.11634. IR(neat): ν_{max} 3304, 2981, 1712, 1225 cm^{-1} . Elemental Analysis for $\text{C}_{17}\text{H}_{17}\text{N}_4\text{O}\cdot\text{H}_2\text{O}$: Found: C, 51.43; H, 7.44; N, 14.23. Calculated: C, 53.55; H, 6.06; N, 14.63.

9-[*cis*-3-(Hydroxymethyl)cyclobutyl]purine (117)



To a flask containing 40 mL of liquid ammonia at -78°C was added sodium metal until the solution remained a dark blue color. To the blue solution was added 9-[*cis*-3-(benzyloxymethyl)cyclobutyl]-6-chloropurine **128** (0.31 mg, 0.93 mmol) dissolved in 8 mL of THF. The mixture was allowed to stir for 45 minutes and

ammonium chloride (20 mg) was added to quench the reaction. This caused the blue color to lighten to a peach colored mixture. The ammonia was evaporated and the remaining solid was purified by column chromatography (9:1 CH₂Cl₂/MeOH). After further purification by HPLC, the product was obtained as a white solid (53.1 mg, 28%). Mp: 71-73°C. Rf: 0.27 (9:1 CH₂Cl₂/MeOH). ¹H NMR [(CD₃)₂SO], 600 MHz): δ 2.32 – 2.36 (1H, m), 2.39 – 2.44 (2H, m), 2.52 – 2.57 (2H, m), 3.30 (1H, s), 3.51 (2H, t, *J* = 5.4 Hz), 5.00 (1H, m), 8.75 (1H, s), 8.93 (1H, s), 9.15 (1H, s). ¹³C NMR [(CD₃)₂SO], 150 MHz): δ 30.4, 32.2, 44.8, 64.4, 134.0, 145.6, 147.9, 150.9, 151.8. HRMS (ESI): expected for C₁₀H₁₃N₄O (M+H)⁺ 205.10839. Found: 205.10824. IR(neat) *v*_{max}: 3224, 3071, 1601 cm⁻¹. Elemental Analysis for C₁₀H₁₂N₄O·H₂O: Found: C, 54.30; H, 5.90; N, 25.10. Calculated: C, 54.04; H, 6.35; N, 25.21. The relative stereochemistry was established by X-ray crystallographic analysis.

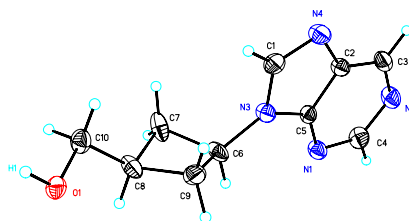


Table 12. Crystal data and structure refinement for KB78.

Identification code	kb78	
Empirical formula	C ₁₀ H ₁₄ N ₄ O ₂	
Formula weight	222.25	
Temperature	173(2) K	
Wavelength	0.71073 Å	
Crystal system	Monoclinic	
Space group	P2(1)/c	
Unit cell dimensions	<i>a</i> = 7.1120(3) Å	∠ = 90°.

	$b = 7.0302(14) \text{ \AA}$	$\beta = 95.92(3)^\circ$.
	$c = 21.7795(14) \text{ \AA}$	$\alpha = 90^\circ$.
Volume	1083.1(2) \AA^3	
Z	4	
Density (calculated)	1.363 Mg/m^3	
Absorption coefficient	0.099 mm^{-1}	
F(000)	472	
Crystal size	0.53 x 0.22 x 0.07 mm^3	
Theta range for data collection	1.88 to 24.71°.	
Index ranges	-8 ≤ h ≤ 8, 0 ≤ k ≤ 8, 0 ≤ l ≤ 25	
Reflections collected	2225	
Independent reflections	2226 [R(int) = 0.0659]	
Completeness to theta = 24.71°	98.8 %	
Absorption correction	Semi-empirical from equivalents	
Max. and min. transmission	0.9931 and 0.9496	
Refinement method	Full-matrix least-squares on F ²	
Data / restraints / parameters	2226 / 0 / 146	
Goodness-of-fit on F ²	1.182	
Final R indices [I > 2σ(I)]	R1 = 0.1195, wR2 = 0.2801	
R indices (all data)	R1 = 0.1244, wR2 = 0.2850	
Largest diff. peak and hole	0.677 and -0.446 e.\AA^{-3}	

Table 13. Atomic coordinates ($\times 10^4$) and equivalent isotropic displacement parameters ($\text{\AA}^2 \times 10^3$) for KB78. $U(\text{eq})$ is defined as one third of the trace of the orthogonalized U_{ij} tensor.

C(1)	2387(7)	5329(7)	942(2)	25(1)
C(2)	2405(7)	4518(6)	-2(2)	23(1)
C(3)	2402(7)	3683(7)	-574(2)	28(1)
C(4)	2474(8)	6641(8)	-1005(2)	31(1)
C(5)	2463(6)	6514(6)	6(2)	20(1)
C(6)	2623(8)	8918(7)	882(2)	28(1)
C(7)	4351(8)	9342(8)	1344(2)	33(1)
C(8)	3041(8)	10485(7)	1734(2)	30(1)

C(9)	1342(8)	9451(8)	1381(2)	33(1)
C(10)	3389(7)	10288(7)	2417(2)	29(1)
N(1)	2498(6)	7635(6)	-484(2)	27(1)
N(2)	2447(7)	4757(6)	-1081(2)	33(1)
N(3)	2472(6)	7008(6)	617(2)	24(1)
N(4)	2378(6)	3802(6)	589(2)	29(1)
O(1)	2039(5)	11392(5)	2704(1)	24(1)
O(1S)	8173(5)	393(5)	2514(2)	39(1)

Table 14. Bond lengths [Å] and angles [°] for KB78.

C(1)-N(4)	1.320(6)	C(9)-H(9A)	0.9900
C(1)-N(3)	1.381(6)	C(9)-H(9B)	0.9900
C(1)-H(1A)	0.9500	C(10)-O(1)	1.428(6)
C(2)-C(3)	1.378(6)	C(10)-H(10A)	0.9900
C(2)-N(4)	1.384(6)	C(10)-H(10B)	0.9900
C(2)-C(5)	1.404(6)	O(1)-H(1)	0.8400
C(3)-N(2)	1.341(6)	O(1S)-H(1S)	1.0079
C(3)-H(3)	0.9500	O(1S)-H(2S)	1.0873
C(4)-N(1)	1.331(6)		
C(4)-N(2)	1.335(7)	N(4)-C(1)-N(3)	113.2(4)
C(4)-H(4)	0.9500	N(4)-C(1)-H(1A)	123.4
C(5)-N(1)	1.328(6)	N(3)-C(1)-H(1A)	123.4
C(5)-N(3)	1.376(6)	C(3)-C(2)-N(4)	133.4(4)
C(6)-N(3)	1.462(6)	C(3)-C(2)-C(5)	115.7(5)
C(6)-C(9)	1.533(7)	N(4)-C(2)-C(5)	110.9(4)
C(6)-C(7)	1.535(7)	N(2)-C(3)-C(2)	120.5(5)
C(6)-H(6)	1.0000	N(2)-C(3)-H(3)	119.8
C(7)-C(8)	1.550(7)	C(2)-C(3)-H(3)	119.8
C(7)-H(7A)	0.9900	N(1)-C(4)-N(2)	128.8(5)
C(7)-H(7B)	0.9900	N(1)-C(4)-H(4)	115.6
C(8)-C(10)	1.488(6)	N(2)-C(4)-H(4)	115.6
C(8)-C(9)	1.546(7)	N(1)-C(5)-N(3)	129.0(4)
C(8)-H(8)	1.0000	N(1)-C(5)-C(2)	125.9(5)

N(3)-C(5)-C(2)	105.1(4)	C(1)-N(4)-C(2)	104.3(4)
N(3)-C(6)-C(9)	118.7(5)	C(10)-O(1)-H(1)	109.5
N(3)-C(6)-C(7)	117.3(4)	H(1S)-O(1S)-H(2S)	108
C(9)-C(6)-C(7)	89.1(4)		
N(3)-C(6)-H(6)	110.1		
C(9)-C(6)-H(6)	110.1		
C(7)-C(6)-H(6)	110.1		
C(6)-C(7)-C(8)	88.5(4)		
C(6)-C(7)-H(7A)	113.9		
C(8)-C(7)-H(7A)	113.9		
C(6)-C(7)-H(7B)	113.9		
C(8)-C(7)-H(7B)	113.9		
H(7A)-C(7)-H(7B)	111.1		
C(10)-C(8)-C(9)	119.7(4)		
C(10)-C(8)-C(7)	116.9(5)		
C(9)-C(8)-C(7)	88.1(4)		
C(10)-C(8)-H(8)	110.1		
C(9)-C(8)-H(8)	110.1		
C(7)-C(8)-H(8)	110.1		
C(6)-C(9)-C(8)	88.6(4)		
C(6)-C(9)-H(9A)	113.9		
C(8)-C(9)-H(9A)	113.9		
C(6)-C(9)-H(9B)	113.9		
C(8)-C(9)-H(9B)	113.9		
H(9A)-C(9)-H(9B)	111.1		
O(1)-C(10)-C(8)	109.7(4)		
O(1)-C(10)-H(10A)	109.7		
C(8)-C(10)-H(10A)	109.7		
O(1)-C(10)-H(10B)	109.7		
C(8)-C(10)-H(10B)	109.7		
H(10A)-C(10)-H(10B)			
C(5)-N(1)-C(4)	111.9(4)		
C(4)-N(2)-C(3)	117.2(4)		
C(5)-N(3)-C(1)	106.5(4)		
C(5)-N(3)-C(6)	127.4(4)		
C(1)-N(3)-C(6)	126.0(4)		

Symmetry transformations used to generate equivalent atoms:

Table 15. Anisotropic displacement parameters ($\text{\AA}^2 \times 10^3$) for KB78. The anisotropic displacement factor exponent takes the form: $-2\pi^2 [h^2 a^{*2} U_{11} + \dots + 2 h k a^* b^* U_{12}]$

	U ₁₁	U ₂₂	U ₃₃	U ₂₃	U ₁₃	U ₁₂
C(1)	30(3)	26(3)	19(2)	5(2)	3(2)	0(2)
C(2)	26(2)	18(2)	26(3)	-1(2)	3(2)	1(2)
C(3)	34(3)	20(2)	28(3)	-4(2)	1(2)	0(2)
C(4)	39(3)	30(3)	24(3)	0(2)	6(2)	-2(2)
C(5)	19(2)	20(2)	22(2)	-4(2)	4(2)	2(2)
C(6)	53(3)	16(2)	15(2)	0(2)	3(2)	1(2)
C(7)	35(3)	31(3)	34(3)	-12(2)	11(2)	-17(3)
C(8)	47(3)	18(2)	27(3)	-4(2)	10(3)	-4(2)
C(9)	40(3)	32(3)	26(3)	-5(2)	3(2)	18(3)
C(10)	32(3)	31(3)	24(3)	-6(2)	2(2)	0(2)
N(1)	34(2)	23(2)	23(2)	-2(2)	4(2)	1(2)
N(2)	42(3)	26(2)	30(2)	-7(2)	8(2)	-1(2)
N(3)	35(2)	21(2)	17(2)	0(2)	6(2)	3(2)
N(4)	44(3)	20(2)	22(2)	0(2)	7(2)	2(2)
O(1)	31(2)	27(2)	15(2)	-1(2)	4(2)	2(2)
O(1S)	30(2)	33(2)	54(3)	-16(2)	6(2)	-1(2)

Table 16. Hydrogen coordinates ($\times 10^4$) and isotropic displacement parameters ($\text{\AA}^2 \times 10^3$) for KB78.

	x	y	z	U(eq)
H(1A)	2341	5277	1376	30
H(3)	2368	2336	-610	33
H(4)	2477	7372	-1372	37

H(6)	2513	9893	546	34
H(7A)	5328	10124	1171	39
H(7B)	4916	8198	1554	39
H(8)	3037	11859	1615	37
H(9A)	884	8344	1604	39
H(9B)	285	10306	1233	39
H(10A)	3285	8935	2534	35
H(10B)	4683	10729	2559	35
H(1)	2167	11188	3086	36
H(1S)	8076	-912	2322	58
H(2S)	9621	892	2518	58

Table 17. Torsion angles [°] for KB78.

N(4)-C(2)-C(3)-N(2)	-179.6(5)
C(5)-C(2)-C(3)-N(2)	-0.2(7)
C(3)-C(2)-C(5)-N(1)	0.6(8)
N(4)-C(2)-C(5)-N(1)	-179.9(4)
C(3)-C(2)-C(5)-N(3)	-179.4(4)
N(4)-C(2)-C(5)-N(3)	0.1(6)
N(3)-C(6)-C(7)-C(8)	-140.2(4)
C(9)-C(6)-C(7)-C(8)	-18.1(4)
C(6)-C(7)-C(8)-C(10)	140.5(5)
C(6)-C(7)-C(8)-C(9)	17.9(4)
N(3)-C(6)-C(9)-C(8)	139.0(5)
C(7)-C(6)-C(9)-C(8)	18.1(4)
C(10)-C(8)-C(9)-C(6)	-138.0(5)
C(7)-C(8)-C(9)-C(6)	-17.9(4)
C(9)-C(8)-C(10)-O(1)	-74.4(6)
C(7)-C(8)-C(10)-O(1)	-178.7(4)
N(3)-C(5)-N(1)-C(4)	180.0(5)
C(2)-C(5)-N(1)-C(4)	0.0(7)
N(2)-C(4)-N(1)-C(5)	-1.0(8)
N(1)-C(4)-N(2)-C(3)	1.4(9)

C(2)-C(3)-N(2)-C(4)	-0.6(8)
N(1)-C(5)-N(3)-C(1)	178.9(5)
C(2)-C(5)-N(3)-C(1)	-1.0(5)
N(1)-C(5)-N(3)-C(6)	-3.4(8)
C(2)-C(5)-N(3)-C(6)	176.6(5)
N(4)-C(1)-N(3)-C(5)	1.8(6)
N(4)-C(1)-N(3)-C(6)	-175.9(5)
C(9)-C(6)-N(3)-C(5)	137.2(5)
C(7)-C(6)-N(3)-C(5)	-117.7(5)
C(9)-C(6)-N(3)-C(1)	-45.6(7)
C(7)-C(6)-N(3)-C(1)	59.5(7)
N(3)-C(1)-N(4)-C(2)	-1.7(5)
C(3)-C(2)-N(4)-C(1)	-179.6(5)
C(5)-C(2)-N(4)-C(1)	1.0(6)

Symmetry transformations used to generate equivalent atoms:

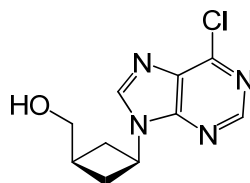
Table 18. Hydrogen bonds for KB78 [\AA and $^\circ$].

D-H...A	d(D-H)	d(H...A)	d(D...A)	$\angle(\text{DHA})$
O(1)-H(1)...N(2)#1	0.84	1.92	2.752(5)	169.6
O(1S)-H(1S)...O(1)#2	1.01	1.90	2.854(5)	157.3
O(1S)-H(2S)...O(1)#3	1.09	1.76	2.827(5)	165.5

Symmetry transformations used to generate equivalent atoms:

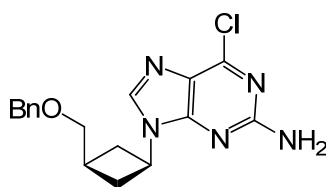
#1 $x, -y+3/2, z+1/2$ #2 $-x+1, y-3/2, -z+1/2$ #3 $x+1, y-1, z$

9-[*cis*-3-(Hydroxymethyl)cyclobutyl]-6-chloropurine (118)



To a 250 mL flask containing 0.32 g of **128** (0.98 mmol) was added 4 mL of dry CH₂Cl₂. The solution was cooled to -78 °C and 4.9 mL of BCl₃ (4.9 mmol, 5 eq) was added dropwise. The mixture was allowed to continue stirring at -78 °C for 7 hours and was then quenched with 3 mL of methanolic ammonia. The mixture was concentrated and purified by column chromatography using 9:1 CH₂Cl₂ as the eluent. This gave the product as a white solid (0.215 g, 92% yield). Rf: 0.56 (9:1 CH₂Cl₂/MeOH). Mp: 104-106°C. ¹H NMR ([(CD₃)₂SO], 300 MHz): δ 2.32 (3H, m), 2.45 (2H, m), 3.46 (2H, d), 4.94 (1H, m), 8.72 (1H, s), 8.79 (1H, s); ¹³C NMR ([(CD₃)₂SO], 75 MHz): δ 30.4, 32.2, 45.4, 131.0, 146.0, 148.8, 151.2, 151.5, 192.3. HRMS (ESI): expected for C₁₀H₁₂ClN₄O (M+H)⁺ 239.06942. Found: 239.06945. IR(neat): ν_{max} 3312, 2980, 1596, 1034 cm⁻¹. Elemental Analysis for C₁₀H₁₁ClN₄O: Found: C, 49.33; H, 4.68; N, 22.83. Calculated: C, 50.32; H, 4.65; N, 23.47.

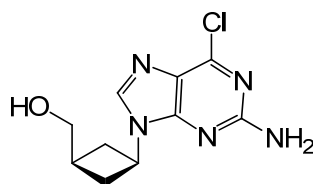
9-[*cis*-3-(Benzyloxymethyl)cyclobutyl]-2-amino-6-chloropurine (**130**)



To a dry 50 mL flask filled with argon was added 9-[*cis*-3-(benzyloxymethyl)cyclobutyl]-6-chloropurine **63** (0.83 g, 4.4 mmol), triphenylphosphine (2.4 g, 9.2 mmol), and 2-amino-6-chloropurine **129** (1.49 g, 8.8 mmol). To the reagents was added 8 mL of dry THF and the mixture was cooled to 0°C. A solution of diisopropyl azodicarboxylate (DIAD) (1.8 mL, 9.1

mmol) in 3.9 mL of dry THF was added dropwise. The mixture was allowed to warm to room temperature and was stirred for 52 hours before quenching with 10 mL of methanol. The solution was then concentrated and purified by short column using 9:1 Hex/EtOAc to 9:1 CH₂Cl₂/MeOH. This yielded 399 mg (27%) of **130** as a white gum. Rf: 0.55 (9:1 CH₂Cl₂/MeOH). ¹H NMR (CDCl₃, 400 MHz): δ 2.48 (3H, m), 2.66 (2H, m), 3.55 (2H, d, *J* = 4.4 Hz), 4.58 (2H, s), 4.80 (1H, m), 5.02 (2H, br s), 7.29-7.38 (5H, m), 7.92 (1H, s); ¹³C NMR (CDCl₃, 100 MHz): δ 28.9, 32.9, 51.0, 72.8, 73.5, 124.0, 127.8, 128.0, 128.7, 131.9, 138.4, 144.0, 151.1, 151.9. HRMS (ESI): expected for C₁₇H₁₉ClN₅O (M+H)⁺ 344.12726. Found: 344.12658. IR(neat): ν_{max} 3328, 3202, 2360, 1611, 1561 cm⁻¹. Elemental Analysis for C₁₇H₁₈ClN₅O: Found: C, 61.36; H, 6.00; N, 17.56. Calculated: C, 59.39; H, 5.28; N, 20.37.

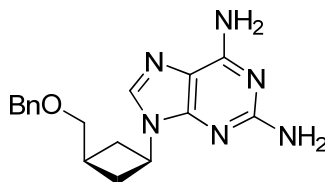
9-[*cis*-3-(Hydroxymethyl)cyclobutyl]-2-amino-6-chloropurine (119)



To a round bottomed flask containing 0.109 g (0.316 mmol) of 9-[*cis*-3-(benzyloxymethyl)cyclobutyl]-2-amino-6-chloropurine **130** was added 3.0 mL of dry CH₂Cl₂. The solution was cooled to -78°C and 3.2 mL of boron trichloride (1.0 M in CH₂Cl₂) was added dropwise. The solution was allowed to stir at -78°C for six hours. The reaction was quenched with 3 mL of 7N methanolic ammonia and was then concentrated. The crude material was purified by column

chromatography using 9:1 CH₂Cl₂/MeOH to give 40.8 mg (50.9% yield) of product as a gummy solid. Rf: 0.42 (9:1 CH₂Cl₂/MeOH). Mp: 150-151 °C. ¹H NMR ([CD₃)₂SO], 600 MHz): δ 2.21 – 2.31 (m, 3H), 2.44 – 2.48 (m, 2H), 3.48 (t, 2H, *J* = 4.8 Hz), 4.65 (t, 1H, *J* = 4.8 Hz), 4.69 – 4.75 (m, 1H), 6.87 (br s, 2H), 8.29 (s, 1H). ¹³C NMR ([CD₃)₂SO], 150 MHz): δ 30.3, 32.3, 44.5, 64.4, 123.7, 141.6, 149.4, 153.8, 159.7. HRMS (ESI): expected for C₁₀H₁₃CIN₅O (M+H)⁺ 254.08031. Found: 254.07976. IR(neat): ν_{max} 3314, 3200, 2929, 1607, 1557 cm⁻¹. Elemental Analysis for C₁₀H₁₂CIN₅O·0.65EtOAc: Found: C, 48.21; H, 5.46 N: 25.01. Calculated: C, 47.85; H, 5.65; N, 24.69.

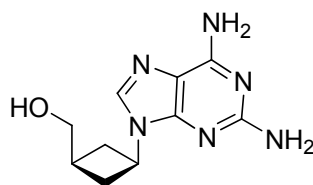
9-[*cis*-3-(Benzyloxymethyl)cyclobutyl]-2,6-diaminopurine (**131**)



To a dry 100 mL flask filled with argon containing 2,6-diaminopurine **132** (0.37 g, 2.5 mmol), 9-[*cis*-3-(benzyloxymethyl)cyclobutyl]-6-chloropurine **63** (0.33 g, 1.2 mmol), K₂CO₃ (0.36 g, 2.6 mmol), and 18-crown-6 (0.36, 1.4 mmol) was added 15 mL of dry DMF. The mixture was heated at 120°C for 15 hours and was then allowed to cool to room temperature. The reaction was quenched with water (30 mL) and the compound was extracted with EtOAc (5 x 50 mL). The organic layers were then washed with brine (2 x 50 mL), dried over MgSO₄, filtered, and concentrated. The crude product was purified by column chromatography using

9:1 CH₂Cl₂/MeOH to give the product as an off-white solid (0.20 g, 50%). Rf: 0.36 (9:1 CH₂Cl₂/MeOH). Mp: 140-141°C. ¹H NMR (CDCl₃, 400 MHz): δ 2.44 (3H, m), 2.65 (2H, m), 3.54 (2H, d), 4.57 (2H, s), 4.77 (1H, m), 4.82 (2H, br s), 5.62 (2H, br s), 7.27-7.38 (5H, m), 7.71 (1H, s); ¹³C NMR (CDCl₃, 100 MHz): δ 28.7, 33.4, 44.8, 73.1, 73.4, 81.8, 84.5, 127.8, 127.9, 128.7, 137.0, 138.5, 155.4, 159.0. HRMS (ESI): expected for C₁₇H₂₁N₆O (M+H)⁺ 325.17714. Found: 325.17668. IR(neat) ν_{max}: 3326, 3186, 1589 cm⁻¹. Elemental Analysis for C₁₇H₂₀N₆O: Found: C, 62.99; H, 6.34; N, 25.61. Calculated: C, 62.95; H, 6.21; N, 25.91.

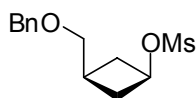
9-[*cis*-3-(Hydroxymethyl)cyclobutyl]-2,6-diaminopurine (120)



To a round bottomed flask containing 0.336 g (1.04 mmol) of 9-[*cis*-3-(benzyloxymethyl)cyclobutyl]-2,6-diaminopurine **131** was added 13.5 mL of dry CH₂Cl₂. The solution was cooled to -78°C and 6.8 mL of boron trichloride (1.0 M in CH₂Cl₂) was added dropwise. The solution was allowed to stir at -78°C for six hours. The reaction was quenched with 10 mL of 7N methanolic ammonia and was then concentrated. The crude material was purified by column chromatography using 9:1 CH₂Cl₂/MeOH to give 183 mg (75% yield) of pure product. Rf: 0.30 (4:1 CH₂Cl₂/MeOH). Mp: 197-198 °C. ¹H NMR ([CD₃]₂SO, 600 MHz): δ 2.23 – 2.27 (3H, m), 2.40 – 2.42 (2H, m), 3.36 (1H, br s), 3.47 (2H, d, *J* = 3 Hz), 4.62 – 4.68 (1H, m), 5.77 (2H, br s), 6.70 (2H, br s), 7.89 (1H, s).

^{13}C NMR ($[(\text{CD}_3)_2\text{SO}]$, 150 MHz): δ 30.1, 32.5, 43.6, 64.4, 113.9, 135.7, 151.6, 156.0, 160.0. HRMS (ESI): expected for $\text{C}_{10}\text{H}_{25}\text{N}_6\text{O}$ ($\text{M}+\text{H}$) $^+$ 235.13019. Found: 235.12978. IR(neat) ν_{max} : 3352, 3130, 2928, 1658, 1589, 1402 cm^{-1} . Elemental Analysis for $\text{C}_{10}\text{H}_{14}\text{N}_6\text{O}\cdot\text{H}_2\text{O}$: Found: C, 47.90; H, 6.43; N: 30.78. Calculated: C, 47.61; H, 6.39; N, 33.31.

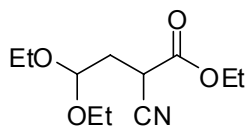
***cis*-3-(Benzyloxymethyl)cyclobutyl methanesulfonate**



To a dry round bottomed flask under argon was added 1.00 g (5.22 mmol) of *cis*-3-(benzyloxymethyl)cyclobutanol **108** and 13.3 mg (0.109 mmol) of DMAP. The oil and solid were dissolved in CH_2Cl_2 (40 mL) and the solution was stirred. Triethylamine (3.6 mL, 25.8 mmol) was then added and the solution was cooled to 0°C . After five minutes of stirring in the ice bath, 0.50 mL (6.43 mmol) of MsCl was added dropwise. The solution was then allowed to warm to room temperature after the addition and stir for 20 hours. The reaction mixture was quenched with water and was then washed with water (2 x 100 mL) and brine (100 mL). The organic layers were dried over anhydrous MgSO_4 , filtered, and concentrated. Purification was performed by column chromatography (1:1 Hex/EtOAc) to give 1.07 g of product (pale yellow oil). (R_f : 0.51; 1:1 Hex/EtOAc). ^1H -NMR (CDCl_3 , 600 MHz): σ 2.11 – 2.22 (m, 3H), 2.52 – 2.56 (m, 2H), 2.98 (s, 3H), 3.47 (d, 2H, $J = 6.0$ Hz), 4.53 (s, 2H), 4.88 – 4.93 (m, 1H), 7.29 – 7.38 (m, 5H). ^{13}C -NMR (CDCl_3 , 150 Mz): σ 26.7, 34.1, 38.5, 71.2, 73.2, 73.4, 127.8,

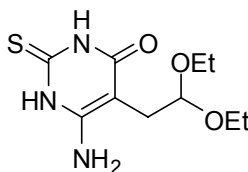
127.9, 128.6, 138.4. HRMS (FAB): expected for $C_{13}H_{19}O_4S$ (M+H)⁺ 271.0926. Found: 271.0921. IR(neat): ν_{\max} 1350, 1170 cm^{-1} .

Ethyl 2-cyano-4,4-diethoxybutanoate (140)



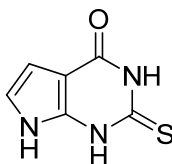
To a dry 3-necked round bottomed flask fitted with a condenser was added 11.3 g (81.5 mmol) of oven dried K_2CO_3 and 0.82 g (5.5 mmol) of NaI. The solids were placed under high vacuum for an hour to ensure dryness. The flask was refilled with argon and 44.0 mL (0.413 mol) of ethyl cyanoacetate was added followed by 13.0 mL (83.8 mmol) of bromoacetal **139**. The yellow mixture was heated to 145°C for 4.5 hours and was then cooled to room temperature. The mixture was dissolved in 100 mL of water and 100 mL of diethyl ether. The organic layer was separated and the aqueous layer was extracted with an additional 100 mL of ether. The organic layers were dried over $MgSO_4$, filtered, and concentrated. The crude material was purified by column chromatography (9:1 Hex/EtOAc) to give 14.2 g (62.0 mmol, 74% yield) of a light yellow oil. (Rf: 0.53; 1:1 Hex/EtOAc). 1H -NMR ($CDCl_3$, 600 MHz): σ 1.18 – 1.22 (m, 6H), 1.31 (t, 3H, $J = 7.2$ Hz), 2.16 – 2.21 (m, 1H), 2.24 – 2.29 (m, 1H), 3.49 – 3.55 (m, 2H), 3.64 – 3.71 (m, 3H), 4.24 (q, 2H, $J = 7.2$ Hz), 4.68 (t, 1H, $J = 5.4$ Hz). ^{13}C -NMR ($CDCl_3$, 150 Mz): σ 14.1, 15.3, 33.7, 62.8, 62.9, 100.1, 116.5, 166.0. HRMS (FAB): expected for $C_{11}H_{20}NO_4$ (M+H)⁺: 230.13868. Found: 230.13861. IR(neat): ν_{\max} 2989, 1774 cm^{-1} .

6-Amino-5-(2,2-diethoxyethyl)-2-thioxo-2,3-dihydropyrimidin-4(1H)-one (141)



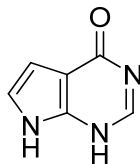
To the 250 mL round bottomed flask containing 14.2 g (61.8 mmol) of ethyl 2,2-diethoxy cyanoacetate **140** was added 110 mL of absolute ethanol followed by 28 mL of sodium ethoxide (21%, 75.0 mmol). Thiourea (5.7 g, 74.5 mmol) was added all at once and the mixture was heated to 95°C and refluxed overnight. The mixture was then cooled to room temperature and concentrated. Water (250 mL) was added and the aqueous layer was washed with diethyl ether (3 x 250 mL). The aqueous layer was then neutralized with acetic acid (1 eq.) and the precipitate was filtered. The yellow solid was dried under vacuum over P₂O₅ overnight to give 9.2 g (35.5 mmol, 57%) of crude product. ¹H-NMR (DMSO, 600 MHz): σ 1.07 (t, 6H, J = 7.2 Hz), 2.43 (d, 2H, J = 5.4 Hz), 3.37 – 3.43 (m, 6H), 3.56 – 3.61 (m, 2H), 4.50 (t, 1H, J = 5.4 Hz), 6.07 (s, 2H), 11.5 (br s, 1H), 11.7 (br s, 1H). ¹³C-NMR (DMSO, 150 Mz): σ 15.4, 27.9, 61.9, 85.7, 101.7, 151.9, 161.8, 172.9. HRMS (FAB): expected for C₁₀H₁₈N₃O₃S (M+H)⁺: 260.10634. Found: 260.10640. IR(neat): ν_{\max} 3342, 3219, 2973, 2879, 1563 cm⁻¹.

2-Thioxo-2,3-dihydro-1H-pyrrolo[2,3-d]pyrimidin-4(7H)-one (142)

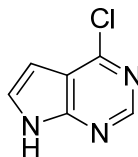


To a 500 mL Erlenmeyer flask containing 9.1 g (35.1 mmol) of 6-Amino-5-(2,2-diethoxyethyl)-2-thioxo-2,3-dihydropyrimidin-4(1H)-one **141** was added 100 mL of 0.2N HCl. The orange-yellow mixture was shaken vigorously for 22 hours. The purple mixture was then filtered under vacuum to give a gray solid. The solid was dried overnight over P₂O₅ to give 5.3 g (31.6 g) of crude product. ¹H-NMR ([[(CD₃)₂SO], 600 MHz): σ 6.33 (s, 1H), 6.72 (s, 1H), 11.28 (s, 1H), 11.86 (s, 1H). ¹³C-NMR ([[(CD₃)₂SO], 150 Mz): σ 102.3, 103.0, 118.4, 138.4, 157.8, 171.8. HRMS (FAB): expected for C₆H₆N₃OS (M+H)⁺: 168.02261. Found: 168.02255. IR(neat): ν_{max} 3534, 3106, 2879, 1669, 1606 cm⁻¹.

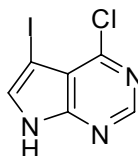
1H-Pyrrolo[2,3-d]pyrimidin-4(7H)-one (**143**)



To a 250 mL round bottomed flask was added 6.3 g of 2-thioxo-2,3-dihydro-1H-pyrrolo[2,3-d]pyrimidin-4(7H)-one **142** followed by 68 mL of H₂O. Aqueous NH₄OH (32 mL) was added followed by Raney Nickel. The mixture was stirred and refluxed for three days. The mixture was then filtered hot over a pad of celite. The filtrate was concentrated to give 2.7g (20.2 mmol, 54% yield) of product. ¹H-NMR ([[(CD₃)₂SO], 600 MHz): σ 6.43 (s, 1H), 7.03 (s, 1H), 7.82 (s, 1H), 11.84 (s, 1H). ¹³C-NMR ([[(CD₃)₂SO], 150 Mz): σ 102.0, 103.4, 107.7, 143.0, 148.1, 158.5. HRMS (ESI): expected for C₆H₆N₃O (M+H)⁺: 135.05054. Found: 136.05038. IR(neat): ν_{max} 3094, 2856, 1661, 1573 cm⁻¹.

4-Chloro-7H-pyrrolo[2,3-d]pyrimidine (144)

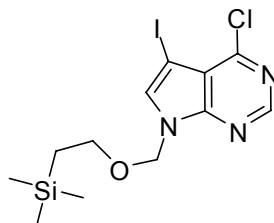
To the 500 mL round bottomed flask containing 2.5 g (18.6 mmol) of 1H-pyrrolo[2,3-d]pyrimidin-4(7H)-one **143** was added 46 mL of POCl₃. The mixture was heated to reflux for five hours. The excess POCl₃ was removed by vacuum. Ice was added and allowed to stir was the residue. The aqueous layer was extracted with diethyl ether until there was no remaining product (as indicated by TLC). The organic layer was dried over MgSO₄, filtered, and concentrated. This resulted in 1.5 g (10.0 mmol, 54% yield) of product as an off-white solid. ¹H-NMR [(CD₃)₂SO], 600 MHz): σ 6.61 (t, 1H, $J = 3$ Hz), 7.70 (t, 1H, $J = 3$ Hz), 8.59 (s, 1H). ¹³C-NMR [(CD₃)₂SO], 150 Mz): σ 98.8, 103.4, 116.6, 128.4, 150.3, 151.8. HRMS (ESI): expected for C₆H₅ClN₃ (M+H)⁺: 154.01665. Found: 154.01644. IR(neat): ν_{\max} 3119, 2962, 2816, 1553 cm⁻¹.

4-Chloro-5-iodo-7H-pyrrolo[2,3-d]pyrimidine (138)

To a dry 250 mL round bottomed flask under argon was added 1.8 g (11.9 mmol) of 4-chloro-7H-pyrrolo[2,3-d]pyrimidine **144** and 3.0 g of *N*-iodosuccinamide (13.1 mmol). The solids were dried under high vacuum for 5 hours and the flask was refilled with argon. Dry DMF (100 mL) was added and the solution was stirred in

the dark for 20 hours. The reaction was quenched with methanol and concentrated. The residue was then diluted with 150 mL of dichloromethane and washed with water (200 mL), saturated aqueous sodium sulfite (200 mL), and brine (100 mL). The organic layers were dried over MgSO₄, filtered, and concentrated. The column was run using 1:1 Hex/EtOAc as the eluent to give a white solid (3.1 g, 11.2 mmol, 95% yield). (R_f: 0.22; 1:1 Hex/EtOAc). mp: 195 – 199 °C (decomposition). ¹H-NMR ([[(CD₃)₂SO], 600 MHz): σ 7.94 (s, 1H), 8.59 (s, 1H). ¹³C-NMR ([[(CD₃)₂SO], 150 Mz): σ 51.7, 115.8, 133.9, 150.4, 150.7, 151.5. HRMS (FAB): expected for C₆H₃ClIN₃I (M+H)⁺: 279.91329. Found: 279.91316. IR(neat): ν_{max} 3061, 2819, 1593, 1158 cm⁻¹. Elemental Analysis for C₆H₃ClIN₃: Found: C, 26.33; H, 1.13; N, 14.94. Calculated: C, 25.79; H, 1.08; N, 15.04.

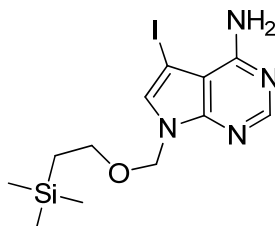
4-Chloro-5-iodo-7-((2-(trimethylsilyl)ethoxy)methyl)-7H-pyrrolo[2,3-d]pyrimidine (153)



To a dry 100 mL round bottomed flask under argon containing 1.1 g (3.8 mmol) of 4-chloro-5-iodo-7H-pyrrolo[2,3-d]pyrimidine **138** was added 0.17 g (4.3 mmol) of sodium hydride (60% in mineral oil). Dry DMF (38 mL) was added and the solution was stirred at room temperature for 40 minutes. Then 0.77 mL of SEMCl was added dropwise and the reaction mixture was allowed to stir to 30

minutes. The reaction was then quenched with brine and the solution was diluted with 150 mL dichloromethane and washed with water (3 x 100 mL). The organic layer was dried over MgSO₄, filtered, and concentrated. The column was run using 9:1 Hex/EtOAc to give 1.3 (3.2 mmol, 86%) of product as a white solid. (Rf: 0.52; 3:1 Hex/EtOAc). mp: 97 – 98 °C. ¹H-NMR (CDCl₃, 600 MHz): σ -0.027 (s, 9H), 0.93 (t, 2H, *J* = 8.1 Hz), 3.5 (t, 2H, *J* = 8.1 Hz), 5.63 (s, 2H), 7.55 (s, br, 1H), 8.66 (s, br, 1H). ¹³C-NMR (CDCl₃, 150 Mz): σ -1.3, 17.9, 52.7, 67.3, 73.4, 101.3, 119.5, 134.7, 151.5, 153.1. HRMS (FAB): expected for C₁₂H₁₇ClN₃IOSi (M+H)⁺: 408.99469. Found: 409.99448. IR(neat): ν_{\max} 3061, 2916, 1727, 1346, 1196 cm⁻¹. Elemental Analysis for C₁₂H₁₇ClIN₃OSi: Found: C, 35.69; H, 4.22; N, 10.21. Calculated: C, 35.18; H, 4.18; N, 10.26.

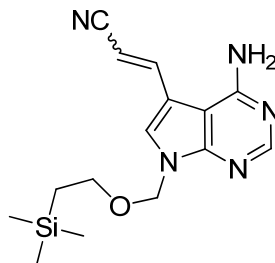
5-iodo-7-((2-(trimethylsilyl)ethoxy)methyl)-7H-pyrrolo[2,3-d]pyrimidin-4-amine (154)



To a pressure vessel was added 1.3 g (3.2 mmol) of 4-chloro-5-iodo-7-((2-(trimethylsilyl)ethoxy)methyl)-7H-pyrrolo[2,3-d] pyrimidine **153** in 81 mL of 1,4-dioxane and 81 mL of ammonium hydroxide. The vessel was sealed and heated to 100°C for five hours. The solution was cooled to room temperature and then concentrated. The residue was diluted with 200 mL CH₂Cl₂. The solution was washed with water (2 x 100 mL) and brine (100 mL). The organic layer was dried over MgSO₄, filtered, and concentrated to yield 1.2 g (3.0 mmol) of product as a

white solid. (Rf: 0.23; 1:1 Hex/EtOAc). mp: 126 - 128 °C. $^1\text{H-NMR}$ (CDCl_3 , 600 MHz): σ -0.038 (s, 9H), 0.92 (t, 2H, $J = 8.4$ Hz), 3.53 (t, 2H, $J = 8.4$ Hz), 5.53 (s, 2H), 5.75 (s, br, 1H), 7.21 (s, 1H), 8.30 (s, 1H). $^{13}\text{C-NMR}$ (CDCl_3 , 150 Mz): σ - 1.2, 17.9, 50.9, 66.8, 73.0, 104.0, 129.1, 151.1, 152.9, 157.2. HRMS (FAB): expected for $\text{C}_{12}\text{H}_{20}\text{IN}_4\text{OSi}$ ($\text{M}+\text{H}$) $^+$: 391.04456. Found: 391.04431. IR(neat): ν_{max} 3464, 3074, 2951, 2898, 1649, 1556, 1263, 1094 cm^{-1} . Elemental Analysis for $\text{C}_{12}\text{H}_{19}\text{IN}_4\text{OSi}$: Found: C, 37.88; H, 5.09; N, 14.05. Calculated: C, 36.93; H, 4.91; N, 14.35.

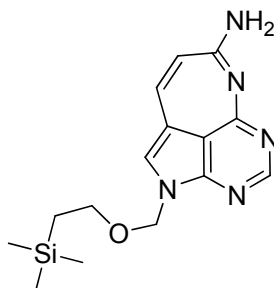
3-(4-amino-7-((2-(trimethylsilyl)ethoxy)methyl)-7H-pyrrolo[2,3-d]pyrimidin-5-yl)acrylonitrile (155)



To the 250 mL round bottomed flask containing 1.2 g (3.0 mmol) of 5-iodo-7-((2-(trimethylsilyl)ethoxy)methyl)-7H-pyrrolo[2,3-d]pyrimidin-4-amine **154** was added 0.17 g (0.92 mmol) of CuI and 27 mL of dry DMF. Then 3.9 mL (59.2 mmol) of acrylonitrile, 0.84 mL (6.0 mmol) of Et_3N , and 0.35 g (0.31 mmol) of $\text{Pd}(\text{Ph}_3\text{P})_4$ were added. The dark red solution was heated to 70 °C. After 24 hours, the solution was cooled to room temperature and stirred for 1 hour with Dowex. The mixture was filtered and the filtrate was concentrated. The residue was diluted with 100 mL of CH_2Cl_2 and washed with water (3 x 100 mL). The organic layer was dried over MgSO_4 , filtered, and concentrated. The column was run using

1:2 Hex/EtOAc (Rf: 0.66; 9:1 CH₂Cl₂/MeOH) to give a yellow solid as a 1:1 mixture of E:Z isomers (81% yield). mp: 161-163 °C. ¹H-NMR (CDCl₃, 600 MHz): σ -0.038 (s, 9H), 0.94 (t, 2H, *J* = 8.4 Hz), 3.54 – 3.60 (m, 2H), 5.36 – 5.44 (m, 2H), 5.59 (s, 1H, minor), 5.62 (s, 1H, major), 5.73 (d, 1H, minor, *J* = 16.2 Hz), 7.32 (d, 1H, major, *J* = 11.4 Hz), 7.45 (m, 1H, major), 7.57 (m, 1H, minor), 8.15 (s, 1H), 8.37 (s, 2H). ¹³C-NMR (CDCl₃, 150 Mz): σ -1.3, 17.9, 67.1, 73.5, 93.1, 95.5, 100.9, 102.0, 112.1, 118.3, 118.5, 126.2, 127.2, 128.8, 132.3, 139.7, 142.8, 151.9, 153.1, 157.5, 157.6. HRMS (ESI): expected for C₁₅H₂₂N₅OSi (M+H)⁺: 316.15881. Found: 316.15841. IR(neat): ν_{max} 3477, 3086, 2954, 2203, 1645, 1577 cm⁻¹. Elemental Analysis for C₁₅H₂₁N₅OSi: Found: C, 58.39; H, 6.71; N, 19.96. Calculated: C, 57.11; H, 6.71; N, 22.20.

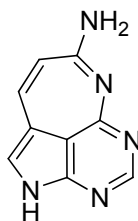
7-amino-2-(2-(trimethylsilyl)ethoxy)methyl)-2H-2,3,5,6-tetraazabenz[cd]azulene (156)



To a dry 100 mL round bottomed flask under argon was added 0.71 g (2.2 mmol) of 3-(4-amino-7-((2-(trimethylsilyl)ethoxy)methyl)-7H-pyrrolo[2,3-d]pyrimidin-5-yl)acrylonitrile **155** and 9.2 mL of 0.5M NaOMe in MeOH. The yellow mixture was heated to 60 °C and stirred for 20 hours. The mixture was concentrated and the column was run using 9:1 CH₂Cl₂/MeOH and then 4:1 CH₂Cl₂/MeOH. (Rf: 0.23, 9:1 CH₂Cl₂/MeOH). mp: 180°C (decomp). ¹H-NMR ([CD₃]₂SO), 600 MHz): σ -

0.073 (s, 9H), 0.83 (t, 2H, $J = 8.4$ Hz), 3.51 (t, 2H, $J = 8.4$ Hz), 5.51 (s, 2H), 5.90 (s, br, 1H), 7.25 (s, br, 1H), 7.69 (s, br, 1H), 8.31 (s, br, 1H). $^{13}\text{C-NMR}$ ($[(\text{CD}_3)_2\text{SO}]$, 150 Mz): σ -0.71, 17.8, 66.6, 73.6, 109.6, 126.1, 139.4, 151.1, 152.9, 157.2. HRMS (FAB): expected for $\text{C}_{15}\text{H}_{22}\text{N}_5\text{OSi}$ ($\text{M}+\text{H}$) $^+$: 316.15881. Found: 316.15871. IR(neat): ν_{max} 3325, 2952, 1624, 1081 cm^{-1} . Elemental Analysis for $\text{C}_{15}\text{H}_{21}\text{N}_5\text{OSi}\cdot 2\text{H}_2\text{O}$: Found: C, 51.09; H, 6.43; N, 19.50. Calculated: C, 51.26; H, 7.17; N, 19.93.

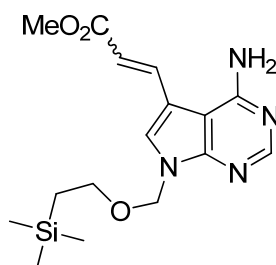
7-amino-2H-2,3,5,6-tetraazabenzocd]azulene (152)



To a dry round bottomed flask containing 0.38 g (1.2 mmol) of 7-amino-2-(2-(trimethylsilyl)ethoxy)methyl)-2H-2,3,5,6-tetraazabenzocd]azulene **156** was added 36 mL of dry CH_2Cl_2 . The yellow solution was cooled to 0°C and 0.76 mL (6.1 mmol) of $\text{BF}_3\cdot\text{OEt}_2$ was added dropwise. The yellow mixture was stirred at 0°C for 30 minutes and then at room temperature for 30 additional minutes. Then 2.2 mL (12.1 mmol) of 5.5M aqueous NaOAc solution was added and the mixture was heated to reflux. The mixture was refluxed for 45 minutes and cooled to room temperature and concentrated. A short column was run using 9:1 $\text{CH}_2\text{Cl}_2/\text{MeOH}$ to prevent the elution of boron salts. However, salts did elute with the extremely polar product, though three separate columns were run. mp: 230°C (decomp). $^1\text{H-NMR}$ (DMSO, 600 MHz): σ 5.89 (d, 1H, $J = 11.4$ Hz), 7.32

(d, 1H, $J = 11.4$ Hz), 7.64 (s, 1H), 8.23 (s, 1H), 8.86 (s, 1H). $^{13}\text{C-NMR}$ (DMSO, 150 Mz): σ 131.2, 141.6, 150.6, 162.5. HRMS (FAB): expected for $\text{C}_9\text{H}_8\text{N}_5$ ($\text{M}+\text{H}$) $^+$: 186.07742. Found: 186.07722. IR(neat): ν_{max} 3118, 1633, 1013 cm^{-1} .

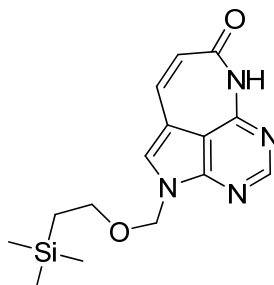
Methyl 3-(4-amino-7-((2-(trimethylsilyl)ethoxy)methyl)-7H-pyrrolo[2,3-d]pyrimidin-5-yl)acrylate (157)



To the 250 mL round bottomed flask containing 0.17 g (0.45 mmol) of 5-iodo-7-((2-(trimethylsilyl)ethoxy)methyl)-7H-pyrrolo[2,3-d]pyrimidin-4-amine was added 0.03 g (0.3 mmol) of CuI and 6.5 mL of dry DMF. Then 0.81 mL (8.9 mmol) of methyl acrylate, 0.13 mL (0.90 mmol) of Et_3N , and 0.05 g (0.048 mmol) of $\text{Pd}(\text{Ph}_3\text{P})_4$ were added. The solution was heated to 70 $^\circ\text{C}$. After 24 hours, the solution was cooled to room temperature and stirred for 1 hour with Dowex. The mixture was filtered and the filtrate was concentrated. The residue was diluted with 100 mL of CH_2Cl_2 and washed with water (3 x 100 mL). The organic layer was dried over MgSO_4 , filtered, and concentrated. The column was run using 1:2 Hex/EtOAc (Rf: 0.34; 9:1 $\text{CH}_2\text{Cl}_2/\text{MeOH}$) to give 102 mg (0.29 mmol, 65%) of product as a yellow gum. mp: 66-68 $^\circ\text{C}$. $^1\text{H-NMR}$ ($[(\text{CD}_3)_2\text{SO}]$, 600 MHz): σ - 0.076 (s, 9H), 0.89 (t, 2H, $J = 7.8$ Hz), 3.52 (t, 2H, $J = 7.8$ Hz), 3.78 (s, 3H), 5.55 (s, 2H), 5.85 (br s, 2H), 6.26 (d, 1H, $J = 16.2$ Hz), 7.41 (s, 1H), 7.83 (d, 1H, $J = 16.2$ Hz), 8.30 (s, 1H). $^{13}\text{C-NMR}$ ($[(\text{CD}_3)_2\text{SO}]$, 150 Mz): σ -1.2, 17.9, 51.9, 66.9,

73.1, 112.4, 117.4, 125.9, 128.6, 132.1, 136.9, 152.5, 157.7, 167.5. HRMS (ESI): expected for $C_{16}H_{25}N_4O_3Si$ ($M+H$)⁺: 349.16904. Found: 349.16910. IR(neat): ν_{max} 3321, 3152, 2951, 1714, 1629, 1579, 1169 cm^{-1} . Elemental Analysis for $C_{16}H_{24}N_4O_3Si \cdot 0.7$ EtOAc: Found: C, 55.93; H, 6.83; N, 13.28. Calculated: C, 55.05; H, 7.27; N, 13.66.

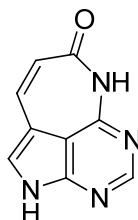
2-(2-(Trimethylsilyl)ethoxy)methyl)-2,6-dihydro-7H-2,3,5,6-tetraazabenzoc[cd]azulen-7-one (158)



To a dry 100 mL round bottomed flask under argon was added 0.10 g (0.29 mmol) of methyl 3-(4-amino-7-((2-(trimethylsilyl)ethoxy)methyl)-7H-pyrrolo[2,3d]pyrimidin-5-yl)acrylate and 13 mL of 0.5M NaOMe in MeOH. The yellow mixture was heated to 60 °C and stirred for 20 hours. The mixture was concentrated and the column was run using 9:1 $CH_2Cl_2/MeOH$ and then 4:1 $CH_2Cl_2/MeOH$ to give 50 mg (0.16 mmol, 55%) of product as a yellow solid. (Rf: 0.28, 9:1 $CH_2Cl_2/MeOH$). mp: 165 - 166 °C. ¹H-NMR ($CDCl_3$, 600 MHz): σ -0.078 (s, 9H), 0.82 (t, 2H, J = 8.4 Hz), 3.53 (t, 2H, J = 8.4 Hz), 5.53 (s, 2H), 5.84 (d, 1H, J = 11.4 Hz), 6.91 (d, 1H, J = 12 Hz), 6.65 (s, 1H), 8.49 (d, 1H, J = 5.4 Hz), 7.19 (s, 1H). ¹³C-NMR ($CDCl_3$, 150 Mz): σ -1.3, 17.6, 66.6, 73.3, 110.3, 119.3, 121.6, 124.6, 133.6, 149.3, 151.5, 152.3, 154.9. HRMS (ESI): expected for $C_{15}H_{21}N_4O_2Si$ ($M+H$)⁺: 317.14283. Found: 317.14220. IR(neat): ν_{max} 3084, 2895,

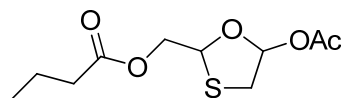
1660, 1615, 1538, 1079 cm^{-1} . Elemental Analysis for $\text{C}_{15}\text{H}_{20}\text{N}_4\text{O}_2\text{Si}$: Found: C, 58.82; H, 7.00; N, 14.07. Calculated: C, 56.94; H, 6.37; N, 17.71.

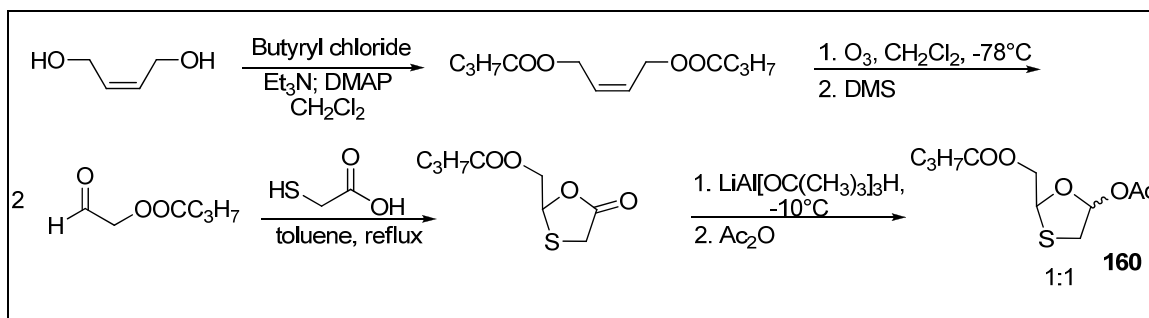
2,6-Dihydro-7H-2,3,5,6-tetraazabenzo[cd]azulen-7-one (135)



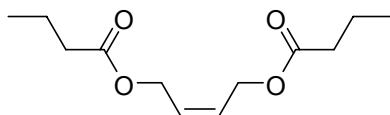
To a dry round bottomed flask containing 0.13 g (1.2 mmol) of 7-amino-2-(2-(trimethylsilyl)ethoxy)methyl)-2H-2,3,5,6-tetraazabenzo[cd]azulene was added 5 mL of EtOH followed by 10 mL of 5N HCl. The yellow solution was heated to reflux for 1.5 hours. The light yellow solution was then cooled to room temperature and neutralized with aqueous K_2CO_3 . The mixture was then concentrated and a short column was run using 9:1 $\text{CH}_2\text{Cl}_2/\text{MeOH}$. mp: 240 $^\circ\text{C}$ (decomp). $^1\text{H-NMR}$ ($[(\text{CD}_3)_2\text{SO}]$, 600 MHz): σ 5.60 (d, 1H, $J = 11.4$ Hz), 7.03 (d, 1H, $J = 12$ Hz), 7.51 (s, 1H), 8.27 (s, 1H), 10.26 (br s, 1H), 10.52 (s, 1H). $^{13}\text{C-NMR}$ ($[(\text{CD}_3)_2\text{SO}]$, 150 Mz): σ 113.8, 119.8, 123.7, 134.3, 152.1, 152.8, 154.1, 166.7. HRMS (APCI): expected for $\text{C}_9\text{H}_7\text{N}_4\text{O}$ ($\text{M}+\text{H}$) $^+$: 187.06144. Found: 187.06113. IR(neat): ν_{max} 3416, 3106, 2919, 2603, 1629 cm^{-1} .

(5-Acetoxy-1,3-oxathiolan-2-yl)methyl butyrate (160)

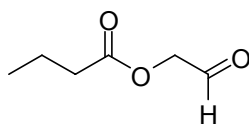




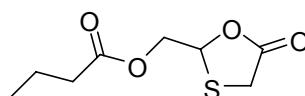
***cis*-But-2-ene-1,4-diol dibutyrate**



To a dry 500 mL round bottomed flask under argon containing 0.04 g (0.355 mmol) of DMAP was added 210 mL of dry CH_2Cl_2 . To the stirred solution was then added 2.92 mL (35.5 mmol) of (*Z*)-but-2-ene-1,4-diol followed by 50 mL (0.359 mol) of triethylamine. The solution was then cooled to 0°C and 8.9 mL of butyryl chloride was added dropwise. After the addition, the solution was warmed to room temperature. After 20 hours of stirring, the tangerine colored solution was quenched with 50 mL of water and then washed with water (200 mL x 2) and brine (200 mL). The washings caused the color of the solution to turn yellow. The organic layers were dried over MgSO_4 , filtered, and concentrated. The crude material was purified by column chromatography using 4:1 Hex/EtOAc as the eluent to give the product in quantitative yield as a colorless oil (R_f : 0.69; 1:1 Hex/EtOAc). $^1\text{H-NMR}$ (CDCl_3 , 600 MHz): σ 0.94 (t, 6H, $J = 7.8$), 1.61 – 1.68 (m, 4H), 2.29 (t, 4H, $J = 7.8$), 4.67 (d, 4H, $J = 5.4$), 5.71 – 5.76 (m, 2H). $^{13}\text{C-NMR}$ (CDCl_3 , 150 Mz): σ 13.8, 18.5, 36.2, 59.9, 128.3, 173.5. HRMS (FAB): expected for $\text{C}_{12}\text{H}_{21}\text{O}_4$ ($\text{M}+\text{H}$) $^+$ 229.14344. Found: 229.14296. IR(neat): ν_{max} 1732 cm^{-1} .

2-Oxoethyl butyrate

To a 250 mL round bottomed flask containing 8.23 g (0.036 mol) of *cis*-But-2-ene-1,4-diol dibutyrate was added 75 mL of CH₂Cl₂. The solution was cooled to -78°C and was ozonized. Upon completion of the ozonolysis, the solution was quenched with dimethyl sulfide (8 mL, 0.11 mol) at -78°C and was allowed to stir at room temperature overnight. The solution was then concentrated and purified by column chromatography (4:1 Hex/EtOAc) to give 6.0 g (64%) of the product as a colorless oil. (R_f: 0.43, 1:1 Hex/EtOAc). ¹H-NMR (CDCl₃, 400 MHz): σ 0.87 – 0.99 (m, 6H), 1.57 – 1.74 (m, 2H), 2.37 – 2.44 (m, 2H), 4.62 – 4.67 (m, 2H), 9.59 (s, 1H). ¹³C-NMR (CDCl₃, 100 Mz): σ 13.7, 18.4, 35.7, 68.7, 173.2, 196.1. HRMS (FAB): expected for C₆H₁₁O₃ (M+H)⁺ 131.07027. Found: 131.07045. IR(neat): ν_{\max} 1736, 1167 cm⁻¹.

(5-oxo-1,3-oxathiolan-2-yl)methyl butyrate

To a 500 mL round bottomed flask fitted with the Dean Stark apparatus and a condenser was added 5.0 g (0.038 mol) of 2-oxoethyl butyrate in 155 mL of toluene. Thioglycolic acid (2.6 mL, 0.038 mol) was added and the flask was heated to reflux for 5 hours. The solution was cooled to room temperature and washed with saturated aqueous NaHCO₃. The aqueous washings were then

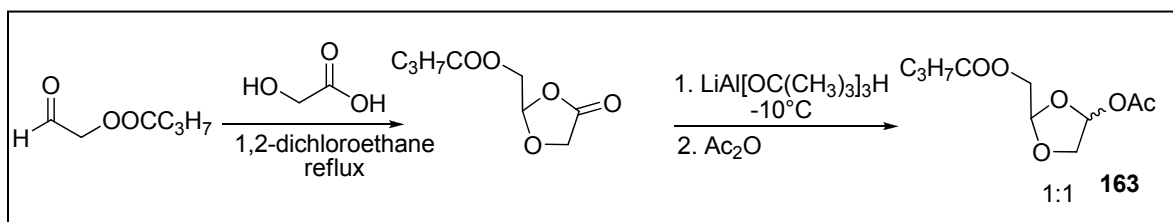
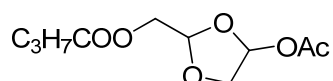
extracted with diethyl ether (2 x 100 mL). The combined extracts were washed with water (2 x 100 mL), dried over MgSO_4 , filtered, and concentrated to give 5.4 g (70% yield) of product as a yellow oil. (R_f : 0.56; 1:1 Hex/EtOAc). $^1\text{H-NMR}$ (CDCl_3 , 400 MHz): σ 0.89 – 0.97 (m, 3H), 1.59 – 1.71 (m, 2H), 2.34 (t, 2H, $J = 7.2$), 3.68 (dd, 2H, $J = 15.2, 16.4$), 4.27 – 4.39 (m, 2H), 5.63 – 5.66 (m, 1 H). $^{13}\text{C-NMR}$ (CDCl_3 , 100 Mz): σ 13.8, 18.4, 30.9, 36.0, 66.2, 78.4, 172.5, 173.0. HRMS (FAB): expected for $\text{C}_8\text{H}_{13}\text{O}_4\text{S}$ ($\text{M}+\text{H}$) $^+$ 205.05291. Found: 205.05276. IR(neat): ν_{max} 1775, 1736, 1151 cm^{-1} .

(5-Acetoxy-1,3-oxathiolan-2-yl)methyl butyrate (160)

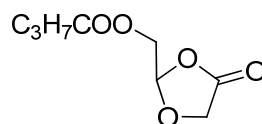
To a 250 mL round bottomed flask containing 1.7 g (8.6 mmol) of (5-oxo-1,3-oxathiolan-2-yl)methyl butyrate was added 40 mL of dry THF. The solution was cooled to -10°C and 9.5 mL of $\text{LiAl}[\text{OC}(\text{CH}_3)_3]_3\text{H}$ was added dropwise. The solution was allowed to stir for three hours and then 8.1 mL of Ac_2O was added dropwise. The solution was warmed to room temperature and stirred overnight. The reaction was quenched with saturate aqueous NaHCO_3 and allowed to stir at room temperature for one hour. The organic layer was washed with 100 mL water and the aqueous layer was back-extracted with 100 mL diethyl ether. The combined organic layers were dried over MgSO_4 , filtered, and concentrated. The column was run using 4:1 Hex/EtOAc to give 2.0 g (8.1 mmol, 94%) of product. $^1\text{H-NMR}$ (CDCl_3 , 600 MHz): σ 0.95 (t, 3H, $J = 7.8$ Hz), 1.61 – 1.69 (m, 2H), 2.10 (s, 3H), 2.30 – 2.34 (m, 2H), 3.13 (d, 1H, minor, $J = 11.4$ Hz), 3.19 (d, 1H, major, $J = 10.8$ Hz), 3.31 (dd, 1H, $J = 6, 4.8$ Hz), 4.13 (dd, 1H, $J = 7.2, 4.8$ Hz), 4.26 –

4.28 (m, 1H), 4.38 (dd, 1H, major, $J = 4.2, 7.8$ Hz), 5.50 – 5.54 (m, 1H), 6.60 (d, 1H, minor, $J = 4.8$ Hz), 6.67 (d, 1H, major, $J = 4.8$ Hz). ^{13}C -NMR (CDCl_3 , 150 Mz): σ 13.8, 18.5, 21.3, 36.1, 67.5, 83.4, 99.3, 119.2, 169.9, 173.3. HRMS (APCI): expected for $\text{C}_{10}\text{H}_{17}\text{O}_5\text{S}$ ($\text{M}+\text{H}$) $^+$ 249.07912. Found: 249.07923. IR(neat): ν_{max} 2965, 2876, 1736, 1373, 1221, 1170 cm^{-1} .

(4-Acetoxy-1,3-dioxolan-2-yl)methyl butyrate (163)



(4-Oxo-1,3-dioxolan-2-yl)methyl butyrate



To a flask containing 2.0 g of 2-oxoethyl butyrate was added 25 mL of 1,2-dichloroethane. Then 0.56 g (7.4 mmol) of glycolic acid was added followed by 54 mg (0.29 mmol) of *p*-TsOH. The mixture was refluxed for 1.5 hours and then a Dean-Stark trap was used to reduce the volume by half. An additional 25 mL of 1,2-dichloroethane was then added and the dark green solution was refluxed for 45 minutes. The solution was cooled to room temperature and concentrated.

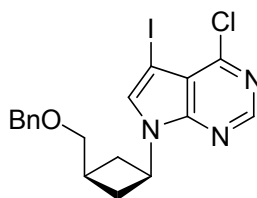
The residue was dissolved in 100 mL of diethyl ether and the solution was washed with 50 mL of NaHCO₃ and 50 mL of water. The organic layers were dried over MgSO₄, filtered, and concentrated to give a yellow-orange oil. Purification by column chromatography using 9:1 Hex/EtOAc provided 0.95 g of product in 39% yield as a colorless oil. (R_f: 0.56; 1:1 Hex/EtOAc). ¹H-NMR (CDCl₃, 400 MHz): σ 0.96 (t, 3H, J = 7.6 Hz), 1.59 – 1.72 (m, 2H), 2.36 (t, 2H, J = 7.6 Hz), 4.25 – 4.31 (m, 2H), 4.34 – 4.41 (m, 2H), 5.84 (t, 1H, J = 3.0 Hz). ¹³C-NMR (CDCl₃, 100 Mz): σ 13.8, 18.5, 36.0, 63.5, 63.7, 102.8, 170.7, 172.9. HRMS (FAB): expected for C₈H₁₃O₅ (M+H)⁺ 189.07575. Found: IR(neat): ν_{\max} 2968, 2878, 1812, 1743, 1214, 1173 cm⁻¹.

(4-Acetoxy-1,3-dioxolan-2-yl)methyl butyrate (163)

To a 250 mL round bottomed flask containing 0.79 g of starting material was added 10.5 mL of dry THF. The solution was cooled to -10°C. Then 3.0 mL of LiAl[OC(CH₃)₃]₃H was added dropwise over 20 minutes. The solution was allowed to continue to stir at -10°C. After 7.5 hours of stirred at -10°C, 2.1 mL of Ac₂O was added dropwise. The solution was allowed to continue stirring overnight at 0°C. The reaction was quenched by adding 1.8 mL of saturated aqueous NaHCO₃ and 0.88 g of Na₂CO₃ at 0°C. The mixture was then stirred at 0°C for one hour. The solution was filtered over silica gel using 4:1 Hex/EtOAc to wash. The solution was concentrated and the column was run using 6:1 Hex/EtOAc to provide 0.51 g of product. R_f: 0.52 (1:1 Hex/EtOAc). ¹H-NMR (CDCl₃, 600 MHz): σ 0.92 - 0.96 (m, 3H), 1.62 – 1.69 (m, 2H), 2.09 (s, 3H), 2.29

– 2.34 (m, 2H), 3.96 (dd, 1H, major, $J = 7.8, 1.8$ Hz), 3.99 (dd, 1H, minor, $J = 5.4, 4.2$ Hz), 4.16 – 4.20 (m, 2H), 4.24 – 4.27 (m, 1H), 5.31 (t, 1H, minor, $J = 4.2$ Hz), 5.39 (t, 1H, major, $J = 4.2$ Hz), 5.82 (t, 1H, $J = 3.6$ Hz), 6.34 (d, 1H, minor, $J = 3.6$ Hz), 6.38 (dd, 1H, major, $J = 2.4, 1.8$). $^{13}\text{C-NMR}$ (CDCl_3 , 150 Mz): σ 13.7, 18.4, 20.8, 36.0, 63.4, 70.9, 94.6, 102.7, 170.4, 173.3. HRMS (FAB): expected for $\text{C}_{10}\text{H}_{17}\text{O}_6$ ($\text{M}+\text{H}$) $^+$ 233.10196. Found: 233.11104. IR(neat): ν_{max} 2966, 2878, 1812, 1737, 1151 cm^{-1} .

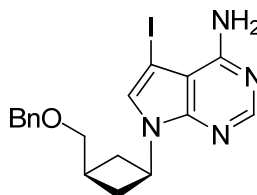
7-((1s,3s)-3-(benzyloxymethyl)cyclobutyl)-4-chloro-5-iodo-7H-pyrrolo[2,3-d]pyrimidine (167)



To a 100 mL round bottomed flask containing 0.33 g (2.1 mmol) of 4-chloro-7H-pyrrolo[2,3-d]pyrimidine was added 0.55 g (2.9 mmol) of *trans*-cyclobutanol **63** and 1.18 g (4.5 mmol) of Ph_3P . Then 12 mL of dry DMF was added and the flask was cooled to 0°C and a solution of DIAD (0.88 mL in 1.9 mL THF) was added dropwise. The flask was then warmed to room temperature and allowed to stir overnight. Methanol was added to quench the reaction and it was concentrated. Then CH_2Cl_2 (50 mL) was added and the organic layer was washed with water and brine, dried over MgSO_4 , filtered, and concentrated. The column was run using 4:1 Hex/EtOAc to give 0.71 g (2.1 mmol) of product. To the 250 mL round bottomed flask containing 0.70 g (2.1 mmol) of 7-((1s,3s)-3-(benzyloxymethyl)cyclobutyl)-4-chloro-7H-pyrrolo[2,3-d]pyrimidine was added

0.54 g (2.4 mmol) of NIS. Then 17.5 mL of dry DMF was added and the reaction was stirred at room temperature in the dark. After overnight stirring, the solution was concentrated and 100 mL of CH₂Cl₂ was added. Then the organic layer was washed twice with 100 mL of saturated aqueous NaHCO₃ and then 100 mL of a sodium sulfite solution. The organic layer was dried over MgSO₄, filtered, and concentrated. The column was run using 4:1 Hex/EtOAc to give 0.79 g (81% yield) of product as a white solid. mp: 130°C. ¹H-NMR (CDCl₃, 600 MHz): σ 2.37 – 2.43 (m, 2H), 2.49 – 2.54 (m, 1H), 2.65 – 2.70 (m, 2H), 3.53 (d, 2H, *J* = 4.2 Hz), 4.60 (s, 2H), 5.23 (q, 1H, *J* = 9 Hz), 7.32 – 7.42 (m, 5H), 7.62 (s, 1H), 8.59 (s, 1H). ¹³C-NMR (CDCl₃, 150 Mz): σ 28.5, 33.3, 45.6, 51.1, 72.7, 73.5, 109.6, 117.2, 127.8, 128.8, 132.7, 138.5, 150.6, 150.7, 152.7. HRMS (ESI): expected for C₁₈H₁₈ClIN₃O (M+H)⁺ 454.01776. Found: 454.01789. IR(neat): ν_{\max} 2941, 2856, 1719, 1575, 1532, 1441, 1214 cm⁻¹. Elemental Analysis for C₁₈H₁₇ClIN₃O: Found: C, 48.60; H, 4.07; N, 8.94. Calculated: C, 47.65; H, 3.78; N, 9.26.

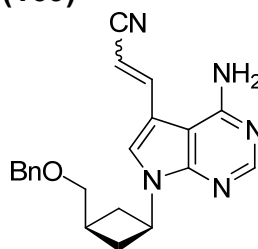
7-((1*s*,3*s*)-3-(Benzyloxymethyl)cyclobutyl)-5-iodo-7H-pyrrolo[2,3-*d*]pyrimidin-4-amine (168)



To a pressure vessel was added 1.5 g (3.4 mmol) of 7-((1*s*,3*s*)-3-(benzyloxymethyl)cyclobutyl)-4-chloro-5-iodo-7H-pyrrolo[2,3-*d*]pyrimidine **168** in

70 mL of 1,4-dioxane and 70 mL of ammonium hydroxide. The vessel was sealed and heated to 100°C for five hours. The solution was cooled to room temperature and then concentrated. The residue was diluted with 200 mL CH₂Cl₂. The solution was washed with water (2 x 100 mL) and brine (100 mL). The organic layer was dried over MgSO₄, filtered, and concentrated to yield 1.3 g (3.0 mmol, 88%) of product. mp: 127 - 129°C. ¹H-NMR (CDCl₃, 600 MHz): σ 2.27 – 2.32 (m, 2H), 2.43 – 2.49 (m, 1H), 2.61 – 2.65 (m, 2H), 3.52 (d, 2H, J = 4.8 Hz), 4.57 (s, 2H), 5.16 (q, 1H, J = 9 Hz), 5.88 (br s, 2H), 7.28 – 7.40 (m, 5H), 8.25 (s, 1H). ¹³C-NMR (CDCl₃, 150 Mz): σ 28.4, 33.7, 45.0, 49.2, 73.1, 73.4, 104.2, 119.3, 126.7, 127.8, 128.5, 128.7, 138.6, 150.1, 152.1, 157.2. HRMS (ESI): expected for C₁₈H₂₀N₄O (M+H)⁺ 435.06763. Found: 435.06690. IR(neat): ν_{\max} 3456, 3296, 2856, 1617, 1578, 1548 cm⁻¹. Elemental Analysis for C₁₈H₁₉N₄O: Found: C, 50.84; H, 4.75; N, 12.16. Calculated: C, 49.78; H, 4.41; N, 12.90.

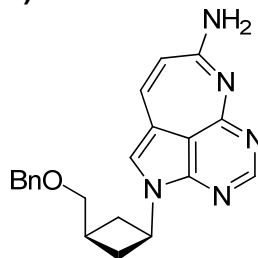
3-(4-Amino-7-((1s,3s)-3-(benzyloxymethyl)cyclobutyl)-7H-pyrrolo[2,3-d]pyrimidin-5-yl)acrylonitrile (169)



To the 250 mL round bottomed flask containing 0.61 g (1.4 mmol) of 7-((1s,3s)-3-(benzyloxymethyl)cyclobutyl)-5-iodo-7H-pyrrolo[2,3-d]pyrimidin-4-amine **168** was added 0.08 g (0.46 mmol) of CuI and 13.5 mL of dry DMF. Then 1.9 mL (28.1 mmol) of acrylonitrile, 0.40 mL (2.9 mmol) of Et₃N, and 0.17 g (0.14 mmol) of

$\text{Pd}(\text{Ph}_3\text{P})_4$ were added. The orange solution was heated to 70 °C. After 24 hours, the solution was cooled to room temperature and stirred for 1 hour with Dowex. The mixture was filtered and the filtrate was concentrated. The residue was diluted with 100 mL of CH_2Cl_2 and washed with water (3 x 100 mL). The organic layer was dried over MgSO_4 , filtered, and concentrated. The column was run using 1:2 Hex/EtOAc and then 1:3 Hex/EtOAc to give a mixture of cis and trans isomers as a brown oil to be used directly in the next step (Rf: 0.50; 9:1 $\text{CH}_2\text{Cl}_2/\text{MeOH}$). $^1\text{H-NMR}$ (CDCl_3 , 600 MHz): σ 2.31 – 2.46 (m, 3H), 2.49 – 2.53 (m, 2H), 2.66 – 2.70 (m, 2H), 3.58 (d, 2H, $J = 3.6$ Hz), 4.58 (s, 2H), 5.21 (q, 1H, $J = 9$ Hz), 5.29 (d, 1H, minor, $J = 11.4$ Hz), 5.34 (d, 1H, major, $J = 16.2$ Hz), 5.56 (br s, 2H), 7.32 – 7.40 (m, 5H), 7.45 – 7.48 (m, 1H, major), 7.54 – 7.57 (m, 1H, minor), 8.31 (s, 1H). $^{13}\text{C-NMR}$ (CDCl_3 , 150 Mz): σ 28.3, 33.0, 33.7, 44.5, 72.7, 73.3, 73.6, 93.9, 119.2, 127.9, 128.1, 128.6, 128.8, 132.2, 141.0, 142.7, 157.2. HRMS (APCI): expected for $\text{C}_{21}\text{H}_{22}\text{N}_5\text{O}$ ($\text{M}+\text{H}$) $^+$ 360.18189. Found: 360.18143. IR(neat): ν_{max} 3324, 3186, 2941, 2856, 2209, 1576, 1439 cm^{-1} .

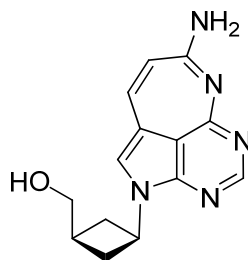
7-amino-2-((1s,3s)-3-(benzyloxymethyl)cyclobutyl)-2H-2,3,5,6-tetraazabeno[cd]azulene (159)



To a dry 250 mL round bottomed flask under argon was added 0.37 g (1.0 mmol) of 3-(4-Amino-7-((1s,3s)-3-(benzyloxymethyl)cyclobutyl)-7H-pyrrolo[2,3d]pyrimi -

din-5-yl)acrylonitrile and 42 mL of 0.5 M NaOMe in MeOH. The yellow mixture was heated to 60 °C and stirred for 20 hours. The mixture was concentrated and the column was run using 9:1 CH₂Cl₂/MeOH to give an orange solid. (Rf: 0.16, 9:1 CH₂Cl₂/MeOH). mp: 104 – 105 °C. ¹H-NMR (CDCl₃, 600 MHz): σ 2.27 – 2.31 (m, 2H), 2.45 (s, 1H), 2.60 – 2.62 (m, 2H), 3.54 (d, 2H, J = 4.2 Hz), 4.56 (s, 2H), 4.89 (q, 1H, J = 8.4 Hz), 5.89 (s, 2H), 6.78 (s, 1H), 7.18 (s, 1H), 7.31 – 7.36 (m, 5H), 8.26 (s, 1H). ¹³C-NMR (CDCl₃, 150 Mz): σ 28.5, 33.3, 45.4, 73.1, 73.5, 109.0, 109.6, 113.3, 115.3, 128.0, 128.7, 138.5, 140.2, 151.6, 164.1, 167.4, 177.8. HRMS (ESI): expected for C₂₁H₂₂N₅O (M+H)⁺ 360.18189. Found: 360.18087. IR(neat): ν_{max} 3306, 3182, 2927, 2853, 1623, 1541 cm⁻¹. Elemental Analysis for C₂₁H₂₁N₅O·5H₂O: Found: C, 56.12; H, 5.12; N, 15.04. Calculated: C, 56.11; H, 6.95; N, 15.58.

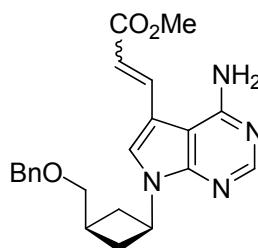
7-amino-2-((1*s*,3*s*)-3-(hydroxymethyl)cyclobutyl)-2*H*-2,3,5,6-tetraazabenzoc[*cd*]azulene (132)



To a dry round bottomed flask containing 0.17 g (0.48 mmol) of 7-amino-2-((1*s*,3*s*)-3-(benzyloxymethyl)cyclobutyl)-2*H*-2,3,5,6-tetraazabenzoc[*cd*]azulene was added 7 mL of dry CH₂Cl₂. The yellow solution was cooled to -78°C and 4.8 mL of 1.0 M BCl₃ was added dropwise. The mixture was stirred at -78°C for 6 hours. Then methanol was added and the solution was concentrated. The column was

run using 9:1 CH₂Cl₂/MeOH and then 4:1 CH₂Cl₂/MeOH (Rf: 0.1; 9:1 CH₂Cl₂/MeOH). mp: 220 °C. ¹H-NMR ([[(CD₃)₂SO], 600 MHz): σ 2.17 – 2.28 (m, 3H), 2.44 – 2.47 (m, 2H), 3.39 (s, 2H), 4.77 (s, 1H), 4.98 (q, 1H, *J* = 9.0 Hz), 6.08 (d, 1H, *J* = 11.4 Hz), 7.33 (d, 1H, *J* = 11.4 Hz), 7.62 (s, 2H), 7.95 (s, 1H), 8.30 (s, 1H). ¹³C-NMR ([[(CD₃)₂SO], 150 Mz): σ 29.9, 32.4, 45.3, 63.8, 113.9, 152.0, 178.5, 181.1. HRMS (ESI): expected for C₁₄H₁₆N₅O (M+H)⁺ 270.13494. Found: 270.13435. IR(neat): ν_{max} 3361, 3120, 2926, 1617, 1384 cm⁻¹.

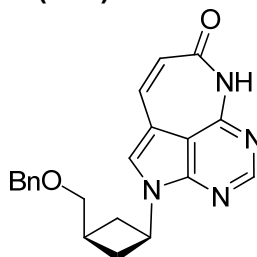
Methyl 3-(4-amino-7-((1*s*,3*s*)-3-(benzyloxymethyl)cyclobutyl)-7H-pyrrolo[2,3-*d*]pyrimidin-5-yl)acrylate (170)



To the 100 mL round bottomed flask containing 0.11 g (0.27 mmol) of 7-((1*s*,3*s*)-3-(benzyloxymethyl)cyclobutyl)-5-iodo-7H-pyrrolo[2,3-*d*]pyrimidin-4-amine was added 15 mg (0.08 mmol) of CuI and 5 mL of dry DMF. Then 0.5 mL (5.5 mmol) of methyl acrylate, 0.075 mL (0.54 mmol) of Et₃N, and 0.032 g (0.029 mmol) of Pd(Ph₃P)₄ were added. The solution was heated to 70 °C. After 24 hours, the solution was cooled to room temperature and stirred for 1 hour with Dowex. The mixture was filtered and the filtrate was concentrated. The residue was diluted with 50 mL of CH₂Cl₂ and washed with water (3 x 50 mL). The organic layer was dried over MgSO₄, filtered, and concentrated. The column was run using 1:2 Hex/EtOAc (Rf: 0.50; 9:1 CH₂Cl₂/MeOH). ¹H-NMR (CDCl₃, 600 MHz): σ 2.30 –

2.40 (m, 3H), 2.45 – 2.52 (m, 2H), 3.54 (d, 2H, $J = 4.2$ Hz), 3.81 (s, 3H), 5.19 (q, 1H, $J = 9$ Hz), 5.30 (s, 2H), 5.43 (br s, 2H), 6.20 (d, 1H, $J = 16.3$ Hz), 7.29 – 7.39 (m, 5H), 7.52 (s, 1H), 7.80 (d, 1H, $J = 16.2$ Hz), 8.31 (s, 1H). ^{13}C -NMR (CDCl_3 , 150 Mz): σ 28.5, 33.4, 44.9, 51.9, 72.9, 73.4, 101.7, 111.4, 116.4, 124.2, 127.8, 127.9, 128.7, 130.7, 137.4, 138.6, 152.7, 155.9, 194.3. HRMS (APCI): expected for $\text{C}_{22}\text{H}_{25}\text{N}_4\text{O}_3$ ($\text{M}+\text{H}$) $^+$ 393.19212. Found: 393.19159. IR(neat): ν_{max} 3322, 3181, 2948, 2853, 1733, 1627, 1581, 1169 cm^{-1} .

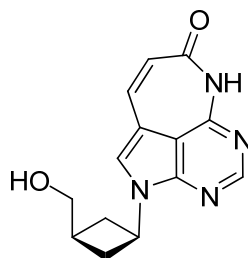
2-(1s,3s)-3-(benzyloxymethyl)cyclobutyl)-2,6-dihydro-7H-2,3,5,6-tetraazabenzo[cd]azulen-7-one (171)



To a dry 100 mL round bottomed flask under argon was added 0.10 g of methyl 3-(4-amino-7-((1s,3s)-3-(benzyloxymethyl)cyclobutyl)-7H-pyrrolo[2,3-d]pyrimidin-5-yl)acrylate and 13.5 mL of 0.5M NaOMe in MeOH. The yellow mixture was heated to 60 °C and stirred for 20 hours. The mixture was concentrated and the column was run using 2.5% MeOH in CH_2Cl_2 to give 58 mg (0.16 mmol) of product. ^1H -NMR (CDCl_3 , 600 MHz): σ 2.36 – 2.42 (m, 3H), 2.48 – 2.51 (m, 2H), 3.54 (d, 2H, $J = 4.8$ Hz), 3.54 (d, 2H, $J = 4.8$ Hz), 4.58 (s, 2H), 5.10 (q, 1H, $J = 9$ Hz), 5.76 (d, 1H, $J = 11.4$ Hz), 6.75 (d, 1H, $J = 12$ Hz), 7.24 (s, 1H), 7.30 – 7.36 (m, 5H), 8.40 (s, 1H), 8.55 (br s, 1H). ^{13}C -NMR (CDCl_3 , 150 Mz): σ 28.4, 33.2, 45.1, 72.8, 73.5, 101.8, 117.7, 120.4, 121.8, 122.9, 128.0, 128.7, 132.2, 132.4,

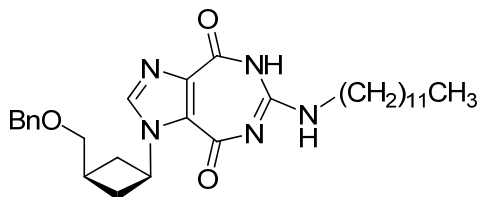
133.9, 154.6, 171.4. HRMS (ESI): expected for $C_{21}H_{21}N_4O_2$ (M+H)⁺ 361.16590. Found: 361.16580. IR(neat): ν_{\max} 2987, 2854, 1626 cm^{-1} .

2-(1s,3s)-3-(benzyloxymethyl)cyclobutyl)-2,6-dihydro-7H-2,3,5,6-tetraazabenz[cd]azulen-7-one (133)



To a dry round bottomed flask containing 58 mg (0.16 mmol) of 2-(1s,3s)-3-(benzyloxymethyl)cyclobutyl)-2,6-dihydro-7H-2,3,5,6-tetraazabenz[cd]azulen-7-one was added 3 mL of dry CH_2Cl_2 . The yellow solution was cooled to $-78^\circ C$ and 1.6 mL of 1.0 M BCl_3 was added dropwise. The mixture was stirred at $-78^\circ C$ for 6 hours. Then methanol was added and the solution was concentrated. The column was run using 9:1 $CH_2Cl_2/MeOH$. mp: 249 – 251 $^\circ C$. 1H -NMR ($[(CD_3)_2SO]$, 600 MHz): σ 2.19 – 2.28 (m, 3H), 2.44 – 2.48 (m, 2H), 3.47 (t, 2H, $J = 4.8$ Hz), 4.65 (t, 1H, $J = 5.4$ Hz), 4.98 (q, 1H, $J = 8.4$ Hz), 5.63 (d, 1H, $J = 11.4$ Hz), 7.04 (d, 1H, $J = 11.4$ Hz), 7.77 (s, 1H), 8.30 (s, 1H), 10.61 (br s, 1H). ^{13}C -NMR ($[(CD_3)_2SO]$, 150 Mz): σ 30.0, 32.4, 44.8, 64.0, 105.6, 111.8, 120.2, 123.9, 133.8, 151.2, 152.8, 153.9, 166.6. HRMS (ESI): expected for $C_{14}H_{15}N_4O_2$ (M+H)⁺ 271.11895. Found: 271.11838. IR(neat): ν_{\max} 3388, 3071, 2981, 2866, 1624 cm^{-1} . Elemental Analysis for $C_{14}H_{15}N_4O_2 \cdot 0.5MeOH$: Found: C, 61.25; H, 5.47; N, 19.10. Calculated: C, 60.83; H, 5.63; N, 19.57.

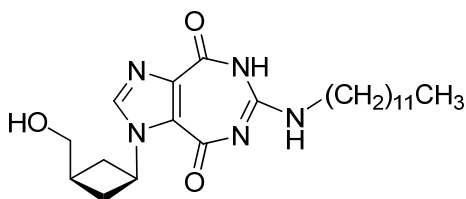
1-((1s,3s)-3-(Benzyloxymethyl)cyclobutyl)-6-(dodecylamino)imidazo[4,5-e][1,3]diazepine-4,8(1H,5H)-dione (181)



To a dry 3-necked round bottomed flask under argon was added 0.26 g (1.4 mmol) *trans*-cyclobutanol **63**, 0.52 g (2.8 mmol) 1H-imidazole-4,5-dicarboxylic acid dimethyl ester, and 0.77 g (2.9 mmol) of triphenylphosphine. Dry THF (8 mL) was added and the mixture was cooled to 0°C. A solution of DIAD (0.58 mL in 1.2 mL of THF) was added dropwise. The yellow mixture was warmed to room temperature and allowed to stir overnight. After 48 hours of stirring at room temperature, the mixture was concentrated and purified by column using 2.5% MeOH in CH₂Cl₂. This yielded 0.30 g (0.83 mmol) of dimethyl1-((1s,3s)-3-(benzyloxymethyl)cyclobutyl)-1H-imidazole-4,5-dicarboxylate (**180**) (Rf: 0.44; 9:1 CH₂Cl₂/MeOH). To a dry 50 mL round bottomed flask under argon was added 0.65 g of dodecylguanidine and 10 mL of dry methanol. The solution was cooled to 0°C and a solution of NaOMe (13 mL, 0.5 M in MeOH) was added. The reaction mixture was stirred at 0°C for 30 minutes. The solution was then added to a flask containing 0.29 g of dimethyl1-((1s,3s)-3-(benzyloxymethyl)cyclobutyl)-1H-imidazole-4,5-dicarboxylate in 15 mL of dry MeOH. A syringe filter was used to prevent any salt from entering the flask. The yellow solution was stirred at room temperature overnight. The solution was then concentrated and the column was run using 5% MeOH in CH₂Cl₂. This yielded 0.36 g (0.65 mmol) of product as a white solid. mp: 144 - 145 °C. ¹H-NMR (CDCl₃, 600 MHz): σ 0.88 (t,

3H, $J = 7.2$ Hz), 1.24 – 1.30 (m, 18H), 1.56 (t, 2H, $J = 6.6$ Hz), 2.34 – 2.38 (m, 3H), 2.48 – 2.50 (m, 2H), 3.43 (t, 2H, $J = 6.6$ Hz), 3.49 (d, 2H, $J = 5.4$ Hz), 4.55 (s, 2H), 5.40 (t, 1H, $J = 7.8$ Hz), 7.29 – 7.37 (m 5H), 7.95 (s, 1H). ^{13}C -NMR (CDCl_3 , 150 Mz): σ 12.4, 14.3, 22.9, 23.9, 27.1, 28.5, 29.5, 29.8, 32.1, 33.6, 69.6, 72.7, 74.3, 101.7, 104.3, 127.8, 128.7, 144.8, 161.7. HRMS (ESI): expected for $\text{C}_{30}\text{H}_{44}\text{N}_5\text{O}_3$ ($\text{M}+\text{H}$) $^+$ 522.34387. Found: 522.34351. IR(neat): ν_{max} 3201, 3130, 2926, 2879, 1595, 1306, 1029 cm^{-1} . Elemental Analysis for $\text{C}_{30}\text{H}_{43}\text{N}_5\text{O}_3$: Found: C, 63.13; H, 8.43; N: 24.33. Calculated: C, 69.07; H, 8.31; N, 13.42.

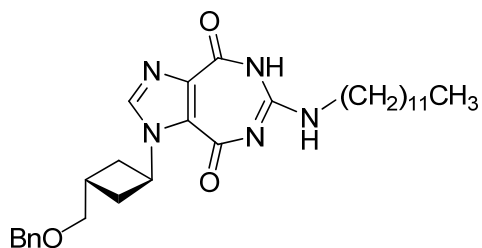
6-(Dodecylamino)-1-((1s,3s)-3-(hydroxymethyl)cyclobutyl)imidazo[4,5-e][1,3]diazepine-4,8(1H,5H)-dione (177)



To the 100 mL round bottomed flask containing 0.33 g of 1-((1s,3s)-3-(benzyloxymethyl)cyclobutyl)-6-(dodecylamino)imidazo[4,5-e][1,3]diazepine-4,8(1H,5H)-dione was added 7.5 mL of CH_2Cl_2 . The solution was cooled to -78°C and solution of BCl_3 (6.5 mL; 1.0 M in CH_2Cl_2) was added dropwise over 10 minutes. The reaction mixture continued to stir at -78°C for 7 hours, and was then quenched with 3 mL of 7N NH_3 in MeOH. The reaction mixture was concentrated and the column was run using 9:1 $\text{CH}_2\text{Cl}_2/\text{MeOH}$ and then 6:1 $\text{CH}_2\text{Cl}_2/\text{MeOH}$. mp: 221 - 222 $^\circ\text{C}$. ^1H -NMR ($[(\text{CD}_3)_2\text{SO}]$, 600 MHz): σ 0.84 (t, 3H, $J = 6.6$ Hz), 1.23 – 1.26 (m, 18H), 1.47 (t, 2H, $J = 6.6$ Hz), 2.08 – 2.15 (m, 2H),

2.19 – 2.23 (m, 1H), 2.42 – 2.51 (m, 2H), 3.19 – 3.22 (m, 2H), 3.38 – 3.42 (m, 2H), 4.60 (t, 1H, $J = 5.4$ Hz), 5.13 (q, 1H, $J = 9.0$ Hz), 7.08 (t, 1H, $J = 4.8$ Hz), 8.27 (s, 1H), 10.40 (s, 1H). $^{13}\text{C-NMR}$ ($[(\text{CD}_3)_2\text{SO}]$, 150 Mz): σ 14.0, 22.1, 26.3, 28.3, 28.7, 29.0, 30.1, 31.3, 32.7, 41.1, 47.2, 63.9, 111.3, 131.1, 134.1, 140.2, 147.6, 159.3, 161.8. HRMS (ESI): expected for $\text{C}_{23}\text{H}_{38}\text{N}_5\text{O}_3$ ($\text{M}+\text{H}$) $^+$ 432.29692. Found: 432.29598. IR(neat): ν_{max} 3224, 2920, 2851, 1712, 1582, 1494, 1464 cm^{-1} .
 1. Elemental Analysis for $\text{C}_{23}\text{H}_{37}\text{N}_5\text{O}_3$: Found: C, 63.08; H, 8.46; N, 16.19. Calculated: C, 64.01; H, 8.64; N, 16.23.

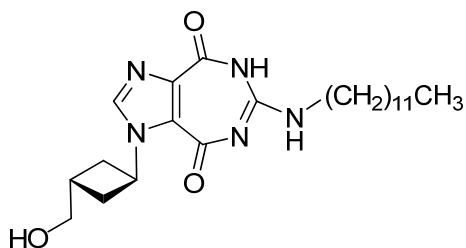
1-((*trans*)-3-(Benzyloxymethyl)cyclobutyl)-6-(dodecylamino)imidazo[4,5-*e*][1,3]diazepine-4,8(1H,5H)-dione (183)



To a dry 3-necked round bottomed flask under argon was added 0.28 g (1.4 mmol) *cis*-cyclobutanol **108**, 0.55 g (3.0 mmol) 1H-imidazole-4,5-dicarboxylic acid dimethyl ester, and 0.82 g (3.1 mmol) of triphenylphosphine. Dry THF (8.5 mL) was added and the mixture was cooled to 0°C. A solution of DIAD (0.61 mL in 1.3 mL of THF) was added dropwise. The yellow mixture was warmed to room temperature and allowed to stir overnight. After 26 hours of stirring at room temperature, the mixture was concentrated and purified by column using 2.5% MeOH in CH_2Cl_2 to give dimethyl 1-((*trans*)-3-(benzyloxymethyl)cyclobutyl)-1H-imidazole-4,5-dicarboxylate (**182**). To a dry 50 mL round bottomed flask under

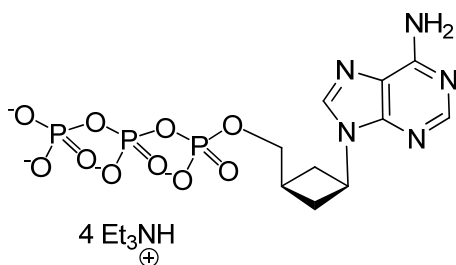
argon was added 0.65 g of dodecylguanidine and 15 mL of dry methanol. The solution was cooled to 0°C and a solution of NaOMe (30 mL, 0.5 M in MeOH) was added. The reaction mixture was stirred at 0°C for 30 minutes. The solution was then added to a flask containing 0.29 g of dimethyl1-((1*s*,3*s*)-3-(benzyloxymethyl)cyclobutyl)-1*H*-imidazole-4,5-dicarboxylate in 20 mL of dry MeOH. A syringe filter was used to prevent any salt from entering the flask. The yellow solution was stirred at room temperature overnight. The solution was then concentrated and the column was run using 2.5% MeOH in CH₂Cl₂. This yielded 0.49 g (0.94 mmol) of product. mp: 185 - 188 °C. ¹H-NMR (CDCl₃, 600 MHz): σ 0.88 (t, 3H, J = 7.2 Hz), 1.24 – 1.29 (m, 18H), 1.55 (t, 2H, J = 6.6 Hz), 2.46 – 2.51 (m, 3H), 2.57 – 2.60 (m, 2H), 3.41 (t, 2H, J = 6.6 Hz), 3.61 (d, 2H, J = 6.6 Hz), 4.57 (s, 2H), 5.57 (q, 1H, J = 7.8 Hz), 7.29 – 7.37 (m 5H), 8.00 (s, 1H). ¹³C-NMR (CDCl₃, 150 Mz): σ 12.4, 14.3, 22.9, 27.1, 29.0, 29.2, 29.5, 29.8, 32.1, 32.6, 33.0, 42.4, 50.7, 72.9, 73.5, 104.3, 119.2, 119.4, 127.9, 128.6, 138.4, 144.6. HRMS (ESI): expected for C₃₀H₄₄N₅O₃ (M+H)⁺ 522.34387. Found: 522.34302. IR(neat): ν_{\max} 3202, 3131, 2922, 2850, 1708, 1525 cm⁻¹. Elemental Analysis for C₃₀H₄₃N₅O₃: Found: C, 68.74; H, 8.42; N, 12.96. Calculated: C, 69.07; H, 8.31; N, 13.42.

6-(Dodecylamino)-1-((*trans*)-3-(hydroxymethyl)cyclobutyl)imidazo[4,5-*e*][1,3]diazepine-4,8(1*H*,5*H*)-dione (178)



To the 100 mL round bottomed flask containing 0.48 g of 1-((trans)-3-(benzyloxymethyl)cyclobutyl)-6-(dodecylamino)imidazo[4,5-e][1,3]diazepine-4,8 (1H,5H)-dione was added 16 mL of CH₂Cl₂. The solution was cooled to -78°C and solution of BCl₃ (4.6 mL; 1.0 M in CH₂Cl₂) was added dropwise over 10 minutes. The reaction mixture continued to stir at -78°C for 7 hours, and was then quenched with 3 mL of 7N NH₃ in MeOH. The reaction mixture was concentrated and the column was run using 9:1 CH₂Cl₂/MeOH to give a white solid. mp: 234 - 236 °C. ¹H-NMR ([CD₃)₂SO], 600 MHz): σ 0.84 (t, 3H, *J* = 6.6 Hz), 1.23 – 1.26 (m, 18H), 1.47 (t, 2H, *J* = 6.6 Hz), 2.29 – 2.37 (m, 3H), 2.41 – 2.43 (m, 2H), 3.18 – 3.24 (m, 2H), 3.50 (t, 2H, *J* = 6.0 Hz), 4.73 (t, 1H, *J* = 5.4 Hz), 5.33 (q, 1H, *J* = 7.8 Hz), 7.12 (t, 1H, *J* = 4.8 Hz), 8.40 (s, 1H), 10.4 (s, 1H). ¹³C-NMR ([CD₃)₂SO], 150 Mz): σ 14.0, 22.1, 26.3, 28.3, 28.7, 29.0, 30.2, 31.3, 31.4, 31.7, 41.1, 49.2, 63.7, 67.3, 113.9, 115.4, 131.2, 134.1, 140.3, 154.9, 159.3, 161.8. HRMS (ESI): expected for C₂₃H₃₈N₅O₃ (M+H)⁺ 432.29692. Found: 432.29715. IR(neat): ν_{max} 3211, 3066, 2917, 2849, 1693, 1583, 1525, 1494 cm⁻¹. Elemental Analysis for C₂₃H₃₇N₅O₃·H₂O: Found: C, 60.97; H, 8.37; N, 15.70. Calculated: C, 61.45; H, 8.74; N, 15.58.

4'-O-Triphosphate of 9-[*cis*-3-hydroxymethyl)cyclobutyl]adenine (184)



To a 100 mL flask with 9-[*cis*-3-hydroxymethyl)cyclobutyl]adenine **100** (66 mg, 0.25 mmol) was added 2.0 mL of PO(OMe)₃. The yellow solution was cooled to 0°C and POCl₃ (0.05 mL, 0.5 mmol) was added dropwise. The solution was stirred at 0°C for 6 hr. The reaction was quenched with water and refrigerated overnight. The column was run using HP-20SS resin. To the collected monophosphate was then added 3 mL of water and 3 mL of *t*-BuOH. Then 35 μL of morpholine was added and the solution was heated to gentle reflux. Then a solution of 82 mg of DCC in 2 mL of *t*-BuOH was added dropwise. The solution was allowed to continue heating under reflux for five hours and was then cooled to room temperature. The mixture was filtered to remove precipitate from the solution. The filtrate was concentrated to give an aqueous solution, which was extracted with diethyl ether (3 x 25 mL). The aqueous layer was concentrated to give a viscous yellow-orange oil which was then triturated to provide a pale yellow solid. Then 0.29 g of (HNBu₃)₂H₂P₂O₇ (0.65 mmol) was added and 4 mL of dry DMF under argon to give a colorless solution. The solution was stirred at room temperature for 4 days and was directly applied to the DEAE-sephadex dianion exchange column (11 mm X 220 mm, eluent from 0.1 M TEAB to 0.6 M TEAB). After analyzing the fractions by HPLC with C-18 reverse phase column (250 mm X 4.6 mm), all the fractions containing product were collected and lyophilized to give the triethylammonium salt of 4'-O-triphosphate of 9-[*cis*-3-

hydroxymethyl)cyclobutyl]adenine (**184**) as a light yellow sticky solid. ^1H NMR ($[(\text{CD}_3)_2\text{SO}]$, 400 MHz): δ 1.11 (br s, 22H), 2.40 (m, 2H), 2.90 (br s, 15H), 3.86 (m, 1H), 4.87 (q, 1H, $J = 8.4$ Hz), 7.20 (s, 2H), 8.12 (s, 1H), 8.36 (s, 1H). ^{31}P NMR ($[(\text{CD}_3)_2\text{SO}]$, 162 MHz): δ -7.45 (γ), -9.67 (α), -20.55 (β).

4'-O-Triphosphate of 7-amino-2-((1s,3s)-3-(hydroxymethyl)cyclobutyl)-2H-2,3,5,6-tetraazabenzocd]azulene (185)

The triphosphate was synthesized in the same manner as described above to give a yellow solid as the product. ^1H NMR ($[(\text{CD}_3)_2\text{SO}]$, 400 MHz): δ 1.10 – 1.41 (br s, 15 H), 1.51 – 1.70 (br s, 2H), 2.43 – 2.61 (m, 3H), 2.81 – 2.93 (m, 2H), 3.10 (br s, 3H), 3.68 (br s, 6H), 4.10 (m, 1H), 4.80 (s, 1H), 7.82 (s, 1H), 8.26 (s, 1H), 8.40 (s, 1H). LRMS(APCI). Expected for $\text{C}_{14}\text{H}_{18}\text{N}_5\text{O}_{10}\text{P}_3$: 509.24. Found: 510.1.

4'-O-Triphosphate of 6-(Dodecylamino)-1-((trans)-3-(hydroxymethyl)cyclobutyl)imidazo[4,5-e][1,3]diazepine-4,8(1H,5H)-dione (186)

The triphosphate was synthesized in the same manner as described above to give a white sticky solid as the product. ^1H NMR ($[(\text{CD}_3)_2\text{SO}]$, 400 MHz): δ 0.91 (t, 3H, $J = 10.8$ Hz), 1.19 (m, 6H), 1.28 – 1.34 (m, 2H), 1.59 – 1.63 (m, 2H), 2.52 (s, 6H), 2.97 – 3.08 (m, 21 H), 3.45 – 3.51 (br s, 33H), 3.77 (m, 16H), 9.25 (br s, 1H). LRMS(APCI). Expected for $\text{C}_{23}\text{H}_{36}\text{N}_5\text{O}_{12}\text{P}_3^{4-}$: 666.4. Found: 667.5.

1.7 References

- (1) Zu, T.; Korber, B. T.; Nahmias, A. J.; Hooper, E.; Sharp, P. M.; Ho, D. D. *Nature* **1998**, 391, 594-597.
- (2) <http://www.until.org/statistics.shtml> 2004-2006.
- (3) Painter, G. R.; Almond, M. R.; Mao, S.; Liotta, D. C. *Current Topics in Medicinal Chemistry* **2004**, 4, 1035-1044.
- (4) Shulman, N.; Winters, M. *Current Drug Targets - Infectious Disorders* **2003**, 3, 273-281.
- (5) Li, Y.; Mao, S.; Hager, M. W.; Becnel, K. D.; Schinazi, R. F.; Liotta, D. C. *Bioorganic and Medicinal Chemistry Letters* **2007**, 17, 3398-3401.
- (6) UNAIDS/WHO *UNAIDS* **2007**, 07.27E.
- (7) Tozser, J. *Current Topics in Medicinal Chemistry* **2003**, 3, 1447-1457.
- (8) Barbaro, G.; Scozzafava, A.; Mastrolorenzo, A.; Supuran, C. T. *Current Pharmaceutical Design* **2005**, 11, 1805-1843.
- (9) Warnke, D.; Barreto, J.; Temesgen, Z. *Journal of Clinical Pharmacology* **2007**, 47, 1570-1579.
- (10) Weiss, R. A. *Nature* **2001**, 410, 963-967.
- (11) Portsmouth, S.; Stebbing, J.; Gazzard, B. *Current Topics in Medicinal Chemistry* **2003**, 3, 1458-1466.
- (12) De Clercq, E. *Nature Reviews: Drug Discovery* **2007**, 6, 1001-1018.
- (13) Cherry, C.; Wesselingh, S. L. *Journal of Antimicrobial Chemotherapy* **2003**, 51, 1091-1093.
- (14) Melroy, J.; Nair, V. *Current Pharmaceutical Design* **2005**, 11, 3847-3852.

- (15) Shibuyama, S.; Gevorkyan, A.; Yoo, U.; Tim, S.; Dzhangiryan, K.; Scott, J. D. *Current Pharmaceutical Design* **2006**, *12*, 1075-1090.
- (16) Sluis-Cremer, N.; Arion, D.; Parniak, M. A. *Cellular and Molecular Life Sciences* **2000**, *57*, 1408-1422.
- (17) Schinazi, R. F.; Hernandez-Santiago, B. I.; Hurwitz, S. J. *Antiviral Research* **2006**, *71*, 322-334.
- (18) Perno, C.-F.; Moyle, G.; Tsoukas, C.; Ratanasuwan, W.; Gatell, J.; Schechter, M. *Journal of Medical Virology* **2008**, *80*, 565-576.
- (19) Sharma, P. L.; Nurpeisov, V.; Hernandez-Santiago, B. I.; Beltran, T.; Schinazi, R. F. *Current Topics in Medicinal Chemistry* **2004**, *4*, 895-919.
- (20) Wainberg, M. A. *AIDS* **2004**, *18*, S63-S68.
- (21) Frenkel, L. M.; Tobin, N. H. *Therapeutic Drug Monitoring* **2004**, *26*, 116-121.
- (22) Ray, A. S.; Yang, Z.; Shi, J.; Hobbs, A.; Schinazi, R. F.; Chu, C. K.; Anderson, K. A. *Biochemistry* **2002**, *41*, 5150-5162.
- (23) Yin, P. D.; Das, D.; Mitsuya, H. *Cellular and Molecular Life Sciences* **2006**, *63*, 1706-1724.
- (24) Roquebert, B.; Marcelin, A.-G. *Journal of Antimicrobial Chemotherapy* **2008**, *61*, 973-975.
- (25) Boyer, P. L.; Sarafianos, S. G.; Arnold, E.; Hughes, S. H. *Journal of Virology* **2001**, *75*, 4832-4842.
- (26) Smith, A. J.; Scott, W. A. *Current Pharmaceutical Design* **2006**, *12*, 1827-1841.

- (27) Sarafianos, S. G.; Das, K.; Hughes, S. H.; Arnold, E. *Current Opinion in Structural Biology* **2004**, *14*, 716-730.
- (28) Sarafianos, S. G.; Das, K.; Clark Jr., A. D.; Ding, J.; Boyer, P. L.; Hughes, S. H.; Arnold, E. *Proceedings of the National Academy of Sciences USA* **1999**, *96*, 10027-10032.
- (29) Turner, D.; Brenner, B.; Wainberg, M. A. *Clinical and Diagnostic Laboratory Immunology* **2003**, *10*, 979-981.
- (30) Turner, D.; Brenner, B.; Wainberg, M. A. *Journal of Antimicrobial Chemotherapy* **2004**, *53*, 53-57.
- (31) Sarafianos, S. G.; Hughes, S. H.; Arnold, E. *International Journal of Biochemistry and Cell Biology* **2004**, *36*, 1706-1715.
- (32) Shimada, N.; Hasegawa, S.; Harada, T.; Tomisawa, T.; Fukii, A.; Takita, T. *The Journal of Antibiotics* **1986**, *39*, 1623-1625.
- (33) Hoshino, H.; Shimizu, N.; Shimada, N.; Takita, T.; Takeuchi, T. *The Journal of Antibiotics* **1987**, *40*, 1077-1078.
- (34) Norbeck, D. W.; Kern, E.; Hayashi, S.; Rosenbrook, W.; Sham, H.; Herrin, T.; Plattner, J. J.; Erickson, J.; Clement, J.; Swanson, R.; Shipkowitz, N.; Hardy, D.; Marsh, K.; Arnett, G.; Shannon, W.; Broder, S.; Mitsuya, H. *Journal of Medicinal Chemistry* **1990**, *33*, 1281-1285.
- (35) Bauld, N. L.; Cessac, J. *Journal of the American Chemical Society* **1977**, *99*, 942-943.
- (36) Bauld, N. L.; Cessac, J.; Holloway, R. T. *Journal of the American Chemical Society* **1977**, *99*, 8140-8144.

- (37) Huryñ, D. M.; Okabe, M. *Chemical Reviews* **1992**, *92*, 1745-1768.
- (38) Ichikawa, E.; Kato, K. *Synthesis* **2002**, 1-28.
- (39) Ortuno, R. M.; Moglioni, A. G.; Moltrasio, G. Y. *Current Organic Chemistry* **2005**, *9*, 237-259.
- (40) Brannock, K. C.; Burpitt, R. D.; Thweatt, J. G. *Journal of Organic Chemistry* **1964**, *29*, 940-941.
- (41) Slusarchyk, W. A.; Young, M. G.; Bisacchi, G. S.; Hockstein, D. R.; Zahler, R. *Tetrahedron Letters* **1989**, *30*, 6453-6456.
- (42) Saleem, A. *Tetrahedron Letters* **1991**, *32*, 6997-7000.
- (43) Ichikawa, Y.-I.; Narita, A.; Shiozawa, A.; Hayashi, Y.; Narasaka, K. *Journal of the Chemical Society, Chemical Communications* **1989**, 1919-1921.
- (44) Hsiao, C.-N.; Hannick, S. M. *Tetrahedron Letters* **1990**, *31*, 6609-6612.
- (45) Katagiri, N.; Sato, H.; Kaneko, C. *Chemical and Pharmaceutical Bulletin* **1990**, *38*, 288-290.
- (46) Izawa, T.; Ogino, Y.; Nishiyama, S.; Yamamura, S.; Kato, K.; Takita, T. *Tetrahedron* **1992**, *48*, 1573-1580.
- (47) Brown, B.; Hegedus, L. S. *Journal of Organic Chemistry* **1998**, *63*, 8012-8018.
- (48) Cotterill, I. C.; Roberts, S. M. *Journal of the Chemical Society, Perkin Transactions 1* **1992**, 2585-2586.
- (49) Jung, M. E.; Sledeski, A. W. *Journal of the Chemical Society, Chemical Communications* **1993**, 589-591.

- (50) Somekawa, K.; Hara, R.; Kinnami, K.; Muraoka, F.; Suishu, T.; Shimo, T. *Chemistry Letters* **1995**, *24*, 407-408.
- (51) Ito, H.; Taguchi, T.; Hanzawa, Y. *Tetrahedron Letters* **1993**, *34*, 7639-7640.
- (52) Gourdel-Martin, M.-E.; Huet, F. *Journal of Organic Chemistry* **1997**, *62*, 2166-2172.
- (53) Gharbaoui, T.; Legraverend, M.; Ludwig, O.; Bisagni, E.; Aubertin, A.-M.; Chertanova, L. *Tetrahedron* **1995**, *51*, 1641-1652.
- (54) Boumchita, H.; Legraverend, M.; Guilhem, J.; Bisagni, E. *Heterocycles* **1991**, *32*, 867-871.
- (55) Kaiwar, V.; Reese, C. B.; Gray, E. J.; Neidle, S. *Journal of the Chemical Society, Perkin Transactions 1* **1995**, 2281-2287.
- (56) Guan, H.-P.; Ksebati, M. B.; Kern, E. R.; Zemlicka, J. *Journal of Organic Chemistry* **2000**, *65*, 5177-5184.
- (57) Fernández, F.; Lópezand, C.; Hergueta, A. R. *Tetrahedron* **1995**, *51*, 10317-10322.
- (58) Hergueta, A. R.; López, C.; Fernández, F.; Caamaño, O.; Blanco, J. M. *Tetrahedron, Asymmetry* **2003**, *14*, 3773-3778.
- (59) Rouge, P. D.; Moglioni, A. G.; Moltrasio, G. Y.; Ortuño, R. M. *Tetrahedron, Asymmetry* **2003**, *14*, 193-195.
- (60) Okabe, M.; Sun, R. C.; Tam, S. Y. K.; Todaro, L. J.; Coffen, D. L. *Journal of Organic Chemistry* **1988**, *53*, 4780-4786.

- (61) Bisacchi, G. S.; Singh, J.; Godfrey, J. D.; Kissick, T. P.; Mitt, T.; Malley, M. F.; Di Marco, J. D.; Gougoutas, J. Z.; Mueller, R. H.; Zahler, R. *Journal of Organic Chemistry* **1995**, *60*, 2902-2905.
- (62) Peterson, M. L.; Vince, R. *Journal of Medicinal Chemistry* **1991**, *34*, 2787-2797.
- (63) Jacobs, G. A.; Tino, J. A.; Zahler, R. *Tetrahedron Letters* **1989**, *30*, 6955-6958.
- (64) Wu, J.; Schneller, S. W.; Seley, K. L.; Snoeck, R.; Andrei, G.; Balzarini, J.; De Clercq, E. *Journal of Medicinal Chemistry* **1997**, *40*, 1401-1406.
- (65) Shaw, G.; Warrener, R. N. *Proceedings of the Chemical Society of London* **1958**, 81-82.
- (66) Shaw, G.; Warrener, R. N. *Journal of the Chemical Society* **1958**, 153-156.
- (67) Shaw, G.; Warrener, R. N. *Journal of the Chemical Society* **1958**, 157-161.
- (68) Shaw, G.; Warrener, R. N.; Maguire, M. H.; Ralph, R. K. *Journal of the Chemical Society* **1958**, 2294-2299.
- (69) Shealy, Y. F.; Odell, C. A. *Journal of Heterocyclic Chemistry* **1976**, *13*, 1015-1020.
- (70) Ichikawa, E.; Kato, K. *Current Medicinal Chemistry* **2001**, *8*, 385.
- (71) Milewska, Z.; Panusz, H. *Analytical Biochemistry* **1974**, *57*, 8-13.
- (72) Burgess, K.; Cook, D. *Chemical Reviews* **2000**, *100*, 2047-2060.

- (73) Yoshikawa, M.; Kato, T.; Takenishi, T. *Tetrahedron Letters* **1967**, *8*, 5065-5068.
- (74) Ludwig, J. *Acta Biochimica et Biophysica Academiae Scientiarum Hungaricae* **1981**, *16*, 131-133.
- (75) Smith, M.; Khorana, H. G. *Journal of the American Chemical Society* **1958**, *80*, 1141-1145.
- (76) Moffatt, J. G. *Canadian Journal of Chemistry* **1964**, *42*, 599-604.
- (77) Ludwig, J.; Eckstein, F. *Journal of Organic Chemistry* **1989**, *54*, 631-635.
- (78) Frieden, M.; Giraud, M.; Reese, C. B.; Song, Q. L. *Journal of the Chemical Society-Perkin Transactions 1* **1998**, 2827-2832.
- (79) Liotta, D. C.; Mao, S.; Hager, M. 2006; Vol. WO2006063281.
- (80) Geen, G. R.; Grinter, T. J.; Kincey, P. M.; Jarvest, R. L. *Tetrahedron* **1990**, *46*, 6903-6914.
- (81) Porcari, A. R.; Ptak, R. G.; Borysko, K. Z.; Breitenbach, J. M.; Vittori, S.; Wotring, L. L.; Drach, J. C.; Townsend, L. B. *Journal of Medicinal Chemistry* **2000**, *43*, 2438-2448.
- (82) Cook, P. D.; Ewing, G.; Jin, Y.; Lambert, J.; Prhavic, M.; Rajappan, V.; Rajwanshi, V. K.; Sakthivel, K.; (Biota, Inc., USA). Application: WO, 2005, p 106 pp.
- (83) Porcari, A. R.; Ptak, R. G.; Borysko, K. Z.; Breitenbach, J. M.; Drach, J. C.; Townsend, L. B. *Journal of Medicinal Chemistry* **2000**, *43*, 2457-2463.
- (84) An, H.; Hong, Z.; Smith, K.; Ding, Y.; Girardet, J.-I.; (Ribapharm Inc., USA). Application: WO, 2003, p 65 pp.

- (85) Davoll, J. *Journal of the Chemical Society* **1960**, 131-138.
- (86) Pudlo, J. S.; Nassiri, M. R.; Kern, E. R.; Wotring, L. L.; Drach, J. C.; Townsend, L. B. *Journal of Medicinal Chemistry* **1990**, *33*, 1984-1992.
- (87) Eissenstat, M. A.; Weaver, J. D. *Tetrahedron Letters* **1995**, *36*, 2029-2032.
- (88) Sobolov, S. B.; Sun, J.; Cooper, B. A. *Tetrahedron Letters* **1998**, *39*, 5685-5688.
- (89) Eller, G. A.; Holzer, W. *Heterocycles* **2004**, *63*, 2537-2555.
- (90) Edstrom, E. D.; Wei, Y. *Journal of Organic Chemistry* **1993**, *58*, 403-407.
- (91) Taylor, E. C.; Liu, B. *Journal of Organic Chemistry* **2001**, *66*, 3726-3738.
- (92) Jones, M. I.; Froussios, C.; Evans, D. A. *Journal of the Chemical Society, Chemical Communications* **1976**, 472-473.
- (93) Seela, F.; Zulauf, M. *Synthesis* **1996**, 726-730.
- (94) Bajwa, J. S.; Chen, G. P.; Prasad, K.; Repic, J.; Blacklock, T. J. *Tetrahedron Letters* **2006**, *47*, 6425-6427.
- (95) Amat, M.; Hadida, S.; Sathyanarayana, S.; Bosch, J. *Journal of Organic Chemistry* **1994**, *59*, 10-11.
- (96) Edstrom, E. D.; Wei, Y. *Journal of Organic Chemistry* **1995**, *60*, 5069-5076.
- (97) Edstrom, E. D.; Feng, X.; Tumkevicius, S. *Tetrahedron Letters* **1996**, *37*, 759-762.
- (98) Hess, S.; Muller, C. E.; Frobenius, W.; Reith, U.; Klotz, K. N.; Eger, K. *Journal of Medicinal Chemistry* **2000**, *43*, 4636-4646.

- (99) Chien, T. C.; Meade, E. A.; Hinkley, J. M.; Townsend, L. B. *Organic Letters* **2004**, *6*, 2857-2859.
- (100) Eger, K.; Pfahl, J. G.; Folkers, G.; Roth, H. J. *Journal of Heterocyclic Chemistry* **1987**, *24*, 425-430.
- (101) Kondo, T.; Nakatsuka, S.; Goto, T. *Chemistry Letters* **1980**, 559-562.
- (102) Seela, F.; Bussmann, W.; Gotze, A.; Rosemeyer, H. *Journal of Medicinal Chemistry* **1984**, *27*, 981-985.
- (103) Ohno, H.; Terui, T.; Kitawaki, T.; Chida, N. *Tetrahedron Letters* **2006**, *47*, 5747-5750.
- (104) Gunic, E.; Girardet, J.-L.; Pietrzkowski, Z.; Esler, C.; Wang, G. *Bioorganic & Medicinal Chemistry* **2001**, *9*, 163-170.
- (105) Bera, S.; Malik, L.; Bhat, B.; Carroll, S. S.; MacCoss, M.; Olsen, D. B.; Tomassini, J. E.; Eldrup, A. B. *Bioorganic & Medicinal Chemistry Letters* **2003**, *13*, 4455-4458.
- (106) Jeang, K. T.; Yedavalli, V. *Nucleic Acids Research* **2006**, *34*, 4198-4205.
- (107) Zhang, N.; Chen, H. M.; Koch, V.; Schmitz, H.; Minczuk, M.; Stepien, P.; Fattom, A. I.; Naso, R. B.; Kalicharran, K.; Borowski, P.; Hosmane, R. S. *Journal of Medicinal Chemistry* **2003**, *46*, 4776-4789.
- (108) Zhang, N.; Chen, H. M.; Koch, V.; Schmitz, H.; Liao, C. L.; Bretner, M.; Bhadti, V. S.; Fattom, A. I.; Naso, R. B.; Hosmane, R. S.; Borowski, P. *Journal of Medicinal Chemistry* **2003**, *46*, 4149-4164.

- (109) Schinazi, R. F.; Sommadossi, J. P.; Saalman, V.; Cannon, D. L.; Xie, M. Y.; Hart, G. C.; Smith, G. A.; Hahn, E. F. *Antimicrobial Agents and Chemotherapy* **1990**, *34*, 1061-1067.
- (110) Stuyver, L. J.; Lostia, S.; Adams, M.; Mathew, J. S.; Pai, B. S.; Grier, J.; Tharnish, P. M.; Choi, Y.; Chong, Y.; Choo, H.; Chu, C. K.; Otto, M. J.; Schinazi, R. F. *Antimicrobial Agents and Chemotherapy* **2002**, *46*, 3854-3860.
- (111) Stuyver, L. J.; Whitaker, T.; McBrayer, T. R.; Hernandez-Santiago, B. I.; Lostia, S.; Tharnish, P. M.; Ramesh, M.; Chu, C. K.; Jordan, R.; Shi, J. X.; Rachakonda, S.; Watanabe, K. A.; Otto, M. J.; Schinazi, R. F. *Antimicrobial Agents and Chemotherapy* **2003**, *47*, 244-254.

Part II: Improvement of Glycosylation Regioselectivity in Purine Nucleoside Analogue Synthesis

2.1 Statement of Purpose

Nucleosides and their analogues have been employed in the treatment of infectious disease, viral infections, and cancer.¹ Many of these FDA approved nucleoside agents contain purine nucleobases, including acyclovir (used for the treatment of herpes simplex virus and herpes zoster), didanosine (an anti-HIV agent) and the anti-cancer agent clofarabine (Figure 1). Thus, in the discovery efforts for new agents, purine analogues are often explored.

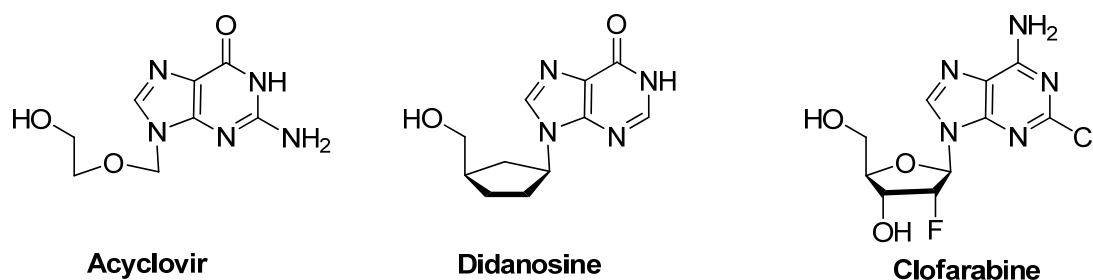
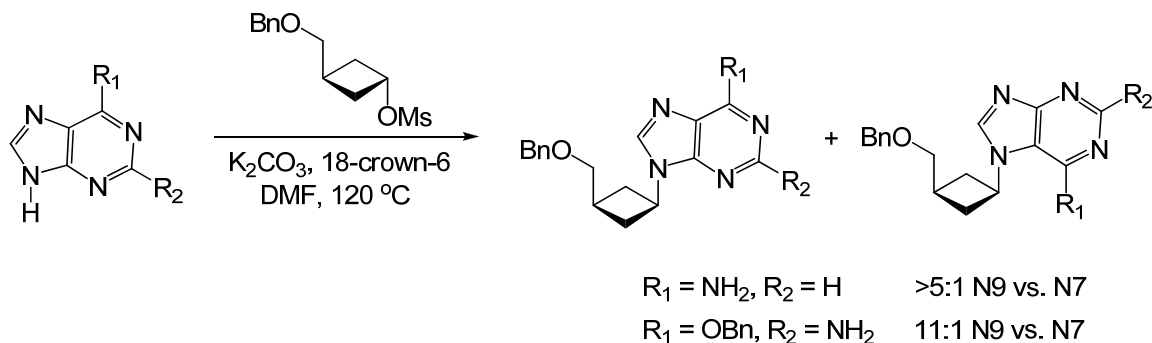


Figure 1: Representative FDA approved purine nucleoside analogues

While there are several methods that are able to reliably synthesize these analogues, control of the regioselectivity of these couplings presents a major challenge. There are existing methods developed that selectively couple to the N9 position, including the use of purine tetrabutylammonium salts and also the rearrangement of the N7 product to the N9 coupled product under acidic conditions.^{2,3} These methods, however, are not suitable for all systems.

We have chosen to address this issue in terms of steric discrimination. In order to improve the N9 vs. N7 selectivity, we envision that a bulky and easily

removable group is needed on position 6 to block the N7 position. This should leave only N9 open for glycosylation, which increases the regioselectivity as seen with the O⁶-benzylguanine coupling (Part I). Because the benzyloxy group is much more bulky than the amino group, the regioselectivity increased from 5:1 to 11:1 for the cyclobutyl coupling of adenine vs. O⁶-benzylguanine, respectively.



Scheme 1: Glycosylation regioselectivity on cyclobutyl coupling with adenine and O⁶-benzylguanine

The substitution of 6-chloropurine with a trisubstituted silyl group in the C6 position should increase the regioselectivity similarly. The silyl group was chosen due to its ability to be easily derivitized into different purine nucleobases.

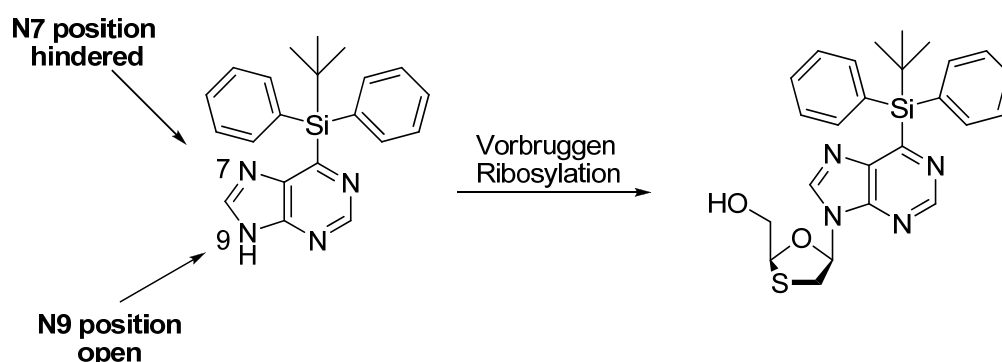


Figure 2: Hypothesized N9 vs. N7 glycosylation regioselectivity with 6-silyl substituted purines

2.2 Introduction and Background

The regioselective glycosylation of purines at the N9 position is difficult to accomplish. There are many factors that have been identified which greatly influence the N9 to N7 glycosylation ratios. Among these are the base, solvent, and temperature used in the reaction.^{4,5} However, the developed regioselective methods tend to be highly specific for the purine and carbohydrate components used in the coupling, and are not easily applied to other systems. It has been previously recognized that the use of large substituents at the C6 position can result in larger N9 to N7 ratios of the coupled nucleoside analogues.^{6,7} We have chosen to further explore this method of derivatizing the C6 position of 6-chloropurine in order to achieve regioselective coupling.

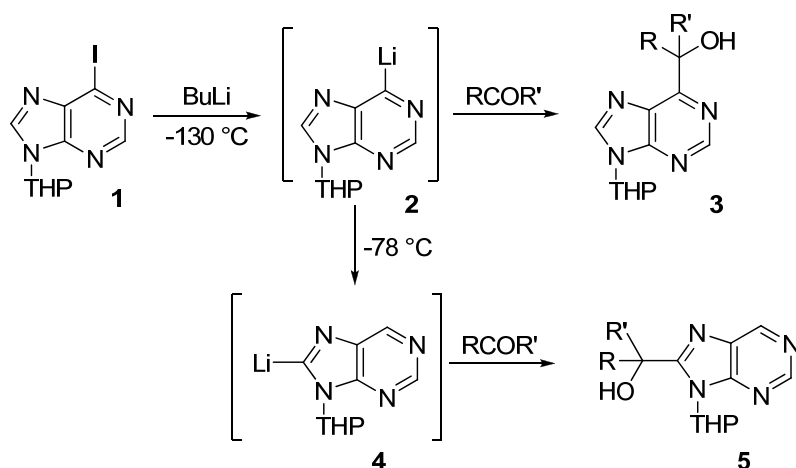
The traditional ways of derivatizing the 6-position of purines involve either heterocyclization or nucleophilic substitution. The cyclization method requires multistep procedures and results in low yields of the 6-substituted purine. The nucleophilic substitution method is limited to only certain types of functional groups. Thus, efforts have been made in applying organometallic reactions to the development of 6-substituted purines.⁸ Major methods that have been employed in this arena involve the use of organometallic purine compounds and also the cross-coupling reactions between halopurines and organometallics.

The generation of organometallic purine reagents has been used to reliably synthesize 2-, 6-, and 8-substituted purines. The general method involves the use of a leaving group on the purine, including halogens and activated hydroxyl groups, with organometallic compounds based upon Li, Mg,

Cu, Al, Zn, Sn, and B. In addition, halopurines have been treated with organometallic reagents in the presence of Pd and Ni catalysts. Both methods have been used to create alkyl, alkenyl, alkynyl, aryl, and hetaryl derivatives. The following sections describe selected methods that have been used to derivatize the C-6 position of purines.

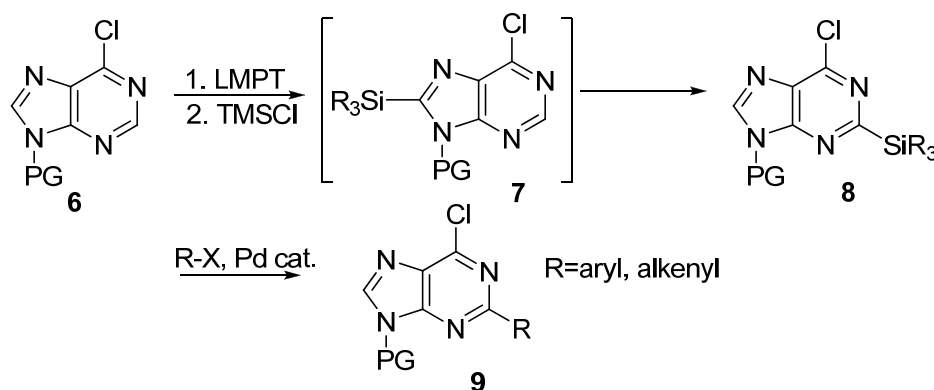
2.2.1 Organolithium Reagents

Purines can be lithiated to form a variety of substituted compounds depending upon the reaction conditions. It has been found that changing the temperature when reacting an N9 protected 6-iodopurine with *n*-BuLi can affect the regioselectivity of the reaction.⁹ When reacting the purine with *n*-BuLi at -78°C, the more acidic C-8 proton was abstracted to form the 8-lithiopurine derivative. However, when the temperature was lowered to -130 °C, the lithium halogen exchange occurred to form the C-6 anion. Warming the reaction to -78 °C resulted in the isomerization of the kinetic 6-lithiopurine intermediate to the thermodynamic 8-lithio derivative.



Scheme 2: Regioselectivity in C6 vs. C8 lithiated purine generation

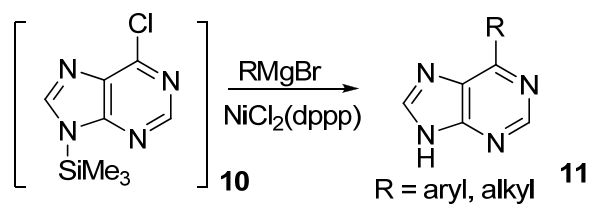
The silylation of these purines has been reported in both the 2- and 8-positions of the purine.¹⁰⁻¹² This was shown with the reaction of 6-chloropurine and LTMP. Lithiation of the purine and quenching with R_3SiCl resulted in the 2-silyl product. This was as a result of migration of the silyl group from C-8 to C-2 (Scheme 3).



Scheme 3: Silyl group migration in purine derivatization

2.2.2 Organomagnesium Reagents

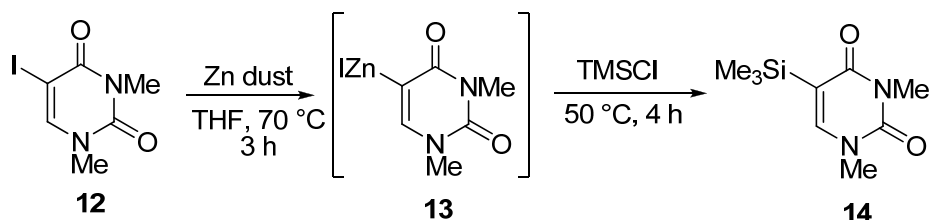
Organomagnesium reagents can be used for both addition and cross-coupling reactions with purines. In these reactions between organomagnesium reagents and halopurines, nickel catalysts tend to be more effective than palladium (Scheme 4).¹³ It was shown that 9-protected-6-chloropurines could be reacted with 2.5 eq of a Grignard reagent to give the 6-aryl or 6-alkylpurine in moderate (60 – 70%) yields. Because Grignard reagents are highly reactive and have low tolerance to functional groups, their use in cross-coupling reactions with purines is limited.



Scheme 4: Purine cross-coupling with organomagnesium reagents

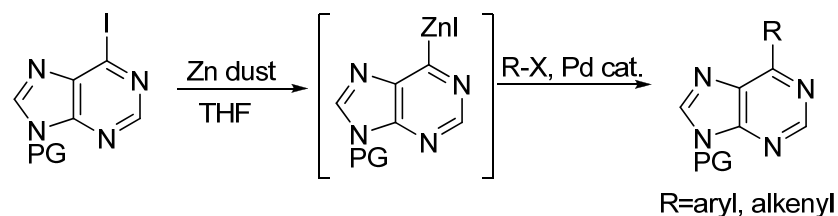
2.2.3 Organozinc Reagents

Knochel and coworkers developed a method of preparing zincated nucleobases through a zinc dust insertion.¹⁴ These systems were able to undergo cross-couplings effectively with a variety of electrophiles. It was also noted that although organozinc halides do not ordinarily react with TMSCl, the iodozinc uracil derivative was able to react with TMSCl without the need of catalyst to provide the silylated product in 78% yield (Scheme 5).¹⁵



Scheme 5: Silylation of iodozinc uracil

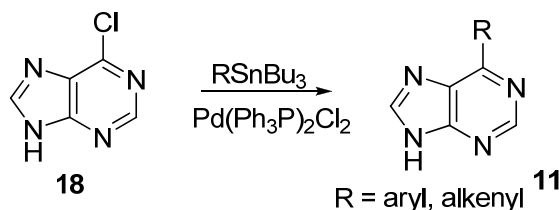
It has also been shown that the 6-iodopurines can be transformed into the zincated 6-iodopurine through the use of activated zinc metal (Scheme 6). These purines can then be cross-coupled under Negishi conditions with a variety of aryl and alkenyl halides to create 6-substituted derivatives.^{14,15} In addition, halopurines can be coupled with organozinc compounds. This method has been used to introduce alkyl, alkenyl, aryl, and hetaryl groups.



Scheme 6: Use of 6-zincated iodopurine for C6 derivatization

2.2.4 Organostannane Reagents

The Stille coupling remains the most commonly used method for synthesizing 2-, 6-, and also 8- substituted purines. This is because a wide variety of derivatives can be created, especially when using alkenyl tributylstannanes. It has been shown that unprotected 6-chloropurine can be treated with alkenyl and aryl tributylstannanes to provide the corresponding alkenyl and aryl purine derivatives (Scheme 7).^{16,17} A major problem with the use of organostannane reagents is the toxicity and difficulties in separation.



Scheme 7: Purine cross-coupling with organostannane reagents

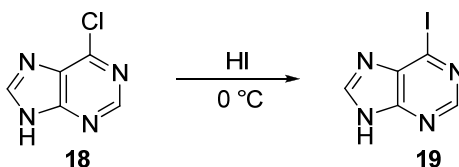
2.3 Results and Discussion

The synthesis of the 6-silylpurine was explored by a variety of methods. This includes the generation of organolithium and organomagnesium purines and also the cross-couplings of halopurines.

2.3.1 Organolithium Generation

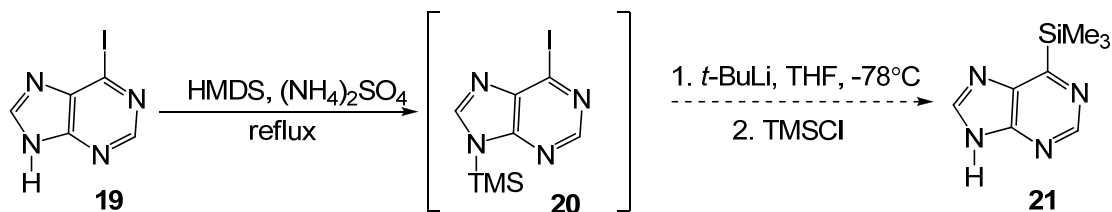
Lithium/Halogen Exchange

The generation of an organolithium heterocycle through a lithium/halogen exchange method is the most common way of performing the desired transformation.¹⁸⁻²⁰ When applied to this system, a halogenated purine derivative would be treated with a lithium reagent, and then with a silyl electrophile to generate the desired product. The initial lithium reagent used in this study was *t*-BuLi. This is because studies have been performed previously with *n*-BuLi, which gave varying 2-, 6-, and 8-lithiated purines depending upon reaction conditions. Use of *t*-BuLi has not been explored, though. Because the C8 proton is very acidic, it is reasonable that the more nucleophilic *n*-BuLi reagent would result in C8 product.⁹ However, the *t*-BuLi reagent is more likely to undergo exchange with the halogen. In addition, the commercially available 6-chloropurine was iodinated to form 6-iodopurine, as the chloro group is not as readily exchangeable (Scheme 8).^{21,22}



Scheme 8: Synthesis of 6-iodopurine

The purine was refluxed in HMDS with ammonium sulfate in order to silylate the N9 position (Scheme 9). This increases the solubility of the base in THF. Following this, *t*-BuLi was added at -78°C to induce the lithium-halogen exchange. The TMSCl electrophile was added which should have produced the silylated base. There was no product formation, however.



Scheme 9: Attempts towards the synthesis of 6-trimethylsilyl-purine

The amounts of *t*-BuLi, TMSCl, and the time lapsed between the addition of *t*-BuLi and the silyl electrophile were varied in efforts of synthesizing the product (Table 1). Initially, it was hypothesized that the lithium-halogen exchange was not occurring. Thus, the time in between the *t*-BuLi and TMSCl addition was varied. Longer reaction times, however, did not give the desired product. Also, the amounts of *t*-BuLi and TMSCl were both increased. These changes did not result in product either. Finally, the electrophile was introduced into the reaction before the lithium reagent. It was hypothesized that the organolithium may form rapidly; thus, the electrophile should be added prior to the reagent to act as a trapping agent. However, this method failed to produce the silylated nucleobase.

<i>t</i>-BuLi (eq)	TMSCl (eq)	Time before TMSCl (hrs)	Temp (°C)
2.0	1.2	1	-78 to rt
2.0	1.2	2	-78 to rt
2.0	1.2	3	-78 to rt
3.2	20.0	4	-78 to rt
3.2	100.0	8	-78 to rt
5.0	10.0	0	-78 to rt

Table 1: Conditions used for 6-iodopurine silylation using *t*-BuLi

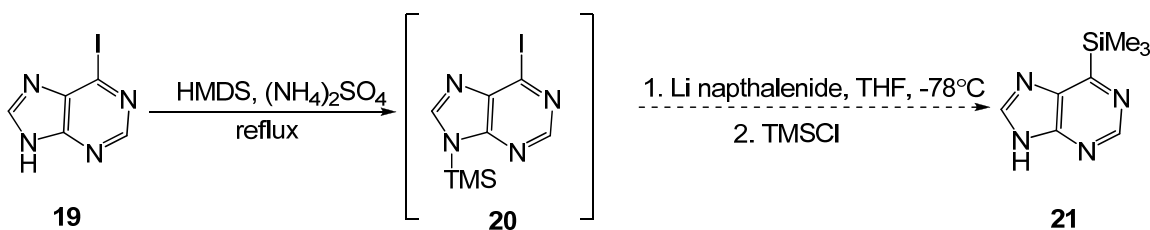
In one instance, a trace amount of the 6-*t*-butylpurine was detected in the crude product mixture. In the event that the *t*-butyl group was competing for C-6 addition, the lithium reagent was changed to LiTMS.²³ Thus, if the lithium counterion added into the C-6 position, it would still produce the desired product. Again, the amounts of LiTMS and TMSCl were varied in these trials, but there was no product formation. For the last trial shown, higher temperatures were used; however, this effort failed as well (Table 2). These reactions were also tried with the LiTBDPS reagent.²⁴

LiTMS (eq)	TMSCl (eq)	Time before TMSCl (hrs)	Temp (°C)
3.2	100.0	3	-78 to rt
3.2	100.0	5	-78 to rt
3.2	20.0	4	-78 to rt
3.2	3.1	2.5	-78 to rt
3.2	3.1	1	-78 to rt
3.2	3.1	1	-20 to 0

Table 2: Conditions used for 6-iodopurine silylation using LiTMS

Another trial was done using lithium naphthalenide²⁵, which is a more hindered base than *t*-BuLi (Scheme 10). This was done to prevent addition of

the lithium counter ion. In this case, however, only starting material was recovered.

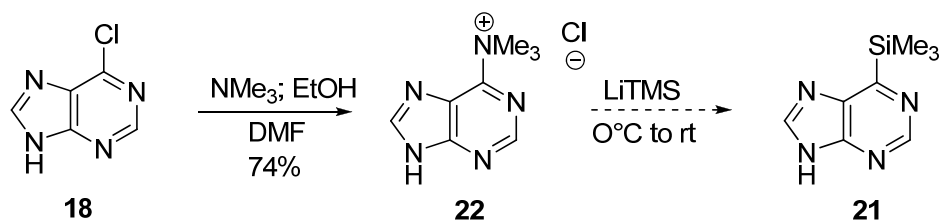


Scheme 10: Attempts towards the synthesis of 6-trimethylsilylpurine using Li naphthalenide

It has been reported that because strong bases such as the alkylolithiums can also act as nucleophiles, it may be necessary to use a weaker base, such as LTMP, to produce the organolithiate. Lithiation has been accomplished with LTMP in a number of heteroaromatic systems, including pyrimidines.^{26,27} However, the use of this reagent to induce the lithium/halogen exchange and treatment with electrophile did not result in product.

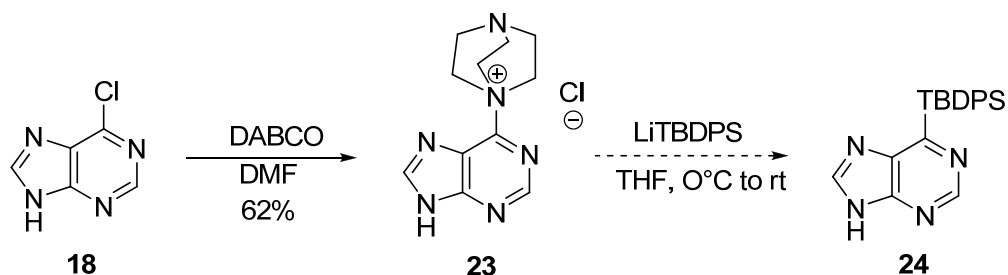
DABCO and Trimethylammonium Purine

The failure of the above methods to produce the desired 6-silylpurine derivative was most likely due to the lithium/halogen exchange not occurring. Thus, it was necessary to employ a readily exchangeable group on the purine. A method that has been employed previously to displace substituents in the C-6 position of purines is the use of the 6-trimethylammonium intermediate.²⁸⁻³¹ It has been shown that this group undergoes addition-elimination much faster than chloride. Thus, it was employed in the synthesis of the 6-silylpurine. However, there was no product formation.



Scheme 11: Use of trimethylammonium purine for silylation

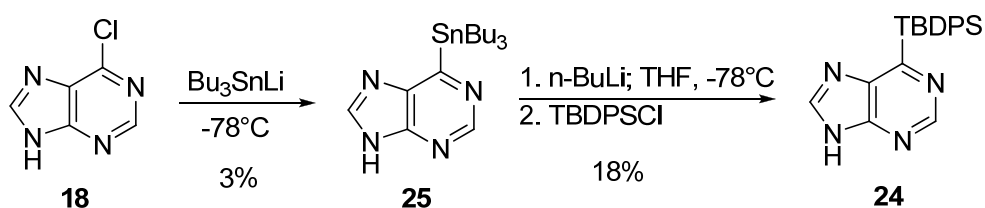
The DABCO purine was prepared and used, as it has also been reported to be a better leaving group than chloride in the addition-elimination reaction, though not as effective as the trimethylammonium. The order of displacement of groups from the 6-position of purines is $\text{Me}_3\text{N} > \text{DABCO} > \text{Cl}$ (relative rates *ca.* 100:10:1).³² It does, however, have certain benefits over the trimethylammonium purine. The trimethylammonium purine is prepared through the reaction of 6-chloropurine with trimethylamine, which is volatile, toxic, and has an unpleasant odor. In addition, it has been shown that nucleophiles can attack a methyl group on the trimethylammonium group through an $\text{S}_{\text{N}}2$ displacement that is competitive with addition-elimination.³³ The DABCO purine reagents have been shown to undergo displacement reactions with a number of alkoxides.^{32,34,35} However, the reaction failed with the silylation method, using both LiTBDS and LiTMS (Scheme 12). The *in situ* trapping method through the early addition of silyl electrophile did not result in product either.



Scheme 12: Use of DABCO purine to generate silyl purine

Lithium/Tin Exchange

Organostannyl reagents have been employed extensively in transmetalation reactions to form organolithium species. This is because these reagents are stable and easy to handle, and can often be used in the synthesis of organolithiates that cannot be formed directly.³⁶ The lithium/tin exchange method has been used with hetarylstannanes, including pyrroles, imidazoles, and pyrimidines to create the desired lithiated species.^{37,38} This method was applied to the synthesis of the 6-silylpurines and was able to generate the 6-TBDPS-purine as a mixture in low yields (Scheme 13). Though this is not an ideal method due to the low yield and non-reproducibility, it does prove that the silyl purine derivative is stable enough to be isolated.

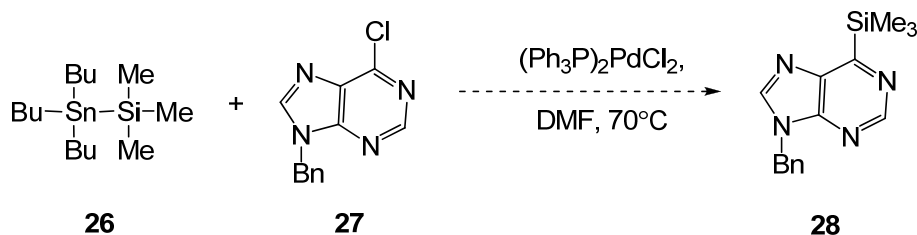


Scheme 13: Use of lithium/tin exchange to prepare silyl purine

2.3.2 Palladium Catalyzed Cross-Couplings

Stille Coupling

Cross-coupling reactions catalyzed by palladium have been used extensively in the derivatization of the C-6 position of purines. The Stille coupling has been used for the C-C bond formation in the 2-, 6-, and 8-positions of the purine.³⁹⁻⁴¹ The Stille coupling was employed to introduce the silyl group to the C6 position of the base (Scheme 14). In this case, the base was benzylated first in order to solvate it.⁴² The purine was treated with the silylstannane, derived from LDA and tributyltin hydride reacting with trimethylsilyl chloride.^{43,44} The reaction was heated to 70°C for 20 hours; however, only starting material was recovered.



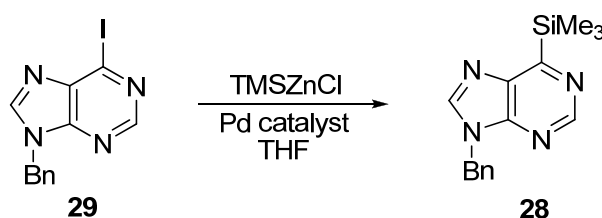
Scheme 14: Stille coupling used for nucleobase silylation

Negishi Coupling

The Negishi coupling has also been employed in the synthesis of 6-substituted purines, and was thus applied to this system. This method has been used to create amino acid-nucleobase conjugates by using iodozincalanines and 6-iodopurines.⁴⁵

The benzylated iodopurine was employed in order to solvate the purine. Treatment of the purine with TMSZnCl resulted in the formation of minimal

product. Palladium catalysts were used, with addition occurring at 0 °C and warming of the reaction mixture after completion of silyl zinc addition. The use of additives and different palladium catalysts did not assist the coupling.⁴⁶ The 6-chloropurine derivative did not react at all. Though this method afforded product, it is not the method of choice as it is necessary to deprotect the N-9 position. This will result, of course, in lower yields than that already obtained. With this additional knowledge that the trimethylsilyl purine is stable, methods to generate the modified nucleobase without using an N9 protective group were sought.



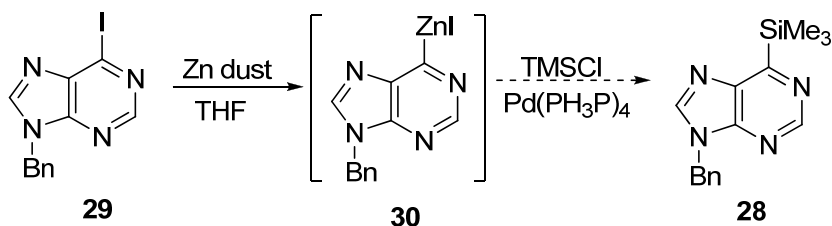
Scheme 15: Negishi coupling used for nucleobase silylation

TMSZnCl (eq)	Pd catalyst	Time (hrs)	Temp (°C)	Additive	Yield
1.3	Pd(Ph ₃ P) ₂ Cl ₂	20	0 to r.t.	none	15%
2.5	Pd(Ph ₃ P) ₂ Cl ₂	20	0 to r.t.	none	21%
3.0	Pd(Ph ₃ P) ₂ Cl ₂	20	0 to 50	none	11%
3.0	Pd(Ph ₃ P) ₄	20	0 to 50	none	14%
3.0	Pd(dba) ₂ /TFP	20	0 to 60	none	8%
1.3	Pd(Ph ₃ P) ₄	24	0 to 75	NMP	-
1.3	Pd(Ph ₃ P) ₂ Cl ₂	24	0 to 75	NMP	-
3.0	Pd(Ph ₃ P) ₄	24	0 to 50	CuI	-

Table 3: Conditions for Negishi coupling

There are examples in the literature that create the metallated nucleobase as the nucleophile in the reaction, though this is not commonly done due to the

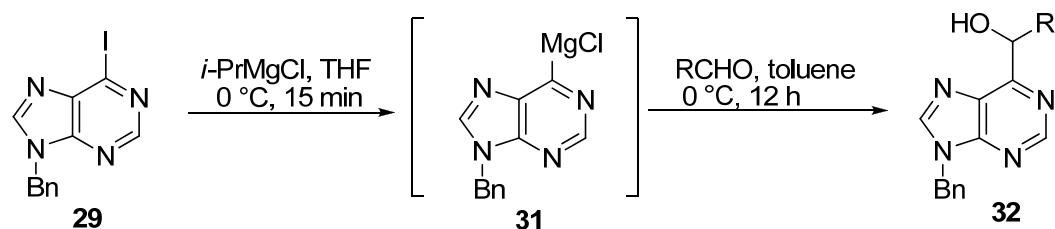
difficulties in preparing these species.¹⁴ Formation of the 6-iodozinc purine and subsequent treatment with the TMSCl electrophile did not result in any product (Scheme 16).



Scheme 16: Attempted Negishi coupling using iodozinc purine

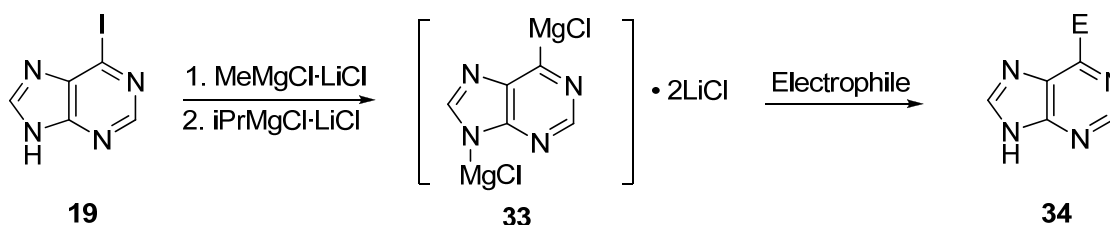
2.3.3 Halogen/Magnesium Exchange

A different approach for performing the halogen exchange has been proposed to occur through a purine-derived Grignard reagent. It was hypothesized that these reagents are more stable than the corresponding lithium reagents and are more reactive than the zinc reagents.⁴⁷ The magnesiated purine was successfully synthesized through an exchange reaction with *i*-PrMgCl in THF at -80 °C in less than 30 minutes. It was shown that the benzylated magnesium purine is stable at this temperature and up to 0 °C. However, slow decomposition results at temperatures above this. There is no migration of magnesium to the 8-position, however. The purine was then treated with a variety of electrophiles, including aldehydes, ketones, esters, and nitriles. However, only aldehydes reacted with this reagent to give the corresponding alcohols (Scheme 17).



Scheme 17: Reaction of aldehydes with 6-magnesiated purines

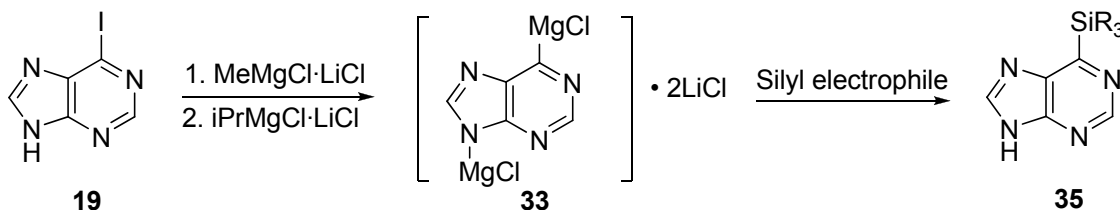
A modification of this method has been reported by Knochel and coworkers.⁴⁸ This method involves the use of MeMgCl to deprotonate the purine, and lithium chloride to improve the solubility of the reagent and also to assist in the exchange reaction with *i*-PrMgCl. The dimagnesiated species can then be treated with an electrophile (Scheme 18). This method is more attractive than the initial method in that the purine is protected *in situ*, thus eliminating two additional steps from the synthesis. Also, this reagent and its pyrimidine counterpart have been shown to react with a wider variety of electrophiles, including aldehydes, alkyl halides, sulfonates, and even TMSCl in the case of pyrimidines.



Scheme 18: Functionalization of unprotected nucleobases using magnesium/halogen exchange

This reaction was employed for the system of this project. Different silyl electrophiles were used, including TMSCl, hexamethyldisilane, and hexamethyldisilazane. No product was isolated in these attempts, even when

using additives such as CuI, which may have assisted with the transmetalation (Table 4). Analysis of the reaction mixture shows that the protonated purine is the major product isolated from this reaction. This proves that the halogen/magnesium exchange is occurring with the system. Thus, either the electrophile is not suitable, or the product is not stable enough.



Scheme 19: Attempted silylation of magnesiated purine

Electrophile	Equivalents	Temp (°C)	Time (hrs)	Additive
TMSCl	3.5	-30 to rt	24	-
TMSCl	7.0	-30 to rt	24	-
(SiMe ₃) ₂ NH	3.3	-30 to 50	24	TMSCl
TMSCl	3.3	-30 to 50	24	CuI
(SiMe ₃) ₂	3.3	-30 to 50	24	-
TBDPSCI	3.3	-30 to rt	24	-

Table 4: Conditions for halogen/magnesium exchange

The reaction was monitored by mass spectrometry. The crude mixture for the TBDPSCI reaction showed the presence of product. However, after purification by column chromatography, no product was detected. The reaction was then performed again using TMSCl as the silyl electrophile, but with lower reaction temperatures. It was shown in the earlier halogen/magnesium exchange methodology that the magnesium species can be formed in 30 minutes

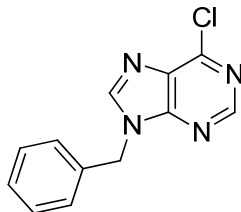
at -78 °C. Thus, in order to prevent side reactions with the reactive species, the reaction was performed at -78°C and only warmed to room temperature after addition of the electrophile. The crude product was analyzed by mass spectrometry and also NMR, which showed the formation of the 6-trimethylsilyl-purine. Attempts to re-crystallize the crude product failed using different solvents. The product was then purified by column chromatography, which resulted in decomposition of the product.

2.4 Conclusion

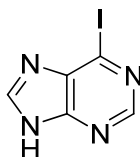
The 6-silyl purine was successfully prepared in both the free nucleobase and N9-benzyl forms. However, these compounds were not able to be isolated in high yields. Purification of the compounds by column chromatography resulted in decomposition. In addition, efforts to recrystallize the compound failed. It will be necessary to develop conditions to efficiently isolate this compound, and then couple the 6-silyl purine to various pseudosugars and determine the N9 vs N7 regioselective enhancement.

2.5 Experimental

General: ^1H -NMR spectra were recorded at either 400 MHz on an INOVA-400 spectrometer, or at 600 MHz on an INOVA-600 spectrometer. ^{13}C -NMR spectra were recorded at either 100 MHz or 150 MHz on the above mentioned instruments, respectively. NMR samples were prepared in either deuterated chloroform (CDCl_3) or dimethyl sulfoxide (d^6 -DMSO) with residual solvent peaks serving as the internal standards. Chemical shifts (δ) are reported in parts per million, and the coupling constants (J) are reported in Hertz. Mass spectra were obtained on either a VG 70-S Nier Johnson or JEOL Mass Spectrometer. HPLC analyses were conducted on a Varian ProStar system. Infrared spectra were recorded on a Thermo Nicolet Avatar 370 FT-IR spectrometer as neat films. Analytical TLC was performed on Whatman precoated glass plates (0.25 mm) with silica gel (60 F254). Flash column chromatography was performed with silica gel 60 (230 – 400 mesh, EM Science). Anhydrous reactions were performed with anhydrous solvents in flame-dried, argon-filled glassware. Reagents were obtained from commercial suppliers and used without further purification. Solvents were purchased as anhydrous or dried over 4Å molecular sieves. Organic extracts were dried over commercially available anhydrous MgSO_4 or Na_2SO_4 . Evaporations were performed under reduced pressure using a Buchi rotary evaporator at 35 °C, unless otherwise noted.

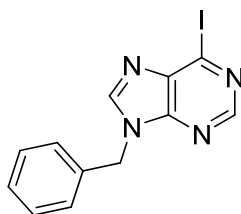
9-benzyl-6-chloro-9H-purine (27)

To the 250 mL round bottomed flask containing 3.33 g (21.5 mmol) of 6-chloropurine was added 8.93 g (64.6 mmol) of potassium carbonate. Then 102 mL of dry DMF was added to the flask followed by 3.7 mL (32.1 mmol) of benzyl chloride. The orange slurry was stirred at room temperature overnight. The mixture was filtered and the filtrate was diluted with 100 mL of CH₂Cl₂. The organic layer was washed with water (4 x 150 mL) and brine (100 mL). The organic layer was dried over MgSO₄, filtered, and concentrated. The column was run using 1:1 Hex/EtOAc to give 3.0 g (12.3 mmol, 57% yield) of a white solid. (R_f: 0.69; 9:1 CH₂Cl₂/MeOH). Mp: 85-87 °C. (Lit. 86-87 °C).⁴⁹ ¹H-NMR (CDCl₃, 600 MHz): σ 5.44 (s, 2H), 7.28 – 7.36 (m, 5H), 8.10 (s, 1H), 8.75 (s, 1H). ¹³C-NMR (CDCl₃, 150 Mz): σ 48.0, 128.0, 128.9, 129.3, 131.6, 134.6, 145.1, 151.1, 152.0, 152.2. HRMS (APCI): expected for C₁₂H₁₀ClN₄ (M+H)⁺ 245.05885. Found 245.05826. IR(neat): ν_{\max} 3062, 3031, 1595, 1556, 1445 cm⁻¹.

6-iodo-9H-purine (19)

A 100 mL round bottomed flask containing 30 mL of HI (55%) was cooled to 0 °C. Then 3.45 g (22.3 mmol) of 6-chloropurine was added slowly. The slurry was then stirred at 0 °C for 2 hours. The slurry was filtered and the solid obtained was added to an Erlenmeyer flask containing 33 mL of cold water. The solution was neutralized with ammonium hydroxide and the mixture was chilled for four hours. The mixture was filtered and the solid was added to an Erlenmeyer flask containing 75 mL of water and 5 mL of ammonium hydroxide. The pH of the solution was adjusted to 5 with glacial acetic acid. The solid was filtered and dried under high vacuum to give 3.51 g (14.3 mmol, 64% yield) of a yellow solid. (Rf: 0.51; 9:1 CH₂Cl₂/MeOH). Mp: 160 °C, decomp. (Lit. 165 °C, decomp).²¹ ¹H-NMR ([CD₃)₂SO], 600 MHz): σ 3.37 (br s, 1H), 8.57 (s, 1H), 8.63 (s, 1H). ¹³C-NMR ([CD₃)₂SO], 150 Mz): σ 120.8, 137.9, 145.4, 149.9, 152.4. HRMS (APCI): expected for C₅H₄IN₄ (M+H)⁺ 246.94752. Found 246.94695. IR(neat): ν_{\max} 3030, 2940, 2790, 1556 cm⁻¹.

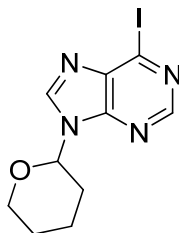
9-benzyl-6-iodo-9H-purine (29)



To the 250 mL round bottomed flask containing 3.48 g (14.2 mmol) of 6-iodo-9H-purine was added 5.89 g (42.6 mmol) of potassium carbonate. Then 60 mL of dry DMF was added to the flask followed by 2.5 mL (21.7 mmol) of benzyl chloride. The orange slurry was stirred at room temperature overnight. The

mixture was filtered and the filtrate diluted with 150 mL of CH₂Cl₂. The organic layer was washed with water (3 x 150 mL) and brine (150 mL). The organic layer was dried over MgSO₄, filtered, and concentrated. The column was run using 1:1 Hex/EtOAc to give 3.33 g (9.91 mmol, 70% yield) of product as a white solid. (Rf: 0.24; 1:1 Hex/EtOAc). Mp: 143-144 °C. (Lit. 142 °C).⁵⁰ (Lit. 152-154 °C)⁵¹ ¹H-NMR (CDCl₃, 600 MHz): σ 5.43 (s, 2H), 7.28 – 7.36 (m, 5H), 8.11 (s, 1H), 8.66 (s, 1H). ¹³C-NMR (CDCl₃, 150 Mz): σ 48.0, 128.0, 129.0, 129.4, 134.7, 138.7, 144.5, 145.1, 148.3, 152.4. HRMS (APCI): expected for C₁₂H₁₀IN₄ (M+H)⁺ 336.99447. Found 336.99408. IR(neat): ν_{\max} 3087, 3053, 1550 cm⁻¹.

6-iodo-9-(tetrahydro-2H-pyran-2-yl)-9H-purine (1)



To the 100 mL round bottomed flask containing 3.64 g (14.8 mmol) of 6-iodopurine was added 48 mg of *p*-TsOH followed by 30 mL of dry THF. The slurry was stirred at 60 °C for 20 minutes and then 1.75 mL (19.3 mmol) of 3,4-dihydropyran was added dropwise. The slurry was heated to 60 °C to give an orange solution. After five hours of stirring, the solution was cooled to room temperature and 1.4 mL of ammonium hydroxide was added. The resulting solution was stirred for five minutes, and was then diluted with EtOAc and washed with water (4 x 50 mL), dried over Na₂SO₄, filtered, and concentrated. The column was run using 1:1 Hex/EtOAc to give 3.57 g (10.8 mmol, 73% yield)

of yellow solid. (Rf: 0.67; 9:1 CH₂Cl₂/MeOH). Mp: 78-81 °C. ¹H-NMR (CDCl₃, 600 MHz): σ 1.63 – 1.65 (m, 1H), 1.70 – 1.81 (m, 2H), 1.99 – 2.07 (m, 2H), 2.12 – 2.15 (m, 1H), 3.73 – 3.77 (m, 1H), 4.14 – 4.16 (m, 1H), 5.73 (dd, 1H, *J* = 7.8, 2.4), 8.32 (s, 1H), 8.60 (s, 1H). ¹³C-NMR (CDCl₃, 150 Mz): σ 22.8, 24.9, 31.9, 69.0, 82.6, 122.3, 138.8, 142.5, 147.3, 152.1. HRMS (APCI): expected for C₁₀H₁₂IN₄O (M+H)⁺ 331.00503. Found 331.00464. IR(neat): ν_{max} 3113, 3051, 2926, 2865, 1549 cm⁻¹.

2.6 References

- (1) Robins, M. J.; Zhong, M.; (Brigham Young University, Transfer Technology Office, USA). Application: WO, 2006, p 73pp.
- (2) Bisacchi, G. S.; Singh, J.; Godfrey, J. D.; Kissick, T. P.; Mitt, T.; Malley, M. F.; Di Marco, J. D.; Gougoutas, J. Z.; Mueller, R. H.; Zahler, R. *Journal of Organic Chemistry* **1995**, *60*, 2902-2905.
- (3) Geen, G. R.; Kincey, P. M.; Spoons, P. G. *Tetrahedron Letters* **2001**, *42*, 1781-1784.
- (4) Kjellberg, J.; Liljenberg, M.; Johansson, N. G. *Tetrahedron Letters* **1986**, *27*, 877-880.
- (5) Liu, M.-C.; Kuzmich, S.; Lin, T.-S. *Tetrahedron Letters* **1984**, *25*, 613-616.
- (6) Geen, G. R.; Grinter, T. J.; Kincey, P. M.; Jarvest, R. L. *Tetrahedron* **1990**, *46*, 6903-6914.
- (7) Alarcon, K.; Martelli, A.; Demeunynck, M.; Lhomme, J. *Tetrahedron Letters* **2000**, *41*, 7211-7215.
- (8) Hocek, M. *European Journal of Organic Chemistry* **2003**, 245-254.
- (9) Leonard, N. J.; Bryant, J. D. *Journal of Organic Chemistry* **1979**, *44*, 4612-4616.
- (10) Kato, K.; Hayakawa, H.; Tanaka, H.; Kumamoto, H.; Miyasaka, T. *Tetrahedron Letters* **1995**, *36*, 6507-6510.
- (11) Kato, K.; Hayakawa, H.; Tanaka, H.; Kumamoto, H.; Shindoh, S.; Shuto, S.; Miyasaka, T. *Journal of Organic Chemistry* **1997**, *62*, 6833-6841.

- (12) Kumamoto, H.; Tanaka, H.; Tsukioka, R.; Ishida, Y.; Nakamura, A.; Kimura, S.; Hayakawa, H.; Kato, K.; Miyasaka, T. *Journal of Organic Chemistry* **1999**, *64*, 7773-7780.
- (13) Estep, K. G.; Josef, K. A.; Bacon, E. R.; Carabateas, P. M.; Rumney, S.; Pilling, G. M.; Krafft, D. S.; Volberg, W. A.; Dillon, K.; Dugrenier, N.; Briggs, G. M.; Canniff, P. C.; Gorczyca, W. P.; Stankus, G. P.; Ezrin, A. M. *Journal of Medicinal Chemistry* **1995**, *38*, 2582-2595.
- (14) Stevenson, T. M.; Prasad, A. S. B.; Citineni, J. R.; Knochel, P. *Tetrahedron Letters* **1996**, *37*, 8375-8378.
- (15) Prasad, A. S. B.; Stevenson, T. M.; Citineni, J. R.; Nyzam, V.; Knochel, P. *Tetrahedron* **1997**, *53*, 7237-7254.
- (16) Gundersen, L.-L. *Tetrahedron Letters* **1994**, *35*, 3155-3158.
- (17) Gundersen, L.-L.; Kristin Bakkestuen, A.; Jørgen Aasen, A.; Øveras, H.; Rise, F. *Tetrahedron* **1994**, *50*, 9743-9756.
- (18) Muchowski, J. M.; Naef, R. *Helvetica Chimica Acta* **1984**, *67*, 1168-1172.
- (19) Therkelsen, F. D.; Rottlander, M.; Thorup, N.; Pedersen, E. B. *Organic Letters* **2004**, *6*, 1991-1994.
- (20) Rajkumar, T. V.; Binkley, S. B. *Journal of Medicinal Chemistry* **1963**, *6*, 550-554.
- (21) Elion, G. B.; Hitchings, G. H. *Journal of the American Chemical Society* **1956**, *78*, 3508-3510.
- (22) Namavari, M.; Satyamurthy, N.; Phelps, M. E.; Barrio, J. R. *Tetrahedron Letters* **1990**, *31*, 4973-4976.

- (23) Hibino, J.; Nakatsukasa, S.; Fugami, K.; Matsubara, S.; Oshima, K.; Nozaki, H. *Journal of the American Chemical Society* **1985**, *107*, 6416-6417.
- (24) Cuadrado, P., Gonzalez, A.M., Gonzalez, B., Pulido, F.J. *Synthetic Communications* **1989**, *19*, 275-283.
- (25) Kondo, Y., Murata, N., Sakamoto, T. *Heterocycles* **1994**, *37*, 1467-1468.
- (26) Ple, N.; Turck, A.; Couture, K.; Queguiner, G. *Journal of Organic Chemistry* **1995**, *60*, 3781-3786.
- (27) Ple, N.; Turck, A.; Heynderickx, A.; Queguiner, G. *Journal of Heterocyclic Chemistry* **1997**, *34*, 551-556.
- (28) Kiburis, J.; Lister, J. H. *Journal of the Chemical Society C-Organic* **1971**, 3942-3947.
- (29) Lewis, L. R.; Schneider, F. H.; Robins, R. K. *Journal of Organic Chemistry* **1961**, *26*, 3837-3842.
- (30) Gaffney, B. L.; Jones, R. A. *Tetrahedron Letters* **1982**, *23*, 2253-2256.
- (31) Ashwell, M.; Bleasdale, C.; Golding, B. T.; O'Neill, I. K. *Journal of the Chemical Society-Chemical Communications* **1990**, 955-956.
- (32) Lembicz, N. K.; Grant, S.; Clegg, W.; Griffin, R. J.; Heath, S. L.; Golding, B. T. *Journal of the Chemical Society-Perkin Transactions 1* **1997**, 185-186.
- (33) Kiburis, J.; Lister, J. H. *Journal of the Chemical Society C-Organic* **1971**, 1587-1589.

- (34) Liu, X.; Zheng, Q. H.; Hutchins, G. D.; Fei, X. S.; Erickson, L. C.; Miller, K. D.; Mock, B. H.; Glick-Wilson, B. E.; Winkle, W. L.; Stone, K. L.; Carlson, K. A. *Synthetic Communications* **2003**, *33*, 941-952.
- (35) Linn, J. A.; McLean, E. W.; Kelley, J. L. *Journal of the Chemical Society-Chemical Communications* **1994**, 913-914.
- (36) Sandosham, J.; Undheim, K. *Tetrahedron* **1994**, *50*, 275-284.
- (37) Iddon, B.; Lim, B. L. *Journal of the Chemical Society-Perkin Transactions 1* **1983**, 271-277.
- (38) Martinez, G. R.; Grieco, P. A.; Srinivasan, C. V. *Journal of Organic Chemistry* **1981**, *46*, 3760-3761.
- (39) Brathe, A.; Gundersen, L. L.; Nisson-Meyer, J.; Rise, F.; Spilsberg, B. *Bioorganic & Medicinal Chemistry Letters* **2003**, *13*, 877-880.
- (40) Langli, G.; Gundersen, L. L.; Rise, F. *Tetrahedron* **1996**, *52*, 5625-5638.
- (41) Darabantu, M.; Bouilly, L.; Turck, A.; Ple, N. *Tetrahedron* **2005**, *61*, 2897-2905.
- (42) Kim, B. Y.; Ahn, J. B.; Lee, H. W.; Kang, S. K.; Lee, J. H.; Shin, J. S.; Ahn, S. K.; Hong, C. I.; Yoon, S. S. *European Journal of Medicinal Chemistry* **2004**, *39*, 433-447.
- (43) Warren, S.; Chow, A.; Fraenkel, G.; Rajanbabu, T. V. *Journal of the American Chemical Society* **2003**, *125*, 15402-15410.
- (44) Luo, F. T.; Wang, R. T. *Tetrahedron Letters* **1991**, *32*, 7703-7706.
- (45) Capek, P.; Pohl, R.; Hocek, M. *Journal of Organic Chemistry* **2004**, *69*, 7985-7988.

- (46) Zhou, J. R.; Fu, G. C. *Journal of the American Chemical Society* **2003**, *125*, 12527-12530.
- (47) Tobrman, T.; Dvorak, D. *Organic Letters* **2003**, *5*, 4289-4291.
- (48) Kopp, F.; Knochel, P. *Organic Letters* **2007**, *9*, 1639-1641.
- (49) Montgomery, J. A.; Temple, C. *Journal of the American Chemical Society* **1961**, *83*, 630-635.
- (50) Guthmann, H.; Konemann, M.; Bach, T. *European Journal of Organic Chemistry* **2007**, 632-638.
- (51) McKenzie, T. C.; Epstein, J. W. *Journal of Organic Chemistry* **1982**, *47*, 4881-4884.

Part III: Enantioselective Synthesis of β -D-Dioxolane-T and β -D-FDOC

3.1 Statement of Purpose

The stereochemistry of nucleoside analogues has a significant effect on the anti-viral activity, as shown with FDOC. Initially, the β -D enantiomer of 2', 3'-dideoxy-5-fluoro-oxacytidine (FDOC) was not considered as a potential anti-HIV treatment due to significant toxicity that the analogue displayed. However, it was discovered that the tested compound contained a small amount (3-5%) of the α -L-enantiomer. Separation of the mixture and subsequent testing of the enantiopure β -D-FDOC revealed that this analogue is highly potent with very low toxicity. The toxicity that was initially displayed was due to the presence of the α -L-enantiomer, which is highly toxic at 1.4 μ M. Thus, enantioselective syntheses of nucleoside analogues are very desirable, as the anti-viral profile differs significantly between isomers.

There have been methods developed to selectively produce specific enantiomers, including an enzymatic kinetic resolution method as well as chiral salt crystallization techniques. However, these methods result in the loss of half of the material. Thus, methods to enantioselectively synthesize dioxolane analogues, namely β -D-dioxolane-T and β -D-FDOC, will be explored.

The enantioselective synthesis will be explored at two points of the general scheme. A variety of chiral reagents will be used to induce chirality in the glycosylation step using racemic acetate. A second approach will be to determine conditions for the enantioselective lactonization. In this method, efforts

will also be made to retain this chirality throughout the remainder of the synthesis.

3.2 Introduction and Background

Nucleoside analogues in which the 3'-carbon has been replaced by a heteroatom have been a subject of intense interest over the last 20 years. These derivatives, which include the oxathiolane (3'-sulfur) and dioxolane (3'-oxygen) pseudosugars, have had significant clinical success as anti-viral agents. In fact, there are currently two FDA approved oxathiolane derived analogues (3TC and FTC) that are used in the treatment of HIV (Figure 1).

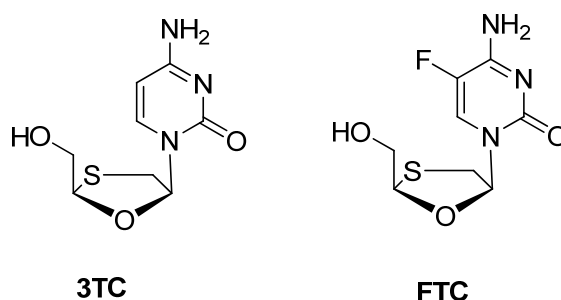


Figure 1: Structures of 3TC and FTC

There are also a number of dioxolane derived nucleosides that are in development or in clinical trials as anti-HIV agents. Among these are DAPD, D-FDOC, and Dioxolane-T (Figure 2). DAPD, or (-)- β -D-2, 6-diaminopurine dioxolane, acts as a water soluble prodrug of the guanine dioxolane derivative. It has displayed positive phase II clinical trial results when used in combination with AZT.¹⁻⁴ Both enantiomers of 2', 3'-dideoxy-5-fluoro-oxacytidine (FDOC) were synthesized and display drastically different anti-HIV properties.⁵ The L enantiomer was found to be highly toxic at low levels (1.4 μ M). The D enantiomer, however, showed excellent potency (EC_{50} = 0.04 μ M in primary human lymphocytes infected with HIV-1_{LA1}) and no toxicity up to 100 μ M.⁶⁻⁸

Dioxolane-T was synthesized as well and was shown to exhibit modest anti-HIV activity *in vivo* and no cellular toxicity.⁹⁻¹¹

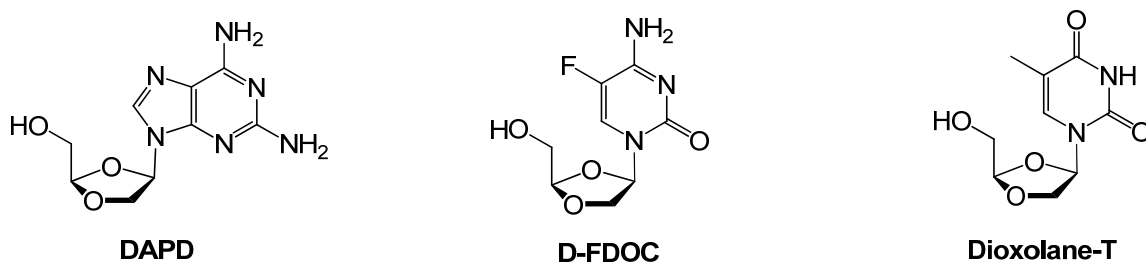
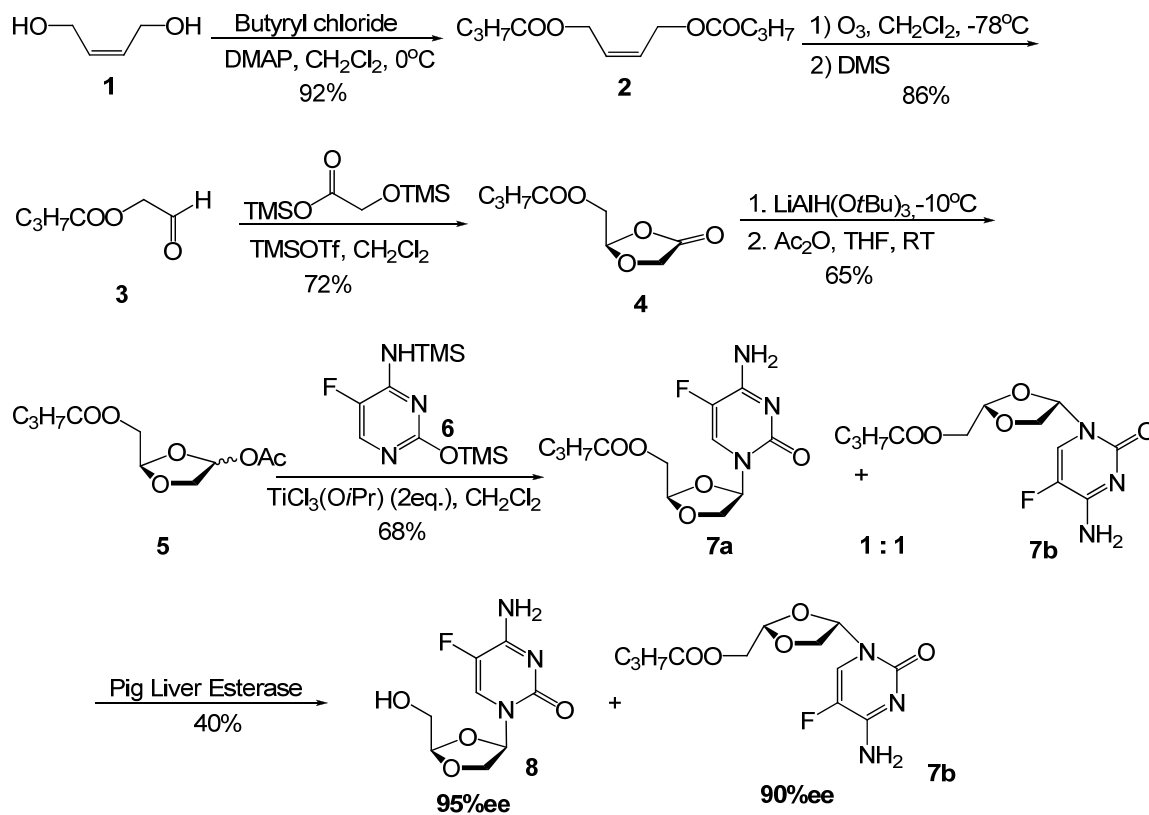


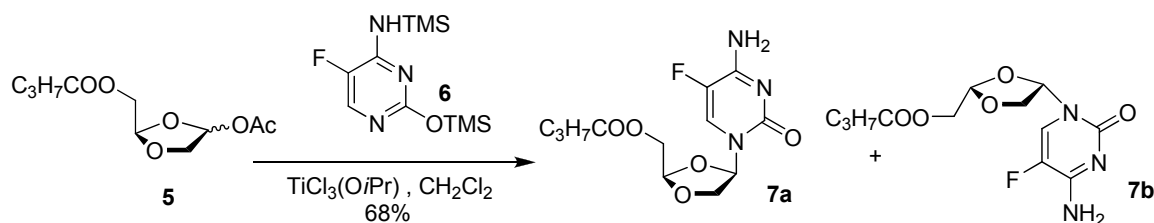
Figure 2: Structures of dioxolane nucleoside analogues

A useful method of synthesizing dioxolane nucleosides developed by the Liotta group has been applied to a variety of derivatives. (Scheme 1).¹²



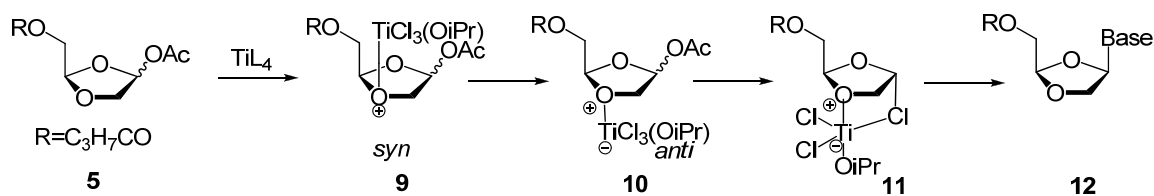
Scheme 1: Synthesis of FDOC **8** using Vorbrüggen ribosylation

This common method of glycosylation with dioxolanes involves the use of titanium trichloroisopropoxide to undergo the Vorbrüggen ribosylation with a silylated nucleobase as the key step.¹² It has been shown that the use of 2 equivalents of the titanium reagent effectively induces β -selective glycosylation (β : α >20:1) in moderate yields when reacting with racemic acetate **5** (Scheme 2).¹³



Scheme 2: β -Selective glycosylation using $TiCl_3(OiPr)$

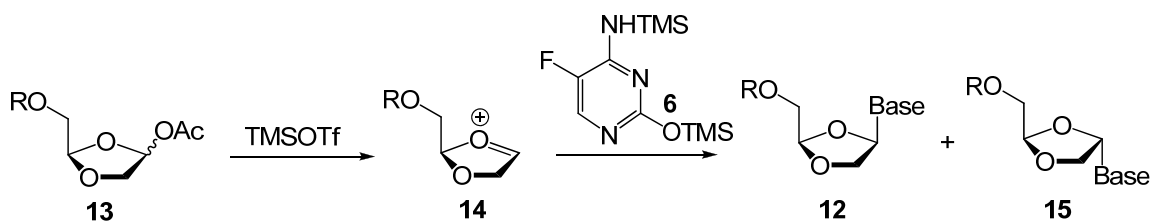
In efforts of selectively producing each enantiomer of FDOC, the enantiopure oxolactone (ee > 99%) was subjected to the same process.¹³ However, complete racemization resulted from this method. This is hypothesized to be due to the complexation of the Lewis acid, which renders the C-O bond labile and results in racemization of the substrate (Scheme 3).^{5,12,14}



Scheme 3: Mechanism of titanium mediated glycosylation reaction

Less oxophilic Lewis acids, such as TMSOTf, are able to retain the chirality of the lactol acetate, but result in 1:1 β : α mixtures. This is due to the

generation of the oxonium ion **14**, which results in no stereocontrol when reacted with the silylated base (Scheme 4).



Scheme 4: Generation of oxonium ion with TMSOTf

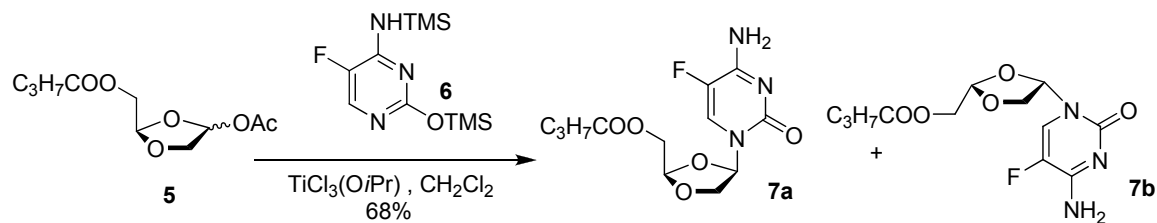
Enantiomerically pure D-FDOC was finally obtained through the use of a kinetic enzymatic resolution and chiral salt crystallization technique. This method, though effective in producing the desired enantiopure dioxolane analogue, results in loss of half of the glycosylated product.¹³ Though the L-FDOC butyrate was recycled through a racemization process while maintaining the β -selectivity, it is desirable to develop a method that selectively produces the D-dioxolane analogue directly. Thus, alternative methods, including the use of chiral Lewis acids and chiral auxiliaries on the dioxolane, will be explored.

3.3 Results and Discussion

The enantioselective synthesis of β -D-FDOC and β -D-dioxolane-T was explored by two methods. The first method involves the use of chiral Lewis acids to induce stereoselective glycosylation in the Vorbrüggen coupling. The second method entails the use of chiral Lewis acids in the lactonization step, and the development of conditions to retain the chirality in subsequent reactions. Though the enantioselective syntheses of both β -D-FDOC and β -D-dioxolane-T were explored using these methods, the following sections will focus on that of β -D-FDOC as it was explored most extensively in this methodology.

3.3.1 Asymmetric Glycosylation

The asymmetric glycosylation using chiral Lewis acids was explored as the initial approach. The reaction was first explored with 2 equivalents of titanium trichloroisopropoxide (Scheme 5). The reaction proceeded similarly to that reported in the literature, producing a 1:1 mixture of D (**17a**) and L (**17b**) isomers in 68% yield. Also, only the β -isomer was detected when using the silylated thymine in the dioxolane-T synthesis.



Scheme 5: Glycosylation with racemic dioxolane acetate and silylated 5-fluorocytosine

Chiral catalysts were then employed to determine if the ratios of D to L butyryl dioxolone-T would change. The binaphthol-derived titanium Lewis acid was explored initially (Figure 3). This species has been shown to be an efficient catalyst for glyoxylate-ene reactions to provide enantiopure α -hydroxy esters.¹⁵ Thus, the $\text{TiCl}_2(\text{BINOL})$ reagent was prepared by reacting $\text{TiCl}_2(\text{OiPr})_2$ with 1 equivalent of (R)-BINOL. The use of this reagent in the glycosylation reaction resulted in no product, even with extended reaction times and elevated reaction temperatures. It was revealed in a subsequent publication that the active catalyst in the glyoxylate-ene reaction was not the expected $\text{TiCl}_2(\text{BINOL})$ reagent, but instead the μ_3 -oxo titanium catalyst.¹⁶ This was discovered through the realization that while the reaction proceeds in high enantioselectivity and yield when performed in the presence of unactivated 4 Å MS, the absence or use of activated sieves both resulted in low yields and enantioselectivities. The study proved that the $\text{TiCl}_2(\text{BINOL})$ reagent served as a “pre-catalyst” in the reaction, with the active μ_3 -oxo titanium catalyst resulting after hydrolysis of the titanium “pre-catalyst” due to H_2O donation from the sieves and also the trapping of the resulting HCl. Thus, the glycosylation was performed in the presence of unactivated 4 Å MS as well to determine if the same μ_3 -oxo titanium species would induce selectivity. However, there was no reaction in this case either. It is possible that the di-oxygenated reagent does not possess enough Lewis acidic character to mediate the reaction.

Thus, it was decided to use the more Lewis acidic chiral camphor sulfonic acid reagent, and determine if any chiral induction resulted. The entire series of

these reagents were prepared including the mono-, di-, tri-, and tetra-CSA substituted titanium reagent and used in the reaction (Table 1). In all cases, only the β -glycosylation product was observed. Thus, these ligands do not affect the coordination of the titanium catalyst to the dioxolane. However, the catalyst was not able to effectively induce enantioselective formation, with the greatest result seen with the tri-substituted species, which had an 0.86:1 ratio of D to L isomers as shown by chiral HPLC. The same study was attempted with camphanic acid. However, the reagent was difficult to work with and resulted in decomposition of the reaction mixture.

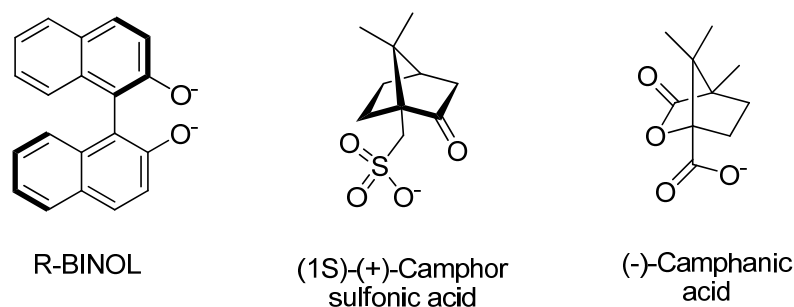
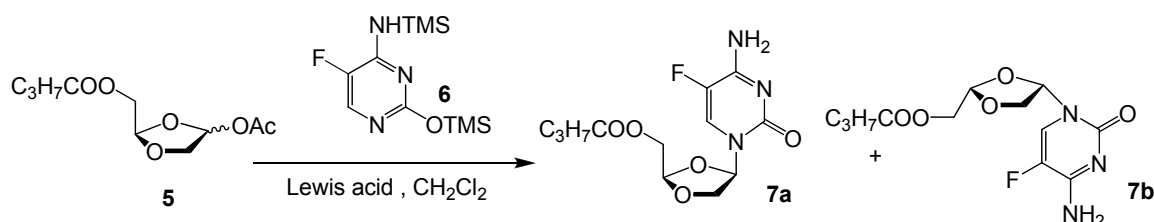


Figure 3: Chiral Lewis acid ligands used in asymmetric glycosylation reactions



Scheme 6: Asymmetric glycosylation general reaction

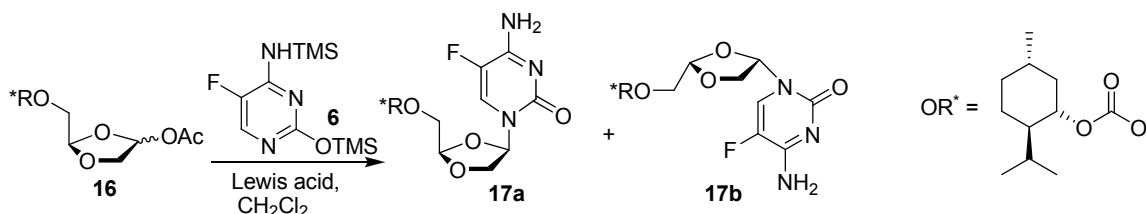
Entry	Lewis acid	Temp (°C)	D:L	Yield
1	TiCl ₃ (O <i>i</i> Pr)	rt	1:1	37%
2	TiCl ₃ (CSA)	rt	1:1	24%
3	TiCl ₂ (CSA) ₂	rt	1:1	44%
4	TiCl(CSA) ₃	0	0.90:1	10%
5	TiCl(CSA) ₃	rt; 0 (quench)	0.86:1	21%

6	TiCl(CSA) ₃	rt; then -78	0.86:1	23%
7	Ti(CSA) ₄	rt; 0 (quench)	0.93:1	11%
8	TiCl ₂ (R-BINOL)	rt	-	-
9	TiCl ₃ (CA)	rt	-	-

Note: Each trial used 2 eq of Lewis acid.

Table 1: Attempts at asymmetric glycosylation using chiral Lewis acids

Because the reaction with the chiral Lewis acids was mainly unsuccessful, it was decided that a chiral auxiliary should be used to see if there would be any resultant stereinduction (Scheme 7). The menthol dioxolane acetate **16** was treated with a variety of Lewis acids to determine the D to L ratios (Table 2). However, this reaction did not take place in the presence of titanium Lewis acids. The use of the well-explored TiCl₃(OiPr) and TiCl₄ Lewis acids resulted in no product. The Ti-BINOL derived catalyst also resulted in no yield. The lack of reactivity of the titanium Lewis acids may be as a result of intense complexation with the menthol and dioxolane components of the substrate. Thus, a large excess (5.1 equivalents) of Lewis acid was used to determine if the reaction would proceed; however, only starting material was recovered from this reaction as well. When less oxaphilic TMSOTf and SnCl₄ Lewis acids were employed, racemic D to L product (**17a** and **17b**) was detected. As expected, there was also a mixture of the β and α glycosylated products. Thus, the chiral menthol dioxolane is not suitable for the β-selective glycosylation reactions.



Scheme 7: Asymmetric glycosylation general reaction with chiral dioxolane

Entry	Lewis acid	Eq.	D:L	Yield
1	TiCl ₃ (O <i>i</i> Pr)	1.0	-	-
2	TiCl ₃ (O <i>i</i> Pr)	2.0	-	-
3	TiCl ₄	1.2	-	-
4	TiCl ₄	2.0	-	-
5	TiCl ₄	2.7	-	-
6	TiCl ₄	5.1	-	-
7	TiCl ₂ (R-BINOL)	2.2	-	-

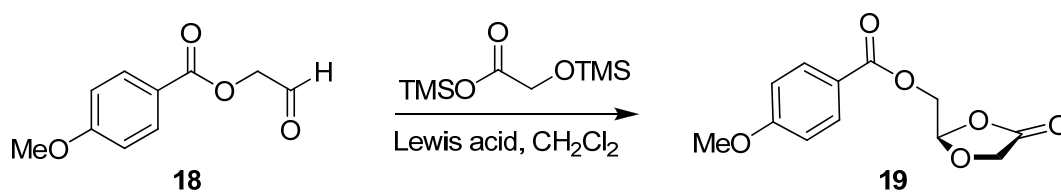
Table 2: Attempts at asymmetric glycosylation using menthol dioxolane

3.3.2 Asymmetric Lactonization

The use of chiral substrates and Lewis acids proved ineffective to enantioselectively enhance the production of D-glycosylated dioxolane; thus, it was decided that the induction should be focused on another reaction of the synthesis. The lactonization step is where the first chiral center is produced. Thus, the enantioselective formation of this center, following by mild conditions that will allow the retention of the dioxolane chirality for the remainder of the reaction sequence should result in the desired product. The use of chiral Lewis acids will be employed in this methodology. The use of the chiral auxiliary on the dioxolane hindered the glycosylation reaction using titanium catalysts. Thus, the chiral auxiliary will not be suitable to include in this methodology, as a titanium catalyst will be needed for β -glycosylation.

The lactonization was first performed using the normal protocol with 0.2 equivalents of TMSOTf at 0 °C. This produced the racemic lactone in 82% yield. The use of the Ti-BINOL reagent did not result in product, even with stoichiometric amounts of Lewis acid and increases in temperature. In order to

induce the reaction, a catalytic amount of TMSOTf should be added after allowing the chiral Lewis acid time to complex with the aldehyde. The racemic product was obtained, which shows that it is likely that TMSOTf alone produced the result. The mono-substituted chiral titanium CSA reagent was then used to undergo the reaction. Product was obtained, but in very low yield. In addition, there was no enantiomeric selectivity. Employment of the di-substituted catalyst resulted in a higher yield, with a slight enhancement of the L-dioxolone.



Scheme 8: Asymmetric lactonization general reaction with chiral Lewis acid

Entry	Lewis acid	Eq.	Temp (°C)	D:L	Yield
1	TMSOTf	0.2	0	1:1	82%
2	TiCl ₂ (R-BINOL)	0.8	0	-	-
3	TiCl ₂ (R-BINOL)	1.0	-10 to rt	-	-
4	TiCl ₂ (R-BINOL)/TMSOTf	0.2 / 0.2	0	1:1	55%
5	TiCl ₃ (CSA)	1.0	-40 to 0	1:1	7%
6	TiCl ₂ (CSA) ₂	2.0	-5	0.9:1	52%

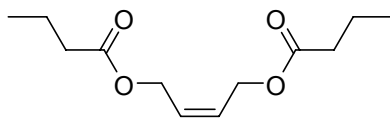
Table 3: Attempts at asymmetric lactonization using chiral Lewis acids

3.4 Conclusion

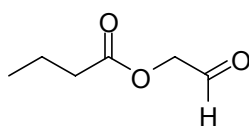
The enantioselective enhancement of β -D-dioxolane-T was explored through the use of chiral reagents in both asymmetric center forming reactions. The first method involved the use of chiral Lewis acids and chiral auxiliaries in the glycosylation step. While no significant enantiomeric selectivity was displayed, the use of an entire series of chiral titanium camphor sulfonic acid reagents was explored and proven effective for β -glycosylation. The use of the menthol chiral auxiliary on the dioxolane hindered the β -selective reaction, as no product was obtained using titanium catalysts. Control of the stereoselectivity in the lactonization step did not result in enantiomerically enhanced product either. This shows that the scrambling of racemic starting material is not an effective approach to synthesizing enantiopure β -D-dioxolane-T. Thus, the focus should be changed to determining conditions under which the chirality of the substrate will be retained. The chiral lactone can be obtained through an enzymatic resolution using Lipase PS.¹⁷ This produces the enantiopure chiral lactone in low yield (22%), but high ee (95%). Reduction of the lactone and subsequent acetylation results in the acetate with retention of chirality. Different titanium Lewis acids should be explored, including the chiral titanium CSA series described herein, to determine conditions that do not scramble the chiral center.

3.5 Experimental

General: ^1H -NMR spectra were recorded at either 400 MHz on an INOVA-400 spectrometer, or at 600 MHz on an INOVA-600 spectrometer. ^{13}C -NMR spectra were recorded at either 100 MHz or 150 MHz on the above mentioned instruments, respectively. NMR samples were prepared in either deuterated chloroform (CDCl_3) or dimethyl sulfoxide (d^6 -DMSO) with residual solvent peaks serving as the internal standards. Chemical shifts (δ) are reported in parts per million, and the coupling constants (J) are reported in Hertz. Mass spectra were obtained on either a VG 70-S Nier Johnson or JEOL Mass Spectrometer. HPLC analyses were conducted on a Varian ProStar system. Infrared spectra were recorded on a Thermo Nicolet Avatar 370 FT-IR spectrometer as neat films. Analytical TLC was performed on Whatman precoated glass plates (0.25 mm) with silica gel (60 F254). Flash column chromatography was performed with silica gel 60 (230 – 400 mesh, EM Science). Anhydrous reactions were performed with anhydrous solvents in flame-dried, argon-filled glassware. Reagents were obtained from commercial suppliers and used without further purification. Solvents were purchased as anhydrous or dried over 4Å molecular sieves. Organic extracts were dried over commercially available anhydrous MgSO_4 or Na_2SO_4 . Evaporations were performed under reduced pressure using a Buchi rotary evaporator at 35 °C, unless otherwise noted.

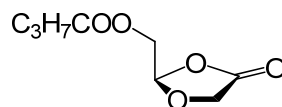
cis-But-2-ene-1,4-diol dibutyrate (2)

To a dry 500 mL round bottomed flask under argon containing 0.04 g (0.355 mmol) of DMAP was added 210 mL of dry CH₂Cl₂. To the stirred solution was then added 2.92 mL (35.5 mmol) of (Z)-but-2-ene-1,4-diol **1** followed by 50 mL (0.359 mol) of triethylamine. The solution was then cooled to 0°C and 8.9 mL of butyryl chloride was added dropwise. After the addition, the solution was warmed to room temperature. After 20 hours of stirring, the tangerine colored solution was quenched with 50 mL of water and then washed with water (200 mL x 2) and brine (200 mL). The washings caused the color of the solution to turn yellow. The organic layers were dried over MgSO₄, filtered, and concentrated. The crude material was purified by column chromatography using 4:1 Hex/EtOAc as the eluent to give the product in quantitative yield as a colorless oil (R_f: 0.69; 1:1 Hex/EtOAc). ¹H-NMR (CDCl₃, 600 MHz): σ 0.94 (t, 6H, *J* = 7.8), 1.61 – 1.68 (m, 4H), 2.29 (t, 4H, *J* = 7.8), 4.67 (d, 4H, *J* = 5.4), 5.71 – 5.76 (m, 2H). ¹³C-NMR (CDCl₃, 150 Mz): σ 13.8, 18.5, 36.2, 59.9, 128.3, 173.5. HRMS (FAB): expected for C₁₂H₂₁O₄ (M+H)⁺ 229.14344. Found: 229.14296. IR(neat): ν_{max} 2965, 2876, 1732, 1166 cm⁻¹.

2-Oxoethyl butyrate (3)

To a 250 mL round bottomed flask containing 8.23 g (0.036 mol) of *cis*-but-2-ene-1,4-diol dibutyrate **2** was added 75 mL of CH₂Cl₂. The solution was cooled to -78°C and was ozonized. Upon completion of the ozonolysis, the solution was quenched with dimethyl sulfide (8 mL, 0.11 mol) at -78°C and was allowed to stir at room temperature overnight. The solution was then concentrated and purified by column chromatography (4:1 Hex/EtOAc) to give 6.0 g (64%) of the product as a colorless oil. (R_f: 0.43, 1:1 Hex/EtOAc). ¹H-NMR (CDCl₃, 400 MHz): σ 0.87 – 0.99 (m, 6H), 1.57 – 1.74 (m, 2H), 2.37 – 2.44 (m, 2H), 4.62 – 4.67 (m, 2H), 9.59 (s, 1H). ¹³C-NMR (CDCl₃, 100 Mz): σ 13.7, 18.4, 35.7, 68.7, 173.2, 196.1. HRMS (FAB): expected for C₆H₁₁O₃ (M+H)⁺ 131.07027. Found: 131.07045. IR(neat): ν_{\max} 2967, 2878, 1736, 1167 cm⁻¹.

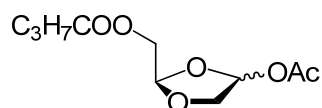
(4-Oxo-1,3-dioxolan-2-yl)methyl butyrate (4)



To a 500 mL round bottomed flask containing 6.67 g (0.051 mol) of 2-oxoethyl butyrate **3** was added 200 mL of CH₂Cl₂. The solution was cooled to 0°C and 13.0 mL (0.053 mol) of trimethylsilyl (trimethylsilyloxy)acetate was added. The solution was allowed to stir and then 1.85 mL (0.010 mol) of TMSOTf was added dropwise. The solution was allowed to stir at 0°C for six hours. The reaction was then quenched with 200 mL of saturated aqueous NaHCO₃ and the mixture was stirred for 10 minutes. The aqueous layer was separated and extracted with CH₂Cl₂ (3 x 100 mL). The combined organic layers were dried over MgSO₄ and filtered. The solution was then concentrated and purified by column

chromatography (4:1 Hex/EtOAc) to give 7.1 g (74%) of the product as yellow oil. (R_f: 0.53, 1:1 Hex/EtOAc). ¹H-NMR (CDCl₃, 400 MHz): σ 0.96 (t, 3H, *J* = 7.6 Hz), 1.59 – 1.72 (m, 2H), 2.36 (t, 2H, *J* = 7.6 Hz), 4.25 – 4.31 (m, 2H), 4.34 – 4.41 (m, 2H), 5.84 (t, 1H, *J* = 3.0 Hz). ¹³C-NMR (CDCl₃, 100 Mz): σ 13.8, 18.5, 36.0, 63.5, 63.7, 102.8, 170.7, 172.9. HRMS (FAB): expected for C₈H₁₃O₅ (M+H)⁺ 189.07575. Found: IR(neat): ν_{max} 2968, 2878, 1812, 1743, 1214, 1173 cm⁻¹.

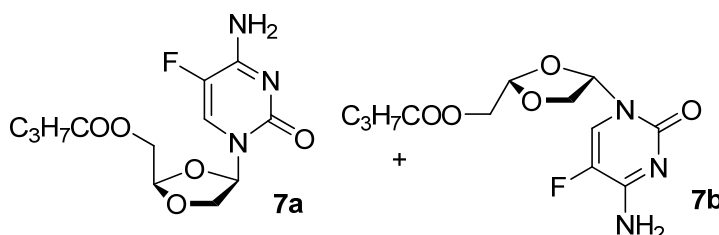
(4-Acetoxy-1,3-dioxolan-2-yl)methyl butyrate (5)



To a 500 mL round bottomed flask containing 7.09 g (37.7 mmol) of (4-oxo-1,3-dioxolan-2-yl)methyl butyrate **4** was added 185 mL of dry THF. The flask was cooled to -10 °C and 40.0 mL of LiAl[OC(CH₃)₃]₃H (1.0 M in THF) was added dropwise. The solution continued to stir at -10 °C for 2 hours, and then 36 mL of acetic anhydride (381 mmol) was added. The solution was warmed to 0 °C and stirred overnight. Then 150 mL of saturated aqueous NaHCO₃ was added and the mixture was stirred for 1 hour. Then the aqueous layer was separated and extracted with diethyl ether. The combined organic layers were dried over MgSO₄, filtered, and concentrated. The column was run using 6:1 Hex/EtOAc to give 5.0 g (21 mmol) of product as a colorless oil. R_f: 0.52 (1:1 Hex/EtOAc). ¹H-NMR (CDCl₃, 600 MHz): σ 0.92 - 0.96 (m, 3H), 1.62 – 1.69 (m, 2H), 2.09 (s, 3H), 2.29 – 2.34 (m, 2H), 3.96 (dd, 1H, major, *J* = 7.8, 1.8 Hz), 3.99 (dd, 1H, minor, *J* = 5.4, 4.2 Hz), 4.16 – 4.20 (m, 2H), 4.24 – 4.27 (m, 1H), 5.31 (t, 1H, minor, *J* = 4.2 Hz), 5.39 (t, 1H, major, *J* = 4.2 Hz), 5.82 (t, 1H, *J* = 3.6 Hz), 6.34 (d, 1H,

minor, $J = 3.6$ Hz), 6.38 (dd, 1H, major, $J = 2.4, 1.8$), . $^{13}\text{C-NMR}$ (CDCl_3 , 150 Mz): σ 13.7, 18.4, 20.8, 36.0, 63.4, 70.9, 94.6, 102.7, 170.4, 173.3. HRMS (FAB): expected for $\text{C}_{10}\text{H}_{17}\text{O}_6$ ($\text{M}+\text{H}$) $^+$ 233.10196. Found: 233.11104. IR(neat): ν_{max} 2966, 2878, 1812, 1737, 1151 cm^{-1} .

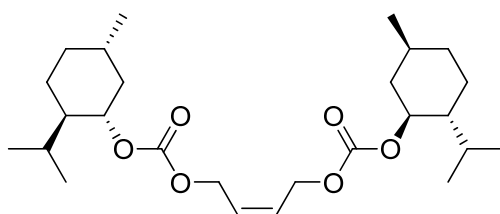
5'-Butyrate-2', 3'-dideoxy-5-fluoro-cytosine (7a & 7b)



To a dry 25 mL flask containing bis-TMS-5-fluorocytosine **6** (0.469 mmol) was added 5 mL anhydrous methylene chloride to give a clear solution. Then, 0.69 mL (0.69 mmol) $\text{TiCl}_3(\text{O}i\text{Pr})$ was added dropwise to give a rusty red clear solution. In a dry round bottomed flask filled with argon was added 5'-butyrate dioxolane acetate **5** (80.1 mg, 0.35 mmol) and 5 mL anhydrous methylene chloride. Then the solution of $\text{TiCl}_3(\text{O}i\text{Pr})$ and the silylated base was added dropwise to the solution of **5** at 0 °C to give the same rusty red clear solution. After overnight stirring, the reaction was quenched with mixture of 12 mL EtOH (absolute) and 3 mL NH_4OH (concentrated) at RT for 30 min, followed by filtration through a two-inch celite column and solvent removal *in vacuo* to give a crude light yellow solid. The crude material was purified by column chromatography using 9:1 EtOAc/: EtOH to afford the product as a white powder. Mp: 145-146 °C Yield: 70.2 mg, 68%. $^1\text{H NMR}$ (CDCl_3 , 600 MHz): δ 0.94 (t, 3H, $J = 7.2$ Hz), 1.64-1.70 (m, 2H), 2.36 (t, 2H, $J = 7.2$ Hz), 4.15 - 4.31 (m, 3H), 4.53 (dd, 1H, $J =$

10.8, 2.4 Hz), 5.17 (s, 1H), 6.23 (d, 1H, $J = 5.4$ Hz), 7.87 (d, 1H, $J = 6.6$ Hz), 8.60 (br s, 1H). ^{13}C NMR (CDCl_3 , 150 MHz): δ 13.7, 18.5, 35.9, 61.6, 72.6, 82.5, 103.2, 125.2, 136.0, 154.3, 158.5, 173.0. HRMS (ESI): expected for $\text{C}_{12}\text{H}_{16}\text{FN}_3\text{O}_5$ ($\text{M}+\text{H}$) $^+$ Found. IR (neat): ν_{max} 3324, 3098, 2965, 1740, 1681, 1504, 1100 cm^{-1} . Chiral HPLC analysis: mobile phase: EtOH: hexane=15:85, flow rate: 1.2 mL/min, Chiralpak AS-10 m, 25×4.6 cm, detection at 271 nm. The retention time for D-butyrate-FDOC is 18.9 min and 21.8 min for L-butyrate-FDOC.

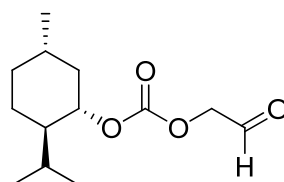
(Z)-but-2-ene-1,4-diyl bis((1S,2R,5S)-2-isopropyl-5-methylcyclohexyl) dicarbonate



To a dry 250 mL round bottomed flask under argon containing 0.02 g (0.175 mmol) of DMAP was added 100 mL of dry CH_3CN . To the stirred solution was then added 1.4 mL (17.0 mmol) of (Z)-but-2-ene-1,4-diol **1** followed by 8.2 mL (0.101 mol) of pyridine. The solution was then cooled to 0°C and 7.2 mL of menthyl chloroformate was added dropwise. After the addition, the solution was warmed to room temperature. After 20 hours of stirring, the pink colored solution was concentrated. The residue was diluted with 200 mL of CH_2Cl_2 and then washed with water (200 mL \times 2). The organic layers were dried over MgSO_4 , filtered, and concentrated. The crude material was purified by column chromatography using 9:1 Hex/EtOAc as the eluent to give the product in 81% yield (6.2 g, 13.7 mmol) as a colorless oil (R_f : 0.81; 1:1 Hex/EtOAc). ^1H -NMR

(CDCl₃, 600 MHz): σ 0.79 (d, 6H J = 7.2 Hz), 0.89 – 0.93 (m, 12H), 1.02 – 1.09 (m, 4H), 1.38 – 1.43 (m, 2H), 1.46 – 1.52 (m, 2H), 1.68 (d, 4H, J = 12Hz), 1.96 (qd, 2H, J = 4.2, 3 Hz), 2.06 – 2.10 (m, 2H), 4.52 (td, 2H, J = 6.6, 4.8 Hz), 4.70 – 4.77 (m, 4H), 5.81 (t, 2H, J = 4.2 Hz). ¹³C-NMR (CDCl₃, 150 Mz): σ 20.9, 22.2, 23.5, 26.2, 31.6, 40.9, 47.2, 63.1, 78.9, 128.2, 154.9. HRMS (FAB): expected for C₂₆H₄₅O₆ (M+H)⁺ 453.32107. Found: 453.32154. IR(neat): ν_{\max} 2955, 2870, 1740, 1249 cm⁻¹.

(1S,2R,5S)-2-isopropyl-5-methylcyclohexyl 2-oxoethyl carbonate

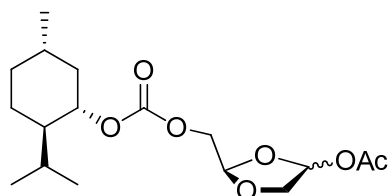


To a 500 mL round bottomed flask containing 6.19 g (13.7 mmol) of (Z)-but-2-ene-1,4-diyl bis((1S,2R,5S)-2-isopropyl-5-methylcyclohexyl) dicarbonate was added 250 mL of CH₂Cl₂. The solution was cooled to -78°C and was ozonized. Upon completion of the ozonolysis, the solution was quenched with dimethyl sulfide (9.5 mL, 0.129 mol) at -78°C and was allowed to stir at room temperature overnight. The solution was then concentrated and purified by column chromatography (4:1 Hex/EtOAc) to give 6.4 g (96%) of the product as a colorless oil. (R_f: 0.77; 1:1 Hex/EtOAc). ¹H-NMR (CDCl₃, 600 MHz): σ 0.78 – 0.81 (m, 3H), 0.86 – 1.03 (m, 7H), 1.04 – 1.13 (m, 2H), 1.43 – 1.51 (m, 2H), 1.67 – 1.72 (m, 2H), 1.97 – 2.00 (m, 1H), 2.07 – 2.12 (m, 1H), 4.55 – 4.59 (m, 1H), 4.55 – 4.59 (m, 1H), 4.67 (s, 1H), 9.66 (s, 1H). ¹³C-NMR (CDCl₃, 150 Mz): σ 16.5, 20.9, 22.2, 23.6, 26.4, 31.6, 34.2, 40.8, 47.2, 71.2, 79.9, 154.7, 195.9.

HRMS (FAB): expected for $C_{13}H_{23}O_4$ (M+H)⁺ 243.15909. Found: 243.15957.

IR(neat): ν_{\max} 3468, 2955, 2870, 1740, 1257 cm^{-1} .

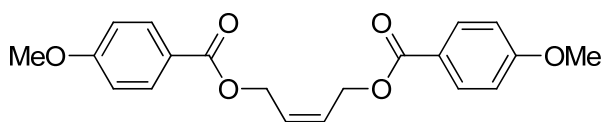
2-(((1S,2R,5S)-2-isopropyl-5-methylcyclohexyloxy)carbonyloxy)methyl)-1,3-dioxolan-4-yl acetate (16)



To a 100 mL round bottomed flask containing 0.26 g (1.12 mmol) of (1S,2R,5S)-2-isopropyl-5-methylcyclohexyl 2-oxoethyl carbonate was added 20 mL of CH_2Cl_2 . The solution was cooled to 0°C and 0.28 mL (1.14 mol) of trimethylsilyl (trimethylsilyloxy)acetate was added. The solution was allowed to stir and then 40 μL (0.22 mmol) of TMSOTf was added dropwise. The solution was allowed to stir at 0°C for six hours. The reaction was then quenched with saturated aqueous NaHCO_3 and the mixture was stirred for 10 minutes. The aqueous layer was separated and extracted with CH_2Cl_2 (3 x 200 mL). The combined organic layers were dried over MgSO_4 and filtered. The solution was then concentrated to give 0.26 g of the crude lactone. (R_f : 0.74, 1:1 Hex/EtOAc). The material was dissolved in 4 mL of dry THF and cooled to -10°C . Then 0.9 mL of $\text{LiAl}[\text{OC}(\text{CH}_3)_3]_3\text{H}$ (1.0 M in THF) was added dropwise. The solution continued to stir at -10°C for 2 hours, and then 0.76 mL of acetic anhydride (8.0 mmol) was added. The solution was warmed to 0°C and stirred overnight. Then 150 mL of saturated aqueous NaHCO_3 was added and the mixture was stirred for 1 hour. Then the aqueous layer was separated and extracted with diethyl ether. The

combined organic layers were dried over MgSO_4 , filtered, and concentrated. The column was run using 4:1 Hex/EtOAc to give 0.21 g (0.62 mmol) of product as a colorless oil. $^1\text{H-NMR}$ (CDCl_3 , 600 MHz): σ 0.78 – 0.80 (m, 3H), 0.85 – 0.93 (m, 7H), 1.02 – 1.09 (m, 6H), 1.39 – 1.49 (m, 2H), 1.68 (d, 2H, $J = 10.2$ Hz), 1.92 – 1.98 (m, 1H), 2.10 (s, 3H), 3.98 (dd, 1H, major, $J = 7.8, 1.8$ Hz), 4.01 (dd, 1H, minor, $J = 6.0, 3.6$ Hz), 4.17 – 4.22 (m, 2H), 4.30 – 4.41 (m, 1H), 4.50 – 4.56 (m, 1H), 5.35 (q, 1H, minor, $J = 4.2$ Hz), 5.43 (t, 1H, major, $J = 4.2$ Hz), 5.83 (t, 1H, $J = 3$ Hz), 6.36 (t, 1H, minor, $J = 3$ Hz), 6.41 (q, 1H, major, $J = 1.8$ Hz). $^{13}\text{C-NMR}$ (CDCl_3 , 150 Mz): σ 16.4, 20.9, 23.4, 31.6, 34.2, 40.7, 47.1, 63.6, 67.1, 71.0, 102.5, 103.5, 154.7, 170.4. HRMS (FAB): expected for $\text{C}_{17}\text{H}_{29}\text{O}_7$ ($\text{M}+\text{H}$) $^+$ 345.19078. Found: 345.19109. IR(neat): ν_{max} 2955, 2871, 1742, 1258 cm^{-1} .

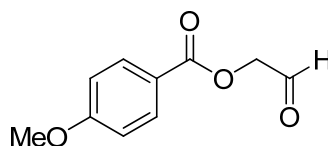
(Z)-but-2-ene-1,4-diyl bis(4-methoxybenzoate)



To a dry 250 mL round bottomed flask under argon containing 0.02 g (0.166 mmol) of DMAP was added 85 mL of dry CH_2Cl_2 . To the stirred solution was then added 1.25 mL (15.2 mmol) of (Z)-but-2-ene-1,4-diol **1** followed by 21 mL (0.151 mol) of triethylamine. The solution was then cooled to 0°C and 8.9 mL of *p*-methoxybenzoyl chloride was added dropwise. After the addition, the solution was warmed to room temperature. After overnight stirring, the solution was

quenched with 50 mL of aqueous NH_4Cl and then washed with water (200 mL x 2) and brine (200 mL). The washings caused the color of the solution to turn yellow. The organic layers were dried over MgSO_4 , filtered, and concentrated. The crude material was purified by column chromatography using 9:1 Hex/EtOAc as the eluent to give the product (4.95 g, 91% yield) as a colorless oil (R_f : 0.69; 1:1 Hex/EtOAc). $^1\text{H-NMR}$ (CDCl_3 , 600 MHz): σ 3.86 (s, 6H), 4.97 (d, 4H, $J = 4.8$ Hz), 5.94 (t, 2H, $J = 4.8$ Hz), 6.91 (d, 4H, $J = 9$ Hz), 8.00 (d, 4H, $J = 9$ Hz). $^{13}\text{C-NMR}$ (CDCl_3 , 150 Mz): σ 55.6, 60.5, 113.8, 122.6, 128.6, 131.9, 163.6, 166.3. HRMS (FAB): expected for $\text{C}_{20}\text{H}_{21}\text{O}_6$ ($\text{M}+\text{H}$) $^+$ 357.13326. Found: 357.13340. IR(neat): ν_{max} 2964, 2843, 1708, 1696, 1605, 1345, 1167 cm^{-1} .

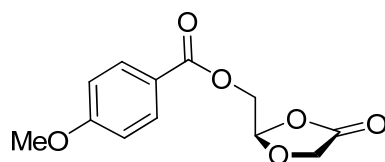
2-oxoethyl 4-methoxybenzoate (18)



To a 500 mL round bottomed flask containing 4.93 g (0.014 mol) of (Z)-but-2-ene-1,4-diyl bis(4-methoxybenzoate) was added 250 mL of CH_2Cl_2 . The solution was cooled to -78°C and was ozonized. Upon completion of the ozonolysis, the solution was quenched with dimethyl sulfide (9.5 mL, 0.129 mol) at -78°C and was allowed to stir at room temperature overnight. The solution was then concentrated and purified by column chromatography (4:1 Hex/EtOAc) to give 5.2 g (97%) of the product as a colorless oil. $^1\text{H-NMR}$ (CDCl_3 , 600 MHz): σ 3.87 (s, 3H), 4.86 (s, 2H), 6.95 (d, 2H, $J = 7.8$ Hz), 8.06 (d, 2H, $J = 7.8$ Hz), 9.72 (s, 1H). $^{13}\text{C-NMR}$ (CDCl_3 , 150 Mz): σ 55.7, 69.0, 114.0, 121.3, 132.2, 164.1, 165.9,

196.6. HRMS (ESI): expected for $C_{10}H_{11}O_4$ $(M+H)^+$ 195.06519. Found: 195.06550. IR(neat): ν_{max} 3458, 2937, 2840, 1709, 1604, 1253, 1168 cm^{-1} .

(4-oxo-1,3-dioxolan-2-yl)methyl 4-methoxybenzoate (19)



To a 100 mL round bottomed flask containing 0.14 g (0.73 mmol) of 2-oxoethyl 4-methoxybenzoate (**18**) was added 10 mL of CH_2Cl_2 . The solution was cooled to $0^\circ C$ and 0.18 mL (0.74 mmol) of trimethylsilyl (trimethylsilyloxy)acetate was added. The solution was allowed to stir and then 26 μL (0.14 mmol) of TMSOTf was added dropwise. The solution was allowed to stir at $0^\circ C$ overnight. The reaction was then quenched with saturated aqueous $NaHCO_3$ and the mixture was stirred for 10 minutes. The aqueous layer was separated and extracted with CH_2Cl_2 (3 x 20 mL). The combined organic layers were dried over $MgSO_4$ and filtered. The solution was then concentrated and purified by column chromatography (9:1 Hex/EtOAc) to give 0.15 g (82%) of the product as colorless oil. 1H -NMR ($CDCl_3$, 600 MHz): σ 3.88 (s, 3H), 4.32 (d, 1H, $J = 15$ Hz), 4.42 (d, 1H, $J = 15$ Hz), 4.51 (dd, 1H, $J = 10.2, 2.4$ Hz), 4.56 (dd, 1H, $J = 9, 3.6$ Hz), 5.96 (t, 1H, $J = 3$ Hz), 6.94 (d, 2H, $J = 8.4$ Hz), 7.99 (d, 2H, $J = 9$ Hz). ^{13}C -NMR ($CDCl_3$, 150 Mz): σ 30.0, 55.8, 63.8, 103.1, 114.1, 121.6, 132.1, 164.1, 165.6, 170.8. HRMS (ESI): expected for $C_{12}H_{13}O_6$ $(M+H)^+$ 253.07066. Found: 253.07038. IR(neat): ν_{max} 2919, 1810, 1718, 1606, 1258 cm^{-1} . Chiral HPLC analysis: mobile phase: MeOH (isocratic), flow rate: 0.5 mL/min, Chiralpak AD-

RH, 15 × 0.46 cm, detection at 280 nm). The retention time for D-dioxolone is 16.6 min and 26.2 min for L-dioxolone.

3.6 References

- (1) Feng, J. Y.; Parker, W. B.; Krajewski, M. L.; Deville-Bonne, D.; Veron, M.; Krishnan, P.; Cheng, Y.-C.; Borroto-Esoda, K. *Biochemical Pharmacology* **2004**, *68*, 1879-1888.
- (2) Chen, H. C.; Schinazi, R. F.; Rajagopalan, P.; Gao, Z. L.; Chu, C. K.; McClure, H. M.; Boudinot, F. D. *Aids Research and Human Retroviruses* **1999**, *15*, 1625-1630.
- (3) Rajagopalan, P.; Boudinot, F. D.; Chu, C. K.; Tennant, B. C.; Baldwin, B. H.; Schinazi, R. F. *Antiviral Chemistry & Chemotherapy* **1996**, *7*, 65-70.
- (4) Rajagopalan, P.; Gao, Z. L.; Chu, C. K.; Schinazi, R. F.; McClure, H. M.; Boudinot, F. D. *Journal of Chromatography B-Biomedical Applications* **1995**, *672*, 119-124.
- (5) Wilson, L. J.; Choi, W.-B.; Spurling, T.; Liotta, D. C.; Schinazi, R. F.; Cannon, D.; Painter, G. R.; St. Clair, M.; Furman, P. A. *Bioorganic & Medicinal Chemistry Letters* **1993**, *3*, 169-174.
- (6) Hernandez-Santiago, B. I.; Chen, H. C.; Asif, G.; Beltran, T.; Mao, S. L.; Hurwitz, S. J.; Grier, J.; McClure, H. M.; Chu, C. K.; Liotta, D. C.; Schinazi, R. F. *Antimicrobial Agents and Chemotherapy* **2005**, *49*, 2589-2597.
- (7) Schinazi, R. F.; Mellors, J.; Erickson-Viitanen, S.; Mathew, J.; Parikh, U.; Sharma, P.; Otto, M.; Yang, Z.; Chu, C. K.; Liotta, D. C. *Antiviral Therapy* **2002**, *7*, S21.

- (8) Schinazi, R. F.; Gosselin, G.; Faraj, A.; Korba, B. E.; Liotta, D. C.; Chu, C. K.; Mathe, C.; Imbach, J. L.; Sommadossi, J. P. *Antimicrobial Agents and Chemotherapy* **1994**, *38*, 2172-2174.
- (9) Norbeck, D. W.; Spanton, S.; Broder, S.; Mitsuya, H. *Tetrahedron Letters* **1989**, *30*, 6263-6266.
- (10) Chu, C. K.; Ahn, S. K.; Kim, H. O.; Beach, J. W.; Alves, A. J.; Jeong, L. S.; Islam, Q.; Roey, P. V.; Schinazi, R. F. *Tetrahedron Letters* **1991**, *32*, 3791-3794.
- (11) Kim, H. O.; Shanmuganathan, K.; Alves, A. J.; Jeong, L. S.; Warren Beach, J.; Schinazi, R. F.; Chien-Neng, C.; Yung-Chi, C.; Chu, C. K. *Tetrahedron Letters* **1992**, *33*, 6899-6902.
- (12) Choi, W. B.; Wilson, L. J.; Yeola, S.; Liotta, D. C.; Schinazi, R. F. *Journal of the American Chemical Society* **1991**, *113*, 9377-9379.
- (13) Mao, S.; Bouygues, M.; Welch, C.; Biba, M.; Chilenski, J.; Schinazi, R. F.; Liotta, D. C. *Bioorganic & Medicinal Chemistry Letters* **2004**, *14*, 4991-4994.
- (14) Wilson, L. J.; Hager, M. W.; El-Kattan, Y. A.; Liotta, D. C. *Synthesis* **1995**, 1465-1479.
- (15) Mikami, K.; Terada, M.; Nakai, T. *Journal of the American Chemical Society* **1990**, *112*, 3949-3954.
- (16) Terada, M.; Matsumoto, Y.; Nakamura, Y.; Mikami, K. *Chemical Communications* **1997**, 281-282.

- (17) Sznaidman, M.; Painter, G. R.; Almond, M. R.; Cleary, D. G.; Pesyan, A.;
(Emory University, USA). Application: WO, 2005, p 98.